MOTION & CONTROL™

NSK

Technical Report

MOTION & CONTROL™
NSK

Technical Report

CAT. No. E728h

CONTENTS

Pages

1. ISO Dimensional system and bearing numbers

1.1 ISO Dimensional system 6
1.2 Formulation of bearing numbers 8
1.3 Bearing numbers for tapered roller bearings (inch system) 10
1.4 Bearing numbers for miniature ball bearings 12
1.5 Auxiliary bearing symbols 14

2. Dynamic load rating, fatigue life, and static load rating

2.1 Dynamic load rating 18
2.2 Dynamic equivalent load 22
2.3 Dynamic equivalent load of triplex angular contact ball bearings 24
2.4 Average of fluctuating load and speed 26
2.5 Combination of rotating and stationary loads 28
2.6 Life calculation of multiple bearings as a group 30
2.7 Load factor and fatigue life by machine 32
2.8 Radial clearance and fatigue life 34
2.9 Misalignment of inner/outer rings and fatigue life of deep-groove ball bearings 36
2.10 Misalignment of inner/outer rings and fatigue life of cylindrical roller bearings 38
2.11 Fatigue life and reliability 40
2.12 Oil film parameters and rolling fatigue life 42
2.13 EHL oil film parameter calculation diagram 44
2.13.1 Oil film parameter 44
2.13.2 Oil film parameter calculation diagram 44
2.13.3 Effect of oil shortage and shearing heat generation 48
2.14 Fatigue analysis 50
2.14.1 Measurement of fatigue degree 50
2.14.2 Surface and sub-surface fatigues 52
2.14.3 Analysis of practical bearing (1) 54
2.14.4 Analysis of practical bearing (2) 56
2.15 Conversion of dynamic load rating with reference to life at 500 min^{-1} and 3 000 hours 58
2.16 Basic static load ratings and static equivalent loads 60

3. Bearing fitting practice

3.1 Load classifications 62
3.2 Required effective interference due to load 64
3.3 Interference deviation due to temperature rise (aluminum housing, plastic housing) 66
3.4 Fit calculation 68
3.5 Surface pressure and maximum stress on fitting surfaces 70
3.6 Mounting and withdrawal loads 72
3.7 Tolerances for bore diameter and outside diameter 74
3.8 Interference and clearance for fitting (shafts and inner rings) 76
3.9 Interference and clearance for fitting (housing holes and outer rings) 78
3.10 Interference dispersion (shafts and inner rings) 80
3.11 Interference dispersion (housing bores and outer rings) 82
3.12 Fits of four-row tapered roller bearings (metric) for roll necks 84

4. Internal clearance

4.1 Internal clearance 86
4.2 Calculating residual internal clearance after mounting 88
4.3 Effect of interference fit on bearing raceways (fit of inner ring) 90
4.4 Effect of interference fit on bearing raceways (fit of outer ring) 92
4.5 Reduction in radial internal clearance caused by a temperature difference between inner and outer rings 94
4.6 Radial and axial internal clearances and contact angles for single row deep groove ball bearings 96
4.6.1 Radial and axial internal clearances 96
4.6.2 Relation between radial clearance and contact angle 98
4.7 Angular clearances in single-row deep groove ball bearings 100
4.8 Relationship between radial and axial clearances in double-row angular contact ball bearings 102
4.9 Angular clearances in double-row angular contact ball bearings 104
4.10 Measuring method of internal clearance of combined tapered roller bearings (offset measuring method) 106
4.11 Internal clearance adjustment method when mounting a tapered roller bearing 108

5. Bearing internal load distribution and displacement

5.1 Bearing internal load distribution 110
5.2 Radial clearance and load factor for radial ball bearings 112
5.3 Radial clearance and maximum rolling element load 114
5.4 Contact surface pressure and contact ellipse of ball bearings under pure radial loads 116
5.5 Contact surface pressure and contact area under pure radial load (roller bearings) 120
5.6 Rolling contact trace and load conditions 128
5.6.1 Ball bearing 128
5.6.2 Roller bearing 130
5.7 Radial load and displacement of cylindrical roller bearings 132
5.8 Misalignment, maximum rolling-element load and moment for deep groove ball bearings 134
5.8.1 Misalignment angle of rings and maximum rolling-element load 134
5.8.2 Misalignment of inner and outer rings and moment 136
5.9 Load distribution of single-direction thrust bearing due to eccentric load 138

Pages

6. Preload and axial displacement

6.1 Position preload and constant-pressure preload ····· 140
6.2 Load and displacement of position-preloaded bearings ····· 142
6.3 Average preload for duplex angular contact ball bearings ····· 150
6.4 Axial displacement of deep groove ball bearings ····· 156
6.5 Axial displacement of tapered roller bearings ····· 160

7. Starting and running torques

7.1 Preload and starting torque for angular contact ball bearings ····· 162
7.2 Preload and starting torque for tapered roller bearings ····· 164
7.3 Empirical equations of running torque of high-speed ball bearings ····· 166
7.4 Empirical equations for running torque of tapered roller bearings ····· 168

8. Bearing type and allowable axial load

8.1 Change of contact angle of radial ball bearings and allowable axial load ····· 172
8.1.1 Change of contact angle due to axial load ····· 172
8.1.2 Allowable axial load for a deep groove ball bearing ····· 176
8.2 Allowable axial load (break down strength of the ribs) for a cylindrical roller bearings ····· 178

9. Lubrication

9.1 Lubrication amount for the forced lubrication method ····· 180
9.2 Grease filling amount of spindle bearing for machine tools ····· 182
9.3 Free space and grease filling amount for deep groove ball bearings ····· 184
9.4 Free space of angular contact ball bearings ····· 186
9.5 Free space of cylindrical roller bearings ····· 188
9.6 Free space of tapered roller bearings ····· 190
9.7 Free space of spherical roller bearings ····· 192
9.8 NSK' s dedicated greases ····· 194
9.8.1 NS7 and NSC greases for induction motor bearings ····· 194
9.8.2 ENS and ENR greases for high-temperature/speed ball bearings ····· 196
9.8.3 EA3 and EA6 greases for commutator motor shafts ····· 198
9.8.4 WPH grease for water pump bearings ····· 200

10. Bearing materials

10.1 Comparison of national standards of rolling bearing steel ····· 202
10.2 Long life bearing steel (NSK Z steel) ····· 204
10.3 High temperature bearing materials ····· 206
10.4 Dimensional stability of bearing steel ····· 208
10.5 Characteristics of bearing and shaft/housing materials ····· 210
10.6 Engineering ceramics as bearing material ····· 212
10.7 Physical properties of representative polymers used as bearing material ····· 216
10.8 Characteristics of nylon material for cages ····· 218

Pages

10.9 Heat-resistant resin materials for cages ····· 220
10.10 Features and operating temperature range of ball bearing seal material ····· 222

11. Load calculation of gears

11.1 Calculation of loads on spur, helical, and double-helical gears ····· 224
11.2 Calculation of load acting on straight bevel gears ····· 228
11.3 Calculation of load on spiral bevel gears ····· 230
11.4 Calculation of load acting on hypoid gears ····· 232
11.5 Calculation of load on worm gear ····· 236

12. General miscellaneous information

12.1 JIS concerning rolling bearings ····· 238
12.2 Amount of permanent deformation at point where inner and outer rings contact the rolling element ····· 240
12.2.1 Ball bearings ····· 240
12.2.2 Roller bearings ····· 242
12.3 Rotation and revolution speed of rolling element ····· 246
12.4 Bearing speed and cage slip speed ····· 248
12.5 Centrifugal force of rolling elements ····· 250
12.6 Temperature rise and dimensional change ····· 252
12.7 Bearing volume and apparent specific gravity ····· 254
12.8 Projection amount of cage in tapered roller bearing ····· 256
12.9 Natural frequency of individual bearing rings ····· 258
12.10 Vibration and noise of bearings ····· 260
12.11 Application of FEM to design of bearing system ····· 262

13. NSK Special bearings

13.1 Ultra-precision ball bearings for gyroscopes ····· 266
13.2 Bearings for vacuum use — ball bearings for X-ray tube — ····· 272
13.3 Ball bearing for high vacuum ····· 276
13.4 Light-contact-sealed ball bearings ····· 278
13.5 Bearing with integral shaft ····· 280
13.6 Bearings for electromagnetic clutches in car air-conditioners ····· 282
13.7 Sealed clean bearings for transmissions ····· 286
13.8 Double-row cylindrical roller bearings, NN30 T series (with polyamide resin cage) ····· 288
13.9 Single-row cylindrical roller bearings, N10B T series (cage made of polyamide resin) ····· 290
13.10 Sealed clean bearings for rolling mill roll neck ····· 292
13.11 Bearings for chain conveyors ····· 294
13.12 RCC bearings for railway rolling stock ····· 298

1. ISO Dimensional system and bearing numbers

1.1 ISO Dimensional system

The boundary dimensions of rolling bearings, namely, bore diameter, outside diameter, width, and chamfer dimensions have been standardized so that common dimensions can be adopted on a worldwide scale. In Japan, JIS (Japan Industrial Standard) adheres to the boundary dimensions established by ISO. ISO is a French acronym which is translated into English as the International Organization for Standardization. The ISO dimensional system specifies the following dimensions for rolling bearings: bore diameter, d, outside diameter, D, width, B, (or height, T) and chamfer dimension, r, and provides for the diameter to range from a bore size of 0.6 mm to an outside diameter of 2500 mm. In addition, a method to expand the range is laid out so that the bore diameter, d, (d>500 mm) is taken from the geometrical ratio standard R40.

When expanding the dimensional system, the equation for the outside diameter equals $D=d+f_D d^{0.9}$ and the width equals $B=f_B \cdot (D-d)/2$. Both of these are to be used for radial bearings. Dimensions of the width, B, if possible, should be taken from numerical sequence R80 of preferred numbers in JIS Z 8601. The values of factors f_D and f_B are respectively specified for the diameter series and width series in Table 1. Minimum chamfer dimension, $r_{s\ min}$, should be selected from ISO table and in principle be that value which is nearest to, but not larger than 7% of the bearing width, B, or of the sectional height $(D-d)/2$, whichever is the smaller. Rounding-off of fractions has been specified for the above dimensions.

The outside diameter can be obtained from the factor f_D in Table 1 and bore d. Incidentally, the diameter series symbols 9, 0, 2, 3 are used most often. The thickness between the bore and outside diameters is determined by the diameter series. The outside diameter series increases in the order of 7, 8, 9, 0, 1, 2, 3, and 4 (Fig. 1) while the bore size remains the same size. The diameter series are combined with the factor f_B and classified into a few different width series. The dimension series is composed of combinations of the width series and diameter series.

In the United States, many tapered roller bearings are expressed in the inch system rather than the metric system as specified by ISO. Japan and European countries use the metric system which is in accordance with ISO directives.

The expansion of thrust bearings series (single-direction with flat seats) is laid out in a similar manner as the radial bearings with the boundary dimensions as follows: outside diameter, $D=d+f_D d^{0.8}$, and height, $T=f_T \cdot (D-d)/2$. Minimum chamfer dimension, $r_{s\ min}$, should be selected from ISO table and in principle be that value which is nearest to, but not larger than 7% of the bearing height, T, or $(D-d)/2$, whichever is the smaller. Values for the factors f_D and f_T are as shown in Table 2.

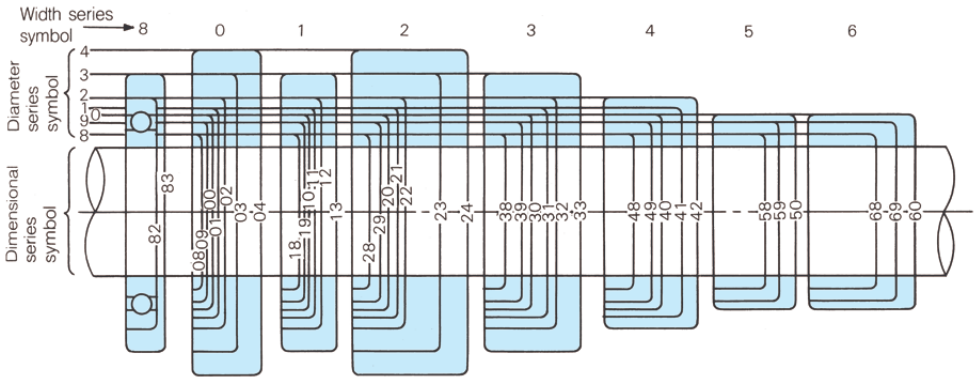

Fig. 1 Cross-sectional profiles of radial bearings by dimensional series

Table 1 f_D and f_B values of radial bearings

Diameter series	7	8	9	0	1	2	3	4
f_D	0.34	0.45	0.62	0.84	1.12	1.48	1.92	2.56

Width series	0	1	2	3	4	5	6	7
f_B	0.64	0.88	1.15	1.5	2.0	2.7	3.6	4.8

Table 2 f_D and f_T values for thrust bearings

Diameter series	0	1	2	3	4	5
f_D	0.36	0.72	1.20	1.84	2.68	3.80

Height series	7	9	1
f_T	0.9	1.2	1.6

1.2 Formulation of bearing numbers

The rolling bearing is an important machine element and its boundary dimensions have been internationally standardized. International standardization of bearing numbers has been examined by ISO but not adopted. Now, manufacturers of various countries are using their own bearing numbers. Japanese manufacturers express the bearing number with 4 or 5 digits by a system which is mainly based on the SKF bearing numbers. The JIS has specified bearing numbers for some of the more commonly used bearings.
A bearing number is composed as follows.

The width series symbol and diameter series symbol are combined and called the dimensional series symbol. For radial bearings, the outside diameter increases with the diameter series symbols 7, 8, 9, 0, 1, 2, 3, and 4. Usually, 9, 0, 2, and 3 are the most frequently used. Width series symbols include 0, 1, 2, 3, 4, 5, and 6 and these are combined with the respective diameter series symbols. Among the width series symbols, 0, 1, 2, and 3 are the most frequently used. Width series symbols become wider in this ordering system to match the respective diameter series symbol.

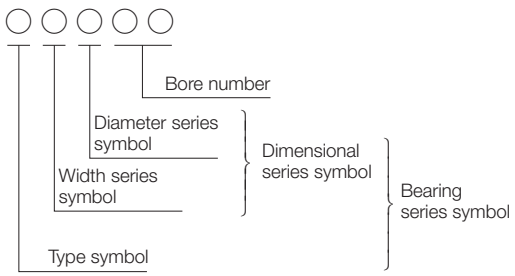

For standard radial ball bearings, the width series symbol is omitted and the bearing number is expressed by 4 digits. Also, it is common practice to omit the width series symbol of the zero for cylindrical roller bearings.

For thrust bearings, there are various combinations between the diameter symbols and height symbols (thrust bearings use the term height symbol rather than width symbol).

The bore diameter symbol is a number which is 1/5 of the bore diameter dimension when bores are 20 mm or greater. For instance, if the bore diameter is 30 mm then the bore diameter symbol is 06. However, when the bore diameter dimension is less than 17 mm, then the bore diameter symbol is by common practice taken from Table 1. Although bearing numbers vary depending on the country, many manufacturers follow this rule when formulating bore symbols.

Numbers and letters are used to form symbols to designate a variety of types and sizes of bearings. For instance, cylindrical roller bearings use letters such as N, NU, NF, NJ and so forth to indicate various roller guide rib positions. The formulation of a bearing number is shown in Table 2.

Table 1

Bore No.	Bore diameter d (mm)
/0.6(1)	0.6
1	1
/1.5(1)	1.5
2	2
/2.5(1)	2.5
3	3
4	4
5	5
6	6
7	7
8	8
9	9
00	10
01	12
02	15
03	17

Notes
(1) NSK 0.6 mm bore bearing is not available. 1X and 2X are used for the NSK bearing number instead of /1.5 and /2.5 respectilely.

Table 2 Formulation of a bearing number

Bearing types		Sample brg	Type No.	Width or height(1) series No.	Dia. Series No.	Bore No.
Radial ball bearing	Single-row deep groove type	629	6	[0] omitted	2	9
		6010	6	[1] omitted	0	10
		6303	6	[0] omitted	3	03
	Single-row angular type	7215A	7	[0] omitted	2	15
	Double-row angular type	3206	3	[3] omitted	2	06
		5312	5	[3] omitted	3	12
	Double-row self-aligning type	1205	1	[0] omitted	2	05
		2211	2	[2] omitted	2	11
Radial roller bearing	Cylindrical roller	NU 1016	NU	1	0	16
		N 220	N	[0] omitted	2	20
		NU 2224	NU	2	2	24
		NN 3016	NN	3	0	16
	Tapered roller	30214	3	0	2	14
	Spherical roller	23034	2	3	0	34
Thrust ball bearing	Single-direction flat seats	51124	5	1	1	24
	Double-direction flat seats	52312	5	2	3	12
	Single-direction self-aligning seats	53318	5	3(2)	3	18
	Double-direction self-aligning seats	54213	5	4(2)	2	13
Thrust roller bearing	Spherical thrust roller	29230	2	9	2	30

Notes (1) Height symbol is used for thrust bearings instead of width.
(2) These express a type symbol rather than a height symbol.

1.3 Bearing numbers for tapered roller bearings (Inch system)

The **ABMA** (The American Bearing Manufacturers Association) standard specifies how to formulate the bearing number for tapered roller bearings in the inch system. The **ABMA** method of specifying bearing numbers is applicable to bearings with new designs. Bearing numbers for tapered roller bearings in the inch system, which have been widely used, will continue to be used and known by the same bearing numbers. Although **TIMKEN** uses **ABMA** bearing numbers to designate new bearing designs, many of its bearing numbers do not conform to **ABMA** rules.

A bearing number is composed as follows.

Load limit symbol	Contact angle number	Series number	Auxiliary number	Auxiliary symbol
AA	○	○○○	○○	AA

"A" indicates an alphabetical character.
"○" indicates a numerical digit.

Tapered roller bearings (Inch system)

The outer ring of a tapered roller bearing is called a "CUP" and the inner ring is a "CONE". A CONE ASSEMBLY consists of tapered rollers, cage and inner ring, though sometimes it is called a "CONE" instead of "CONE ASSEMBLY". Therefore, an inch-system tapered roller bearing consists of one CUP and one CONE (exactly speaking, one CONE ASSEMBLY). Each part is sold separately. Therefore, to obtain a complete set both parts must be ordered.

In the example of page 11, LM11949 is only a CONE. A complete inch-system tapered roller bearing is called a CONE/CUP and is specified by LM11949/LM11910 for this example.

LM 1 19 49

Load limit symbol
Terms such as light load, medium load, and heavy load and so forth are used for metric series bearings. The following symbols are used as load limiting symbols and are arranged from lighter to heavier: EL, LL, L, LM, M, HM, H, HH, EH, J, T
However, the last symbol "T" is reserved for thrust bearings only.

Contact angle number
The number expressing the contact angle is composed as follows.

Cup angle (contact angle × 2)	Number
0° to Less than 24°	1
24° to Less than 25°30'	2
25°30' to Less than 27°	3
27° to Less than 28°30'	4
28°30' to Less than 30°30'	5
30°30' to Less than 32°30'	6
32°30' to Less than 36°	7
36° to Less than 45°	8
Higher than 45° (Other than thrust bearings)	9

Auxiliary symbol
The auxiliary symbol is a suffix composed of 1 or 2 letters and used when the appearance or internal features are modified.
B Outer ring with flange
X Standard type, modified slightly
WA Inner ring with a slot at the back
Others Omitted

Auxiliary number
Excluding the auxiliary symbols, the last and second to last numbers are auxiliary numbers which are peculiar to the inner or outer ring of that bearing.
The numbers, 10 to 19, are used for outer rings with 10 used to label the bearing with the minimum outside diameter.
The numbers, 30 to 49, are used for inner rings with 49 used to label the inner ring with the largest bore diameter.

Series number
A series number is expressed by one, two, or three digits. The relationship with the largest bore diameter of that series is as follows.

Maximum bore diameter in series (mm (inch))		Series number
over	inch	
0	25.4 (1)	00 to 19
25.4 (1)	50.8 (2)	20 to 99
		000 to 029
50.8 (2)	76.2 (3)	039 to 129
……(omitted)……		

1.4 Bearing numbers for miniature ball bearings

Ball bearings with outside diameters below 9 mm (or below 9.525 mm for bearings in the inch design) are called miniature ball bearings and are mainly used in VCRs, computer peripherals, various instruments, gyros, micro-motors, etc. Ball bearings with outside diameters greater than or equal to 9 mm (greater than or equal to 9.525 mm for inch design bearings) and bore diameters less than 10 mm are called extra-small ball bearings.

As in general bearings, special capabilities of miniature ball bearings are expressed by descriptive symbols added after the basic bearing number. However, one distinction of miniature and extra-small ball bearings is that a clearance indicating symbol is always included and a torque symbol is often included even if the frictional torque is quite small.

NSK has established a clearance system for miniature and extra-small ball bearings with 6 gradations of clearance so that NSK can satisfy the clearance demands of its customers. The MC3 clearance is the normal clearance suitable for general bearings.

As far as miniature and extra-small ball bearings are concerned, the ISO standards are applied to bearings in the metric design bearings and **ABMA** standards are applied to inch design bearings.

Miniature ball bearings are often required to have low frictional torque when used in machines. Therefore, torque standards have been established for low frictional torque. Torque symbols are used to indicate the classification of miniature bearings within the frictional standards.

The cage, seal, and shield symbols for miniature ball bearings are the same as those used for general bearings. The material symbol indicating stainless steel is an "S" and is added before the basic bearing number in both inch and metric designs for bearings of special dimensions. However, for metric stainless steel bearings of standard dimensions, an "h" is added after the basic bearing number. The figure below shows the arrangement and meaning and so forth of bearing symbols for miniature and extra-small ball bearings.

Table 1 Formulation of bearing numbers for miniature ball bearings.

Symbol	Contents
ZZS	Shield
ZZ	Shield

Symbol	Contents
J	Pressed-cage
W	Crown type cage
T	Non-metallic cage

Symbol	Contents
Omitted	Bearing steel (SUJ2)
h	Stainless steel (SUS440C)
S	Stainless steel (SUS440C)

Symbol	Radial clearance (μm)
MC1	0 ~ 5
MC2	3 ~ 8
MC3	5 ~ 10
MC4	8 ~ 13
MC5	13 ~ 20
MC6	20 ~ 28

ANSI/ABMA Std.		ISO Std.	
Symbol	Accuracy class	Symbol	Accuracy class
Omitted	ABEC1	Omitted	Class 0
3	ABEC3	P6	Class 6
5P	CLASS5P	P5	Class 5
7P	CLASS7P	P4	Class 4

Symbol	Contents
AF2	Aero-Shell Fluid 12
NS7	NS Hilube grease

Classification	Material symbol
Inch design bearings	S
Special metric design bearings	—
Standard metric design bearings	—
	—

Basic bearing number	Material symbol	Cage symbol	Seal/shield symbol	Clearance symbol	Accuracy symbol	Torque symbol	Lubricatdon symbol
FR133	—	J	ZZS	MC4	7P	L	AF2
MR74	—	W	ZZS	MC3	P5	—	NS7
692	h	J	ZZ	MC3	P5	—	NS7
602	—	J	ZZS	MC4	—	—	NS7

1.5 Auxiliary bearing symbols

Rolling bearings are provided with various capabilities to meet a variety of application demands and methods of use. These special capabilities are classified and indicated by auxiliary symbols attached after the basic bearing number. The entire system of basic and auxiliary symbols should be completely unified but this level of standardization has not been achieved.

Currently, manufacturers use a combination of their own symbols and specified symbols. The internal clearance symbols and accuracy symbols are two sets of symbols which are widely used and specified by JIS. The auxiliary symbols employed by NSK are listed in alphabetical order as follows.

Symbol	Contents	Example
A	Internal design differs from standard design	6307A HR32936JA
A(1)	Angular contact ball bearing with standard contact angle of α =30°	7215A
AH	Removable sleeve type symbol	AH3132
A5(1)	Angular contact ball bearing with standard contact angle of α =25°	7913A5
B	Cylindrical roller bearing: the allowance of roller inscribed circle diameter or circumscribed circle diameter does not comply with JIS standards	NU306B
	Inch series tapered roller bearing with flanged cup	779/772B
B(1)	Angular contact ball bearing with standard contact angle of α =40°	7310B
C(1)	Angular contact ball bearing with standard contact angle of α =15°	7205C
	Tapered roller bearing with contact angle of about 20°	HR32205C
CA	Spherical roller bearing with high load capacity (machined cage)	22324CA
CD	Spherical roller bearing with high load capacity (pressed cage)	22228CD
C1 C2 C3 C4 C5	C1 clearance (smaller than C2) C2 clearance (smaller than normal clearance) C3 clearance (larger than normal clearance) C4 clearance (larger than C3) C5 clearance (larger than C4)	6218C3
CC CC1 CC2 CC3 CC4 CC5	Normal matched clearance of cylindrical roller bearing C1 matched clearance of cylindrical roller bearing C2 matched clearance of cylindrical roller bearing C3 matched clearance of cylindrical roller bearing C4 matched clearance of cylindrical roller bearing C5 matched clearance of cylindrical roller bearing	N238CC2
CC9	Matched clearance of cylindrical roller bearing with tapered bore (smaller than CC1)	NN3017KCC9
CG15	Special radial clearance (indicates median clearance)	6022CG15
CM	Special clearances for general motors of single-row deep groove ball bearing and cylindrical roller bearing (matched)	NU312CM

Note (1) Part of the basic bearing number

Symbol	Contents	Example
D(1)	Tapered roller bearing with contact angle of about 28°	HR30305D
DU	A contact rubber seal on one side	6306DU
DDU	Contact rubber seals on both sides	6205DDU
DB	2-row combination (back-to-back combination)	7208ADB
DBB	4-row combination	7318ADBB
DBD	3-row combination	7318ADBD
DBT	4-row combination	7318ADBT
DBTD	5-row combination	7318ADBTD
DF	2-row combination (front-to-front combination)	7320ADF
DFD	3-row combination	7320ADFD
DFF	4-row combination	7320ADFF
DFT	4-row combination	7320ADFT
DT	2-row combination (tandem combination)	7320ADT
DTD	3-row combination	7320ADTD
DTT	4-row combination	7320ADTT

Symbol	Contents	Example
E	Bearing with notch or oil port	6214E
	High load capacity type cylindrical roller bearing	NU309ET
E4	Cylindrical roller bearing for sheave and spherical roller bearing with oil groove and oil holes in the outer ring	230/560 ME4
F	Steel machined cage	230/570F
g	Case hardened steel (SAE4320H, etc)	456g/454g
h	Stainless steel bearing rings and rolling elements	6203h
H	Adapter type symbol	H318X
	Radial and thrust spherical roller bearings of high load capacity	22210H 29418H
HJ	L-type loose collar type symbol	HJ210
HR (2)	High load capacity type tapered roller bearing	HR30308J
J	Tapered roller bearing with the outer ring raceway small end diameter and angle in conformity with ISO standards	HR30308J
	Pressed steel cage, 2 pieces	R6JZZ
K	Tapered inner ring bore (taper: 1:12)	1210K
	With outer ring spacer	30310DF+K
K30	Tapered inner ring bore (taper: 1:30)	24024CK30
KL	With inner and outer ring spacers (Figure just after KL is spacer width)	7310ADB+KL10
L	With inner ring spacer	30310DB+L
M	Copper alloy machined cage	6219M
MC3	Small size and miniature ball bearings of standard clearance	683MC3
N	With locating snap ring groove in outer ring	6310N
NR	Bearing with locating snap ring	6209NR
NRX	Locating snap ring of special dimension	6209NRX
NRZ	Pressed-steel shield on one side and locating snap ring on the same side (c.f. ZNR)	6207NRZ
PN0	Accuracy class of inch design tapered roller bearings, equivalent to Class 0	575/572PN0
PN3	Accuracy class of inch design tapered roller bearings, equivalent to Class 3	779/772BPN3

Note (2) HR is added before bearing type symbol.

Symbol	Contents		Example
S11	Heat stabilized for operation up to 200℃		22230CAMKE4 C3S11
T	Synthetic resin cage		7204CT
V	No cage		NA4905V
	A non-contact rubber seal on one side		6204V
VV	Non-contact rubber seals on both sides		6306VV
W	One-piece pressed-steel cage		NU210W
	Inch design tapered roller bearing with notch at bearing ring		456W/454
X	Bore or outside diameter or width modified less than 1 mm		6310X
	Shaft washer's outside diameter is smaller than housing washer's outside diameter		51130X
X26	Bearings with enhanced dimensional stability	Bearing operating temperature below 150℃	23032CD C3X26
X28		Operating temperature below 200℃	23032CD C4X28
X29		Operating temperature below 250℃	23032CD C4X29
Y	Pressed-brass cage		608Y
Z	A pressed-steel shield on one side		6203Z
ZN	A pressed-steel shield on one side and a locating-snap-ring groove on the other side		6208ZN
ZNR	A pressed-steel shield on one side and a locating-snap-ring on the other side (c.f. NRZ)		6208ZNR
ZZ	Pressed-steel shields on both sides		6208ZZ

2. Dynamic load rating, fatigue life, and static load rating

2.1 Dynamic load rating

The basic dynamic load rating of rolling bearings is defined as the constant load applied on bearings with stationary outer rings that the inner rings can endure for a rating life (90% life) of one million revolutions. The basic load rating of radial bearings is defined as a central radial load of constant direction and magnitude, while the basic load rating of thrust bearings is defined as an axial load of constant magnitude in the same direction as the central axis.

This basic dynamic load rating is calculated by an equation shown in Table 1. The equation is based on the theory of G. Lundberg & A. Palmgren, and was adopted in ISO R281 : 1962 in 1962 and in JIS B 1518 : 1965 in Japan in March, 1965. Later on, these standards were established respectively as ISO 281 : 1990 and JIS B 1518 (under revision) after some modification.

The fatigue life of a bearing is calculated as follows:

$$L=\left(\frac{C}{P}\right)^{3} \text{ for a ball bearing} \quad \cdots\cdots (1)$$

$$L=\left(\frac{C}{P}\right)^{10/3} \text{ for a roller bearing} \quad \cdots\cdots (2)$$

where, L: Rating fatigue life (10^6 rev)
P: Dynamic equivalent load (N), {kgf}
C: Basic dynamic load rating (N), {kgf}

The factor f_c used in the calculation of Table 1 has a different value depending on the bearing type, as shown in Tables 2 and 3. The value f_c of a radial ball bearing is the same as specified in JIS B 1518 : 1965, while that of a radial roller bearing was revised to be the maximum possible value. In this way, the factor f_c determined from the processing accuracy and material has been at about the same level for the past 20 years.

During this period, however, bearings have undergone substantial improvement in terms of not only material, but also processing accuracy. As a result, the practical bearing life is extended considerably. It would be easier to use the above equations for calculations with improved bearings because the dynamic load rating already reflects the life extension factor. This concept of ISO 281 : 1990 and JIS B 1518 (under revision) has led to the increase of the basic dynamic load rating by multiplying by the rating factor b_m. The value of the rating factor b_m is as shown in Table 4.

Table 1 Calculation equation of basic dynamic load rating

Classification		Ball bearing	Roller bearing
Radial bearing		$b_m f_c (i \cos\alpha)^{0.7} Z^{2/3} D_w^{1.8}$	$b_m f_c (i L_{we} \cos\alpha)^{7/9} Z^{3/4} D_{we}^{29/27}$
Single-row thrust bearing	$\alpha=90°$	$b_m f_c Z^{2/3} D_w^{1.8}$	$b_m f_c L_{we}^{7/9} Z^{3/4} D_{we}^{29/27}$
	$\alpha\neq 90°$	$b_m f_c (\cos\alpha)^{0.7} \tan\alpha\, Z^{2/3} D_w^{1.8}$	$b_m f_c (L_{we} \cos\alpha)^{7/9} \tan\alpha\, Z^{3/4} D_{we}^{29/27}$
Quantity symbols in equations		b_m: Rating factor depending on normal material and manufacture quality f_c: Coefficient determined from shape, processing accuracy, and material of bearing parts i: Number of rows of rolling elements in one bearing α: Nominal contact angle (°) Z: Number of rolling elements per row D_w: Diameter of ball (mm) D_{we}: Diameter of roller used in calculation (1) (mm) L_{we}: Effective length of roller (mm)	

Note (1) Diameter at the middle of the roller length
Tapered roller: Arithmetic average value of roller large and small end diameters assuming the roller without chamfers
Convex roller (asymmetric): Approximate value of roller diameter at the contact point of the roller and ribless raceway (generally outer ring raceway) without applying load

Remarks When D_w>25.4 mm, $D_w^{1.8}$ becomes 3.647 $D_w^{1.4}$

Table 2 f_c value of radial ball bearings

$\frac{D_w \cos\alpha}{D_{pw}}$ (1)	f_c		
	Single-row deep groove ball bearing, single/double row angular contact ball bearing	Double-row deep groove ball bearing	Self-aligning ball bearing
0.05	46.7 {4.76}	44.2 {4.51}	17.3 {1.76}
0.06	49.1 {5.00}	46.5 {4.74}	18.6 {1.90}
0.07	51.1 {5.21}	48.4 {4.94}	19.9 {2.03}
0.08	52.8 {5.39}	50.0 {5.10}	21.1 {2.15}
0.09	54.3 {5.54}	51.4 {5.24}	22.3 {2.27}
0.10	55.5 {5.66}	52.6 {5.37}	23.4 {2.39}
0.12	57.5 {5.86}	54.5 {5.55}	25.6 {2.61}
0.14	58.8 {6.00}	55.7 {5.68}	27.7 {2.82}
0.16	59.6 {6.08}	56.5 {5.76}	29.7 {3.03}
0.18	59.9 {6.11}	56.8 {5.79}	31.7 {3.23}
0.20	59.9 {6.11}	56.8 {5.79}	33.5 {3.42}
0.22	59.6 {6.08}	56.5 {5.76}	35.2 {3.59}
0.24	59.0 {6.02}	55.9 {5.70}	36.8 {3.75}
0.26	58.2 {5.93}	55.1 {5.62}	38.2 {3.90}
0.28	57.1 {5.83}	54.1 {5.52}	39.4 {4.02}
0.30	56.0 {5.70}	53.0 {5.40}	40.3 {4.11}
0.32	54.6 {5.57}	51.8 {5.28}	40.9 {4.17}
0.34	53.2 {5.42}	50.4 {5.14}	41.2 {4.20}
0.36	51.7 {5.27}	48.9 {4.99}	41.3 {4.21}
0.38	50.0 {5.10}	47.4 {4.84}	41.0 {4.18}

Note (1) D_{pw} is the pitch diameter of balls.
Remarks Figures in { } for kgf unit calculation

Table 3 f_c value of radial roller bearings

$\frac{D_{we}\cos\alpha}{D_{pw}}$ (2)	f_c
0.01	52.1 {5.32}
0.02	60.8 {6.20}
0.03	66.5 {6.78}
0.04	70.7 {7.21}
0.05	74.1 {7.56}
0.06	76.9 {7.84}
0.07	79.2 {8.08}
0.08	81.2 {8.28}
0.09	82.8 {8.45}
0.10	84.2 {8.59}
0.12	86.4 {8.81}
0.14	87.7 {8.95}
0.16	88.5 {9.03}
0.18	88.8 {9.06}
0.20	88.7 {9.05}
0.22	77.2 {9.00}
0.24	87.5 {8.92}
0.26	86.4 {8.81}
0.28	85.2 {8.69}
0.30	83.8 {8.54}

Note (2) D_{pw} is the pitch diameter of rollers.
Remarks 1. The f_c value in the above table applies to a bearing in which the stress distribution in the length direction of roller is nearly uniform.
2. Figures in { } for kgf unit calculation

Table 4 Value of rating factor b_m

Bearing type		b_m
Radial Bearings	Deep groove ball bearing	1.3
	Magneto bearing	1.3
	Angular contact ball bearing	1.3
	Ball bearing for rolling bearing unit	1.3
	Self-aligning ball bearing	1.3
	Spherical roller bearing	1.15
	Filling slot ball bearing	1.1
	Cylindrical roller bearing	1.1
	Tapered roller bearing	1.1
	Solid needle roller bearing	1.1
Thrust Bearings	Thrust ball bearing	1.3
	Thrust spherical roller bearing	1.15
	Thrust tapered roller bearing	1.1
	Thrust cylindrical roller bearing	1
	Thrust needle roller bearing	1

2.2 Dynamic equivalent load

In some cases, the loads applied on bearings are purely radial or axial loads; however, in most cases, the loads are a combination of both. In addition, such loads usually fluctuate in both magnitude and direction.

In such cases, the loads actually applied on bearings cannot be used for bearing life calculations; therefore, a hypothetical load should be estimated that has a constant magnitude and passes through the center of the bearing, and will give the same bearing life that the bearing would attain under actual conditions of load and rotation. Such a hypothetical load is called the equivalent load.

Assuming the equivalent radial load as P_r, the radial load as F_r, the axial load as F_a, and the contact angle as α, the relationship between the equivalent radial load and bearing load can be approximated as follows:

$$P_r = XF_r + YF_a \quad \cdots\cdots (1)$$

where, X: Radial load factor, Y: Axial load factor } See Table 1

The axial load factor varies depending on the contact angle. Though the contact angle remains the same regardless of the magnitude of the axial load in the cases of roller bearings, such as single-row deep groove ball bearings and angular contact ball bearings experience an increase in contact angle when the axial load is increased. Such change in the contact angle can be expressed by the ratio of the basic static load rating C_{0r} and axial load F_a. Table 1, therefore, shows the axial load factor at the contact angle corresponding to this ratio. Regarding angular contact ball bearings, the effect of change in the contact angle on the load factor may be ignored under normal conditions even if the contact angle is as large as 25°, 30° or 40°.

For the thrust bearing with the contact angle of α=90° receiving both radial and axial loads simultaneously, the equivalent axial load P_a becomes as follows:

$$P_a = XF_r + YF_a \quad \cdots\cdots (2)$$

Bearing type		$\frac{C_{0r}}{F_a}$
Single-row deep groove ball bearings		5
		10
		15
		20
		25
		30
		50
Angular contact ball bearings	15°	5
		10
		15
		20
		25
		30
		50
	25°	—
	30°	—
	40°	—
Self-aligning ball bearings		—
Magnet ball bearings		—
Tapered roller bearings Spherical roller bearings		—
Thrust ball bearings	45°	—
	60°	—
Thrust roller bearings		—

Table 1 Value of factors X and Y

Single-row bearing				Double-row bearing				e
$F_a/F_r \leqq e$		$F_a/F_r > e$		$F_a/F_r \leqq e$		$F_a/F_r > e$		
X	Y	X	Y	X	Y	X	Y	
			1.26					0.35
			1.49					0.29
			1.64					0.27
1	0	0.56	1.76	—	—	—	—	0.25
			1.85					0.24
			1.92					0.23
			2.13					0.20
			1.10		1.23		1.79	0.51
			1.21		1.36		1.97	0.47
			1.28		1.43		2.08	0.44
1	0	0.44	1.32	1	1.48	0.72	2.14	0.42
			1.36		1.52		2.21	0.41
			1.38		1.55		2.24	0.40
			1.44		1.61		2.34	0.39
1	0	0.41	0.87	1	0.92	0.67	1.41	0.68
1	0	0.39	0.76	1	0.78	0.63	1.24	0.80
1	0	0.35	0.57	1	0.55	0.57	0.93	1.14
—	—	—	—	1	$0.42\cot\alpha$	0.65	$0.65\cot\alpha$	$1.5\tan\alpha$
1	0	0.5	2.5	—	—	—	—	0.2
1	0	0.4	$0.4\cot\alpha$	1	$0.45\cot\alpha$	0.67	$0.67\cot\alpha$	$1.5\tan\alpha$
—	—	0.66	1	1.18	0.59	0.66	1	1.25
—	—	0.92	1	1.90	0.55	0.92	1	2.17
—	—	$\tan\alpha$	1	$1.5\tan\alpha$	0.67	$\tan\alpha$	1	$1.5\tan\alpha$

Remarks 1. Two similar single-row angular contact ball bearings are used.
(1) DF or DB combination: Apply X and Y of double-row bearing. However, if obtain the axial load ratio of C_{0r}/F_a, C_{0r} should be half of C_{0r} for the bearing set.
(2) DT combination: Apply X and Y of single-row bearing. C_{0r} should be half of C_{0r} for the bearing set.
2. This table differs from JIS and ISO standards in the method of determining the axial load ratio C_{0r}/F_a.

2.3 Dynamic equivalent load of triplex angular contact ball bearings

Three separate single-row bearings may be used side by side as shown in the figure when angular contact ball bearings are to be used to carry a large axial load. There are three patterns of combination, which are expressed by combination symbols of DBD, DFD, and DTD.

As in the case of single-row and double-row bearings, the dynamic equivalent load, which is determined from the radial and axial loads acting on a bearing, is used to calculate the fatigue life for these combined bearings.

Assuming the dynamic equivalent radial load as P_r, the radial load as F_r, and axial load as F_a, the relationship between the dynamic equivalent radial load and bearing load may be approximated as follows:

$$P_r = XF_r + YF_a \quad \cdots\cdots (1)$$

where, X: Radial load factor, Y: Axial load factor } See Table 1

The axial load factor varies with the contact angle. In an angular contact ball bearing, whose contact angle is small, the contact angle varies substantially when the axial load increases.

A change in the contact angle can be expressed by the ratio between the basic static load rating C_{0r} and axial load F_a. Accordingly, for the angular contact ball bearing with a contact angle of 15°, the axial load factor at a contact angle corresponding to this ratio is shown. If the angular contact ball bearings have contact angles of 25°, 30° and 40°, the effect of change in the contact angle on the axial load factor may be ignored and thus the axial load factor is assumed as constant.

Arrangement	Load direction
3 row matched stack, axial load is supported by 2 rows. (Symbol DBD or DFD)	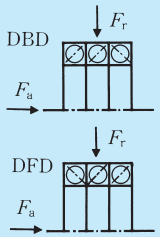
3 row matched stack, axial load is supported by 1 row. (Symbol DBD or DFD)	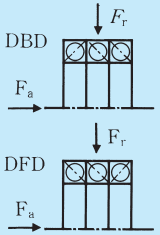
3 row tandem matched stack (Symbol DTD)	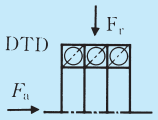

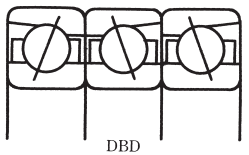

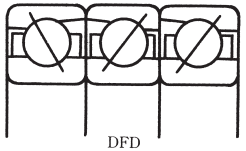

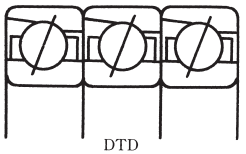

Table 1 Factors X and Y of triplex angular contact ball bearing

Contact angle α	j	$\frac{C_{0r}}{jF_a}$	$\frac{F_a}{F_r} \leqq e$		$\frac{F_a}{F_r} > e$		e	Basic load rating of 3 row ball bearings	
			X	Y	X	Y		C_r	C_{0r}
15°	1.5	5	1	0.64	0.58	1.46	0.51	2.16 times of single bearing	3 times of single bearing
		10		0.70		1.61	0.47		
		15		0.74		1.70	0.44		
		20		0.76		1.75	0.42		
		25		0.78		1.81	0.41		
		30		0.80		1.83	0.40		
		50		0.83		1.91	0.39		
25°	—	—	1	0.48	0.54	1.16	0.68		
30°	—	—	1	0.41	0.52	1.01	0.80		
40°	—	—	1	0.29	0.46	0.76	1.14		
15°	3	5	1	2.28	0.95	2.37	0.51	2.16 times of single bearing	3 times of single bearing
		10		2.51		2.61	0.47		
		15		2.64		2.76	0.44		
		20		2.73		2.85	0.42		
		25		2.80		2.93	0.41		
		30		2.85		2.98	0.40		
		50		2.98		3.11	0.39		
25°	—	—	1	1.70	0.88	1.88	0.68		
30°	—	—	1	1.45	0.84	1.64	0.80		
40°	—	—	1	1.02	0.76	1.23	1.14		
15°	1	5	1	0	0.44	1.10	0.51	2.16 times of single bearing	3 times of single bearing
		10				1.21	0.47		
		15				1.28	0.44		
		20				1.32	0.42		
		25				1.36	0.41		
		30				1.38	0.40		
		50				1.44	0.39		
25°	—	—	1	0	0.41	0.87	0.68		
30°	—	—	1	0	0.39	0.76	0.80		
40°	—	—	1	0	0.35	0.57	1.14		

2.4 Average of fluctuating load and speed

When the load applied on a bearing fluctuates, an average load which will yield the same bearing life as the fluctuating load should be calculated.

(1) When the relation between load and rotating speed can be partitioned into groups of rectangles (Fig. 1),

Load F_1; Speed n_1; Operating time t_1
Load F_2; Speed n_2; Operating time t_2
⋮
Load F_n; Speed n_n; Operating time t_n

then the average load F_m may be calculated using the following equation:

$$F_m = \sqrt[p]{\frac{F_1^p n_1 t_1 + F_2^p n_2 t_2 + \cdots + F_n^p n_n t_n}{n_1 t_1 + n_2 t_2 + \cdots\cdots + n_n t_n}} \quad \cdots\cdots (1)$$

where, F_m: Average of fluctuating load (N), {kgf}
p=3 for ball bearings
p=10/3 for roller bearings

The average speed n_m may be calculated as follows:

$$n_m = \frac{n_1 t_1 + n_2 t_2 + \cdots\cdots + n_n t_n}{t_1 + t_2 + \cdots\cdots + t_n} \quad \cdots\cdots (2)$$

(2) When the load fluctuates almost linearly (Fig. 2), the average load may be calculated as follows:

$$F_m \fallingdotseq \frac{1}{3}(F_{min} + 2F_{max}) \quad \cdots\cdots (3)$$

where, F_{min}: Minimum value of fluctuating load (N), {kgf}
F_{max}: Maximum value of fluctuating load (N), {kgf}

(3) When the load fluctuation is similar to a sine wave (Fig. 3), an approximate value for the average load F_m may be calculated from the following equation:

In the case of Fig. 3 (a)
$F_m \fallingdotseq 0.65\ F_{max}$ ..... (4)
In the case of Fig. 3 (b)
$F_m \fallingdotseq 0.75\ F_{max}$ ..... (5)

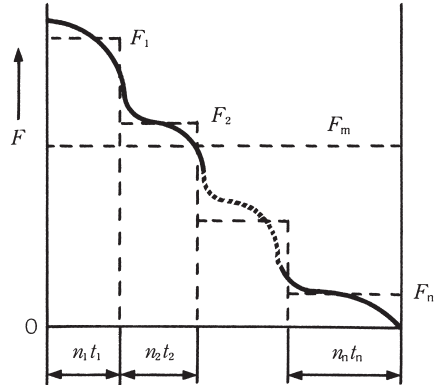

Fig. 1 Incremental load variation

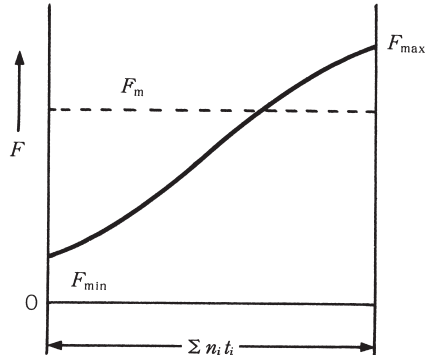

Fig. 2 Simple load fluctuation

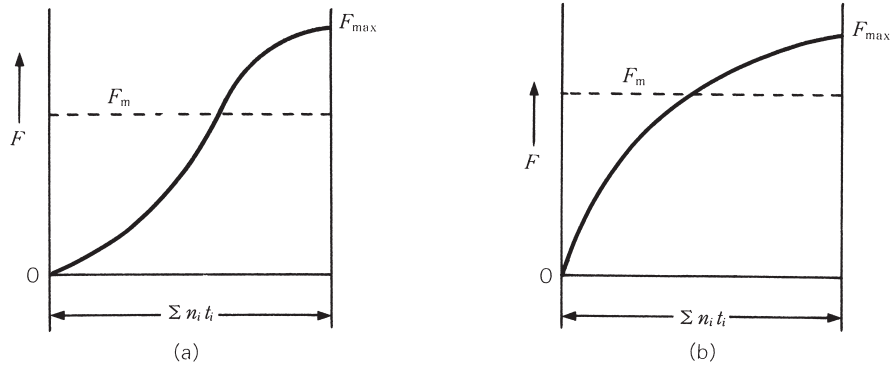

Fig. 3 Sinusoidal load variation

2.5 Combination of rotating and stationary loads

Generally, rotating, static, and indeterminate loads act on a rolling bearing. In certain cases, both the rotating load, which is caused by an unbalanced or a vibration weight, and the stationary load, which is caused by gravity or power transmission, may act simultaneously. The combined mean effective load when the indeterminate load caused by rotating and static loads can be calculated as follows. There are two kinds of combined loads; rotating and stationary which are classified depending on the magnitude of these loads, as shown in Fig. 1.

Namely, the combined load becomes a running load with its magnitude changing as shown in Fig. 1 (a) if the rotating load is larger than the static load. The combined load becomes an oscillating load with a magnitude changing as shown in Fig. 1 (b) if the rotating load is smaller than the stationary load.

In either case, the combined load F is expressed by the following equation:

$$F=\sqrt{F_R^2+F_S^2-2F_RF_S\cos\theta} \quad \cdots\cdots (1)$$

where, F_R: Rotating load (N), {kgf}
F_S: Stationary load (N), {kgf}
θ: Angle defined by rotating and stationary loads

The value F can be approximated by Load Equations (2.1) and (2.2) which vary sinusoidally depending on the magnitude of F_R and F_S, that is, in such a manner that F_R+F_S becomes the maximum load F_{max} and F_R-F_S becomes the minimum load F_{min} for $F_R \gg F_S$ or $F_R \ll F_S$.

$$F_R \gg F_S,\ F=F_R-F_S\cos\theta \quad \cdots\cdots (2.1)$$
$$F_R \ll F_S,\ F=F_S-F_R\cos\theta \quad \cdots\cdots (2.2)$$

The value F can also be approximated by Equations (3.1) and (3.2) when $F_R \fallingdotseq F_S$.

$F_R>F_S$,

$$F=F_R-F_S+2F_S\sin\frac{\theta}{2} \quad \cdots\cdots (3.1)$$

$F_R>F_S$,

$$F=F_S-F_R+2F_R\sin\frac{\theta}{2} \quad \cdots\cdots (3.2)$$

Curves of Equations (1), (2.1), (3.1), and (3.2) are as shown in Fig. 2.

The mean value F_m of the load varying as expressed by Equations (2.1) and (2.2) or (3.1) and (3.2) can be expressed respectively by Equations (4.1) and (4.2) or (5.1) and (5.2).

$F_m=F_{min}+0.65\,(F_{max}-F_{min})$

$$F_R \geqq F_S,\ F_m=F_R+0.3F_S \quad \cdots\cdots (4.1)$$
$$F_R \leqq F_S,\ F_m=F_S+0.3F_R \quad \cdots\cdots (4.2)$$

$F_m=F_{min}+0.75\,(F_{max}-F_{min})$

$$F_R \geqq F_S,\ F_m=F_R+0.5F_S \quad \cdots\cdots (5.1)$$
$$F_R \leqq F_S,\ F_m=F_S+0.5F_R \quad \cdots\cdots (5.2)$$

Generally, as the value F exists somewhere among Equations (4.1), (4.2), (5.1), and (5.2), the factor 0.3 or 0.5 of the second terms of Equations (4.1) and (4.2) as well as (5.1) and (5.2) is assumed to change linearly along with F_S/F_R or F_R/F_S. Then, these factors may be expressed as follows:

$$0.3+0.2\frac{F_S}{F_R},\ 0 \leqq \frac{F_S}{F_R} \leqq 1$$

or $$0.3+0.2\frac{F_R}{F_S},\ 0 \leqq \frac{F_R}{F_S} \leqq 1$$

Accordingly, F_m can be expressed by the following equation:

$F_R \geqq F_S$,

$$F_m=F_R+\left(0.3+0.2\frac{F_S}{F_R}\right)F_S$$
$$=F_R+0.3F_S+0.2\frac{F_S^2}{F_R} \quad \cdots\cdots (6.1)$$

$F_R \geqq F_S$,

$$F_m=F_S+\left(0.3+0.2\frac{F_R}{F_S}\right)F_R$$
$$=F_S+0.3F_R+0.2\frac{F_R^2}{F_S} \quad \cdots\cdots (6.2)$$

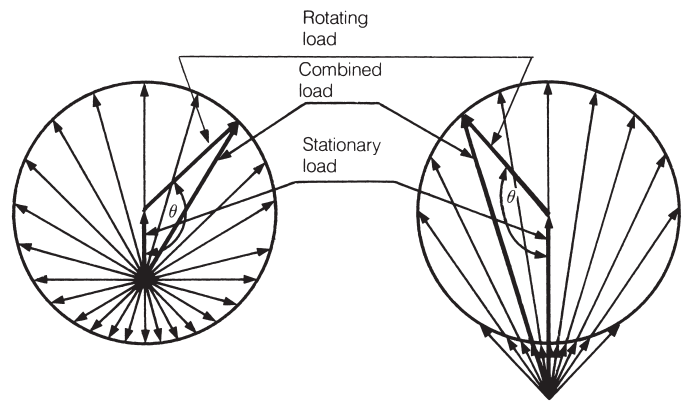

(a) Rotating load > stationary load (b) Rotating load < stationary load

Fig. 1 Combined load of rotating and stationary loads

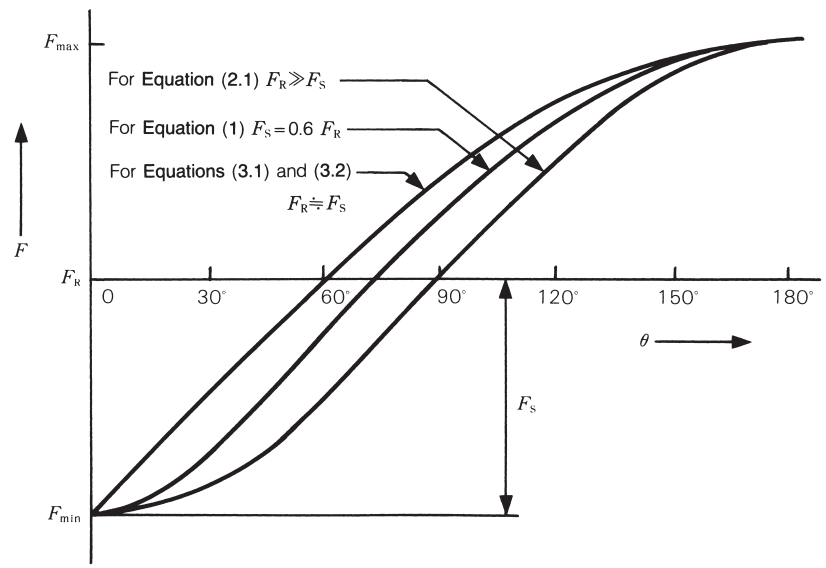

Fig. 2 Chart of combined loads

2.6 Life calculation of multiple bearings as a group

When multiple rolling bearings are used in one machine, the fatigue life of individual bearings can be determined if the load acting on individual bearings is known. Generally, however, the machine becomes inoperative if a bearing in any part fails. It may therefore be necessary in certain cases to know the fatigue life of a group of bearings used in one machine.

The fatigue life of the bearings varies greatly and our fatigue life calculation equation

$L=\left(\frac{C}{P}\right)^{p}$ applies to the 90% life (also called the rating fatigue life, which is either the gross number of revolution or hours to which 90% of multiple similar bearings operated under similar conditions can reach).

In other words, the calculated fatigue life for one bearing has a probability of 90%. Since the endurance probability of a group of multiple bearings for a certain period is a product of the endurance probability of individual bearings for the same period, the rating fatigue life of a group of multiple bearings is not determined solely from the shortest rating fatigue life among the individual bearings. In fact, the group life is much shorter than the life of the bearing with the shortest fatigue life.

Assuming the rating fatigue life of individual bearings as L_1, L_2, L_3 ... and the rating fatigue life of the entire group of bearings as L, the below equation is obtained:

$$\frac{1}{L^e}=\frac{1}{L_1^e}+\frac{1}{L_2^e}+\frac{1}{L_3^e}+\cdots\cdots \quad (1)$$

where, e=1.1 (both for ball and roller bearings)

L of Equation (1) can be determined with ease by using Fig. 1.

Take the value L_1 of Equation (1) on the L_1 scale and the value of L_2 on the L_2 scale, connect them with a straight line, and read the intersection with the L scale. In this way, the value L_A of

$$\frac{1}{L_A^e}=\frac{1}{L_1^e}+\frac{1}{L_2^e}$$

is determined. Take this value L_A on the L_1 scale and the value L_3 on the L_2 scale, connect them with a straight line, and read an intersection with the L scale.
In this way, the value L of

$$\frac{1}{L^e}=\frac{1}{L_1^e}+\frac{1}{L_2^e}+\frac{1}{L_3^e}$$

can be determined.

Example

Assume that the calculated fatigue life of bearings of automotive front wheels as follows:

280 000 km for inner bearing

320 000 km for outer bearing

Then, the fatigue life of bearings of the wheel can be determined at 160 000 km from Fig. 1. If the fatigue life of the bearing of the right-hand wheel takes this value, the fatigue life of the left-hand wheel will be the same. As a result, the fatigue life of the front wheels as a group will become 85 000 km.

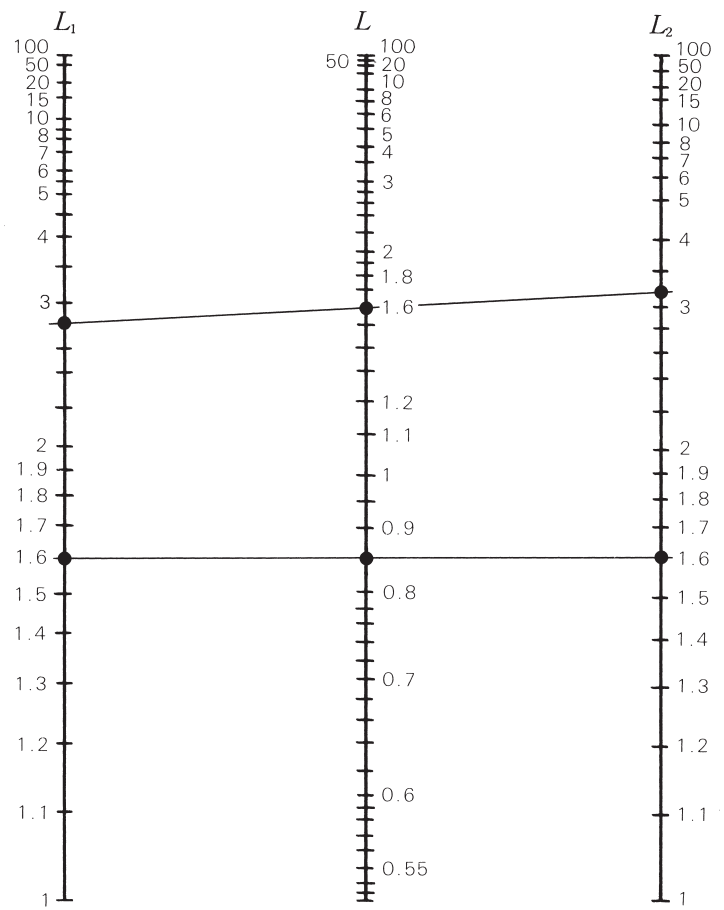

Fig. 1 Chart for life calculation

2.7 Load factor and fatigue life by machine

Loads acting on the bearing, rotating speed, and other conditions must be taken into account when selecting a bearing for a machine. Basic loads acting on a bearing are considered normally to include the weight of a rotating body supported by the bearing, load developed by power transmitted gears and belt, and other loads which can be estimated by calculation.
Actually, in addition to the above loads, there are loads caused by unbalance of a rotating body, load developed due to vibration and shock during operation, etc., which are, however, difficult to determine accurately. In order to assume the dynamic equivalent load P necessary for selection of the bearing, therefore, the above basic load F_c is converted into a practical mean effective load by multiplying it by a certain factor. This factor is called the load factor f_w, which is an empirical value. Table 1 shows the guideline of load factor f_w for each machine and operating conditions. For example, when a part incorporating a bearing is subject to a radial load of F_{rc} and an axial load of F_{ac}, the dynamic equivalent load P can be expressed as follows, with load factors assumed respectively as f_{w1} and f_{w2}:

$$P = X f_{w1} F_{rc} + Y f_{w2} F_{ac} \quad \cdots\cdots (1)$$

Setting an unnecessarily long fatigue life during selection of a bearing is not economical because it will lead to a larger bearing. Moreover, the fatigue life of a bearing may not be the sole standard in certain cases in view of the strength, rigidity, and mounting dimensions of the shaft. In general, the bearing design life is set as a guideline for each machine and operation conditions to ensure selection of an adequate yet economical bearing.

Such a design life requires an empirical value called the fatigue life factor f_h. Table 2 shows the fatigue life factors which are summarized for each machine and operating conditions. It is therefore necessary to determine the basic load rating C from the fatigue life factor f_h appropriate to the bearing application purpose while using the equation as follows:

$$C \geqq \frac{f_h \cdot P}{f_n} \quad \cdots\cdots (2)$$

where, C: Basic dynamic load rating (N), {kgf}
f_n: Speed factor

The bearing must satisfy the calculated basic dynamic load rating C as shown above.

Table 1 Value of load factor f_w

Running conditions	Typical machine	f_w
Smooth operation free from shock	Electric motors, machine tools, air conditioners	1 to 1.2
Normal operation	Air blowers, compressors, elevators, cranes, paper making machines	1.2 to 1.5
Operation exposed to shock and vibration	Construction equipment, crushers, vibrating screens, rolling mills	1.5 to 3

Table 2 Fatigue life factor f_h for various bearing applications

Operating periods	Fatigue life factor f_h and machine				
	≤3	2 to 4	3 to 5	4 to 7	≥6
Infrequently or only for short periods	•Small motors for home appliances like vacuum cleaners •Hand powered tools	•Agricultural equipment			
Only occasionally but reliability is important		•Motors for home heaters and air conditioners •Construction equipment	•Conveyors •Elevators		
Intermittently for relatively long periods	•Rolling mill roll necks	•Small motors •Deck cranes •General cargo cranes •Pinion stands •Passenger cars	•Factory motors •Machine tools •Transmissions •Vibrating screens •Crushers	•Crane sheaves •Compressors •Specialized transmissions	
Intermittently for more than eight hours daily		•Escalators	•Centrifugal separators •Air conditioning equipment •Blowers •Woodworking machines •Large motors •Axle boxes on railway rolling stock	•Mine hoists •Press fly-wheels •Railway traction motors •Locomotive axle boxes	•Papermaking machines
Continuously and high reliability is important					•Waterworking pumps •Electric power station •Mine draining pumps

2.8 Radial clearance and fatigue life

As shown in the catalog, etc., the fatigue life calculation equation of rolling bearings is Equation (1):

$$L=\left(\frac{C}{P}\right)^{p} \quad \cdots\cdots (1)$$

where, L: Rating fatigue life (10^6rev)
C: Basic dynamic load rating (N), {kgf}
P: Dynamic equivalent load (N), {kgf}
p: Index Ball bearing p=3,

Roller bearing $p=\frac{10}{3}$

The rating fatigue life L for a radial bearing in this case is based on a prerequisite that the load distribution in the bearing corresponds to the state with the load factor $\varepsilon = 0.5$ (Fig. 1). The load factor ε varies depending on the magnitude of load and bearing internal clearance. Their relationship is described in 5.2 (Radial Internal Clearance and Load Factor of Ball Bearing).

The load distribution with ε=0.5 is obtained when the bearing internal clearance is zero. In this sense, the normal fatigue life calculation is intended to obtain the value when the clearance is zero. When the effect of the radial clearance is taken into account, the bearing fatigue life can be calculated as follows. Equations (2) and (3) can be established between the bearing radial clearance Δ_r and a function $f(\varepsilon)$ of load factor ε:

For deep groove ball bearing

$$\left.\begin{aligned} f(\varepsilon)&=\frac{\Delta_r \cdot D_w^{1/3}}{0.00044\left(\frac{F_r}{Z}\right)^{2/3}} \quad \cdots\cdots (\mathrm{N}) \\ f(\varepsilon)&=\frac{\Delta_r \cdot D_w^{1/3}}{0.002\left(\frac{F_r}{Z}\right)^{2/3}} \quad \cdots\cdots \{\mathrm{kgf}\} \end{aligned}\right\} \cdots\cdots (2)$$

For cylindrical roller bearing

$$\left.\begin{aligned} f(\varepsilon)&=\frac{\Delta_r \cdot L_{we}^{0.8}}{0.000077\left(\frac{F_r}{Z \cdot i}\right)^{0.9}} \quad \cdots\cdots (\mathrm{N}) \\ f(\varepsilon)&=\frac{\Delta_r \cdot L_{we}^{0.8}}{0.0006\left(\frac{F_r}{Z \cdot i}\right)^{0.9}} \quad \cdots\cdots \{\mathrm{kgf}\} \end{aligned}\right\} \cdots\cdots (3)$$

where, Δ_r: Radial clearance (mm)
F_r: Radial load (N), {kgf}
Z: Number of rolling elements
i: No. of rows of rolling elements
D_w: Ball diameter (mm)
L_{we}: Effective roller length (mm)
L_ε: Life with clearance of Δ_r
L: Life with zero clearance, obtained from Equation (1)

The relationship between load factor ε and $f(\varepsilon)$, and the life ratio L_ε/L, when the radial internal clearance is Δ_r can also be obtained as shown in Table 1.

Fig. 2 shows the relationship between the radial clearance and bearing fatigue life while taking 6208 and NU208 as examples.

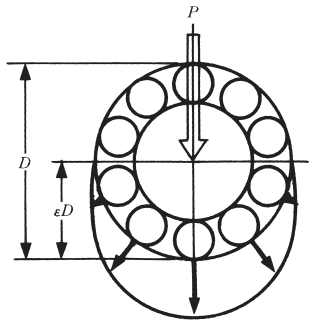

Fig. 1 Load distribution with ε=0.5

Table 1 ε and $f(\varepsilon)$, L_ε/L

ε	Deep groove ball bearing		Cylindrical roller bearing	
	$f(\varepsilon)$	$\frac{L_\varepsilon}{L}$	$f(\varepsilon)$	$\frac{L_\varepsilon}{L}$
0.1	33.713	0.294	51.315	0.220
0.2	10.221	0.546	14.500	0.469
0.3	4.045	0.737	5.539	0.691
0.4	1.408	0.889	1.887	0.870
0.5	0	1.0	0	1.0
0.6	− 0.859	1.069	− 1.133	1.075
0.7	− 1.438	1.098	− 1.897	1.096
0.8	− 1.862	1.094	− 2.455	1.065
0.9	− 2.195	1.041	− 2.929	0.968
1.0	− 2.489	0.948	− 3.453	0.805
1.25	− 3.207	0.605	− 4.934	0.378
1.5	− 3.877	0.371	− 6.387	0.196
1.67	− 4.283	0.276	− 7.335	0.133
1.8	− 4.596	0.221	− 8.082	0.100
2.0	− 5.052	0.159	− 9.187	0.067
2.5	− 6.114	0.078	−11.904	0.029
3	− 7.092	0.043	−14.570	0.015
4	− 8.874	0.017	−19.721	0.005
5	−10.489	0.008	−24.903	0.002
10	−17.148	0.001	−48.395	0.0002

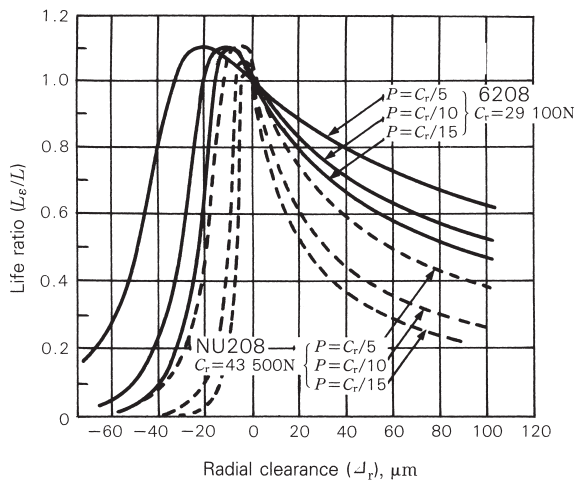

Fig. 2 Radial clearance and bearing life ratio

2.9 Misalignment of inner/outer rings and fatigue life of deep-groove ball bearings

A rolling bearing is manufactured with high accuracy, and it is essential to take utmost care with machining and assembly accuracies of surrounding shafts and housing if this accuracy is to be maintained. In practice, however, the machining accuracy of parts around the bearing is limited, and bearings are subject to misalignment of inner/outer rings caused by the shaft deflection under external load.

The allowable misalignment is generally 0.0006 ~ 0.003 rad (2′ to 10′) but this varies depending on the size of the deep-groove ball bearing, internal clearance during operation, and load.

This section introduces the relationship between the misalignment of inner/outer rings and fatigue life. Four different sizes of bearings are selected as examples from the 62 and 63 series deep-groove ball bearings.

Assume the fatigue life without misalignment as $L_{\theta=0}$ and the fatigue life with misalignment as L_θ. The effect of the misalignment on the fatigue life may be found by calculating $L_\theta/L_{\theta=0}$. The result is shown in Figs. 1 to 4.

As an example of ordinary running conditions, the radial load F_r (N) {kgf} and axial load F_a (N) {kgf} were assumed respectively to be approximately 10% (normal load) and 1% (light preload) of the dynamic load rating C_r (N) {kgf} of a bearing and were used as load conditions for the calculation. Normal radial clearance was used and the shaft fit was set to around j5. Also taken into account was the decrease of the internal clearance due to expansion of the inner ring.

Moreover, assuming that the temperature difference between the inner and outer rings was 5°C during operation, inner/outer ring misalignment, $L_\theta/L_{\theta=0}$ was calculated for the maximum, minimum, and mean effective clearances.

As shown in Figs. 1 to 4, degradation of the fatigue life is limited to 5 to 10% or less when the misalignment ranges from 0.0006 to 0.003 rad (2′ to 10′), thus not presenting much problem.

When the misalignment exceeds a certain limit, however, the fatigue life degrades rapidly as shown in the figure. Attention is therefore necessary in this respect.

When the clearance is small, not much effect is observed as long as the misalignment is small, as shown in the figure. But the life decreases substantially when the misalignment increases. As previously mentioned, it is essential to minimize the mounting error as much as possible when a bearing is to be used.

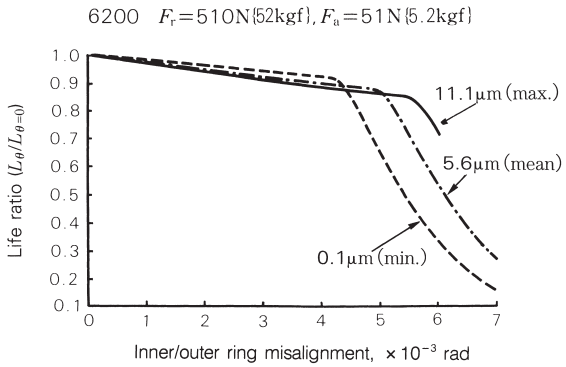

Fig. 1

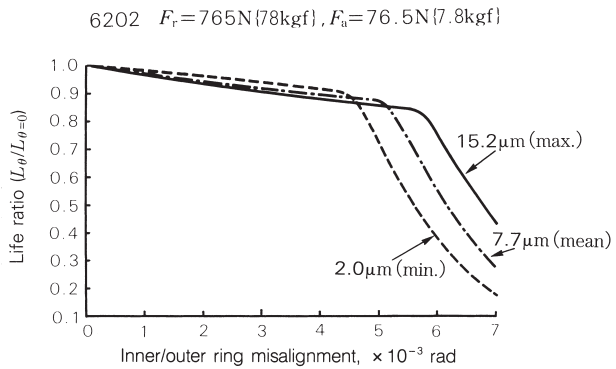

Fig. 2

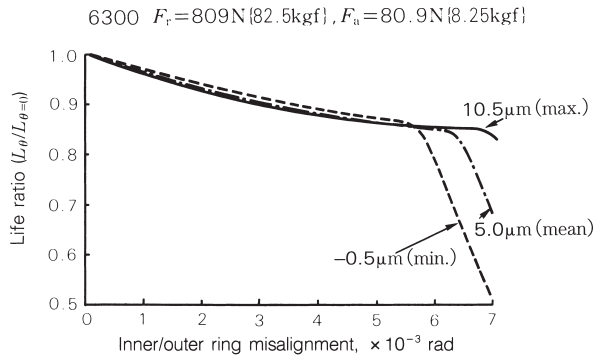

Fig. 3

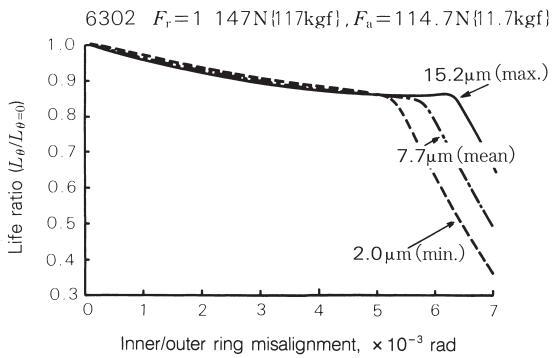

Fig. 4

2.10 Misalignment of inner/outer rings and fatigue life of cylindrical roller bearings

When a shaft supported by rolling bearings is deflected or there is some inaccuracy in a shoulder, there arises misalignment between the inner and outer rings of the bearings, thereby lowering their fatigue life. The degree of life degradation depends on the bearing type and interior design but also varies depending on the radial internal clearance and the magnitude of load during operation.

The relationship between the misalignment of inner/outer rings and fatigue life was determined, as shown in **Figs. 1** to **4**, while using cylindrical roller bearings NU215 and NU315 of standard design.

In these figures, the horizontal axis shows the misalignment of inner/outer rings (rad) while the vertical axis shows the fatigue life ratio $L_\theta/L_{\theta=0}$. The fatigue life without misalignment is $L_{\theta=0}$ and that with misalignment is L_θ.

Figs. 1 and 2 show the case with constant load (10% of basic dynamic load rating C_r of a bearing) for each case when the internal clearance is a normal, C3 clearance, or C4 clearance. **Figs. 3** and **4** show the case with constant clearance (normal clearance) when the load is 5%, 10%, and 20% of the basic dynamic load rating C_r.

Note that the median effective clearance in these examples was determined using m5/H7 fits and a temperature difference of 5°C between the inner and outer rings.

The fatigue life ratio for the clearance and load shows the same trend as in the case of other cylindrical roller bearings. But the life ratio itself differs among bearing series and dimensions, with life degradation rapid in 22 and 23 series bearings (wide type). It is advisable to use a bearing of special design when considerable misalignment is expected during application.

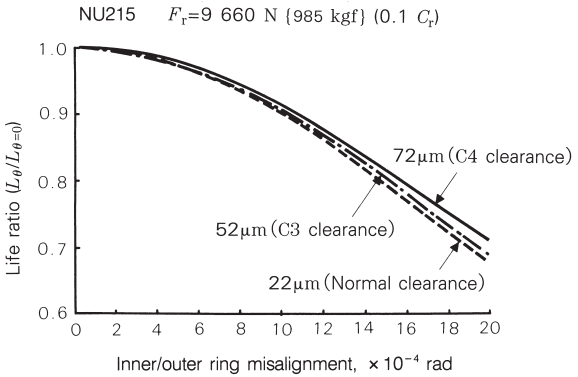

Fig. 1

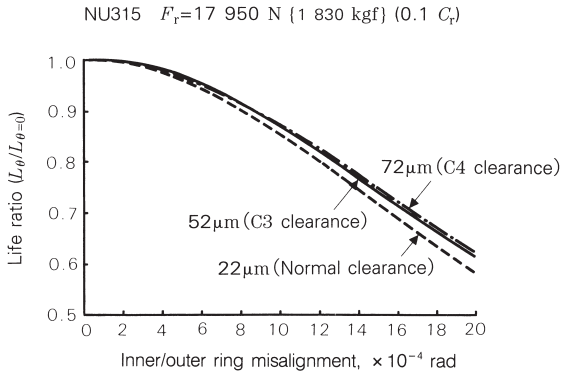

Fig. 2

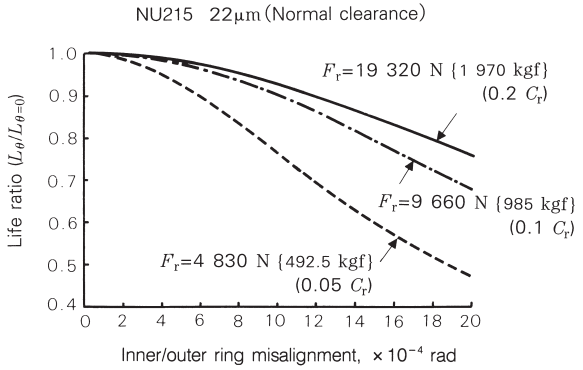

Fig. 3

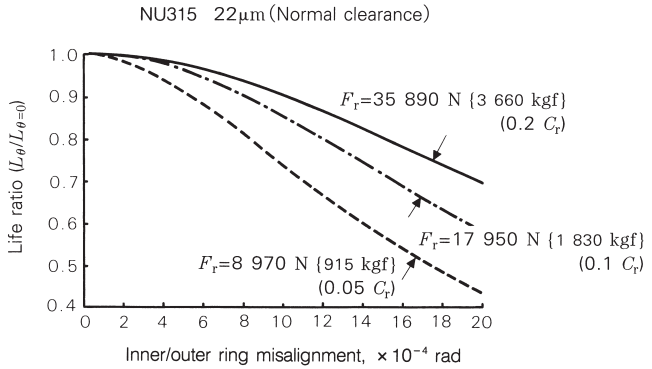

Fig. 4

2.11 Fatigue life and reliability

Where any part failure may result in damage to the entire machine and repair of damage is impossible, as in applications such as aircraft, satellites, or rockets, greatly increased reliability is demanded of each component. This concept is being applied generally to durable consumer goods and may also be utilized to achieve effective preventive maintenance of machines and equipment.

The rating fatigue life of a rolling bearing is the gross number of revolutions or the gross rotating period when the rotating speed is constant for which 90% of a group of similar bearings running individually under similar conditions can rotate without suffering material damage due to rolling fatigue. In other words, fatigue life is normally defined at 90% reliability. There are other ways to describe the life. For example, the average value is employed frequently to describe the life span of human beings. However, if the average value were used for bearings, then too many bearings would fail before the average life value is reached. On the other hand, if a low or minimum value is used as a criterion, then too many bearings would have a life much longer than the set value. In this view, the value 90% was chosen for common practice. The value 95% could have been taken as the statistical reliability, but nevertheless, the slightly looser reliability of 90% was taken for bearings empirically from the practical and economical viewpoint. A 90% reliability however is not acceptable for parts of aircraft or electronic computers or communication systems these days, and a 99% or 99.9% reliability is demanded in some of these cases.

The fatigue life distribution when a group of similar bearings are operated individually under similar conditions is shown in Fig. 1. The Weibull equation can be used to describe the fatigue life distribution within a damage ratio of 10 to 60% (residual probability of 90 to 40%). Below the damage ratio of 10% (residual probability of 90% or more), however, the rolling fatigue life becomes longer than the theoretical curve of the Weibull distribution, as shown in Fig. 2. This is a conclusion drawn from the life test of numerous, widely-varying bearings and an analysis of the data.

When bearing life with a failure ratio of 10% or less (for example, the 95% life or 98% life) is to be considered on the basis of the above concept, the reliability factor a_1 as shown in the table below is used to check the life. Assume here that the 98% life L_2 is to be calculated for a bearing whose rating fatigue life L_{10} was calculated at 10 000 hours. The life can be calculated as L_2=0.33×L_{10}=3 300 hours. In this manner, the reliability of the bearing life can be matched to the degree of reliability required of the equipment and difficulty of overhaul and inspection.

Table 1 Reliability factor

Reliability, %	90	95	96	97	98	99
Life, L_a	L_{10} rating life	L_5	L_4	L_3	L_2	L_1
Reliability factor, a_1	1	0.62	0.53	0.44	0.33	0.21

Apart from rolling fatigue, factors such as lubrication, wear, sound, and accuracy govern the durability of a bearing. These factors must be taken into account, but the endurance limit of these factors varies depending on application and conditions.

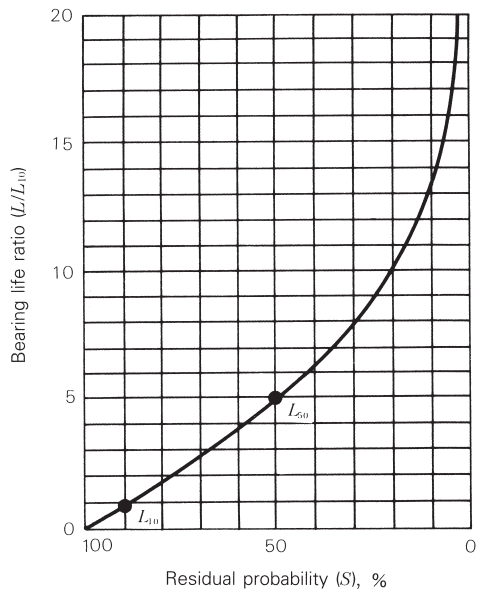

Fig. 1 Bearing life and residual probability

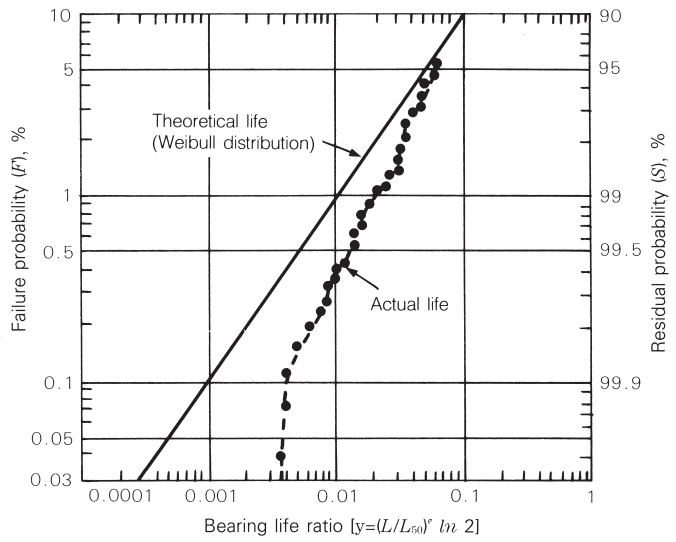

Fig. 2 Life distribution in the low failure ratio range

2.12 Oil film parameters and rolling fatigue life

Based on numerous experiments and experiences, the rolling fatigue life of rolling bearings can be shown to be closely related to the lubrication.

The rolling fatigue life is expressed by the maximum number of rotations, which a bearing can endure, until the raceway or rolling surface of a bearing develops fatigue in the material, resulting in flaking of the surface, under action of cyclic stress by the bearing. Such flaking begins with either microscopic non-uniform portions (such as non-metallic inclusions, cavities) in the material or with microscopic defect in the material's surface (such as extremely small cracks or surface damage or dents caused by contact between extremely small projections in the raceway or rolling surface). The former flaking is called sub-surface originating flaking while the latter is surface-originating flaking.

The oil film parameter (Λ), which is the ratio between the resultant oil film thickness and surface roughness, expresses whether or not the lubrication state of the rolling contact surface is satisfactory. The effect of the oil film grows with increasing Λ. Namely, when Λ is large (around 3 in general), surface-originating flaking due to contact between extremely small projections in the surface is less likely to occur. If the surface is free from defects (flaw, dent, etc.), the life is determined mainly by sub-surface originating flaking. On the other hand, a decrease in Λ tends to develop surface-originating flaking, resulting in degradation of the bearing's life. This state is shown in Fig. 1.

NSK has performed life experiments with about 370 bearings within the range of Λ=0.3 ~ 3 using different lubricants and bearing materials (● and ▲ in Fig. 2). Fig. 2 shows a summary of the principal experiments selected from among those reported up to now. As is evident, the life decreases rapidly at around $\Lambda \fallingdotseq 1$ when compared with the life values at around Λ=3 ~ 4 where life changes at a slower rate. The life becomes about 1/10 or less at $\Lambda \leqq 0.5$. This is a result of severe surface-originating flaking.

Accordingly, it is advisable for extension of the fatigue life of rolling bearings to increase the oil film parameter (ideally to a value above 3) by improving lubrication conditions.

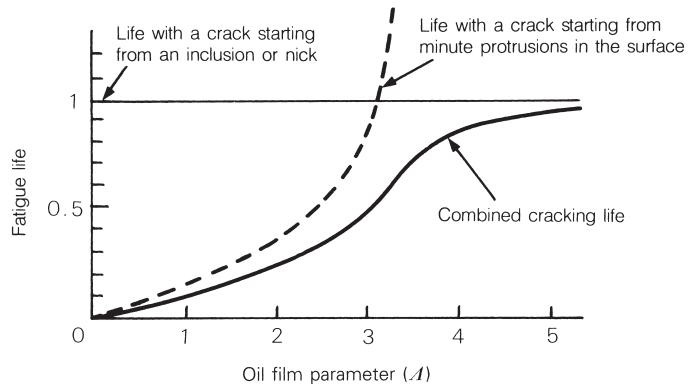

Fig. 1 Expression of life according to Λ (Tallian, et al.)

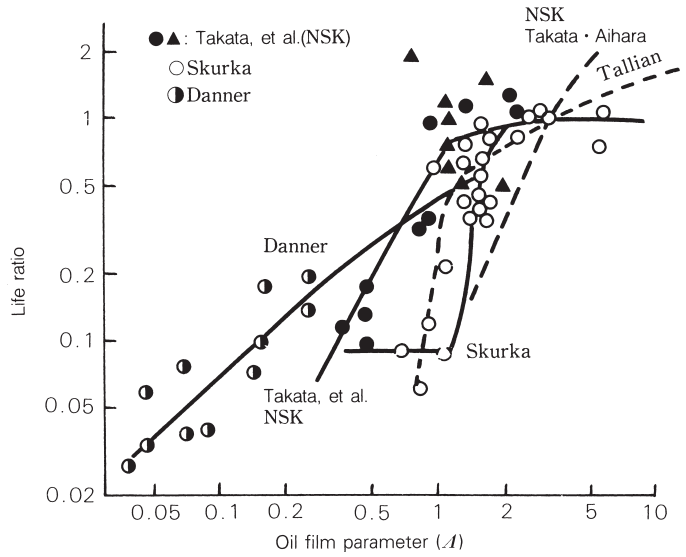

Fig. 2 Typical experiment with Λ and rolling fatigue life
(Expressed with reference to the life at Λ=3)

2.13 EHL oil film parameter calculation diagram

Lubrication of rolling bearings can be expressed by the theory of elastohydrodynamic lubrication (EHL). Introduced below is a method to determine the oil film parameter (oil film − surface roughness ratio), the most critical among the EHL qualities.

2.13.1 Oil film parameter

The raceway surfaces and rolling surfaces of a bearing are extremely smooth, but have fine irregularities when viewed through a microscope. As the EHL oil film thickness is in the same order as the surface roughness, lubricating conditions cannot be discussed without considering this surface roughness. For example, given a particular mean oil film thickness, there are two conditions which may occur depending on the surface roughness. One consists of complete separation of the two surfaces by means of the oil film (Fig. 1 (a)). The other consists of metal contact between surface projections (Fig. 1 (b)). The degradation of lubrication and surface damage is attributed to case (b). The symbol lambda (Λ) represents the ratio between the oil film thickness and roughness. It is widely employed as an oil film parameter in the study and application of EHL.

$$\Lambda = h/\sigma \quad \cdots\cdots (1)$$

where h: EHL oil film thickness
σ: Combined roughness ($\sqrt{\sigma_1^2+\sigma_2^2}$)

σ_1, σ_2: Root mean square (rms) roughness of each contacting surface

The oil film parameter may be correlated to the formation of the oil film as shown in Figs. 2 and the degree of lubrication can be divided into three zones as shown in the figure.

2.13.2 Oil film parameter calculation diagram

The Dowson-Higginson minimum oil film thickness equation shown below is used for the diagram:

$$H_{\min} = 2.65 \frac{G^{0.54} U^{0.7}}{W^{0.13}} \quad \cdots\cdots (2)$$

The oil film thickness to be used is that of the inner ring under the maximum rolling element load (at which the thickness becomes minimum).

Equation (2) can be expressed as follows by grouping into terms (R) for speed, (A) for viscosity, (F) for load, and (J) for bearing technical specifications. t is a constant.

$$\Lambda = t \cdot R \cdot A \cdot F \cdot J \quad \cdots\cdots (3)$$

R and A may be quantities not dependent on a bearing. When the load P is assumed to be between 98 N {10 kgf} and 98 kN {10 tf}, F changes by 2.54 times as $F \propto P^{-0.13}$. Since the actual load is determined roughly from the bearing size, however, such change may be limited to 20 to 30%. As a result, F is handled as a lump with the term J of bearing specifications [$F=F$ (J)]. Traditional Equation (3) can therefore be grouped as shown below:

$$\Lambda = T \cdot R \cdot A \cdot D \quad \cdots\cdots (4)$$

where, T: Factor determined by the bearing Type
R: Factor related to Rotation speed
A: Factor related to viscosity (viscosity grade α: Alpha)
D: Factor related to bearing Dimensions

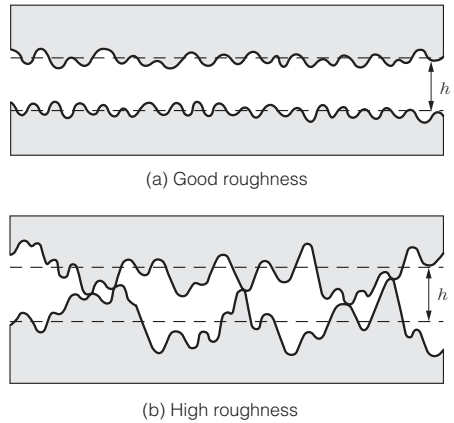

Fig. 1 Oil film and surface roughness

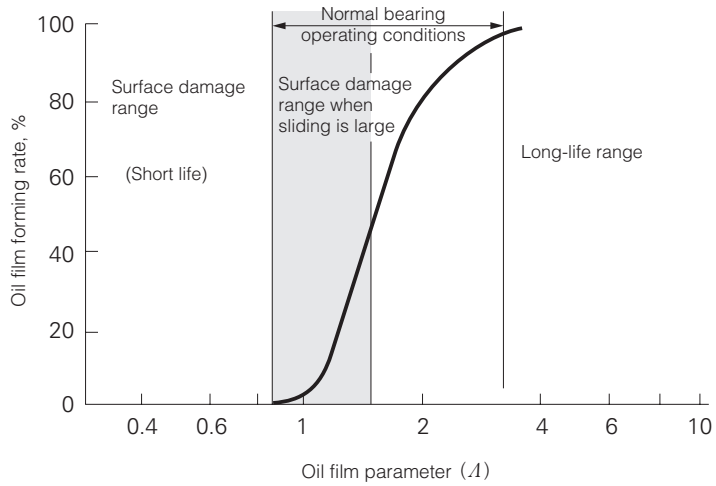

Fig. 2 Effect of oil film on bearing performance

The oil film parameter Λ, which is most vital among quantities related to EHL, is expressed by a simplified equation shown below. The fatigue life of rolling bearings becomes shorter when Λ is smaller.

In the equation $\Lambda = T \cdot R \cdot A \cdot D$ terms include A for oil viscosity η_0 (mPa·s, {cp}), R for the speed n (min^{-1}), and D for bearing bore diameter d (mm). The calculation procedure is described below.

(1) Determine the value T from the bearing type (Table 1).

(2) Determine the R value for n (min^{-1}) from Fig. 3.

(3) Determine A from the absolute viscosity (mPa·s, {cp}) and oil kind in Fig. 4. Generally, the kinematic viscosity ν_0 (mm^2/s, {cSt}) is used and conversion is made as follows:

$$\eta_0 = \rho \cdot \nu_0 \quad \cdots\cdots (5)$$

ρ is the density (g/cm^3) and uses the approximate value as shown below:

Mineral oil ρ=0.85
Silicon oil ρ=1.0
Diester oil ρ=0.9

When it is not known whether the mineral oil is naphthene or paraffin, use the paraffin curve shown in Fig. 4.

(4) Determine the D value from the diameter series and bore diameter d (mm) in Fig. 5.

(5) The product of the above values is used as an oil film parameter.

Table 1 Value T

Bearing type	Value T
Ball bearing	1.5
Cylindrical roller bearing	1.0
Tapered roller bearing	1.1
Spherical roller bearing	0.8

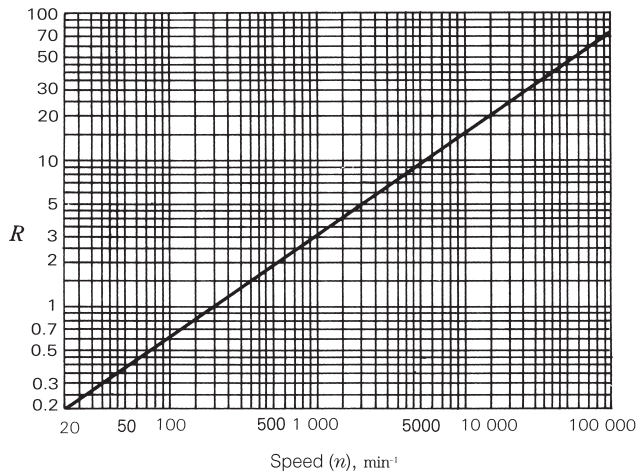

Fig. 3 Speed term, R

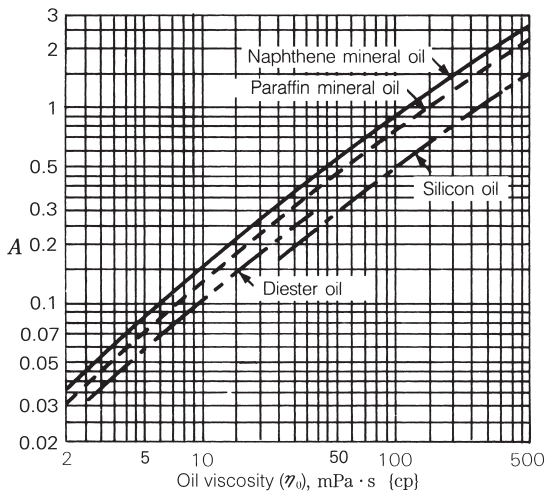

Fig. 4 Term related to lubricant viscosity, A

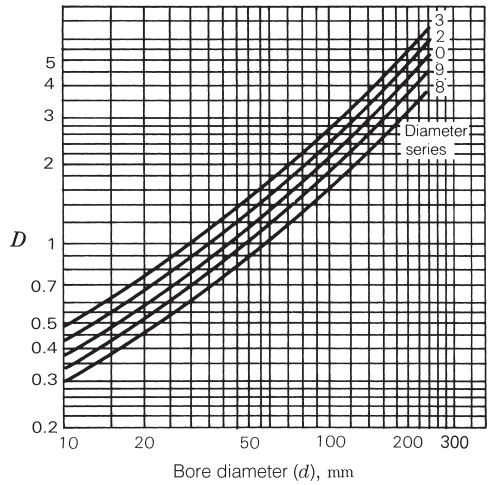

Fig. 5 Term related to bearing specifications, D

Examples of EHL oil film parameter calculation are described below.

(Example 1)

The oil film parameter is determined when a deep groove ball bearing 6312 is operated with paraffin mineral oil (η_0=30 mPa·s, {cp}) at the speed n =1 000 min^{-1}.

(Solution)

d=60 mm and D=130 mm from the bearing catalog.

T=1.5 from Table 1

R=3.0 from Fig. 3

A=0.31 from Fig. 4

D=1.76 from Fig. 5

Accordingly, Λ=2.5

(Example 2)

The oil film parameter is determined when a cylindrical roller bearing NU240 is operated with paraffin mineral oil (η_0=10 mPa·s, {cp}) at the speed n=2 500 min^{-1}.

(Solution)

d=200 mm and D=360 mm from the bearing catalog.

T=1.0 from Table 1

R=5.7 from Fig. 3

A=0.13 from Fig. 4

D=4.8 from Fig. 5

Accordingly, Λ=3.6

2.13.3 Effect of oil shortage and shearing heat generation

The oil film parameter obtained above is the value when the requirements, that is, the contact inlet fully flooded with oil and isothermal inlet are satisfied. However, these conditions may not be satisfied depending on lubrication and operating conditions.

One such condition is called starvation, and the actual oil film paramerer value may become smaller than determined by Equation (4). Starvation might occur if lubrication becomes limited. In this condition, a guideline for adjusting the oil film parameter is 50 to 70% of the value obtained from Equation (4).

Another effect is the localized temperature rise of oil in the contact inlet due to heavy shearing during high-speed operation, resulting in a decrease of the oil viscosity. In this case, the oil film parameter becomes smaller than the isothermal theoretical value. The effect of shearing heat generation was analyzed by Murch and Wilson, who established the decrease factor of the oil film parameter. An approximation using the viscosity and speed (pitch diameter of rolling element set D_{pw} × rotating speed per minute n as parameters) is shown in Fig. 6. By multiplying the oil film parameter determined in the previous section by this decrease factor Hi the oil film parameter considering the shearing heat generation is obtained.

Nameny;

$$\Lambda = Hi \cdot T \cdot R \cdot A \cdot D \quad \text{.....} \quad (6)$$

Note that the average of the bore and outside diameters of the bearings may be used as the pitch diameter D_{pw} (d_m) of rolling element set.

Conditions for the calculation (Example 1) include $d_m n$=9.5 × 10^4 and η_0=30 mPa·s, {cp}, and Hi is nearly equivalent to 1 as is evident from Fig. 6. There is therefore almost no effect of shearing heat generation.

Conditions for (Example 2) are $d_m n$=7×10^5 and η_0=10 mPa·s, {cp} while Hi=0.76, which means that the oil film parameter is smaller by about 25%. Accordingly, Λ is actually 2.7, not 3.6.

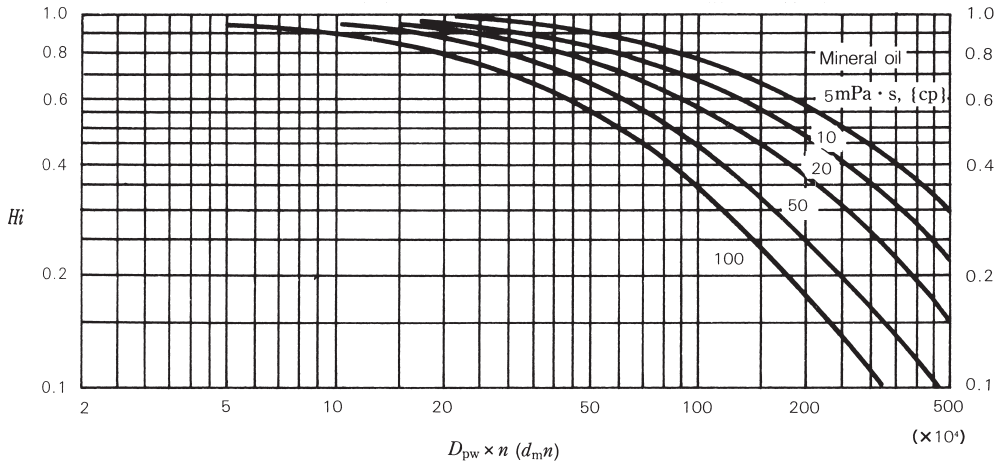

Fig. 6 Oil film thickness decrease factor Hi due to shearing heat generation

2.14 Fatigue analysis

It is necessary for prediction of the fatigue life of rolling bearings and estimation of the residual life to know all fatigue break-down phenomena of bearings. But, it will take some time before we reach a stage enabling prediction and estimation. Rolling fatigue, however, is fatigue proceeding under compressive stress at the contact point and known to develop extremely great material change until breakdown occurs. In many cases, it is possible to estimate the degree of fatigue of bearings by detecting material change. However, this estimation method is not effective in the cases where the defects in the raceway surface cause premature cracking or chemical corrosion occurs on the raceway. In these two cases, flaking grows in advance of the material change.

2.14.1 Measurement of fatigue degree

The progress of fatigue in a bearing can be determined by using an X-ray to measure changes in the residual stress, diffraction half-value width, and retained austenite amount.

These values change as the fatigue progresses as shown in Fig. 1. Residual stress, which grows early and approaches the saturation value, can be used to detect extremely small fatigue. For large fatigue, change of the diffraction half-value width and retained austenite amount may be correlated to the progress of fatigue. These measurements with X-ray are put together into one parameter (fatigue index) to determine the relationship with the endurance test period of a bearing.

Measured values were collected by carrying out endurance test with many ball, tapered roller, and cylindrical roller bearings under various load and lubrication conditions. Simultaneously, measurements were made on bearings used in actual machines.

Fig. 2 summarizes the data. Variance is considerable because data reflects the complexity of the fatigue phenomenon. But, there exists correlation between the fatigue index and the endurance test period or operating hours. If some uncertainty is allowed, the fatigue degree can be handled quantitatively.

Description of “sub-surface fatigue” in Fig. 2 applies to the case when fatigue is governed by internal shearing stress. “Surface fatigue” shows correlation when the surface fatigue occurs earlier and more severely than sub-surface fatigue due to contamination or oil film breakdown of lubricating oil.

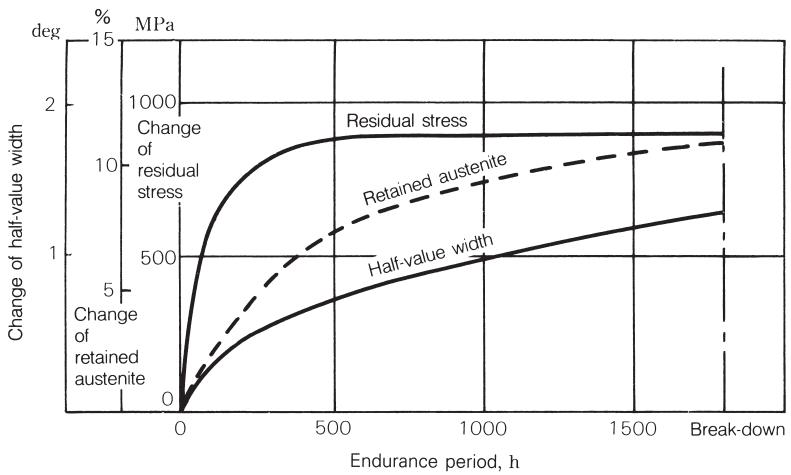

Fig. 1 Change in X-ray measurements

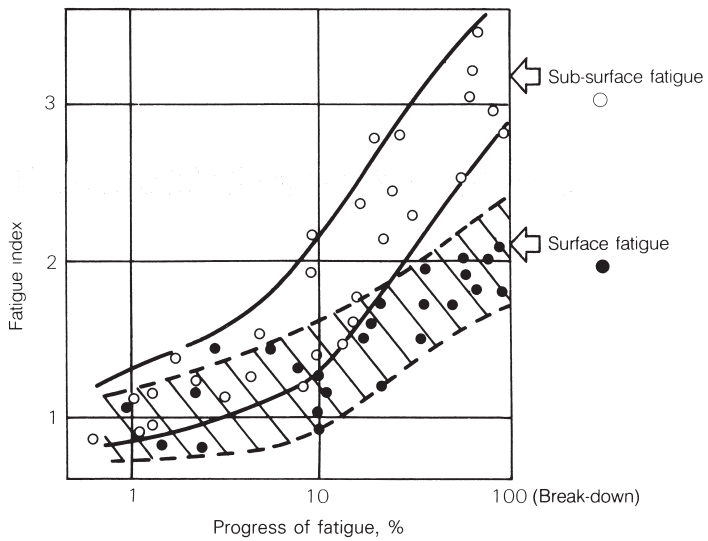

Fig. 2 Fatigue progress and fatigue index

2.14.2 Surface and sub-surface fatigues

Rolling bearings have an extremely smooth finish surface and enjoy relatively satisfactory lubrication conditions. It has been considered that internal shearing stress below the rolling surface governs the failure of a bearing.

Shearing stress caused by rolling contact becomes maximum at a certain depth below the surface, with a crack (which is an origin of break-down) occurring initially under the surface. When the raceway is broken due to such sub-surface fatigue, the fatigue index as measured in the depth direction is known to increase according to the theoretical calculation of shearing stress, as is evident from an example of the ball bearing shown in Fig. 3.

The fatigue pattern shown in Fig. 3 occurs mostly when lubrication conditions are satisfactory and oil film of sufficient thickness is formed in rolling contact points. The basic dynamic load rating described in the bearing catalog is determined using data of bearing failures according to the above internal fatigue pattern.

Fig. 4 shows an example of a cylindrical roller bearing subject to endurance test under lubrication conditions causing unsatisfactory oil film. It is evident that the surface fatigue degree rises much earlier than the calculated life.

In this test, all bearings failed before sub-surface fatigue became apparent. In this way, bearing failure due to surface fatigue is mostly attributed to lubrication conditions such as insufficient oil film due to excessively low oil viscosity or entry of foreign matters or moisture into lubricant.

Needless to say, bearing failure induced by surface fatigue occurs in advance of that by sub-surface fatigue. Bearings in many machines are exposed frequently to danger of initiating such surface fatigue and, in most of the cases, failure by surface fatigue prior to failure due to sub-surface fatigue (which is the original life limit of bearings).

Fatigue analysis of bearings used in actual machines shows not the sub-surface fatigue pattern, but the surface fatigue pattern as shown in the figure in overwhelmingly high percentage.

In this manner, knowing the distribution of the fatigue index in actually used bearings leads to an understanding of effective information not only on residual life of bearings, but also on lubrication and load conditions.

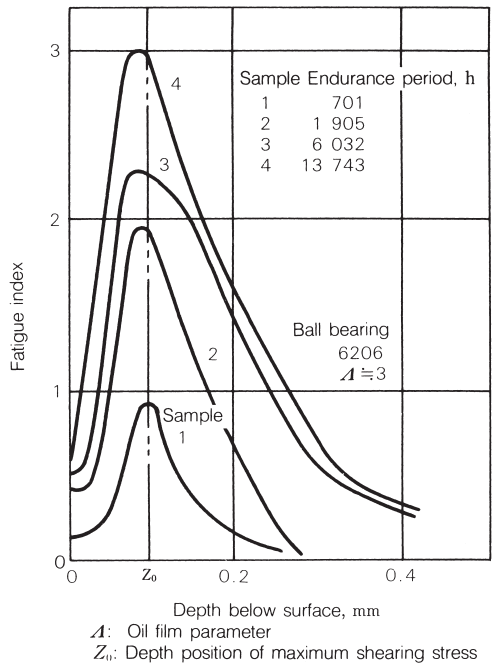

Fig. 3 Progress of sub-surface fatigue

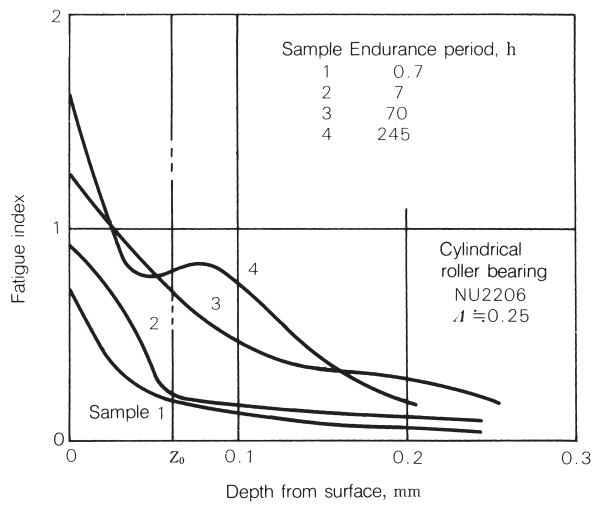

Fig. 4 Progress of surface fatigue

2.14.3 Analysis of practical bearing (1)

Bearings for automotive transmissions must overcome difficult problems of size and weight reduction as well as extension of durable life to meet the ever increasing efforts to conserve energy.

Fig. 5 shows an example of fatigue analysis of bearings used in the transmission of an actual passenger car. Analysis of the transmission bearings of various vehicles reveals the surface fatigue pattern as shown in Fig. 5, but almost no progress of sub-surface fatigue which is used as a criterion for calculating the bearing life.

In other words, these bearings develop less fatigue under external bearing loads but they eventually suffer damage due to fatigue by surface force on the rolling surface though they can be used for a long time.

This may be attributable to indentations caused by inclusions of extremely small foreign matters from the gear oil, which in turn cause excessive fatigue of the surface.

As is evident from Fig. 5, the fatigue index is heaviest in the counter front bearing where the load is most severe, followed by the counter rear bearing where the load is lightest. This surprising fact may be due to the fact that the counter shaft bearings are immersed in gear oil which often has many foreign particles suspend in it. Thus, metal chips in the gear oil eventually contact and abrade the counter shaft bearings.

Fig. 6 shows the result of the durability test and fatigue analysis data with two kinds of bearings used in a transmission of an actual vehicle.

As is known from above the analytical result, a bearing with a special seal (sealed clean bearing), which prevents entry of foreign matter in gear oil while allowing entry of oil only, offers remarkably extended life. In this way, the life is extended by more than ten times when compared with an open type bearing without a seal.

The fatigue pattern shows change in the sub-surface fatigue pattern in the sealed clean bearing, indicating that reduction of surface fatigue contributes greatly to the remarkable life extension.

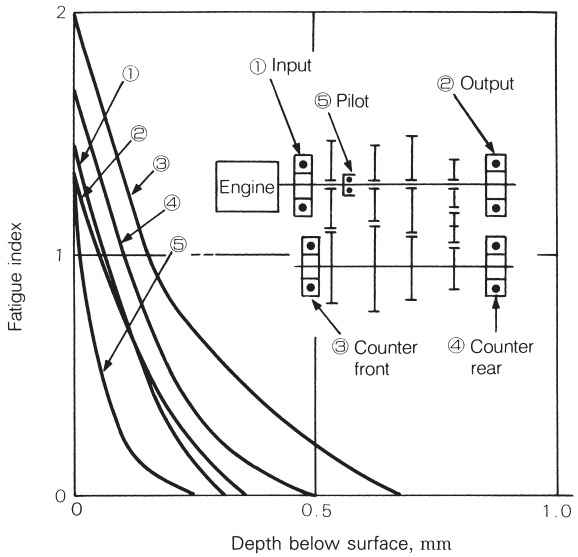

Fig. 5 Fatigue index distribution of transmission bearings (used in actual vehicle)

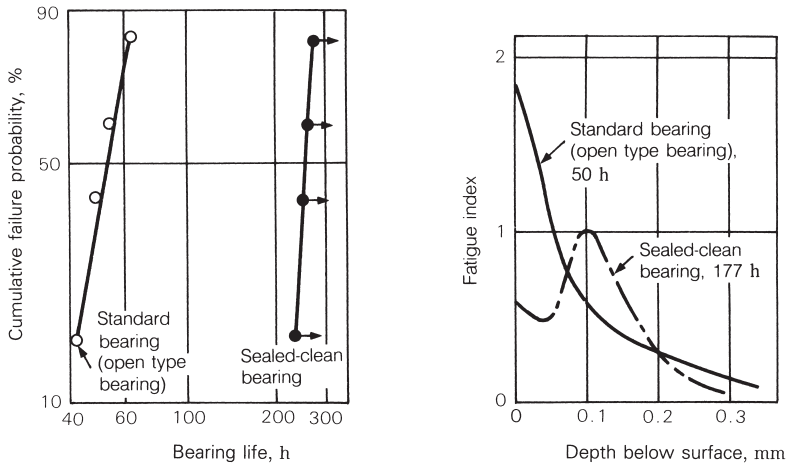

Fig. 6 Comparison between open type bearing and sealed-clean bearing in transmission durability test

2.14.4 Analysis of practical bearing (2)

As shown in the above examples, the cause of fatigue failure can be presumed through measurement of the fatigue index. There are also other applications. Namely, prediction of residual life, prediction of breakdown life by parts (inner and outer rings, rolling elements, etc.), and understanding of surface or sub-surface fatigue are possible. This information can be utilized for improved design. Specifically, this information may be used to reduce the size and weight, to optimize lubrication conditions, expand the applications for sealed clean bearings, and to enhance the load rating. Measurement of the fatigue index begins also to be applied in roller bearings to prevent the edge load of rollers to obtain a more ideal linear contact state. Improvements in the accuracy of fatigue index measurements can lead to better bearing designs.

In the future, prediction of residual life may be used to shorten the durability test period and optimize the interval between replacements.

Fig. 7 shows the measurement of the fatigue index distribution on the raceway surface of a pinion gear shaft incorporating a needle roller bearing. Heavy fatigue is observed on the raceway end nearest to the gear, indicating the necessity of a countermeasure against edge load of the roller.

Fig. 8 shows an example of estimating the durable life on the Weibull chart while interrupting the bearing durability test and predicting the life from the respective measurements of the fatigue index.

Practical examples as above introduced are expected to increase as fatigue analysis technology moves forward.

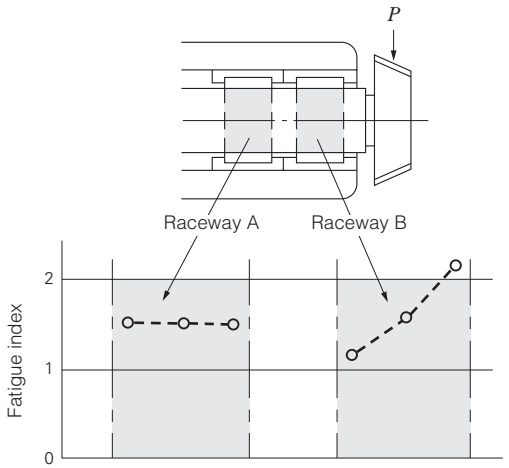

Fig. 7 Distribution of fatigue index in the raceway surface of the pinion shaft

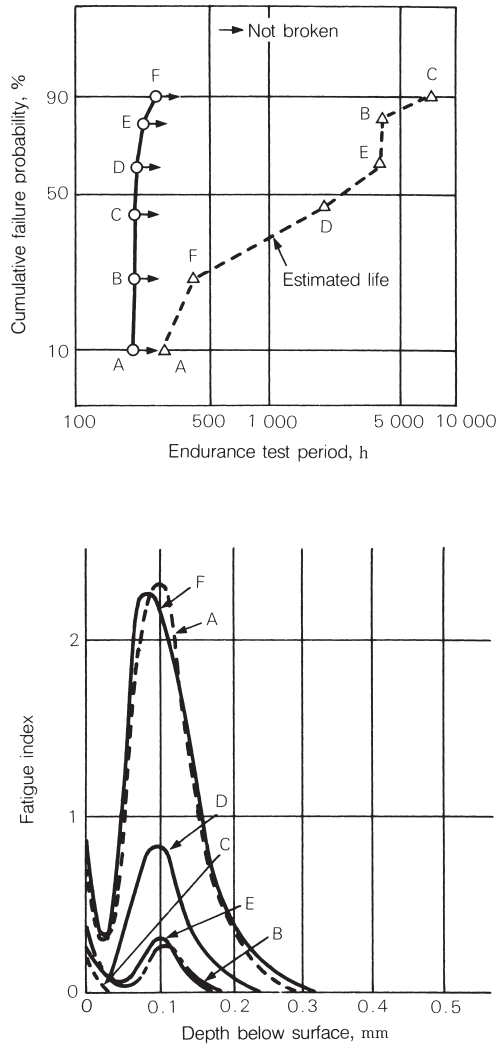

Fig. 8 Estimation of life for bearings whose durability test was interrupted halfway

2.15 Conversion of dynamic load rating with reference to life at 500 min⁻¹ and 3 000 hours

The basic dynamic load rating of rolling bearings is the load without fluctuation in the direction and magnitude, at which the rating fatigue life of a group of similar bearings operated with inner rings rotating and outer rings stationary reaches one million revolutions. The standard load rating is 33.3 min^{-1} and 500 hours ($33.3\times500\times60=10^6$). The calculation equation is specified in JIS B 1518. Some other makers, however, are using a calculation equation of dynamic load rating unique and different from ours, and comparison may encounter difficulties due to difference in standards. One of these differences is concerned with the gross number of revolutions.

For example, TIMKEN of the USA determines the dynamic load rating of tapered roller bearing by using the gross number of revolutions for the rotating speed of 500 min^{-1} for 3 000 hours, that is, 500×3 000×60=90 000 000 revolutions, as a standard.
TORRINGTON uses 33.3 min^{-1} and 500 hours, that is, 33.3×500×60=1 000 000 revolutions as a standard as in the case of JIS. Assuming that the dynamic load rating calculation equation is basically similar between both companies, except for the gross number of revolutions standard, the difference in the gross number of revolutions may be converted as follows in terms of dynamic load rating:

$$L_T=\left(\frac{C_T}{P_T}\right)^p\times n_T \quad\cdots\cdots (1)$$

$$L_R=\left(\frac{C_R}{P_R}\right)^p\times n_R \quad\cdots\cdots (2)$$

where, L: Rating fatigue life as expressed by gross number of revolutions
C: Basic dynamic load rating (N), {kgf}
P: Load (N), {kgf}
p: Power
n: Standard of gross number of revolutions

A suffix "T" stands for TIMKEN while "R" for TORRINGTON.

Assuming that the internal specification of a bearing is completely similar between both companies, setting loads $P_T=P_R$ lead to the following equation from Equations (1) and (2):

$$\frac{L_T}{L_R}=\frac{\left(\frac{C_T}{P_T}\right)^p\times n_T}{\left(\frac{C_R}{P_R}\right)^p\times n_R}=1 \quad\cdots\cdots (3)$$

$$C_R{}^p=\frac{n_T}{n_R}C_T{}^p \quad\cdots\cdots (4)$$

Set n_T=90 000 000, n_R=1 000 000, and power $p=\frac{10}{3}$ (applicable to roller bearings) in Equation (4):

$$C_R=\left(\frac{n_T}{n_R}\right)^{\frac{1}{p}}C_T$$

$$=\left(\frac{90\ 000\ 000}{1\ 000\ 000}\right)^{\frac{3}{10}}C_T$$

$$=90^{\frac{3}{10}}C_T \quad\cdots\cdots (5)$$

Namely, the value 3.857 times the dynamic load rating C_T of TIMKEN is equivalent to C_R of TORRINGTON. Actually, however, the internal specification is not necessarily the same because every bearing maker undertakes design and manufacture from its unique viewpoint. In case of a difference in the units (SI unit and pound), simple conversion is enough.

Relationship among Equations (3) to (5) can be established only when the dynamic load rating calculation equation is basically the same as described.
If it is evident that the equation is based on different standards, comparison or conversion using apparent numerical figures should be considered only as reference. Reasonable judgement is possible only by performing recalculation according to a similar calculation method.

2.16 Basic static load ratings and static equivalent loads

(1) Basic static load rating

When subjected to an excessive load or a strong shock load, rolling bearings undergo a local permanent deformation of the rolling elements and raceway surface if the elastic limit is exceeded. The nonelastic deformation increases in both area and depth as the load increases, and when the load exceeds a certain limit, the smooth running of the bearing is impeded.

The basic static load rating is defined as that static load which produces the following calculated contact stress at the center of the contact area between the rolling element subjected to the maximum stress and the raceway surface.

For self-aligning ball bearings
4 600 MPa {469 kgf/mm^2}
For other ball bearings
4 200 MPa {428 kgf/mm^2}
For roller bearings
4 000 MPa {408 kgf/mm^2}

In this most heavily stressed contact area, the sum of the permanent deformation of the rolling element and that of the raceway is nearly 0.0001 times the rolling element's diameter. The basic static load rating C_0 is written C_{0r} for radial bearings and C_{0a} for thrust bearings in the bearing tables.

In addition, following the modification of the criteria for the basic static load rating by ISO, the new C_0 values for NSK's ball bearings became about 0.8 to 1.3 times the past values and those for roller bearings about 1.5 to 1.9 times. Consequently, the values of permissible static load factor f_s have also changed, so please pay attention to this.

In the above description, the static load rating is not the load for failure (crack) of rolling element and bearing ring. Since the load necessary to crush a rolling element is more than seven times the static load rating, this is a sufficient safety factor against failure load when considering general machine equipment.

(2) Static equivalent load

The static equivalent load must be considered for radial bearings exposed to synthetic loads or axial loads only and for thrust bearings exposed to axial loads and slight radial loads.

The static equivalent load is a hypothetical load of a magnitude causing a contact stress (equivalent to the maximum contact stress occurring under actual load conditions) in the contact between the rolling element and raceway under maximum load when the bearing is stationary (including extremely low speed rotation and low-speed oscillation). This equivalent load is the radial load acting through a bearing center for radial bearings and the axial load in a direction aligned to the central axis in the case of thrust bearings.

(a) Static equivalent load of radial bearings
The static equivalent load of radial bearings is taken as the larger value of the two values obtained from the two equations below:

$$P_0=XF_r+Y_0F_a \quad \cdots\cdots (1)$$

$$P_0=F_r \quad \cdots\cdots (2)$$

where, P_0: Static equivalent load (N), {kgf}
F_r: Radial load (N), {kgf}
F_a: Axial load (N), {kgf}
X_0: Static radial load factor
Y_0: Static axial load factor

(b) Static equivalent load of thrust bearings

$$P_0=X_0F_r+F_a \quad \alpha\neq 90° \quad \cdots\cdots (3)$$

where, P_0: Static equivalent load (N), {kgf}
α : Nominal contact angle

Note that the accuracy of this equation decreases when $F_a<X_0F_r$.
Values X_0 and Y_0 of Equations (1) and (3) are as shown in Table 2.
Note that $P_0=F_a$ for a thrust bearing with $\alpha=90°$

(3) Static allowable load factor

The static equivalent load allowed for bearings varies depending on the basic static load rating, requirements of the bearings and bearing operating conditions.

The allowable static load factor f_s for review of the safety factor against the basic static load rating is determined from Equation (4). Generally recommended values of f_s are shown in Table 1.

Due care must be taken during application because the value of f_s for roller bearings (particularly, with the large C_0 value) has been changed along with the change of the static load rating.

$$f_s=\frac{C_0}{P_0} \quad \cdots\cdots (4)$$

where, C_0: Basic static load rating (N), {kgf}
P_0: Static equivalent load (N), {kgf}

Normally, $f_s\geqq 4$ applies to spherical thrust roller bearings.

Table 1 Value of permissible static load factor, f_s

Running conditions	Lower limit of f_s	
	Ball bearings	Roller bearings
Low-noise applications	2	3
Vibration and shock loads	1.5	2
Standard running conditions	1	1.5

Table 2 Static epuivalent load

Bearing type		Single row		Double row	
		X_0	Y_0	X_0	Y_0
Deep groove ball bearings		0.6	0.5	0.6	0.5
Angular contact ball bearings	$\alpha=15°$	0.5	0.46	1	0.92
	$\alpha=20°$	0.5	0.42	1	0.84
	$\alpha=25°$	0.5	0.38	1	0.76
	$\alpha=30°$	0.5	0.33	1	0.66
	$\alpha=35°$	0.5	0.29	1	0.58
	$\alpha=40°$	0.5	0.26	1	0.52
	$\alpha=45°$	0.5	0.22	1	0.44
Self-aligning ball bearings	$\alpha\neq 0$	0.5	0.22 cot α	1	0.44 cot α
Tapered roller bearings	$\alpha\neq 0$				
Spherical roller bearings	$\alpha\neq 0$				
Cylindrical roller bearings	$\alpha=0$	$P_0=F_r$			
Thrust ball bearings	$\alpha=90°$	$P_{0a}=F_a$			
Thrust roller bearings	$\alpha=90°$				
Thrust ball bearings	$\alpha\neq 90°$	$P_{0a}=F_a+2.3\,F_r\tan\alpha$ (where, $F_a>2.3\,F_r\tan\alpha$)			
Thrust roller bearings	$\alpha\neq 90°$				

3. Bearing fitting practice

3.1 Load classifications

Bearing loads can be classified in various ways. With respect to magnitude, loads are classified as light, medium, or heavy; with respect to time, they are called stationary, fluctuating, or shock; and with respect to direction, they are divided into rotating (or "circumferential"), stationary (or "spot"), or indeterminate. The terms, "rotating", "static", and "indeterminate", do not apply to the bearing itself, but instead are used to describe the load acting on each of the bearing rings.

Whether an interference fit or a loose fit should be adopted depends on whether the load applied to the inner and outer rings is rotating or stationary. A so-called "rotating load" is one where the loading direction on a bearing ring changes continuously regardless of whether the bearing ring itself rotates or remains stationary. On the other hand, a so called "stationary load" is one where the loading direction on a bearing ring is the same regardless of whether the bearing ring itself rotates or remains stationary.

As an example, when the load direction on a bearing remains constant and the inner ring rotates and the outer ring stays fixed, a rotating load is applied to the inner ring and a stationary load to the outer ring. In the case that the majority of the bearing load is an unbalanced load due to rotation, even if the inner ring rotates and the outer ring stays fixed, a stationary load is applied to the inner ring and a rotating load to the outer ring. (See **Table 1**).

Depending on the actual conditions, the situation is not usually as simple as described above. The loads may vary in complex ways with the load direction being a combination of fixed and rotating loads caused by mass, by imbalance, by vibration, and by power transmission. If the load direction on a bearing ring is highly irregular or a rotating load and stationary load are applied alternatively, such a load is called an indeterminate load.

The fit of a bearing ring on which a rotating load is applied should generally be an interference fit. If a bearing ring, on which a rotating load is applied, is mounted with a loose fit, the bearing ring may slip on the shaft or in the housing and, if the load is heavy, the fitting surface may be damaged or fretting corrosion may occur. The tightness of the fit should be sufficient to prevent the interference from becoming zero as a result of the applied load and a temperature difference between the inner ring and shaft or between the outer ring and housing during operation. Depending on the operation conditions, the inner ring fitting is usually k5, m5, n6, etc. and for the outer ring, it is N7, P7, etc.

For large bearings, to avoid the difficulty of mounting and dismounting, sometimes a loose fit is adopted for the bearing ring on which a rotating load is applied. In such a case, the shaft material must be sufficiently hard, its surface must be well finished, and a lubricant needs to be applied to minimize damage due to slipping.

There is no problem with slipping between the shaft or housing for a bearing ring on which a stationary load is applied; therefore, a loose fit or transition fit can be used. The looseness of the fit depends on the accuracy required in use and the reduction in the load distribution range caused by bearing-ring deformation. For inner rings, g6, h6, js5(j5), etc. are often used, and for outer rings, H7, JS7(J7), etc.

For indeterminate loads, it cannot be determined easily, but in most cases, both the inner and outer rings are mounted with an interference fit.

Table 1 Rotating and stationary load of inner rings

Rotating load on inner ring	(1) When bearing load direction is constant, the inner ring rotates and the outer ring remains fixed. (2) When the inner ring remains fixed, the outer ring rotates, and the load direction rotates with the same speed as the outer ring (unbalanced load, etc.).
Static load on inner ring	(1) When the outer ring remains fixed, the inner ring rotates, and the load direction rotates with the same speed as the inner ring (unbalanced load, etc.). (2) When the load direction is constant, the outer ring rotates, and the inner ring remains fixed.

3.2 Required effective interference due to load

The magnitude of the load is an important factor in determining the fit (interference tolerance) of a bearing.

When a load is applied to the inner ring, it is compressed radially and, at the same time, it expands circumferentially a little; thereby, the initial interference is reduced.

To obtain the interference reduction of the inner ring, **Equation** (1) is usually used.

$$\left.\begin{aligned}\Delta d_F &= 0.08\sqrt{\frac{d}{B}F_r}\times10^{-3} && \text{(N)}\\ &= 0.25\sqrt{\frac{d}{B}F_r}\times10^{-3} && \{\text{kgf}\}\end{aligned}\right\}\quad\cdots\cdots\cdots\cdots (1)$$

where Δd_F: Interference reduction of inner ring due to load (mm)
d: Inner ring bore diameter (mm)
B: Inner ring width (mm)
F_r: Radial load (N), {kgf}

Therefore, the effective interference Δd should be larger than the interference given by **Equation** (1).

The interference given by **Equation** (1) is sufficient for relatively low loads (less than about 0.2 C_{0r} where C_{0r} is the static load rating. For most general applications, this condition applies). However, under special conditions where the load is heavy (when F_r is close to C_{0r}), the interference becomes insufficient.

For heavy radial loads exceeding 0.2 C_{0r}, it is better to rely on **Equation** (2).

$$\left.\begin{aligned}\Delta d &\geqq 0.02\frac{F_r}{B}\times10^{-3} && \text{(N)}\\ &\geqq 0.2\frac{F_r}{B}\times10^{-3} && \{\text{kgf}\}\end{aligned}\right\}\quad\cdots\cdots\cdots\cdots (2)$$

where Δd: Required effective interference due to load (mm)
B: Inner ring width (mm)
F_r: Radial load (N), {kgf}

Creep experiments conducted by NSK with NU219 bearings showed a linear relation between radial load (load at creep occurrence limit) and required effective interference. It was confirmed that this line agrees well with the straight line of **Equation** (2).

For NU219, with the interference given by **Equation** (1) for loads heavier than 0.25 C_{0r}, the interference becomes insufficient and creep occurs.

Generally speaking, the necessary interference for loads heavier than 0.25 C_{0r} should be calculated using **Equation** (2). When doing this, sufficient care should be taken to prevent excessive circumferential stress.

Calculation example

For NU219, B=32 (mm) and assume
F_r=98 100 N {10 000 kgf}
C_{0r}=183 000 N {18 600 kgf}

$$\frac{F_r}{C_{0r}}=\frac{98\ 100}{183\ 000}=0.536>0.2$$

Therefore, the required effective interference is calculated using **Equation** (2).

$$\Delta d=0.02\times\frac{98\ 100}{32}\times10^{-3}=0.061\ \text{(mm)}$$

This result agrees well with **Fig. 1**.

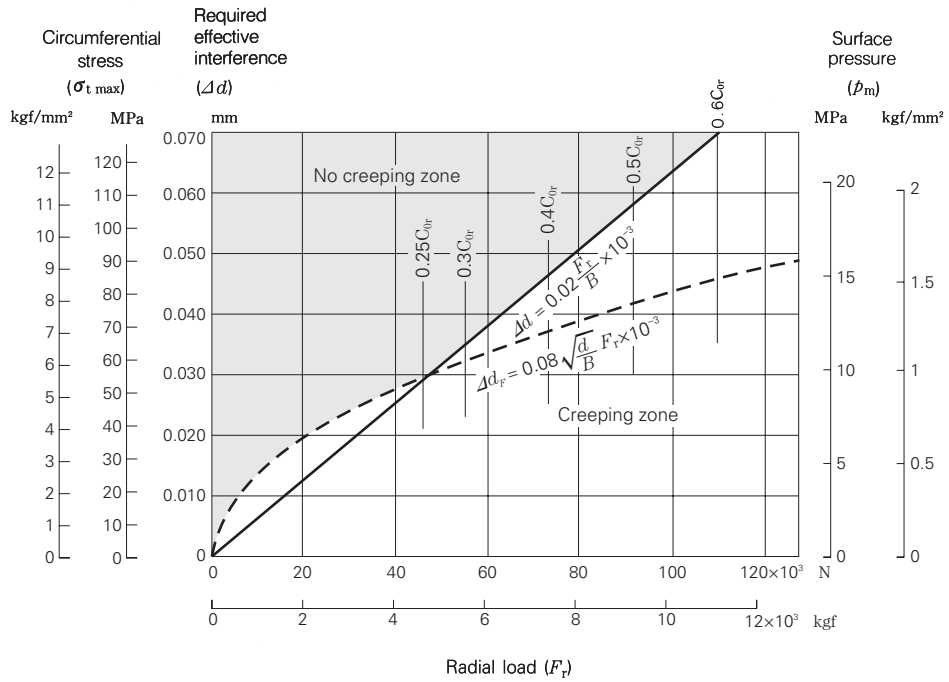

Fig. 1 Load and required effective interference for fit

3.3 Interference deviation due to temperature rise (aluminum housing, plastic housing)

For reducing weight and cost or improving the performance of equipment, bearing housing materials such as aluminum, light alloys, or plastics (polyacetal resin, etc.) are often used.

When non-ferrous materials are used in housings, any temperature rise occurring during operation affects the interference or clearance of the outer ring due to the difference in the coefficients of linear expansion. This change is large for plastics which have high coefficients of linear expansion.

The deviation ΔD_T of clearance or interference of a fitting surface of a bearing's outer ring due to temperature rise is expressed by the following equation:

$$\Delta D_T=(\alpha_1 \cdot \Delta T_1-\alpha_2 \cdot \Delta T_2)D \text{ (mm)} \quad \cdots\cdots (1)$$

where ΔD_T: Change of clearance or interference at fitting surface due to temperature rise

α_1: Coefficient of linear expansion of housing (1/°C)

ΔT_1: Housing temperature rise near fitting surface (°C)

α_2: Coefficient of linear expansion of bearing outer ring
Bearing steel .... $\alpha_2=12.5\times10^{-6}$ (1/°C)

ΔT_2: Outer ring temperature rise near fitting surface (°C)

D: Bearing outside diameter (mm)

In general, the housing temperature rise and that of the outer ring are somewhat different, but if we assume they are approximately equal near the fitting surfaces, ($\Delta T_1 \fallingdotseq \Delta T_2=\Delta T$), Equation (1) becomes,

$$\Delta D_T=(\alpha_1-\alpha_2)\ \Delta T \cdot D \text{ (mm)} \quad \cdots\cdots (2)$$

where ΔT: Temperature rise of outer ring and housing near fitting surfaces (°C)

In the case of an aluminum housing ($\alpha_1=23.7\times10^{-6}$), Equation (2) can be shown graphically as in Fig. 1.

Among the various plastics, polyacetal resin is one that is often used for bearing housings. The coefficients of linear expansion of plastics may vary or show directional characteristics. In the case of polyacetal resin, for molded products, it is approximately 9×10^{-5}. Equation (2) can be shown as in Fig. 2.

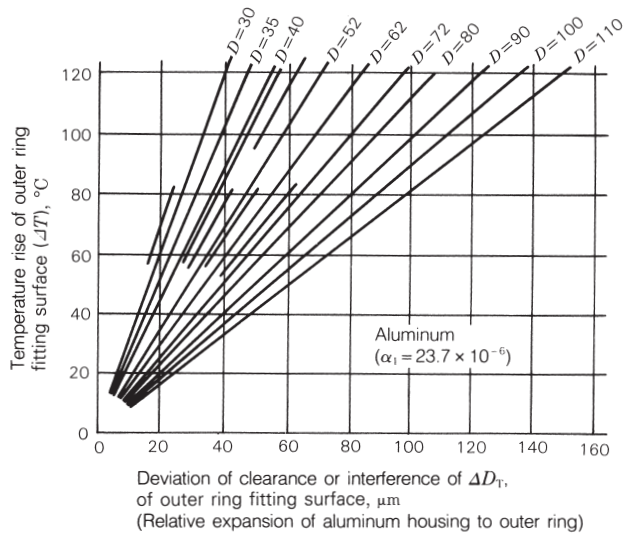

Fig. 1 Aluminum housing

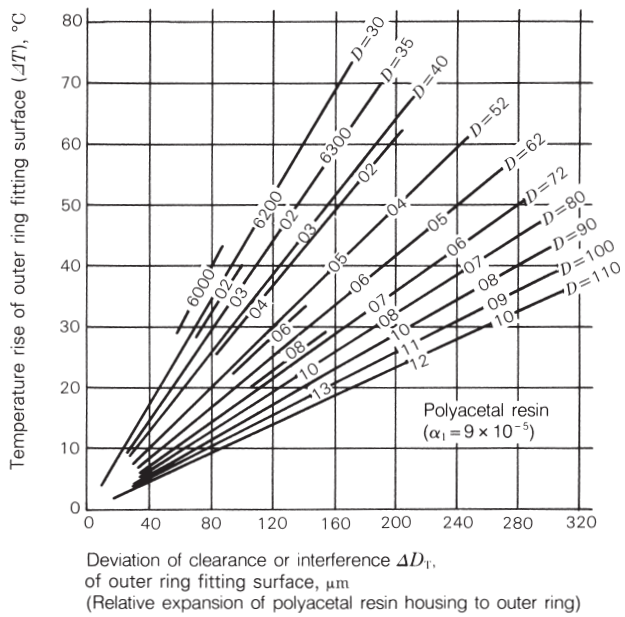

Fig. 2 Polyacetal resin housing

3.4 Fit calculation

It is easier to mount a bearings with a loose fit than with an interference fit. However, if there is clearance between the fitting surfaces or too little interference, depending on the loading condition, creep may occur and damage the fitting surfaces; therefore, a sufficient interference must be chosen to prevent such damage.

The most common loading condition is to have a fixed load and fixed direction with the inner ring (i.e. shaft) rotating and the outer ring stationary. This condition is referred to as a rotating load on the inner ring or a stationary load on the outer ring. In other words, a circumferential load is applied to the inner ring and a spot load on the outer ring.

In the case of automobile wheels, a circumferential load is applied to the outer ring (rotating load on outer ring) and a spot load on the inner ring. In any case, for a spot load, the interference can be almost negligible, but it must be tight for the bearing ring to which a circumferential load is applied.

For indeterminate loads caused by unbalanced weight, vibration, etc., the magnitude of the interference should be almost the same as for circumferential loads. The interference appropriate for the tolerances of the shaft and housing given in the bearing manufacturer's catalog is sufficient for most cases.

If a bearing ring is mounted with interference, the ring becomes deformed and stress is generated. This stress is calculated in the same way as for thick-walled cylinders to which uniform internal and external pressures are applied. The equations for both inner and outer rings are summarized in Table 1. The Young's modulus and Poisson's ratio for the shaft and housing are assumed to be the same as for the inner and outer rings.

What we obtain by measurement is called "apparent interference", but what is necessary is "effective interference" (Δd and ΔD given in Table 1 are effective interferences). Since the effective interference is related to the reduction of bearing internal clearance caused by fit, the relation between apparent interference and effective interference is important.

The effective interference is less than the apparent interference mainly due to the deformation of the fitting surface caused by the fit.

The relation between apparent interference Δd_a and effective interference Δd is not necessarily uniform. Usually, the following equations can be used though they differ a little from empirical equations due to roughness.

For ground shafts: $\Delta d = \dfrac{d}{d+2}\,\Delta d_a$ (mm)

For machined shafts: $\Delta d = \dfrac{d}{d+3}\,\Delta d_a$ (mm)

Satisfactory results can be obtained by using the nominal bearing ring diameter when estimating the expansion/contraction of a ring to correct the internal bearing clearance. It is not necessary to use the mean outside diameter (or mean bore diameter) which gives an equal cross sectional area.

Table 1 Fit conditions

	Inner ring and shaft	Outer ring and housing
Surface pressure p_m (MPa) {kgf/mm²}	Hollow shaft $p_m = \dfrac{\Delta d}{d}\,\dfrac{1}{\left[\dfrac{m_s-1}{m_sE_s}-\dfrac{m_i-1}{m_iE_i}\right]+2\left[\dfrac{k_0^2}{E_s(1-k_0^2)}+\dfrac{1}{E_i(1-k_2)}\right]}$ Solid shaft $p_m = \dfrac{\Delta d}{d}\,\dfrac{1}{\left[\dfrac{m_s-1}{m_sE_s}-\dfrac{m_i-1}{m_iE_i}\right]+\dfrac{2}{E_i(1-k^2)}}$	Housing outside diameter $p_m = \dfrac{\Delta D}{D}\,\dfrac{1}{\left[\dfrac{m_e-1}{m_eE_e}-\dfrac{m_h-1}{m_hE_h}\right]+2\left[\dfrac{h^2}{E_e(1-h^2)}+\dfrac{1}{E_h(1-h_e^2)}\right]}$
Expansion of inner ring raceway ΔD_i (mm) Contraction of outer ring raceway ΔD_e (mm)	$\Delta D_i = 2d\,\dfrac{p_m}{E_i}\,\dfrac{k}{1-k^2}$ $= \Delta d \cdot k\,\dfrac{1-k_0^2}{1-k^2k_0^2}$ (hollow shaft) $= \Delta d \cdot k$ (solid shaft)	$\Delta D_e = 2D\,\dfrac{p_m}{E_e}\,\dfrac{h}{1-h^2}$ $= \Delta D \cdot h\,\dfrac{1-h_0^2}{1-h^2h_0^2}$
Maximum stress $\sigma_{t\,max}$ (MPa) {kgf/mm²}	Circumferential stress at inner ring bore fitting surface is maximum. $\sigma_{t\,max} = p_m\,\dfrac{1+k^2}{1-k^2}$	Circumferential stress at outer ring bore surface is maximum. $\sigma_{t\,max} = p_m\,\dfrac{2}{1-h^2}$
Symbols	d : Shaft diameter, inner ring bore d_0: Hollow shaft bore D_i: Inner ring raceway diameter $k = d/D_i$, $k_0 = d_0/d$ E_i: Inner ring Young's modulus, 208 000 MPa {21 200 kgf/mm²} E_s: Shaft Young's modulus m_i: Inner ring poisson's number, 3.33 m_s: Shaft poisson's number	D : Housing bore diameter, outer ring outside diameter D_0: Housing outside diameter D_e: Outer ring raceway diameter $h = D_e/D$, $h_0 = D/D_0$ E_e: Outer ring Young's modulus, 208 000 MPa {21 200 kgf/mm²} E_h: Housing Young's modulus m_e: Outer ring poisson's number, 3.33 m_h: Housing poisson's number

3.5 Surface pressure and maximum stress on fitting surfaces

In order for rolling bearings to achieve their full life expectancy, their fitting must be appropriate. Usually for an inner ring, which is the rotating ring, an interference fit is chosen, and for a fixed outer ring, a loose fit is used. To select the fit, the magnitude of the load, the temperature differences among the bearing and shaft and housing, the material characteristics of the shaft and housing, the level of finish, the material thickness, and the bearing mounting/dismounting method must all be considered.

If the interference is insufficient for the operating conditions, ring loosening, creep, fretting, heat generation, etc. may occur. If the interference is excessive, the ring may crack. The magnitude of the interference is usually satisfactory if it is set for the size of the shaft or housing listed in the bearing manufacturer's catalog. To determine the surface pressure and stress on the fitting surfaces, calculations can be made assuming a thick-walled cylinder with uniform internal and external pressures. To do this, the necessary equations are summarized in Section 3.4 "Fit calculation". For convenience in the fitting of bearing inner rings on solid steel shafts, which are the most common, the surface pressure and maximum stress are shown in Figs. 2 and 3.

Fig. 2 shows the surface pressure p_m and maximum stress $\sigma_{t\ max}$ variations with shaft diameter when interference results from the mean values of the tolerance grade shaft and bearing bore tolerances. Fig. 3 shows the maximum surface pressure p_m and maximum stress $\sigma_{t\ max}$ when maximum interference occurs.

Fig. 3 is convenient for checking whether $\sigma_{t\ max}$ exceeds the tolerances. The tensile strength of hardened bearing steel is about 1 570 to 1 960 MPa {160 to 200 kgf/mm²}. However, for safety, plan for a maximum fitting stress of 127 MPa {13 kgf/mm²}. For reference, the distributions of circumferential stress σ_t and radial stress σ_r in an inner ring are shown in Fig. 1.

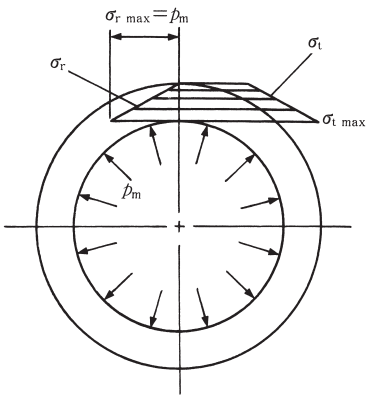

Fig. 1 Distribution of circumferential stress σ_t and radial stress σ_r

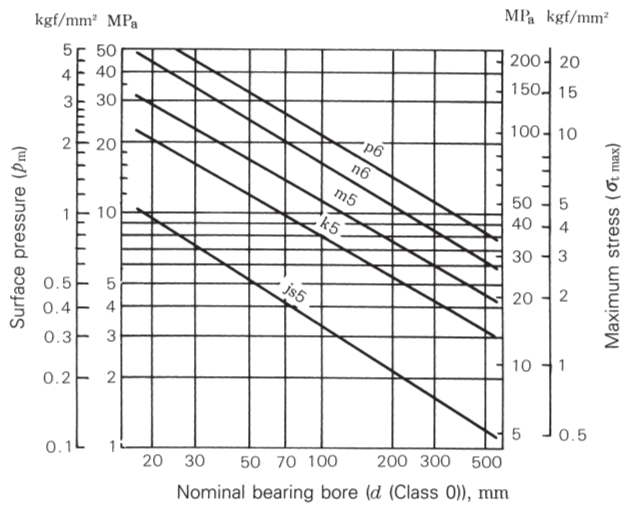

Fig. 2 Surface pressure p_m and maximum stress $\sigma_{t\ max}$ for mean interference in various tolerance grades

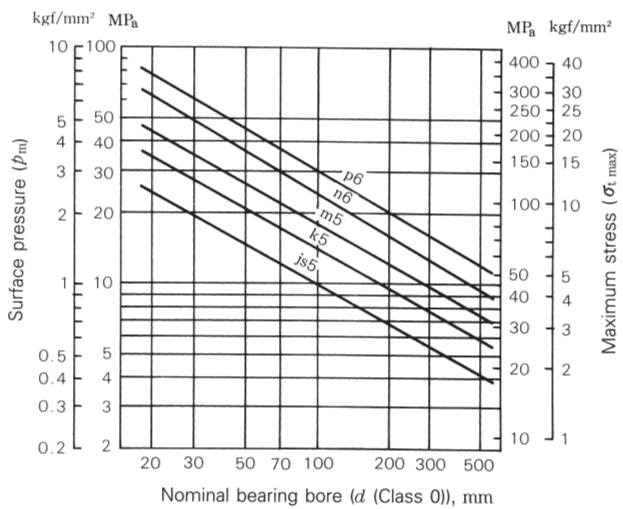

Fig. 3 Surface pressure p_m and maximum stress $\sigma_{t\ max}$ for maximum interference in various tolerance grades

3.6 Mounting and withdrawal loads

The push-up load needed to mount bearings on shafts or in a housing hole with interference can be obtained using the thick-walled cylinder theory.

The mounting load (or withdrawal load) depends upon the contact area, surface pressure, and coefficient of friction between the fitting surfaces.

The mounting load (or withdrawal load) K needed to mount inner rings on shafts is given by Equation (1).

$$K=\mu\ p_m\ \pi\ d\ B\ \text{(N), \{kgf\}} \quad \cdots\cdots (1)$$

where μ: Coefficient of friction between fitting surfaces
μ=0.12 (for mounting)
μ=0.18 (for withdrawal)

p_m: Surface pressure (MPa), {kgf/mm^2}
For example, inner ring surface pressure can be obtained using Table 1 (Page 69)

$$p_m=\frac{E}{2}\ \frac{\Delta d}{d}\ \frac{(1-k^2)\ (1-k_0^2)}{1-k^2\ k_0^2}$$

d: Shaft diameter (mm)
B: Bearing width (mm)
Δd: Effective interference (mm)
E: Young's modulus of steel (MPa), {kgf/mm^2}
E=208 000 MPa {21 200 kgf/mm^2}
k: Inner ring thickness ratio
$k=d/D_i$
D_i: Inner ring raceway diameter (mm)
k_0: Hollow shaft thickness ratio
$k_0=d_0/d$
d_0: Bore diameter of hollow shaft (mm)

For solid shafts, d_0=0, consequently k_0=0. The value of k varies depending on the bearing type and size, but it usually ranges between k=0.7 and 0.9. Assuming that k=0.8 and the shaft is solid, Equation (1) is:

$$\left.\begin{aligned} K &= 118\ 000\mu\ \Delta d\ B\ \text{(N)} \\ &= 12\ 000\mu\ \Delta d\ B\ \text{\{kgf\}} \end{aligned}\right\} \cdots\cdots (2)$$

Equation (2) is shown graphically in Fig. 1. The mounting and withdrawal loads for outer rings and housings have been calculated and the results are shown in Fig. 2.

The actual mounting and withdrawal loads can become much higher than the calculated values if the bearing ring and shaft (or housing) are slightly misaligned or the load is applied unevenly to the circumference of the bearing ring hole. Consequently, the loads obtained from Figs. 1 and 2 should be considered only as guides when designing withdrawal tools, their strength should be five to six times higher than that indicated by the figures.

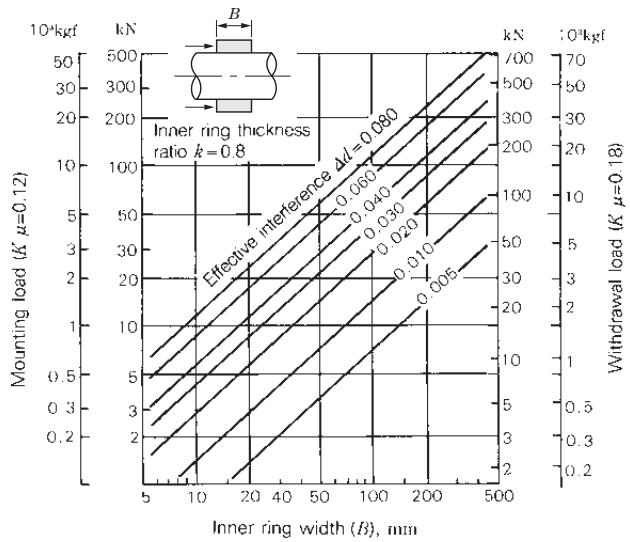

Fig. 1 Mounting and withdrawal loads for inner rings

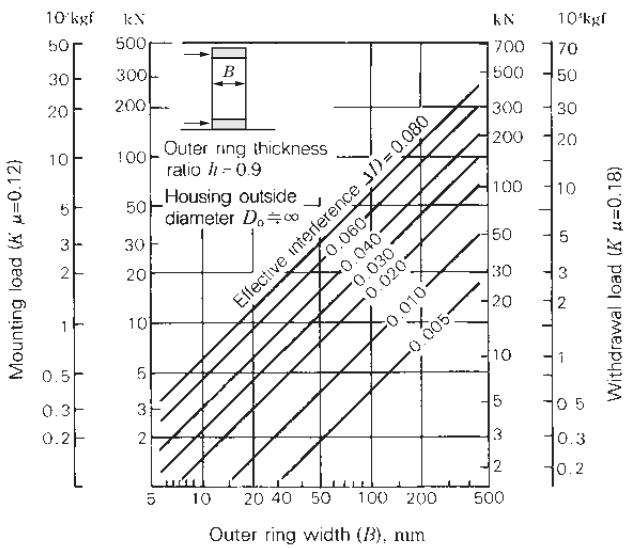

Fig. 2 Mounting and withdrawal loads for outer rings

3.7 Tolerances for bore diameter and outside diameter

The accuracy of the inner-ring bore diameter and outer-ring outside diameter and the width of rolling bearings is specified by JIS which complies with ISO.

In the previous JIS, the upper and lower dimensional tolerances were adopted to the average diameter of the entire bore or outside surfaces (d_m or D_m) regarding the dimensions of inner ring bore diameter and outer ring outside diameter which are important for fitting the shaft and housing.

Consequently, a standard was introduced for the upper and lower dimensional tolerances concerning the bore diameter, d, and outside diameter, D. However, there was no standard for the profile deviation like bore and outside out-of-roundness and cylindricity. Each bearing manufacturer specified independently the tolerances or criteria of the ellipse and cylindricity based on the maximum and minimum tolerances of d_m or D_m and d or D.

In the new JIS (JIS B 1514 : 1986, revised in July 1, 1986, Accuracy of rolling bearings) matched to ISO standards, tolerances, Δ_{dmpI}, Δ_{dmpII}, ... and Δ_{DmpI}, Δ_{DmpII}, ..., of the bore and outside mean diameters in a single radial plane, d_{mpI}, d_{mpII}, ... and D_{mpI}, D_{mpII}, ..., are within the allowable range between upper and lower limits.

The new JIS specifies the maximum values of bore and outside diameter variations within a single plane, V_{dp} and V_{Dp} which are equivalent to the out-of-roundness. Regarding the cylindricity, JIS also specifies the maximum values of the variations of mean bore diameters and mean outside diameters in a single radial plane, V_{dmp} and V_{Dmp}.

Table 1 Tolerances of radial bearing inner rings (Accuracy Class 0) except tapered roller bearings

Units: μm

Nominal bore diameter d (mm)		Single plane mean bore diameter deviation Δ_{dmp}		Diameter series: 7, 8, 9 — Bore diameter variation in a plane V_{dp}	Diameter series: 0, 1 — Bore diameter variation in a plane V_{dp}	Diameter series: 2, 3, 4 — Bore diameter variation in a plane V_{dp}	Mean bore diameter variation V_{dmp}	Radial runout of inner ring K_{ia}	Single bearing — Deviation of inner or outer ring width Δ_{Bs} (or Δ_{Cs})		Matched set bearing(1) — Deviation of inner or outer ring width Δ_{Bs} (or Δ_{Cs})		Inner ring width variation V_{Bs}
over	incl	high	low	max.	max.	max.	max.	max.	high	low	high	low	max.
omitted	omitted	omitted	omitted	omitted	omitted	omitted	omitted	omitted	omitted	omitted	omitted	omitted	omitted
10	**18**	0	− 8	10	8	6	6	10	0	−120	0	−250	20
18	**30**	0	−10	13	10	8	8	13	0	−120	0	−250	20
30	**50**	0	−12	15	12	9	9	15	0	−120	0	−250	20
50	**80**	0	−15	19	19	11	11	20	0	−150	0	−380	25
80	**120**	0	−20	25	25	15	15	25	0	−200	0	−380	25
120	**180**	0	−25	31	31	19	19	30	0	−250	0	−500	30
omitted	omitted	omitted	omitted	omitted	omitted	omitted	omitted	omitted	omitted	omitted	omitted	omitted	omitted

Note (1) Applicable to individual rings manufactured for combined bearings.

[All radial planes]

$$d_m = \frac{d_s\ (\text{max.}) + d_s\ (\text{min.})}{2}$$

$$= \frac{d_{spI}\ (\text{max.}) + d_{spII}\ (\text{min.})}{2}$$

[Radial plane I]

$$d_{mpI} = \frac{d_{spI}\ (\text{max.}) + d_{spI}\ (\text{min.})}{2}$$

$$\Delta_{DmpI} = d_{mpI} - d$$

$$V_{dpI} = d_{spI}\ (\text{max.}) - d_{spI}\ (\text{min.})$$

[Three radial planes]

$$V_{dmp} = d_{mpI} - d_{mpII}$$

Suffix "s" means single measurement, "p" means radial plane.

Mean bore diameter at each plane

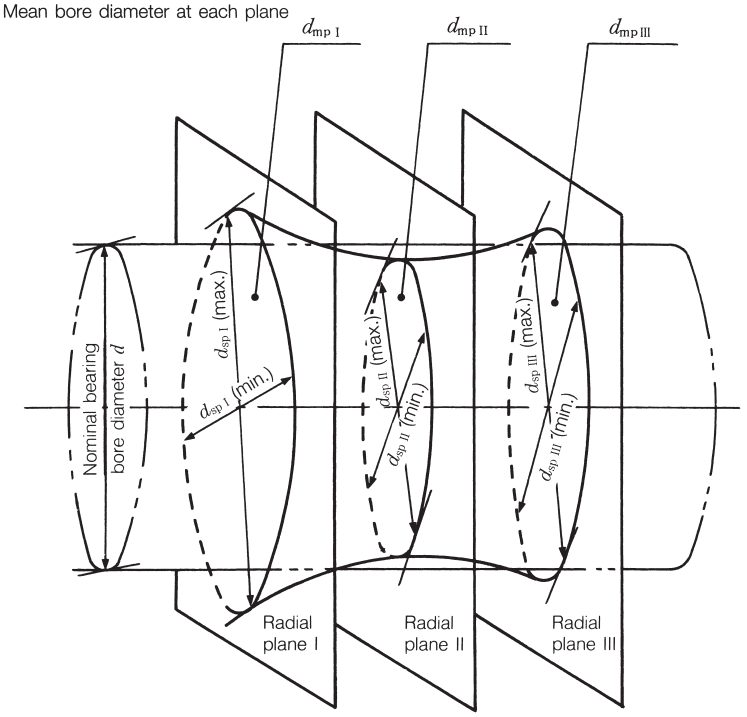

3.8 Interference and clearance for fitting (shafts and inner rings)

The tolerances on bore diameter d and outside diameter D of rolling bearings are specified by ISO. For tolerance Class 0, js5(j5), k5, and m5 are commonly used for shafts and H7, JS7(J7) housings. The class of fit that should be used is given in the catalogs of bearing manufacturers. The maximum and minimum interference for the fit of shafts and inner rings for each fitting class are given in Table 1. The recommended fits given in catalogs are target values; therefore, the machining of shafts and housings should be performed aiming at the center of the respective tolerances.

Table 1 Interferences and clearances for inner ring and shaft fit

Units: μm

Nominal size (mm)		Bearing single plane mean bore diameter deviation (Bearing: Normal class) Δd_{mp}		Interferences or clearances for each shaft tolerance																												Nominal size (mm)	
				f6		g5		g6		h5		h6		js5		j5		js6		j6		k5		k6		m5		m6		n6		p6		r6			
				Clearance		Clearance	Interference	Clearance	Interference	Clearance	Interference	Clearance	Interference	Clearance	Interference	Clearance	Interference	Clearance	Interference	Clearance	Interference	Interference		Interference		Interference		Interference		Interference		Interference		Interference			
over	incl	high	low	max.	min	max.	max.	max.	max.	max.	max.	max.	max.	max.	max.	max.	max.	max.	max.	max.	max.	min.	max.	min.	max.	min.	max.	min.	max.	min.	max.	min.	max.	min.	max.	over	incl
3	**6**	0	−8	18	2	9	4	12	4	5	8	8	8	—	—	—	—	—	—	—	—	—	—	—	—	—	—	—	—	—	—	—	—	—	—	**3**	**6**
6	**10**	0	−8	22	5	11	3	14	3	6	8	9	8	3	11	2	12	4.5	12.5	2	15	—	—	—	—	—	—	—	—	—	—	—	—	—	—	**6**	**10**
10	**18**	0	−8	27	8	14	2	17	2	8	8	11	8	4	12	3	13	5.5	13.5	3	16	—	—	—	—	—	—	—	—	—	—	—	—	—	—	**10**	**18**
18	**30**	0	−10	33	10	16	3	20	3	9	10	13	10	4.5	14.5	4	15	6.5	16.5	4	19	2	21	2	25	—	—	—	—	—	—	—	—	—	—	**18**	**30**
30	**50**	0	−12	41	13	20	3	25	3	11	12	16	12	5.5	17.5	5	18	8	20	5	23	2	25	2	30	9	32	9	37	—	—	—	—	—	—	**30**	**50**
50	**65**	0	−15	49	15	23	5	29	5	13	15	19	15	6.5	21.5	7	21	9.5	24.5	7	27	2	30	2	36	11	39	11	45	—	—	—	—	—	—	**50**	**65**
65	**80**	0	−15	49	15	23	5	29	5	13	15	19	15	6.5	21.5	7	21	9.5	24.5	7	27	2	30	2	36	11	39	11	45	20	54	—	—	—	—	**65**	**80**
80	**100**	0	−20	58	16	27	8	34	8	15	20	22	20	7.5	27.5	9	26	11	31	9	33	3	38	3	45	13	48	13	55	23	65	37	79	—	—	**80**	**100**
100	**120**	0	−20	58	16	27	8	34	8	15	20	22	20	7.5	27.5	9	26	11	31	9	33	3	38	3	45	13	48	13	55	23	65	37	79	—	—	**100**	**120**
120	**140**	0	−25	68	18	32	11	39	11	18	25	25	25	9	34	11	32	12.5	37.5	11	39	3	46	3	53	15	58	15	65	27	77	43	93	63	113	**120**	**140**
140	**160**	0	−25	68	18	32	11	39	11	18	25	25	25	9	34	11	32	12.5	37.5	11	39	3	46	3	53	15	58	15	65	27	77	43	93	65	115	**140**	**160**
160	**180**	0	−25	68	18	32	11	39	11	18	25	25	25	9	34	11	32	12.5	37.5	11	39	3	46	3	53	15	58	15	65	27	77	43	93	68	118	**160**	**180**
180	**200**	0	−30	79	20	35	15	44	15	20	30	29	30	10	40	13	37	14.5	44.5	13	46	4	54	4	63	17	67	17	76	31	90	50	109	77	136	**180**	**200**
200	**225**	0	−30	79	20	35	15	44	15	20	30	29	30	10	40	13	37	14.5	44.5	13	46	4	54	4	63	17	67	17	76	31	90	50	109	80	139	**200**	**225**
225	**250**	0	−30	79	20	35	15	44	15	20	30	29	30	10	40	13	37	14.5	44.5	13	46	4	54	4	63	17	67	17	76	31	90	50	109	84	143	**225**	**250**
250	**280**	0	−35	88	21	40	18	49	18	23	35	32	35	11.5	46.5	16	42	16	51	16	51	4	62	4	71	20	78	20	87	34	101	56	123	94	161	**250**	**280**
280	**315**	0	−35	88	21	40	18	49	18	23	35	32	35	11.5	46.5	16	42	16	51	16	51	4	62	4	71	20	78	20	87	34	101	56	123	98	165	**280**	**315**
315	**355**	0	−40	98	22	43	22	54	22	25	40	36	40	12.5	52.5	18	47	18	58	18	58	4	69	4	80	21	86	21	97	37	113	62	138	108	184	**315**	**355**
355	**400**	0	−40	98	22	43	22	54	22	25	40	36	40	12.5	52.5	18	47	18	58	18	58	4	69	4	80	21	86	21	97	37	113	62	138	114	190	**355**	**400**
400	**450**	0	−45	108	23	47	25	60	25	27	45	40	45	13.5	58.5	20	52	20	65	20	65	5	77	5	90	23	95	23	108	40	125	68	153	126	211	**400**	**450**
450	**500**	0	−45	108	23	47	25	60	25	27	45	40	45	13.5	58.5	20	52	20	65	20	65	5	77	5	90	23	95	23	108	40	125	68	153	132	217	**450**	**500**

Remarks 1. The interference figures are omitted if the stress due to fit between inner ring and shaft is excessive.
2. From now on the js class in recommended instead of the j class.

3.9 Interference and clearance for fitting (housing holes and outer rings)

The maximum and minimum interference for the fit between housings and outer rings are shown in Table 1. Inner rings are interference fitted in most cases, but the usual fit for outer rings is generally a loose or transition fit. With the J6 or N7 classes as shown in the Table 1, if the combination is a transition fit with a maximum size hole and minimum size bearing O.D., there will be a clearance between them. Conversely, if the combination is one with a minimum size hole and maximum size bearing O.D., there will be interference.

If the bearing load is a rotating load on the inner ring, there is no problem with a loose fit (usually H7) of the outer ring. If the loading direction on the outer ring rotates or fluctuates, the outer ring must also be mounted with interference. In such cases, the load characteristics determine whether it shall be a full interference fit or a transition fit with a target interference specified.

Table 1 Interference and clearance of fit of outer rings with housing

Units: μm

Nominal size (mm)		Bearing single plane mean outside diameter deviation (Bearing: Normal class) ΔD_{mp}		Interferences or clearances for each housing tolerance																												Nominal size (mm)	
				G7		H6		H7		H8		J6		JS6		J7		JS7		K6		K7		M6		M7		N6		N7		P6		P7			
				Clearance		Clearance		Clearance		Clearance		Clearance	Interference	Clearance	Interference	Clearance	Interference	Clearance	Interference	Clearance	Interference	Clearance	Interference	Clearance	Interference	Clearance	Interference	Clearance	Interference	Clearance	Interference	Interference		Interference			
over	incl	high	low	max.	min.	max.	min.	max.	min.	max.	min.	max.	max.	max.	max.	max.	max.	max.	max.	max.	max.	max.	max.	max.	max.	max.	max.	max.	max.	max.	max.	min.	max.	min.	max.	over	incl
6	**10**	0	− 8	28	5	17	0	23	0	30	0	13	4	12.5	4.5	16	7	15	7	10	7	13	10	5	12	8	15	1	16	4	19	4	21	1	24	**6**	**10**
10	**18**	0	− 8	32	6	19	0	26	0	35	0	14	5	13.5	5.5	18	8	17	9	10	9	14	12	4	15	8	18	1(1)	20	3	23	7	26	3	29	**10**	**18**
18	**30**	0	− 9	37	7	22	0	30	0	42	0	17	5	15.5	6.5	21	9	19	10	11	11	15	15	5	17	9	21	2(1)	24	2	28	9	31	5	35	**18**	**30**
30	**50**	0	−11	45	9	27	0	36	0	50	0	21	6	19	8	25	11	23	12	14	13	18	18	7	20	11	25	1(1)	28	3	33	10	37	6	42	**30**	**50**
50	**80**	0	−13	53	10	32	0	43	0	59	0	26	6	22.5	9.5	31	12	28	15	17	15	22	21	8	24	13	30	1(1)	33	4	39	13	45	8	51	**50**	**80**
80	**120**	0	−15	62	12	37	0	50	0	69	0	31	6	26	11	37	13	32	17	19	18	25	25	9	28	15	35	1(1)	38	5	45	15	52	9	59	**80**	**120**
120	**150**	0	−18	72	14	43	0	58	0	81	0	36	7	30.5	12.5	44	14	38	20	22	21	30	28	10	33	18	40	2(1)	45	6	52	18	61	10	68	**120**	**150**
150	**180**	0	−25	79	14	50	0	65	0	88	0	43	7	37.5	12.5	51	14	45	20	29	21	37	28	17	33	25	40	5	45	13	52	11	61	3	68	**150**	**180**
180	**250**	0	−30	91	15	59	0	76	0	102	0	52	7	44.5	14.5	60	16	53	23	35	24	43	33	22	37	30	46	8	51	16	60	11	70	3	79	**180**	**250**
250	**315**	0	−35	104	17	67	0	87	0	116	0	60	7	51	16	71	16	61	26	40	27	51	36	26	41	35	52	10	57	21	66	12	79	1	88	**250**	**315**
315	**400**	0	−40	115	18	76	0	97	0	129	0	69	7	58	18	79	18	67	28	47	29	57	40	30	46	40	57	14	62	24	73	11	87	1	98	**315**	**400**
400	**500**	0	−45	128	20	85	0	108	0	142	0	78	7	65	20	88	20	76	31	53	32	63	45	35	50	45	63	18	67	28	80	10	95	0	108	**400**	**500**
500	**630**	0	−50	142	22	94	0	120	0	160	0	—	—	72	22	—	—	85	35	50	44	50	70	24	70	24	96	6	88	6	114	28	122	28	148	**500**	**630**
630	**800**	0	−75	179	24	125	0	155	0	200	0	—	—	100	25	—	—	115	40	75	50	75	80	45	80	45	110	25	100	25	130	13	138	13	168	**630**	**800**
800	**1 000**	0	−100	216	26	156	0	190	0	240	0	—	—	128	28	—	—	145	45	100	56	100	90	66	90	66	124	44	112	44	146	0	156	0	190	**800**	**1 000**

Note (1) Minimum interferences are listed.

Remarks In the future, JS class in recommended instead of J class.

3.10 Interference dispersion (shafts and inner rings)

The residual clearance in bearings is calculated by subtracting from the initial radial clearance the expansion or contraction of the bearing rings caused by their fitting.

In this residual clearance calculation, usually the pertinent bearing dimensions (shaft diameter, bore diameter of inner ring, bore diameter of housing, outside diameter of outer ring) are assumed to have a normal (Guassian) distribution within their respective tolerance specifications.

If the shaft diameter and inner-ring bore diameter both have normal (Gaussian) distributions and their reject ratios are the same, then the range of distribution of interference R (dispersion) that has the same reject ratio as the shaft and inner-ring bore is given by the following equation:

$$R=\sqrt{R_s^2+R_i^2} \quad \cdots\cdots (1)$$

where R_s: Shaft diameter tolerance (range of specification)
R_i: Inner-ring bore diameter tolerance (range of specification)

The mean interference and its dispersion R based on the tolerances on inner-ring bore diameters d of radial bearings of Normal Class and shafts of Classes 5 and 6 are shown in Table 1.

Table 1 Mean value and dispersion of interference for fitting of inner rings with shafts

Units: μm

Nominal size (mm)		Bearing single plane mean bore diameter deviation (Bearing: Normal class) Δd_{mp}		Fit with Class 5 shaft												Fit with Class 6 shaft								
				Mean value of interference												Mean value of interference (1)								Dispersion of interference $R=\sqrt{R_s^2+R_i^2}$
over	incl	high	low	h5	js5	j5	k5	m5	Dispersion of interference $R=\sqrt{R_s^2+R_i^2}$	h6	js6	j6	k6	m6	n6	p6	r6	
—	**3**	0	−8	2	4	4	6	8	±4.5	1	4	5	7	9	11	13	17	±5
3	**6**	0	−8	1.5	4	4.5	7.5	10.5	±4.5	0	4	6	9	12	16	20	23	±5.5
6	**10**	0	−8	1	4	5	8	13	±5	−0.5	4	6.5	9.5	14.5	18.5	23.5	27.5	±6
10	**18**	0	−8	0	4	5	9	15	±5.5	−1.5	4	6.5	10.5	16.5	21.5	27.5	32.5	±7
18	**30**	0	−10	0.5	5	5.5	11.5	17.5	±6.5	−1.5	5	7.5	13.5	19.5	26.5	33.5	39.5	±8
30	**50**	0	−12	0.5	6	6.5	13.5	20.5	±8	−2	6	9	16	23	31	40	48	±10
50	**65**	0	−15	1	7.5	7	16	25	±10	−2	7.5	10	19	28	37	49	58	±12
65	**80**	0	−15	1	7.5	7	16	25	±10	−2	7.5	10	19	28	37	49	60	±12
80	**100**	0	−20	2.5	10	8.5	20.5	30.5	±12.5	−1	10	12	24	34	44	58	72	±15
100	**120**	0	−20	2.5	10	8.5	20.5	30.5	±12.5	−1	10	12	24	34	44	58	75	±15
120	**140**	0	−25	3.5	12.5	10.5	24.5	36.5	±15.5	0	12.5	14	28	40	52	68	88	±17.5
140	**160**	0	−25	3.5	12.5	10.5	24.5	36.5	±15.5	0	12.5	14	28	40	52	68	90	±17.5
160	**180**	0	−25	3.5	12.5	10.5	24.5	36.5	±15.5	0	12.5	14	28	40	52	68	93	±17.5
180	**200**	0	−30	5	15	12	29	42	±18	0.5	15	16.5	33.5	46.5	60.5	79.5	106.5	±21
200	**225**	0	−30	5	15	12	29	42	±18	0.5	15	16.5	33.5	46.5	60.5	79.5	109.5	±21
225	**250**	0	−30	5	15	12	29	42	±18	0.5	15	16.5	33.5	46.5	60.5	79.5	113.5	±21
250	**280**	0	−35	6	17.5	13	33	49	±21	1.5	17.5	17.5	37.5	53.5	67.5	89.5	127.5	±23.5
280	**315**	0	−35	6	17.5	13	33	49	±21	1.5	17.5	17.5	37.5	53.5	67.5	89.5	131.5	±23.5
315	**355**	0	−40	7.5	20	14.5	36.5	53.5	±23.5	2	20	20	42	59	75	100	146	±27
355	**400**	0	−40	7.5	20	14.5	36.5	53.5	±23.5	2	20	20	42	59	75	100	152	±27
400	**450**	0	−45	9	22.5	16	41	59	±26	2.5	22.5	22.5	47.5	65.5	82.5	110.5	168.5	±30

Note (1) Negative mean value of the interference indicates clearance.

3.11 Interference dispersion (housing bores and outer rings)

In a manner similar to the previous interference dispersion for shafts and inner rings, that for housings and outer rings is shown in Table 1. The interference dispersion R in Table 1 is given by the following equation:

$$R=\sqrt{R_e^2+R_H^2} \quad \cdots\cdots (1)$$

where R_e: Tolerance on outside diameter of outer ring (range of specification value)

R_H: Tolerance on bore diameter of housing (range of specification value)

This is based on the property that the sum of two or more numbers, which are normally distributed, is also distributed normally (rule for the addition of Gaussian distributions).

Table 1 shows the mean value and dispersion R of interference for the fitting of radial bearings of Normal Class and housings of Classes 6 and 7.

This rule for the addition of Gaussian distributions is widely used for calculating residual clearance and estimating the overall dispersion of a series of parts which are within respective tolerance ranges.

Table 1 Mean value and dispersion of interference for the fitting of outer rings with housings

Units: μm

Nominal size (mm)		Bearing single plane mean outside diameter deviation (Bearing: Normal class) ΔD_{mp}		Fit with Class 6 housing						Fit with Class 7 housing							
				Mean value of interference (1)					Dispersion of interference	Mean value of interference (1)							Dispersion of interference
over	incl	high	low	H6	J6	JS6	K6	M6	N6	P6	$R=\sqrt{R_e^2+R_H^2}$	H7	J7	JS7	K7	M7	N7	P7	$R=\sqrt{R_e^2+R_H^2}$
3	**6**	0	−8	−8	−5	−4	−2	1	5	9	±5.5	−10	−4	−4	−1	2	6	10	±7
6	**10**	0	−8	−8.5	−4.5	−4	−1.5	3.5	7.5	12.5	±6	−11.5	−4.5	−4	−1.5	3.5	7.5	12.5	±8.5
10	**18**	0	−8	−9.5	−4.5	−4	−0.5	5.5	10.5	16.5	±7	−13	−5	−4	−1	5	10	16	±10
18	**30**	0	−9	−11	−6	−4.5	0	6	13	20	±8	−15	−6	−4.5	0	6	13	20	±11.5
30	**50**	0	−11	−13.5	−7.5	−5.5	−0.5	6.5	14.5	23.5	±9.5	−18	−7	−5.5	0	7	15	24	±13.5
50	**80**	0	−13	−16	−10	−6.5	−1	8	17	29	±11.5	−21.5	−9.5	−6.5	−0.5	8.5	17.5	29.5	±16.5
80	**120**	0	−15	−18.5	−12.5	−7.5	−0.5	9.5	19.5	33.5	±13.5	−25	−12	−7.5	0	10	20	34	±19
120	**150**	0	−18	−21.5	−14.5	−9	−0.5	11.5	23.5	39.5	±15.5	−29	−15	−9	−1	11	23	39	±22
150	**180**	0	−25	−25	−18	−12.5	−4	8	20	36	±17.5	−32.5	−18.5	−12.5	−4.5	7.5	19.5	35.5	±23.5
180	**250**	0	−30	−29.5	−22.5	−15	−5.5	7.5	21.5	40.5	±21	−38	−22	−15	−5	8	22	41	±27.5
250	**315**	0	−35	−33.5	−26.5	−17.5	−6.5	7.5	23.5	45.5	±23.5	−43.5	−27.5	−17.5	−7.5	8.5	22.5	44.5	±31.5
315	**400**	0	−40	−38	−31	−20	−9	8	24	49	±27	−48.5	−30.5	−20	−8.5	8.5	24.5	49.5	±35
400	**500**	0	−45	−42.5	−35.5	−22.5	−10.5	7.5	24.5	52.5	±30	−54	−34	−22.5	−9	9	26	54	±38.5
500	**630**	0	−50	−47	—	−25	−3	23	41	75	±33.5	−60	—	−25	10	36	54	88	±43
630	**800**	0	−75	−62.5	—	−37.5	−12.5	17.5	37.5	75.5	±45	−77.5	—	−37.5	2.5	32.5	52.5	90.5	±55
800	**1000**	0	−100	−78	—	−50	−22	12	34	78	±57.5	−95	—	−50	−5	29	51	95	±67

Note (1) Negative mean value of the interference indicates clearance.

3.12 Fits of four-row tapered roller bearings (metric) for roll necks

Bearings of various sizes and types are used in steel mill rolling equipment, such as rolling rolls, reducers, pinion stands, thrust blocks, table rollers, etc. Among them, roll neck bearings are the ones which must be watched most closely because of their severe operating conditions and their vital role.

As a rule for rolling bearing rings, a tight fit should be used for the ring rotating under a load. This rule applies for roll neck bearings, the fit of the inner ring rotating under the load should be tight.

However, since the rolls are replaced frequently, mounting and dismounting of the bearings on the roll necks should be easy. To meet this requirement, the fit of the roll neck and bearing is loose enabling easy handling. This means that the inner ring of the roll neck bearing which sustains relatively heavy load, may creep resulting in wear or score on the roll neck surface. Therefore, the fitting of the roll neck and bearing should have some clearance and a lubricant (with an extreme pressure additive) is applied to the bore surface to create a protective oil film.

If a loose fit is used, the roll neck tolerance should be close to the figures listed in Table 1. Compared with the bearing bore tolerance, the clearance of the fit is much larger than that of a loose fit for general rolling bearings.

The fit between the bearing outer ring and chock (housing bore) is also a loose fit as shown in Table 2.

Even if the clearance between the roll neck and bearing bore is kept within the values in Table 1, steel particles and dust in the fitting clearance may roughen the fitting surface.

Roll neck bearings are inevitably mounted with a loose fit to satisfy easy mounting/dismounting. If the roll neck bearing replacement interval is long, a tight fit is preferable.

Some rolling mills use tapered roll necks. In this case, the bearing may be mounted and dismounted with a hydraulic device.

Also, there are some rolling mills that use four-row cylindrical roller bearings where the inner ring is tightly fitted with the roll neck. By the way, inner ring replacement is easier if an induction heating device is used.

Table 1 Fits between bearing bore and roll neck

Units: μm

Nominal bore diameter d (mm)		Single plane mean bore diameter deviation Δd_{mp}		Deviation of roll neck diameter		Clearance		Wear limit of roll neck outside diameter
over	incl	high	low	high	low	min.	max.	
50	**80**	0	− 15	− 90	−125	75	125	250
80	**120**	0	− 20	−120	−150	100	150	300
120	**180**	0	− 25	−150	−175	125	175	350
180	**250**	0	− 30	−175	−200	145	200	400
250	**315**	0	− 35	−210	−250	175	250	500
315	**400**	0	− 40	−240	−300	200	300	600
400	**500**	0	− 45	−245	−300	200	300	600
500	**630**	0	− 50	−250	−300	200	300	600
630	**800**	0	− 75	−325	−400	250	400	800
800	**1000**	0	−100	−375	−450	275	450	900
1000	**1250**	0	−125	−475	−500	300	500	1000
1250	**1600**	0	−160	−510	−600	350	600	1200

Table 2 Fits between bearing outside diameter and chock bore

Units: μm

Nominal outside diameter D (mm)		Single plane mean outside diameter ΔD_{mp}		Deviation of chock bore diameter		Clearance		Wear limit and permissible ellipse of chock bore diameter
over	incl	high	low	high	low	min.	max.	
120	**150**	0	− 18	+ 57	+ 25	25	75	150
150	**180**	0	− 25	+100	+ 50	50	125	250
180	**250**	0	− 30	+120	+ 50	50	150	300
250	**315**	0	− 35	+115	+ 50	50	150	300
315	**400**	0	− 40	+110	+ 50	50	150	300
400	**500**	0	− 45	+105	+ 50	50	150	300
500	**630**	0	− 50	+100	+ 50	50	150	300
630	**800**	0	− 75	+150	+ 75	75	225	450
800	**1000**	0	−100	+150	+ 75	75	250	500
1000	**1250**	0	−125	+175	+100	100	300	600
1250	**1600**	0	−160	+215	+125	125	375	750
1600	**2000**	0	−200	+250	+150	150	450	900

4. Internal clearance

4.1 Internal clearance

Internal clearance is one of the most important factors affecting bearing performance. The bearing "internal clearance" is the relative movement of the outer and inner rings when they are lightly pushed in opposite directions. Movement in the diametrical direction is called radial clearance and that in the shaft's direction is called axial clearance.

The reason why the internal clearance is so important for bearings is that it is directly related to their performance in the following respects. The amount of clearance influences the load distribution in a bearing and this can affect its life. It also influences the noise and vibration. In addition, it can influence whether the rolling elements move by rolling or sliding motion.

Normally, bearings are installed with interference for either the inner or outer ring and this leads to its expansion or contraction which causes a change in the clearance. Also, the bearing temperature reaches saturation during operation; however, the temperature of the inner ring, outer ring, and rolling elements are all different from each other, and this temperature difference changes the clearance (Fig. 1). Moreover, when a bearing operates under load, an elastic displacement of the inner ring, outer ring, and rolling elements also leads to a change in clearance. Because of these changes, bearing internal clearance is a very complex subject.

Therefore, what is the ideal clearance? Before considering this question, let us define the following different types of clearance. The symbol for each clearance amount is shown in parentheses.

Measured Internal Clearance (Δ_1)
This is the internal clearance measured under a specified measuring load and can be called "apparent clearance". This clearance includes the elastic deformation (δ_{FO}) caused by the measuring load.

$$\Delta_1=\Delta_0+\delta_{FO}$$

Theoretical Internal Clearance (Δ_0)
This is the radial internal clearance which is the measured clearance minus the elastic deformation caused by the measuring load.

$$\Delta_0=\Delta_1+\delta_{FO}$$

δ_{FO} is significant for ball bearings, but not for roller bearings where it is assumed to be equal to zero, and thus, $\Delta_0=\Delta_1$.

Residual Internal Clearance (Δ_f)
This is the clearance left in a bearing after mounting it on a shaft and in a housing. The elastic deformation caused by the mass of the shaft, etc. is neglected. Assuming the clearance decrease caused by the ring expansion or contraction is δ_f, then:

$$\Delta_f=\Delta_0+\delta_f$$

Effective Internal Clearance (Δ)
This is the bearing clearance that exists in a machine at its operating temperature except that the elastic deformation caused by load is not included. That is to say, this is the clearance when considering only the changes due to bearing fitting δ_f and temperature difference between the inner and outer rings δ_t. The basic load ratings of bearings apply only when the effective clearance Δ=0.

$$\Delta=\Delta_f-\delta_t=\Delta_0-(\delta_f+\delta_t)$$

Operating Clearance (Δ_F)
This is the actual clearance when a bearing is installed and running under load. Here, the effect of elastic deformation δ_F is included as well as fitting and temperature. Generally, the operating clearance is not used in the calculation.

$$\Delta_F=\Delta+\delta_F$$

The most important clearance of a bearing is the effective clearance as we have already explained. Theoretically speaking, the bearing whose effective clearance Δ is slightly negative has the longest life. (The slightly negative clearance means such effective clearance that the operating clearance turns to positive by the influence of bearing load. Strictly speaking, the amount of negative clearance varies with the magnitude of bearing load.) However, it is impossible to make the clearance of all bearings to the ideal effective clearance, and we have to consider the geometrical clearance Δ_0 in order to let the minimum value of effecive clearance be zero or a slightly negative value. To obtain this value, we should have both accurate reduction amount of clearance caused by the interference of the inner ring and outer ring δ_f and accurate amount of clearance change caused by the temperature difference between inner ring and outer ring δ_t. The methods of the calculation are discussed in the following sections.

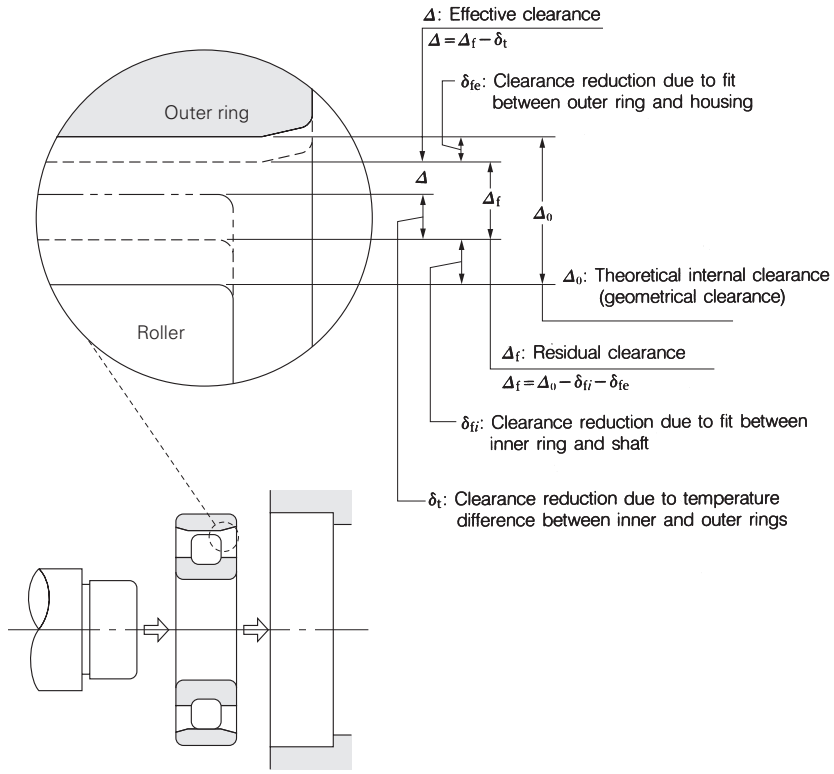

Fig. 1 Changes of radial internal clearance of roller bearing

4.2 Calculating residual internal clearance after mounting

The various types of internal bearing clearance were discussed in Section **4.1**. This section will explain the step by step procedures for calculating residual internal clearance.

When the inner ring of a bearing is press fit onto a shaft, or when the outer ring is press fit into a housing, it stands to reason that radial internal clearance will decrease due to the resulting expansion or contraction of the bearing raceways. Generally, most bearing applications have a rotating shaft which requires a tight fit between the inner ring and shaft and a loose fit between the outer ring and housing. Generally, therefore, only the effect of the interference on the inner ring needs to be taken into account.

Below we have selected a 6310 single row deep groove ball bearing for our representative calculations. The shaft is set at k5, with the housing set at H7. An interference fit is applied only to the inner ring.

Shaft diameter, bore size and radial clearance are the standard bearing measurements. Assuming that 99.7% of the parts are within tolerance, the mean value ($m_{\Delta f}$) and standard deviation ($\sigma_{\Delta f}$) of the internal clearance after mounting (residual clearance) can be calculated. Measurements are given in units of millimeters (mm).

$$\sigma_s=\frac{R_s/2}{3}=0.0018$$

$$\sigma_i=\frac{R_i/2}{3}=0.0020$$

$$\sigma_{\Delta 0}=\frac{R_{\Delta 0}/2}{3}=0.0028$$

$$\sigma_f^2=\sigma_s^2+\sigma_i^2$$

$$m_{\Delta f}=m_{\Delta 0}-\lambda_i\ (m_s-m_i)=0.0035$$

$$\sigma_{\Delta f}=\sqrt{\sigma_{\Delta 0}^2+\lambda_i^2\ \sigma_f^2}=0.0035$$

where, σ_s: Standard deviation of shaft diameter
σ_i: Standard deviation of bore diameter
σ_f: Standard deviation of interference
$\sigma_{\Delta 0}$: Standard deviation of radial clearance (before mounting)
$\sigma_{\Delta f}$: Standard deviation of residual clearance (after mounting)
m_s: Mean value of shaft diameter (ϕ50+0.008)
m_i: Mean value of bore diameter (ϕ50–0.006)
$m_{\Delta 0}$: Mean value of radial clearance (before mounting) (0.014)
$m_{\Delta f}$: Mean value of residual clearance (after mounting)
R_s: Shaft tolerance (0.011)
R_i: Bearing bore tolerance (0.012)
$R_{\Delta 0}$: Range in radial clearance (before mounting) (0.017)
λ_i: Rate of raceway expansion from apparent interference (0.75 from **Fig. 1**)

The average amount of raceway expansion and contraction from apparent interference is calculated from $\lambda_i\ (m_m-m_i)$.

To determine, wihtin a 99.7% probability, the variation in internal clearance after mounting ($R_{\Delta f}$), we use the following equation.

$$R_{\Delta f}=m_{\Delta f}\pm 3\sigma_{\Delta f}=+0.014 \text{ to } -0.007$$

In other words, the mean value of residual clearance ($m_{\Delta f}$) is +0.0035, and the range is from −0.007 to +0.014 for a 6310 bearing.

We will discuss further in Section **4.5** the method used to calculate the amount of change in internal clearance when there is a variation in temperature between inner and outer rings.

Units: mm

Shaft diameter	ϕ50 $^{+0.013}_{+0.002}$
Bearing bore diameter, (d)	ϕ50 $^{0}_{-0.012}$
Radial internal clearance (Δ_0)	0.006 to 0.023(1)

Note (1) Standard internal clearance, unmounted

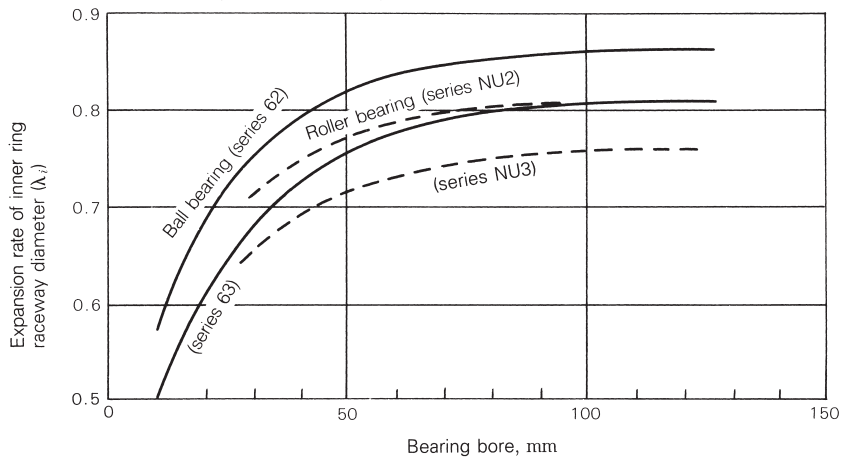

Fig. 1 Rate of inner ring raceway expansion (λ_i) from apparent interference

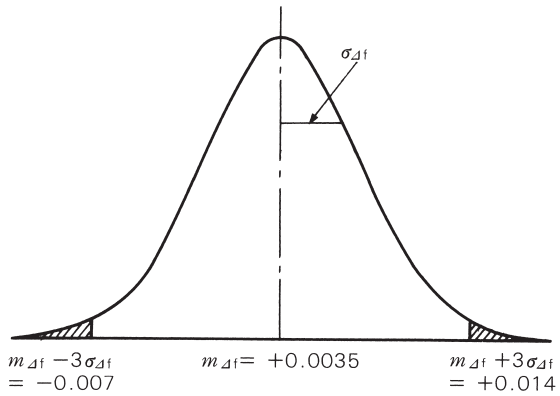

Fig. 2 Distribution of residual internal clearance

4.3 Effect of interference fit on bearing raceways (fit of inner ring)

One of the important factors that relates to radial clearance is the reduction in radial clearance resulting from the mounting fit. When inner ring is mounted on a shaft with an interference fit and the outer ring is secured in a housing with an interference fit, the inner ring will expand and the outer ring will contract.

The means of calculating the amount of ring expansion or contraction were previously noted in Section 3.4, however, the equation for establishing the amount of inner raceway expansion (ΔD_i) is given in Equation (1).

$$\Delta D_i = \Delta d \; k \; \frac{1-k_0^{\,2}}{1-k^2 \, k_0^{\,2}} \quad \cdots\cdots (1)$$

where, Δd: Effective interference (mm)
k: Ratio of bore to inner raceway diameter; $k=d/D_i$
k_0: Ratio of inside to outside diameter of hollow shaft; $k_0=d_0/D_i$
d: Bore or shaft diameter (mm)
D_i: Inner raceway diameter (mm)
d_0: Inside diameter of hollow shaft (mm)

Equation (1) has been translated into a clearer graphical form in Fig. 1.

The vertical axis of Fig. 1 represents the inner raceway diameter expansion in relation to the amount of interference. The horizontal axis is the ratio of inside and outside diameter of the hollow shaft (k_0) and uses as its parameter the ratio of bore diameter and raceway diameter of the inner ring (k).

Generally, the decrease in radial clearance is calculated to be approximately 80% of the interference. However, this is for solid shaft mountings only. For hollow shaft mountings the decrease in radial clearance varies with the ratio of inside to outside diameter of the shaft. Since the general 80% rule is based on average bearing bore size to inner raceway diameter ratios, the change will vary with different bearing types, sizes, and series. Typical plots for Single Row Deep Groove Ball Bearings and for Cylindrical Roller Bearings are shown in Figs. 2 and 3. Values in Fig. 1 apply only for steel shafts.

Let's take as an example a 6220 ball bearing mounted on a hollow shaft (diameter d=100 mm, inside diameter d_0=65 mm) with a fit class of m5 and determine the decrease in radial clearance.

The ratio between bore diameter and raceway diameter, k is 0.87 as shown in Fig. 2. The ratio of inside to outside diameter for shaft, k_0, is $k_0=d_0/d$=0.65. Thus, reading from Fig. 1, the rate of raceway expansion is 73%.

Given that an interference of m5 has a mean value of 30 μm, the amount of raceway expansion, or, the amount of decrease in the radial clearance from the fit is 0.73×30=22 μm.

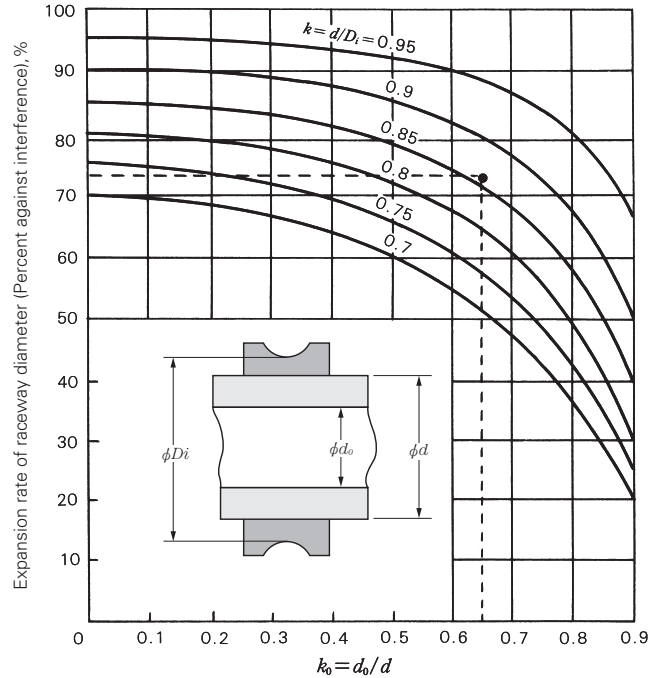

Fig. 1 Raceway expansion in relation to bearing fit (Inner ring fit upon steel shaft)

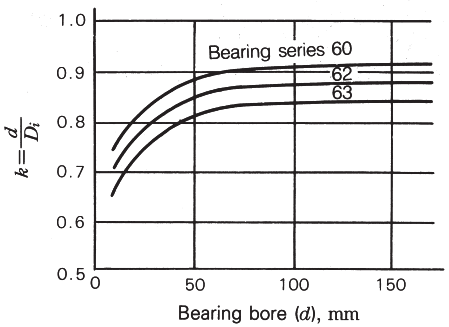

Fig. 2 Ratio of bore size to raceway diameter for single row deep groove ball bearings

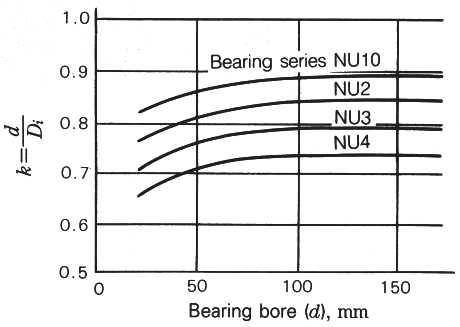

Fig. 3 Ratio of bore size to raceway diameter for cylindrical roller bearings

4.4 Effect of interference fit on bearing raceways (fit of outer ring)

We continue with the calculation of the raceway contraction of the outer ring after fitting.

When a bearing load is applied on a rotating inner ring (outer ring carrying a static load), an interference fit is adopted for the inner ring and the outer ring is mounted either with a transition fit or a clearance fit. However, when the bearing load is applied on a rotating outer ring (inner ring carrying a static load) or when there is an indeterminate load and the outer ring must be mounted with an interference fit, a decrease in radial internal clearance caused by the fit begins to contribute in the same way as when the inner ring is mounted with an interference fit.

Actually, because the amount of interference that can be applied to the outer ring is limited by stress, and because the constraints of most bearing applications make it difficult to apply a large amount of interference to the outer ring, and instances where there is an indeterminate load are quite rare compared to those where a rotating inner ring carries the load, there are few occasions where it is necessary to be cautious about the decrease in radial clearance caused by outer-ring interference.

The decrease in outer raceway diameter ΔD_e is calculated using **Equation** (1).

$$\Delta D_e = \Delta D \cdot h \frac{1-h_0^2}{1-h^2 h_0^2} \quad \cdots\cdots (1)$$

where, ΔD: Effective interference (mm)
h: Ratio between raceway dia. and outside dia. of outer ring, $h=D_e/D$
h_0: Housing thickness ratio, $h_0=D/D_0$
D: Bearing outside diameter (housing bore diameter) (mm)
D_e: Raceway diameter of outer ring (mm)
D_0: Outside diameter of housing (mm)

Fig. 1 represents the above equation in graphic form.

The vertical axis show the outer-ring raceway contraction as a percentage of interference, and the horizontal axis is the housing thickness ratio h_0. The data are plotted for constant values of the outer-ring thickness ratio from 0.7 through 1.0 in increments of 0.05. The value of thickness ratio h will differ with bearing type, size, and diameter series. Representative values for single-row deep groove ball bearings and for cylindrical roller bearings are given in **Figs. 2** and **3** respectively.

Loads applied on rotating outer rings occur in such applications as automotive front axles, tension pulleys, conveyor systems, and other pulley systems.

As an example, we estimate the amount of decrease in radial clearance assuming a 6207 ball bearing is mounted in a steel housing with an N7 fit. The outside diameter of the housing is assumed to be D_0=95, and the bearing outside diameter is D=72. From **Fig. 2**, the outer-ring thickness ratio, h, is 0.9. Because $h_0=D/D_0$=0.76, from **Fig. 1**, the amount of raceway contraction is 71%. Taking the mean value for N7 interference as 18 μm, the amount of contraction of the outer raceway, or the amount of decrease in radial clearance is 0.71×18=13 μm.

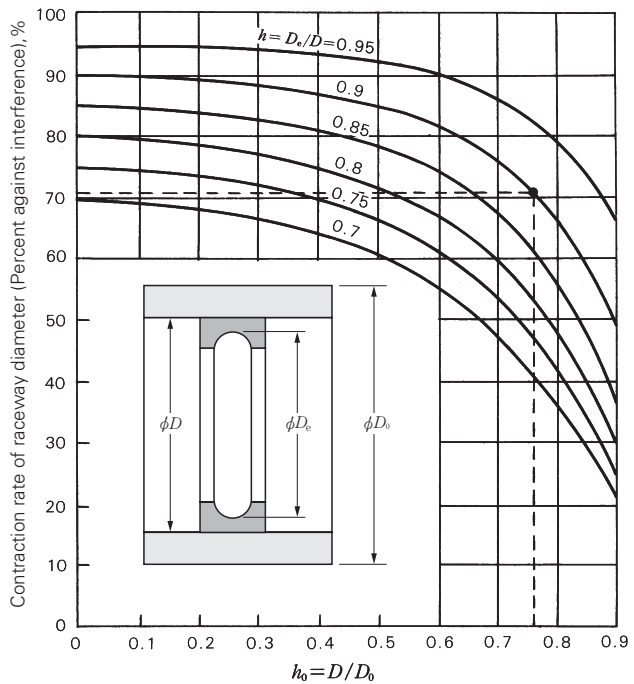

Fig. 1 Raceway contraction in relation to bearing fit (Outer ring fit in steel housing)

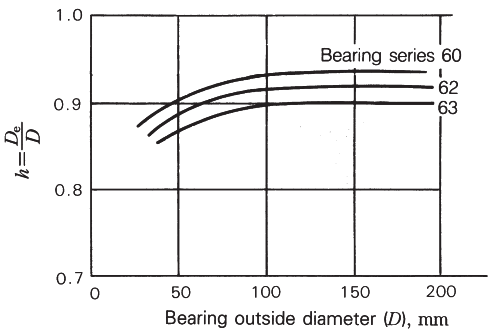

Fig. 2 Ratio of outside diameter to raceway diameter for single row deep groove ball bearings

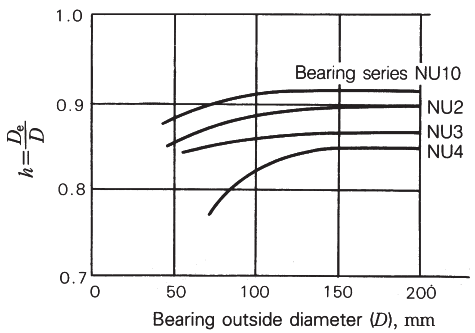

Fig. 3 Ratio of outside diameter to raceway diameter for cylindrical roller bearings

4.5 Reduction in radial internal clearance caused by a temperature difference between inner and outer rings

The internal clearance after mounting was explained in Section 4.2. We continue here by explaining the way to determine the reduction in radial internal clearance caused by inner and outer ring temperature differences and, finally, the method of estimating the effective internal clearance in a systematic fashion.

When a bearing runs under a load, the temperature of the entire bearing will rise. Of course, the rolling elements also undergo a temperature change, but, because the change is extremely difficult to measure or even estimate, the temperature of the rolling elements is generally assumed to be the same as the inner-ring temperature.

We will use the same bearing for our example as we did in Section 4.2, a 6310, and determine the reduction in clearance caused by a temperature difference of 5°C between the inner and outer rings using the equation below.

$$\delta_t=\alpha\Delta_t D_e \fallingdotseq \alpha\Delta_t\frac{4D+d}{5} \quad \cdots\cdots (1)$$

$$\fallingdotseq 12.5\times10^{-6}\times5\times\frac{4\times110+50}{5}$$

$$\fallingdotseq 6\times10^{-3}\ (\mathrm{mm})$$

where δ_t: Decrease in radial internal clearance caused by a temperature difference between the inner and outer rings (mm)

α: Linear thermal expansion coefficient for bearing steel, 12.5×10^{-6} (1/°C)

Δ_t: Difference in temperature between inner ring (or rolling elements) and outer ring (°C)

D: Outside diameter (6310 bearing, 110 mm)

d: Bore diameter (6310 bearing, 50 mm)

D_e: Outer-ring raceway diameter (mm)

The following equations are used to calculate the outer-ring raceway diameter:

Ball Bearings: $D_e=(4D+d)/5$

Roller Bearings: $D_e=(3D+d)/4$

Using the values for Δ_f, the residual clearance arrived at in Section 4.2, and for δ_t, the reduction in radial internal clearance caused by a temperature difference between the inner and outer rings just calculated, we can determine the effective internal clearance (Δ) using the following equation.

$\Delta=\Delta_f-\delta_t=(+0.014 \text{ to } -0.007)-0.006$
$= +0.008 \text{ to } -0.013$

Referring to Fig. 1 below (also see Section 2.8) we can see how the effective internal clearance influences bearing life (in this example with a radial load of 3 350 N {340 kgf}, or approximately 5% of the basic load rating). The longest bearing life occurs under conditions where the effective internal clearance is −13 μm. The lowest limit to the preferred effective internal clearance range is also −13 μm.

To summarize radial internal clearances briefly:

(1) Generally, the radial clearances given in tables and figures are theoretical internal clearances, Δ_0.

(2) The most important clearance for bearings is the effective radial internal clearance, Δ. It is a value determined by taking the theoretical clearance Δ_0 and subtracting δ_f, the reduction in clearance caused by the interference fit of one or both rings, and δ_t, the reduction in clearance caused by a temperature difference between the inner and outer rings. $\Delta=\Delta_0-(\delta_f+\delta_t)$.

(3) Theoretically, the optimum effective internal clearance Δ is a negative number close to zero which gives maximum bearing life. Therefore, it is desirable for a bearing to have an effective internal clearance greater than the ideal minimum value.

(4) To determine the relation between the effective internal clearance and bearing life (strictly speaking, the bearing load should also be considered), there is actually no need to give serious consideration to operating internal clearance Δ_F; the problem lies with the effective internal clearance Δ.

(5) The basic load rating C_r for a bearing is calculated for an effective internal clearance $\Delta=0$.

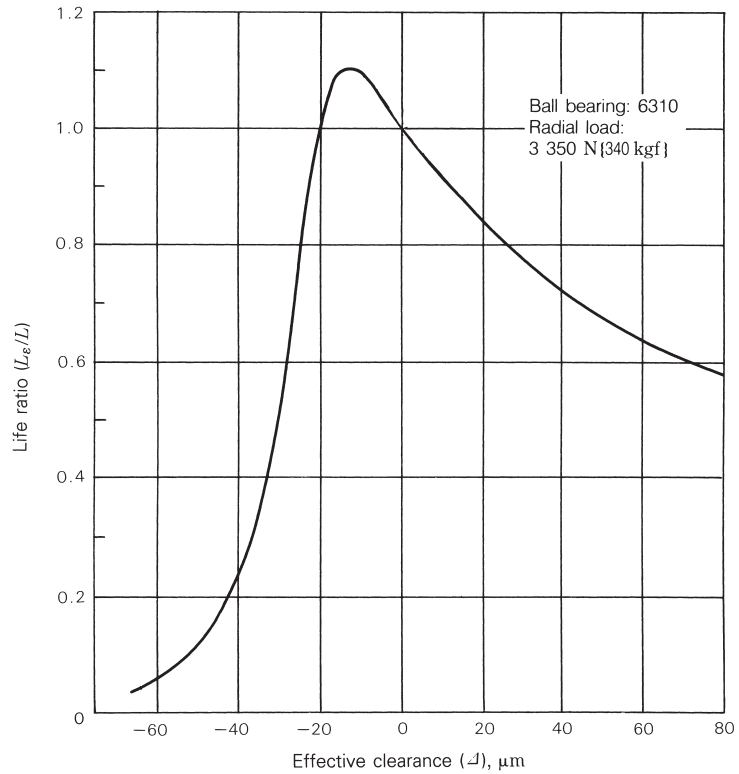

Fig. 1 Relation between effective clearance and bearing life for 6310 ball bearing

Remarks $L\varepsilon$: Life in case of effective clearance $\Delta=\varepsilon$
L: Life in case of effective clearance $\Delta=0$

4.6 Radial and axial internal clearances and contact angles for single row deep groove ball bearings

4.6.1 Radial and axial internal clearances

The internal clearance in single row bearings has been specified as the radial internal clearance. The bearing internal clearance is the amount of relative displacement possible between the bearing rings when one ring is fixed and the other ring does not bear a load. The amount of movement along the direction of the bearing radius is called the radial clearance, and the amount along the direction of the axis is called the axial clearance.

The geometric relation between the radial and axial clearance is shown in Fig. 1.

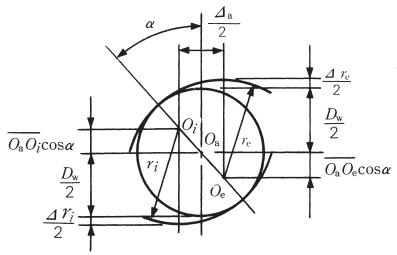

Fig. 1 Relationship Between Δ_r and Δ_a

Symbols used in Fig. 1

- O_a: Ball center
- O_e: Center of groove curvature, outer ring
- O_i: Center of groove curvature, inner ring
- D_w: Ball diameter (mm)
- r_e: Radius of outer ring groove (mm)
- r_i: Radius of inner ring groove (mm)
- α: Contact angle (°)
- Δ_r: Radial clearance (mm)
- Δ_a: Axial clearance (mm)

It is apparent from Fig. 1 that $\Delta_r=\Delta r_e+\Delta r_i$.

From geometric relationships, various equations for clearance, contact angle, etc. can be derived.

$$\Delta_r=2\ (1-\cos\alpha)\ (r_e+r_i-D_w) \quad \cdots\cdots (1)$$

$$\Delta_a=2\ \sin\alpha\ (r_e+r_i-D_w) \quad \cdots\cdots (2)$$

$$\frac{\Delta_a}{\Delta_r}=\cot\frac{\alpha}{2} \quad \cdots\cdots (3)$$

$$\Delta_a \fallingdotseq 2\ (r_e+r_i-D_w)^{1/2}\Delta_r^{1/2} \quad \cdots\cdots (4)$$

$$\alpha=\cos^{-1}\left(\frac{r_e+r_i-D_w-\frac{\Delta_r}{2}}{r_e+r_i-D_w}\right) \quad \cdots\cdots (5)$$

$$=\sin^{-1}\left(\frac{\Delta_a/2}{r_e+r_i-D_w}\right) \quad \cdots\cdots (6)$$

Because $(r_e+r_i-D_w)$ is a constant, it is apparent why fixed relationships between Δ_r, Δ_a and α exist for all the various bearing types.

As was previously mentioned, the clearances for deep groove ball bearings are given as radial clearances, but there are specific applications where it is desirable to have an axial clearance as well. The relationship between deep groove ball bearing radial clearance Δ_r and axial clearance Δ_a is given in Equation (4). To simplify,

$$\Delta_a \fallingdotseq K\ \Delta_r^{1/2} \quad \cdots\cdots (7)$$

where K: Constant depending on bearing design

$K=2\ (r_e+r_i-D_w)^{1/2}$

Fig. 2 shows one example. The various values for K are presented by bearing size in Table 1 below.

Example

Assume a 6312 bearing, for a sample calculation, which has a radial clearance of 0.017 mm. From Table 1, K=2.09. Therefore, the axial clearance Δ_a is:

$\Delta=2.09\times\sqrt{0.017}=2.09\times0.13=0.27$ (mm)

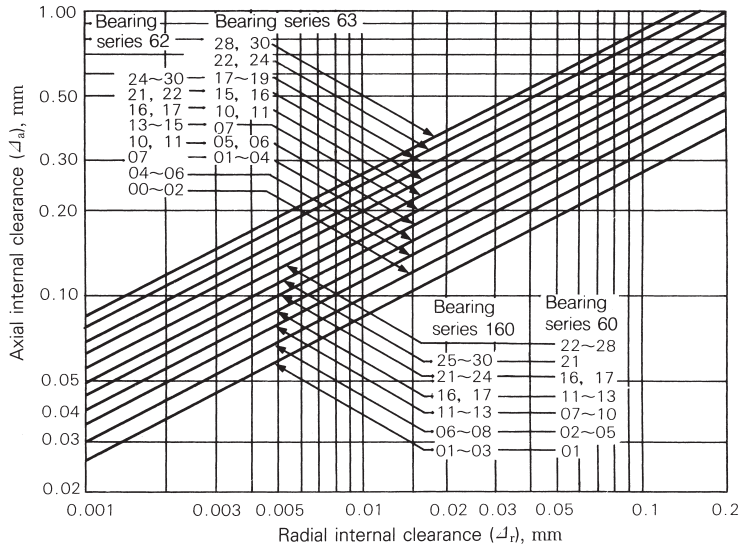

Fig. 2 Radial clearance, Δ_r and axial clearance, Δ_a of deep groove ball bearings

Table 1 Constant values of K for radial and axial clearance conversion

Bearing bore No.	K			
	Series 160	Series 60	Series 62	Series 63
00	—	—	0.93	1.14
01	0.80	0.80	0.93	1.06
02	0.80	0.93	0.93	1.06
03	0.80	0.93	0.99	1.11
04	0.90	0.96	1.06	1.07
05	0.90	0.96	1.06	1.20
06	0.96	1.01	1.07	1.19
07	0.96	1.06	1.25	1.37
08	0.96	1.06	1.29	1.45
09	1.01	1.11	1.29	1.57
10	1.01	1.11	1.33	1.64
11	1.06	1.20	1.40	1.70
12	1.06	1.20	1.50	2.09
13	1.06	1.20	1.54	1.82
14	1.16	1.29	1.57	1.88
15	1.16	1.29	1.57	1.95
16	1.20	1.37	1.64	2.01
17	1.20	1.37	1.70	2.06
18	1.29	1.44	1.76	2.11
19	1.29	1.44	1.82	2.16
20	1.29	1.44	1.88	2.25
21	1.37	1.54	1.95	2.32
22	1.40	1.64	2.01	2.40
24	1.40	1.64	2.06	2.40
26	1.54	1.70	2.11	2.49
28	1.54	1.70	2.11	2.59
30	1.57	1.76	2.11	2.59

4.6.2 Relation between radial clearance and contact angle

Single-row deep groove ball bearings are sometimes used as thrust bearings. In such applications, it is recommended to make the contact angle as large as possible.

The contact angle for ball bearings is determined by the geometric relationship between the radial clearance and the radii of the inner and outer grooves. Using Equations (1) to (6), Fig. 3 shows the particular relationship between the radial clearance and contact angle of 62 and 63 series bearings. The initial contact angle, α_0, is the initial contact angle when the axial load is zero. Application of any load to the bearing will change this contact angle.

If the initial contact angle α_0 exceeds 20°, it is necessary to check whether or not the contact area of the ball and raceway touch the edge of raceway shoulder. (Refer to Section 8.1.2)

For applications when an axial load alone is applied, the radial clearance for deep groove ball bearings is normally greater than the normal clearance in order to ensure that the contact anlgle is relatively large. The initial contact angles for C3 and C4 clearances are given for selected bearing sizes in Table 2 below.

Table 2 Initial contact angle, α_0, with C3 and C4 clearances

Bearing No.	α_0 with C3	α_0 with C4
6205	12.5° to 18°	16.5° to 22°
6210	11.5° to 16.5°	13.5° to 19.5°
6215	11.5° to 16°	15.5° to 19.5°
6220	10.5° to 14.5°	14° to 17.5°
6305	11° to 16°	14.5° to 19.5°
6310	9.5° to 13.5°	12° to 16°
6315	9.5° to 13.5°	12.5° to 15.5°
6320	9° to 12.5°	12° to 15°

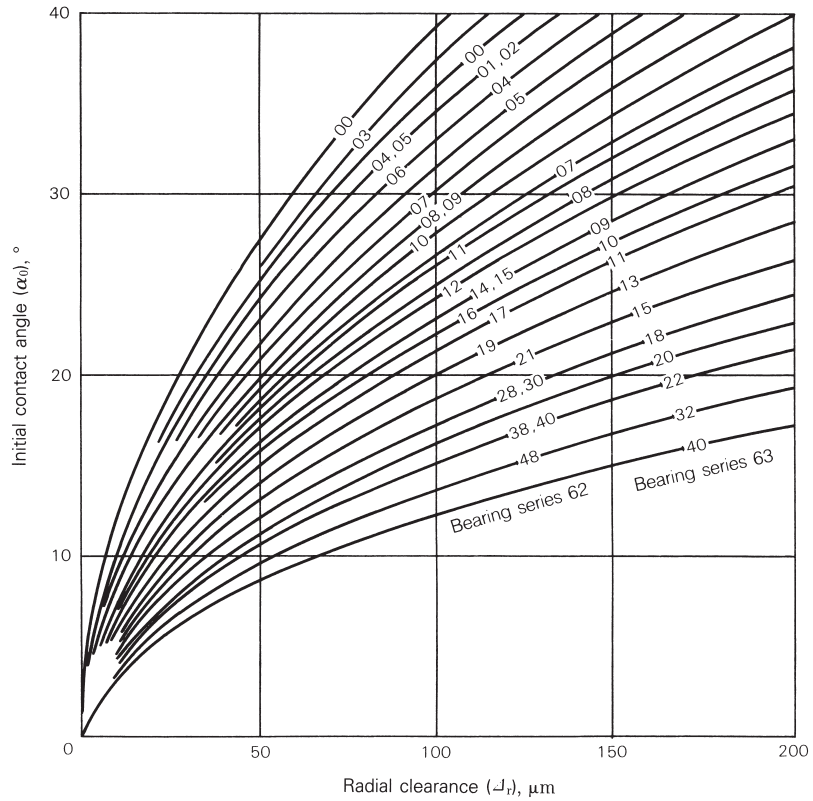

Fig. 3 Radial clearance and contact angle

4.7 Angular clearances in single-row deep groove ball bearings

When estimating bearing loads, the usual loads considered are radial loads, axial loads, or a combination of the two. Under such load, the movement of the inner and outer rings is usually assumed to be parallel.

Actually, there are many occasions when a bearing's inner and outer rings do not operate in true planar rotation because of housing or shaft misalignment, shaft deflection due to the applied load, or a mounting where the bearing is slightly skewed. In such cases, if the inner and outer ring misalignment angle is greater than a half of the bearing's angular clearance, it will create an unusual amount of stress, a rise in temperature, and premature flaking or other fatigue failure. There are more detailed reports available on such topics as how to determine the weight distribution and equivalent load for bearings which must handle moment loads. However, when considering the weight or load calculations, the amount of angular clearance in individual bearings is also of major concern in bearing selection. The angular clearance, which is clearly related to radial clearance, is the maximum angular displacement of the two ring axes when one of the bearing rings is fixed and the other is free and unloaded. An approximation of angular clearance can be determined from Equation (1) below.

$$\tan\frac{\theta_0}{2} \fallingdotseq \frac{2\ \{\Delta_r\ (r_e+r_i-D_w)\}^{1/2}}{D_{pw}}$$

$$= K_0 \cdot \Delta_r^{1/2} \quad \cdots\cdots (1)$$

where, Δ_r: Radial clearance (mm)
r_e: Outer-ring groove radius (mm)
r_i: Inner-ring groove radius (mm)
D_w: Ball diameter (mm)
D_{pw}: Pitch diameter (mm)
K_0: Constant

$$K_0 = \frac{2\ (r_e+r_i-D_w)^{1/2}}{D_{pw}}$$

K_0 is a constant dependent on the individual bearing design. Table 1 gives values for K_0 for single-row deep groove bearing series 60, 62, and 63. Fig. 1 shows the relationship between the radial clearance Δ_r and angular clearance θ_0.

The deflection angle of the inner and outer rings is $\pm\ \theta_0/2$.

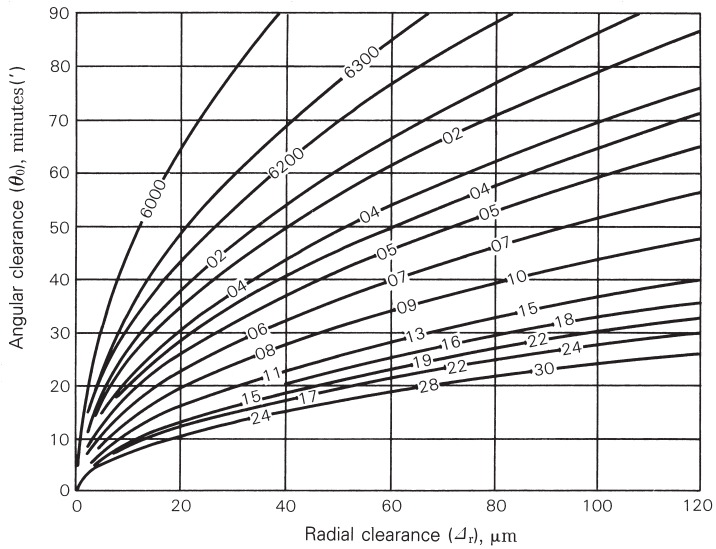

Fig. 1 Radial clearance and angular clearance

Table 1 Constant values of K_0 for radial and angular clearance conversion

Bearing bore No.	K_0		
	Series 60	Series 62	Series 63
	$\times 10^{-3}$	$\times 10^{-3}$	$\times 10^{-3}$
00	67.4	45.6	50.6
01	39.7	42.3	43.3
02	39.7	36.5	36.0
03	35.9	34.0	33.7
04	30.9	31.7	29.7
05	27.0	27.2	27.0
06	23.7	23.0	22.9
07	21.9	23.3	23.5
08	19.5	21.4	22.4
09	18.2	19.8	21.1
10	16.8	19.0	20.0
11	16.6	18.1	19.4
12	15.5	17.4	18.5
13	14.6	16.6	17.8
14	14.3	16.1	17.1
15	13.5	15.2	16.6
16	13.3	14.9	16.0
17	12.7	14.5	15.5
18	12.5	14.1	15.1
19	11.9	13.7	14.6
20	11.5	13.4	14.2
21	11.4	13.2	14.0
22	11.7	12.9	13.6
24	10.9	12.2	12.7
26	10.3	11.7	12.1
28	9.71	10.8	11.8
30	9.39	10.0	11.0

4.8 Relationship between radial and axial clearances in double-row angular contact ball bearings

The relationship between the radial and axial internal clearances in double-row angular contact ball bearings can be determined geometrically as shown in **Fig. 1** below.

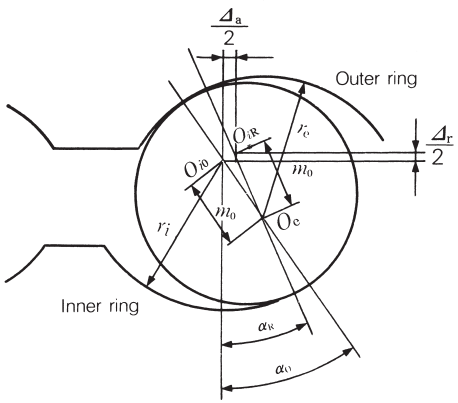

Fig. 1

where, Δ_r: Radial clearance (mm)
Δ_a: Axial clearance (mm)
α_0: Initial contact angle, inner or outer ring displaced axially
α_R: Initial contact angle, inner or outer ring displaced radially
O_e: Center of outer-ring groove curvature (outer ring fixed)
O_{i0}: Center of inner-ring groove curvature (inner ring displaced axially)
O_{iR}: Center of inner-ring groove curvature (inner ring displaced radially)
m_0: Distance between inner and outer ring groove-curvature centers, $m_0=r_i+r_e-D_w$
D_w: Ball diameter (mm)
r_i: Radius of inner-ring groove (mm)
r_e: Radius of outer-ring groove (mm)

The following relations can be derived from **Fig. 1**:

$$m_0 \sin \alpha_0 = m_0 \sin \alpha_R + \frac{\Delta_a}{2} \quad \cdots\cdots (1)$$

$$m_0 \cos \alpha_0 = m_0 \cos \alpha_R + \frac{\Delta_r}{2} \quad \cdots\cdots (2)$$

since $\sin^2\alpha_0 = 1-\cos^2\alpha_0$,

$$(m_0 \sin \alpha_0)^2 = m_0^2 - (m_0 \cos \alpha_0)^2 \quad \cdots\cdots (3)$$

Combined **Equations** (1), (2), and (3), we obtain:

$$\left(m_0 \sin \alpha_R + \frac{\Delta_a}{2}\right)^2 = m_0^2 - \left(m_0 \cos\alpha_R - \frac{\Delta_r}{2}\right)^2 \quad \cdots\cdots (4)$$

$$\therefore \Delta_a = 2\sqrt{m_0^2 - \left(m_0 \cos\alpha_R - \frac{\Delta_r}{2}\right)^2} - 2m_0 \sin \alpha_R \quad \cdots\cdots (5)$$

α_R is 25° for 52 and 53 series bearings and 32° for 32 and 33 series bearings. If we set α_R equal to 0°, **Equation** (5) becomes:

$$\Delta_a = 2\sqrt{m_0^2 - \left(m_0 - \frac{\Delta_r}{2}\right)^2}$$

$$= 2\sqrt{m_0 \Delta_r - \frac{\Delta_r^2}{4}}$$

However, $\frac{\Delta_r^2}{4}$ is negligible.

$$\therefore \Delta_a \fallingdotseq 2 m_0^{1/2} \Delta_r^{1/2} \quad \cdots\cdots (6)$$

This is identical to the relationship between the radial and axial clearances in single-row deep groove ball bearings.

The value of m_0 is dependent on the inner and outer ring groove radii. The relation between Δ_r and Δ_a, as given by **Equation** (5), is shown in **Figs. 2** and **3** for NSK 52, 53, 32, and 33 series double-row angular contact ball bearings. When the clearance range is small, the axial clearance is given approximately by

$$\Delta_a \fallingdotseq \Delta_r \cot \alpha_R \quad \cdots\cdots (7)$$

However, when the clearance is relatively large, (when $\Delta_r/D_w > 0.002$) the error in **Equation** (7) can be quite large.

The contact angle α_R is independent of the radial clearance; however, the initial contact angle α_0 varies with the radial clearance when the inner or outer ring is displaced axially. This relationship is given by **Equation** (2).

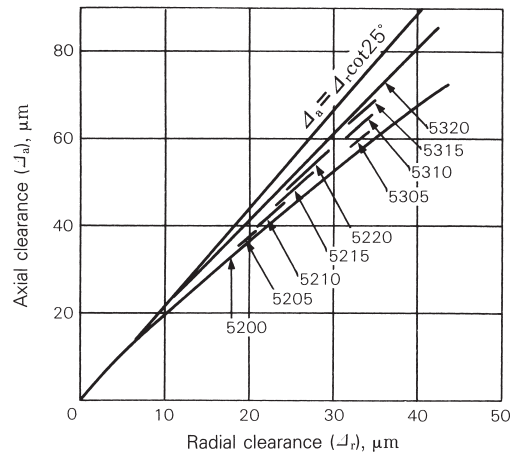

Fig. 2 Radial and axial clearances of bearing series 52 and 53

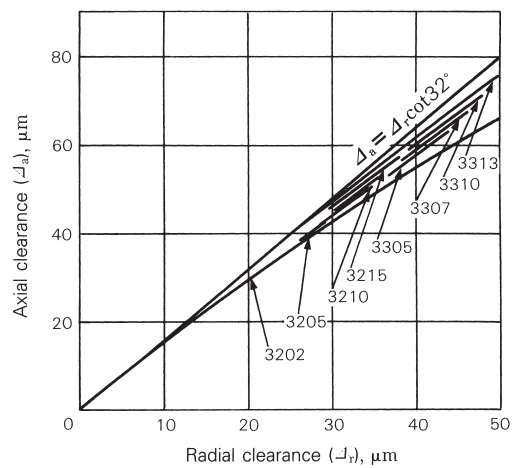

Fig. 3 Radial and axial clearances of bearing series 32 and 33

4.9 Angular clearances in double-row angular contact ball bearings

The angular clearance in double-row bearings is defined in exactly the same way as for single-row bearings; i.e., with one of the bearing rings fixed, the angular clearance is the greatest possible angular displacement of the axis of the other ring.

Since the angular clearance is the greatest total relative displacement of the two ring axes, it is twice the possible angle of inner and outer ring movement (the maximum angular displacement in one direction from the center without creating a moment).

The relationship between axial and angular clearance for double-row angular contact ball bearings is given by Equation (1) below.

$$\Delta_a = 2m_0\left\{\sin\alpha_0 + \frac{\theta R_i}{2m_0} - \sqrt{1-\left(\cos\alpha_0 + \frac{\theta l}{4m_0}\right)^2}\right\} \quad \cdots\cdots (1)$$

where, Δ_a: Axial clearance (mm)
m_0: Distance between inner and outer ring groove curvature centers, $m_0 = r_e + r_i - D_w$ (mm)
r_e: Outer-ring groove radius (mm)
r_i: Inner-ring groove radius (mm)
α_0: Initial contact angle (°)
θ: Angular clearance (rad)
R_i: Distance between shaft center and inner-ring groove curvature center (mm)
l: Distance between left and right groove centers of inner-ring (mm)

The above equation is shown plotted in Fig. 1 for NSK double-row angular contact ball bearings series 52, 53, 32, and 33.

The relationship between radial clearance Δ_r and axial clearance Δ_a for double-row angular contact ball bearings was explained in Section 4.8. Based on those equations, Fig. 2 shows the relationship between angular clearance θ and radial clearance Δ_r.

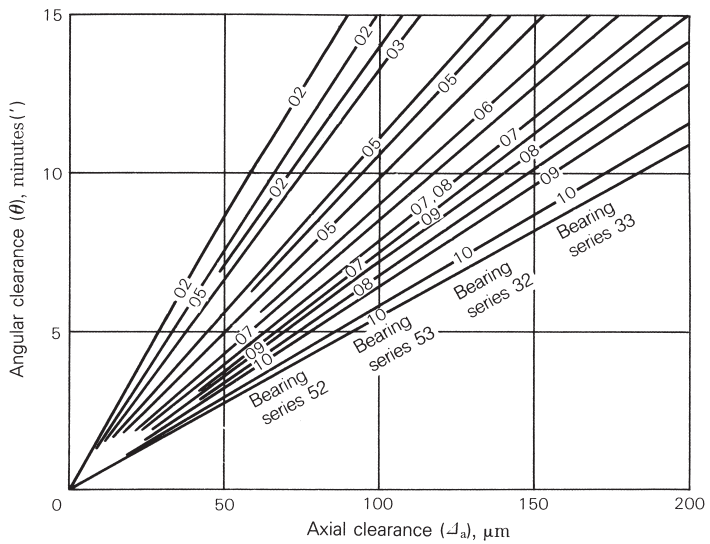

Fig. 1 Relationship between axial and angular clearances

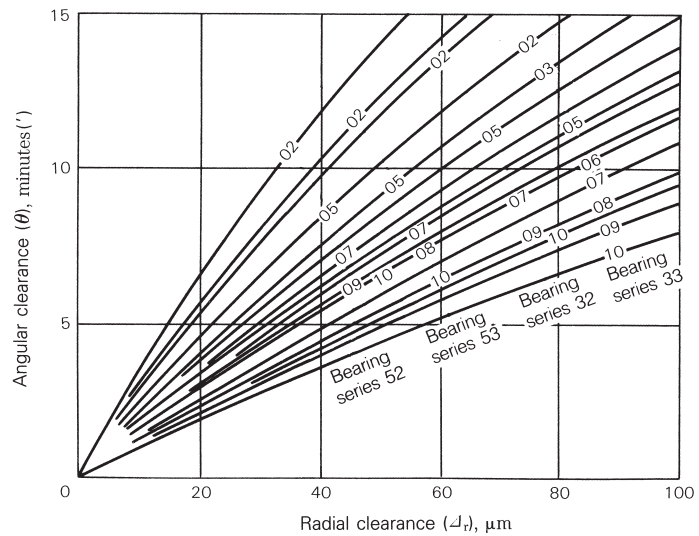

Fig. 2 Relationship between radial and angular clearances

4.10 Measuring method of internal clearance of combined tapered roller bearings (offset measuring method)

Combined tapered roller bearings are available in two types: a back-to-back combination (DB type) and a face-to-face combination (DF type) (see Fig. 1 and Fig. 2). The advantages of these combinations can be obtained by assembly as one set or combined with other bearings to be a fixed- or free-side bearing.

For the DB type of combined tapered roller bearing, as its cage protrudes from the back side of the outer ring, the outer ring spacer (K spacer in Fig. 1) is mounted to prevent mutual contact of cages. For the inner ring, the inner ring spacer (L spacer in Fig. 1), having an appropriate width, is provided to secure the clearance. For the DF type, as shown in Fig. 2, bearings are used with a K spacer.

In general, to use such a bearing arrangement either an appropriate clearance is required that takes into account the heat generated during operation or an applied preload is required that increases the rigidity of the bearings. The spacer width should be adjusted so as to provide an appropriate clearance or preload (minus clearance) after mounting.

Hereunder, we introduce you to a clearance measurement method for a DB arrangement.

(1) As shown in Fig. 3, put the bearing A on the surface plate and after stabilization of rollers by rotating the outer ring (more than 10 turns), measure the offset $f_A=T_A-B_A$.

(2) Next, as shown in Fig. 4, use the same procedure to measure the other bearing B for its offset $f_B=T_B-B_B$.

(3) Next, measure the width of the K and L spacers as shown in Fig. 5.

From the results of the above measurements, the axial clearance Δ_a of the combined tapered roller bearing can be obtained, with the use of symbols shown in Figs. 3 through 5 by Equation (1):

$$\Delta_a=(L-K)-(f_A+f_B) \quad \cdots\cdots (1)$$

As an example, for the combined tapered roller bearing HR32232JDB+KLR10AC3, confirm the clearance of the actual product conforms to the specifications. First, refer to NSK Rolling Bearing Catalog CAT. No. E1102 (Page A93) and notice that the C3 clearance range is Δ_r=110 to 140 μm.

To compare this specification with the offset measurement results, convert it into an axial clearance Δ_a by using Equation (2):

$$\Delta_a=\Delta_r \cot\alpha \fallingdotseq \Delta_r \frac{1.5}{e} \quad \cdots\cdots (2)$$

where, e: Constant determined for each bearing No. (Listed in the Bearing Tables of NSK Rolling Bearings Catalog)

refering to the said catalog (Page B127), with use of e=0.44, the following is obtained:

$$\Delta_a=(110 \text{ to } 140)\times\frac{1.5}{e}$$

$$\fallingdotseq 380 \text{ to } 480\ \mu\text{m}$$

It is possible to confirm that the bearing clearance is C3, by verifying that the axial clearance Δ_a of Equation (1) (obtained by the bearing offset measurement) is within the above mentioned range.

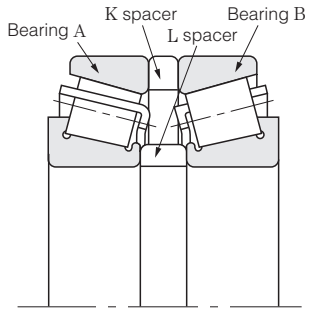

Fig. 1 DB arrangement

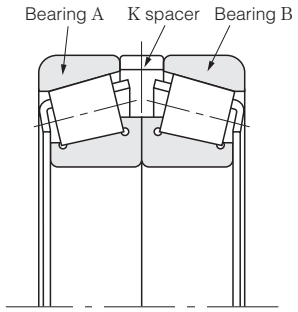

Fig. 2 DF arrangement

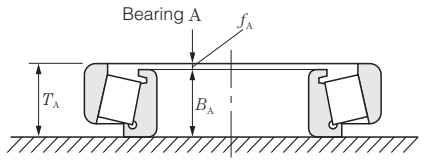

Fig. 3

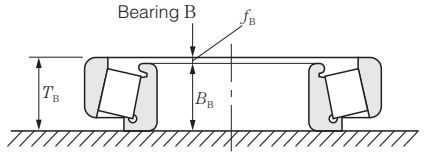

Fig. 4

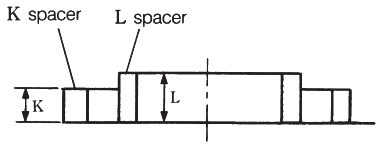

Fig. 5

4.11 Internal clearance adjustment method when mounting a tapered roller bearing

The two single row tapered roller bearings are usually arranged in a configuration opposite each other and the clearance is adjusted in the axial direction. There are two types of opposite placement methods: back-to-back arrangement (DB arrangement) and face-to-face arrangement (DF arrangement).

The clearance adjustment of the back-to-back arrangement is performed by tightening the inner ring by a shaft nut or a shaft end bolt. In Fig. 1, an example using a shaft end bolt is shown. In this case, it is necessary that the fit of the tightening side inner ring with the shaft be a loose fit to allow displacement of the inner ring in the axial direction.

For the face-to-face arrangement, a shim is inserted between the cover, which retains the outer ring in the axial direction, and the housing in order to allow adjustment to the specified axial clearance (Fig. 2). In this case, it is necessary to use a loose fit between the tightening side of the outer ring and the housing in order to allow appropriate displacement of the outer ring in the axial direction. When the structure is designed to install the outer ring into the retaining cover (Fig. 3), the above measure becomes unnecessary and both mounting and dismounting become easy.

Theoretically when the bearing clearance is slightly negative during operation, the fatigue life becomes the longest, but if the negative clearance becomes much bigger, then the fatigue life becomes very short and heat generation quickly increases. Thus, it is generally arranged that the clearance be slightly positive (a little bigger than zero) while operating. In consideration of the clearance reduction caused by temperature difference of inner and outer rings during operation and difference of thermal expansion of the shaft and housing in the axial direction, the bearing clearance after mounting should be decided.

In practice, the clearance C1 or C2 is frequently adopted which is listed in "Radial internal clearances in double-row and combined tapered roller bearing (cylindrical bore)" of NSK Rolling Bearing Catalog CAT. No. E1102, Page A93.

In addition, the relationship between the radial clearance Δ_r and axial clearance Δ_a is as follows:

$$\Delta_a = \Delta_r \cot \alpha \fallingdotseq \Delta_r \frac{1.5}{e}$$

where, α: Contact angle
e: Constant determined for each bearing No. (Listed in the Bearing Tables of NSK Rolling Bearing Catalog)

Tapered roller bearings, which are used for head spindles of machine tools, automotive final reduction gears, etc., are set to a negative clearance for the purpose of obtaining bearing rigidity. Such a method is called a preload method. There are two different modes of preloading: position preload and constant pressure preload. The position preload is used most often.

For the position preload, there are two methods: one method is to use an already adjusted arrangement of bearings and the other method is to apply the specified preload by tightening an adjustment nut or using an adjustment shim.

The constant pressure preload is a method to apply an appropriate preload to the bearing by means of spring or hydraulic pressure, etc. Next we introduce several examples that use these methods:

Fig. 4 shows the automotive final reduction gear. For pinion gears, the preload is adjusted by use of an inner ring spacer and shim. For large gears on the other hand, the preload is controlled by tightening the torque of the outer ring retaining screw.

Fig. 5 shows the rear wheel of a truck. This is an example of a preload application by tightening the inner ring in the axial direction with a shaft nut. In this case, the preload is controlled by measuring the starting friction moment of the bearing.

Fig. 6 shows an example of the head spindle of the lathe, the preload is adjusted by tightening the shaft nut.

Fig. 7 shows an example of a constant pressure preload for which the preload is adjusted by the displacement of the spring. In this case, first find a relationship between the spring's preload and displacement, then use this information to establish a constant pressure preload.

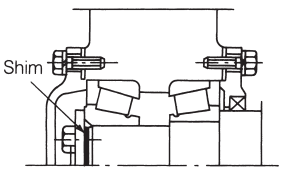

Fig. 1 DB arrangement whose clearance is adjusted by inner rings.

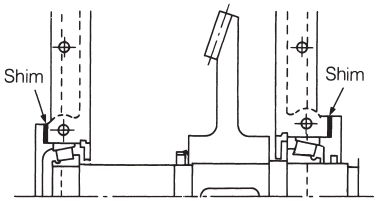

Fig. 2 DF arrangement whose clearance is adjusted by outer rings.

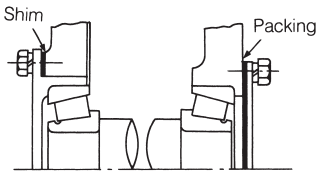

Fig. 3 Examples of clearance adjusted by shim thickness of outer ring cover

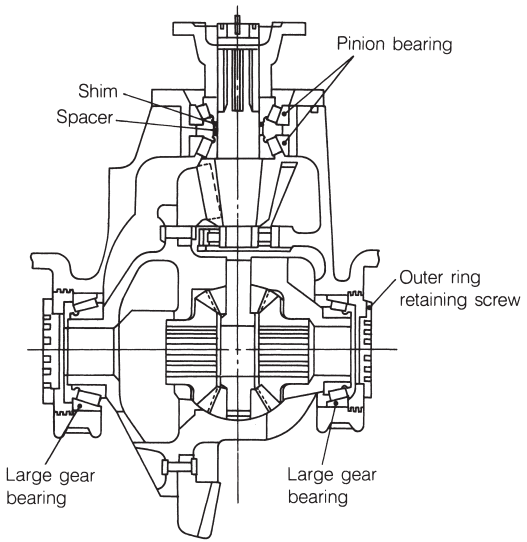

Fig. 4 Automotive final reduction gear

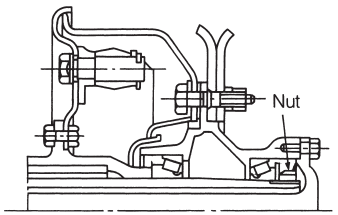

Fig. 5 Rear wheel of truck

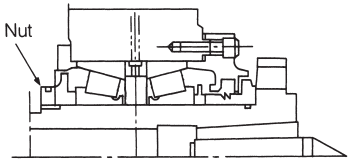

Fig. 6 Head spindle of lathe

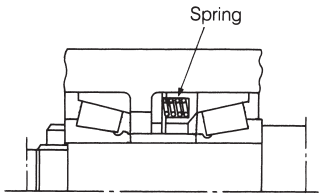

Fig. 7 Constant pressure preload applied by spring

5. Bearing internal load distribution and displacement

5.1 Bearing internal load distribution

This section will begin by examing the effect of a radial load F_r and an axial load F_a applied on a single-row bearing with a contact angle α (angular contact ball bearings, tapered roller bearings, etc.). The ratio of F_a to F_r determines the range of the loading area when just a portion of the raceway sustains the load, or when the entire raceway circumference sustains the load.
The size of the loading area is called the load factor ε. When only a part of the outer circumference bears the load, ε is the ratio between the projected length of the loading area and the raceway diameter. For this example, we use $\varepsilon \leqq 1$. (Refer to **Fig. 1**).

When the entire raceway circumference is subjected to a load, the calculation becomes,

$$\varepsilon = \frac{\delta_{max}}{\delta_{max} - \delta_{min}} \geqq 1$$

where, δ_{max}: Elastic deformation of a rolling element under maximum load
δ_{min}: Elastic deformation of a rolling element under minimum load

The load $Q(\psi)$ on any random rolling element is proportional to the amount of elastic deformation $\delta(\psi)$ of the contact surface raised to the t power. Therefore, it follows that when $\psi=0$ (with maximum rolling element load of Q_{max} and maximum elastic deformation of δ_{max}),

$$\frac{Q(\psi)}{Q_{max}} = \left(\frac{\delta(\psi)}{\delta_{max}}\right)^t \quad \cdots\cdots (1)$$

t=1.5 (point contact), t=1.1 (line contact)

The relations between the maximum rolling element load Q_{max}, radial load F_r, and axial load F_a are as follows:

$$F_r = J_r\, Z\, Q_{max} \cos\alpha \quad \cdots\cdots (2)$$
$$F_a = J_a\, Z\, Q_{max} \sin\alpha \quad \cdots\cdots (3)$$

where Z is the number of rolling elements, and J_r and J_a are coefficients for point and line contact derived from **Equation** (1). The values for J_r and J_a with corresponding ε values are given in **Table 1**. When ε=0.5, (when half of the raceway circumference is subjected to a load), the relationship between F_a and F_r becomes,

$$F_a = 1.216\, F_r \tan\alpha \quad \cdots\cdots \text{(point contact)}$$
$$F_a = 1.260\, F_r \tan\alpha \quad \cdots\cdots \text{(line contact)}$$

The basic load rating of radial bearings becomes significant under these conditions.

Assuming the internal clearance in a bearing Δ=0, ε=0.5 and using a value for J_r taken from **Table 1**, **Equation** (2) becomes,

$$Q_{max} = 4.37 \frac{F_r}{Z\cos\alpha} \text{ point contact} \quad \cdots\cdots (4)$$

$$Q_{max} = 4.08 \frac{F_r}{Z\cos\alpha} \text{ line contact} \quad \cdots\cdots (5)$$

With a pure axial load, F_r=0, $\varepsilon=\infty$, J_a=1, and **Equation** (3) becomes;

$$Q = Q_{max} = \frac{F_a}{Z\sin\alpha} \quad \cdots\cdots (6)$$

(In this case, the rolling elements all share the load equally.)

For a single-row deep groove ball bearing with zero clearance that is subjected to a pure radial load, the equation becomes;

$$Q_{max} = 4.37 \frac{F_r}{Z} \quad \cdots\cdots (7)$$

For a bearing with a clearance Δ>0 subjected to a radial load and with ε<0.5, the maximum rolling element load will be greater than that given by **Equation** (7). Also, if the outer ring is mounted with a clearance fit, the outer ring deformation will reduce the load range. **Equation** (8) is a more practical relation than **Equation** (7), since bearings usually operate with some internal clearance.

$$Q_{max} = 5 \frac{F_r}{Z} \quad \cdots\cdots (8)$$

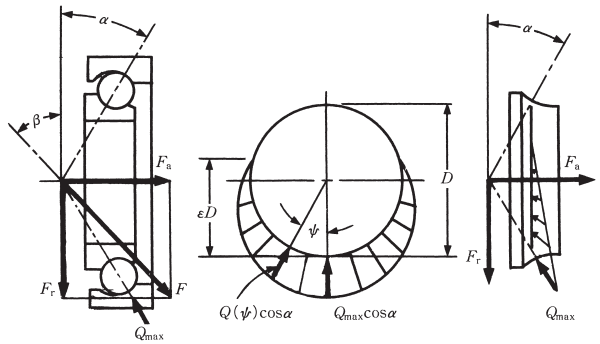

Fig. 1

Table 1 Values for J_r and J_a in single-row bearings

ε	Point contact			Line contact		
	$\frac{F_r \tan\alpha}{F_a}$	J_r	J_a	$\frac{F_r \tan\alpha}{F_a}$	J_r	J_a
0	1	0	0	1	0	0
0.1	0.9663	0.1156	0.1196	0.9613	0.1268	0.1319
0.2	0.9318	0.1590	0.1707	0.9215	0.1737	0.1885
0.3	0.8964	0.1892	0.2110	0.8805	0.2055	0.2334
0.4	0.8601	0.2117	0.2462	0.8380	0.2286	0.2728
0.5	0.8225	0.2288	0.2782	0.7939	0.2453	0.3090
0.6	0.7835	0.2416	0.3084	0.7480	0.2568	0.3433
0.7	0.7427	0.2505	0.3374	0.6999	0.2636	0.3766
0.8	0.6995	0.2559	0.3658	0.6486	0.2658	0.4098
0.9	0.6529	0.2576	0.3945	0.5920	0.2628	0.4439
1.0	0.6000	0.2546	0.4244	0.5238	0.2523	0.4817
1.25	0.4338	0.2289	0.5044	0.3598	0.2078	0.5775
1.67	0.3088	0.1871	0.6060	0.2340	0.1589	0.6790
2.5	0.1850	0.1339	0.7240	0.1372	0.1075	0.7837
5	0.0831	0.0711	0.8558	0.0611	0.0544	0.8909
∞	0	0	1	0	0	1

5.2 Radial clearance and load factor for radial ball bearings

The load distribution will differ if there is some radial clearance. If any load acts on a bearing, in order for the inner and outer rings to maintain parallel rotation, the inner and outer rings must move relative to each other out of their original unloaded position. Movement in the axial direction is symbolized by δ_a and that in the radial direction by δ_r. With a radial clearance Δ_r and a contact angle α, as shown in **Fig. 1**, the total elastic deformation $\delta(\psi)$ of a rolling element at the angle ψ is given by **Equation** (1).

$$\delta(\psi)=\delta_r\cos\psi\cos\alpha+\delta_a\sin\alpha-\frac{\Delta_r}{2}\cos\alpha \quad \cdots\cdots (1)$$

The maximum displacement δ_{max} with $\psi=0$ is given,

$$\delta_{max}=\delta_r\cos\psi+\delta_a\sin\alpha-\frac{\Delta_r}{2}\cos\alpha \quad \cdots\cdots (2)$$

Combining these two equations,

$$\delta(\psi)=\delta_{max}\left\{1-\frac{1}{2\varepsilon}(1-\cos\psi)\right\} \quad \cdots\cdots (3)$$

and,

$$\varepsilon=\frac{\delta_{max}}{2\delta_r\cos\alpha}=\frac{1}{2}\left\{1+\frac{\delta_a}{\delta_r}\tan\alpha-\frac{\Delta_r}{2\delta_r}\right\} \quad \cdots\cdots (4)$$

When there is no relative movement in the axial direction, ($\delta_a=0$), **Equations** (2) and (4) become,

$$\delta_{max}=\left(\delta_r-\frac{\Delta_r}{2}\right)\cos\alpha \quad \cdots\cdots (2)'$$

$$\varepsilon=\frac{1}{2}\left(1-\frac{\Delta_r}{2\delta_r}\right) \quad \cdots\cdots (4)'$$

$$\therefore\ \delta_{max}=\frac{\varepsilon}{1-\varepsilon}\Delta_r\cos\alpha \quad \cdots\cdots (5)$$

From the Hertz equation,

$$\delta_{max}=c\frac{Q_{max}^{2/3}}{D_w^{1/3}} \quad \cdots\cdots (6)$$

The maximum rolling element load Q_{max} is given by,

$$Q_{max}=\frac{F_r}{J_rZ\cos\alpha} \quad \cdots\cdots (7)$$

Combining **Equations** (5), (6), and (7) yields **Equation** (8) which shows the relation among radial clearance, radial load, and load factor.

$$\Delta_r=\left(\frac{1-2\varepsilon}{\varepsilon}J_r^{-2/3}\right)c\left(\frac{F_r}{Z}\right)^{2/3}D_w^{-1/3}\cos^{-5/3}\alpha \quad \cdots\cdots (8)$$

where, Δ_r: Radial clearance (mm)
ε: Load factor
J_r: Radial integral (Page 111, Table 1)
c: Hertz elasticity coefficient
F_r: Radial load (N), {kgf}
Z: Number of balls
D_w: Ball diameter (mm)
α: Contact angle (°)

Values obtained using **Equation** (8) for a 6208 single-row radial ball bearing are plotted in **Fig. 2**.

As an example of how to use this graph, assume a radial clearance of 20 μm and $F_r=C_r/10=2\ 910$ N {297 kgf}. The load factor ε is found to be 0.36 from **Fig. 2** and $J_r=0.203$ (Page 111, **Table 1**). The maximum rolling element load Q_{max} can then be calculated as follows,

$$Q_{max}=\frac{F_r}{J_rZ\cos\alpha}=\frac{2\ 910}{0.203\times9}=1\ 590\text{N}\ \{163\text{kgf}\}$$

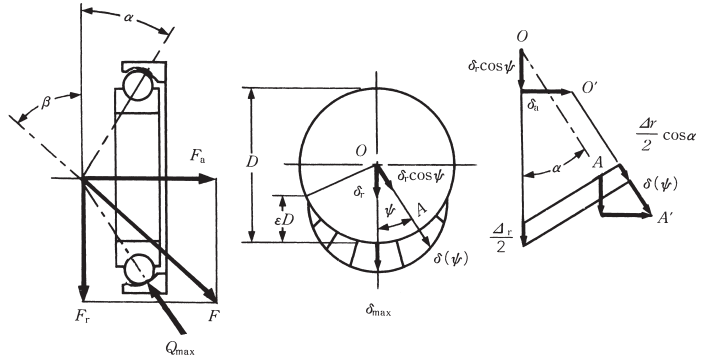

Fig. 1

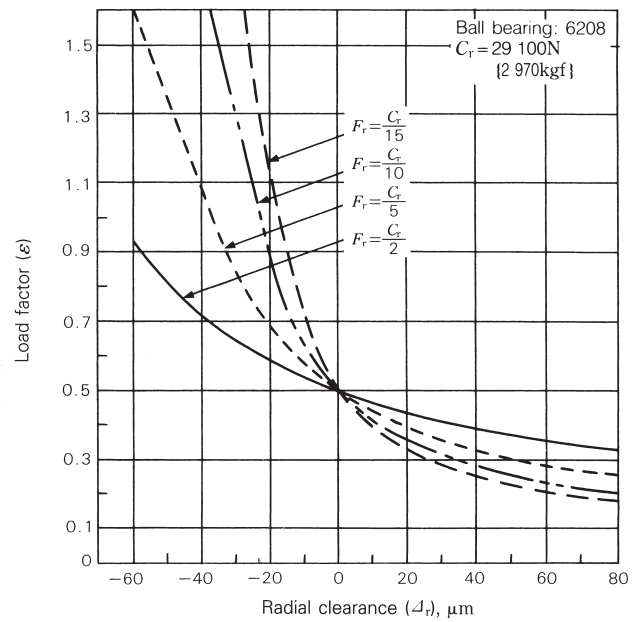

Fig. 2

5.3 Radial clearance and maximum rolling element load

If we consider an example where a deep groove ball bearing is subjected to a radial load and the radial clearance Δ_r is 0, then the load factor ε will be 0.5. When $\Delta_r>0$ (where there is a clearance), $\varepsilon<0.5$; when $\Delta_r<0$, $\varepsilon>0.5$. (See Fig. 1).

Fig. 2 in section 5.2 shows how the load factor change due to clearance decreases with increasing radial load.

When the relationship between radial clearance and load factor is determined, it can be used to establish the relationship between radial clearance and bearing life, and between radial clearance and maximum rolling element load.

The maximum rolling element load is calculated using Equation (1).

$$Q_{max}=\frac{F_r}{J_r Z\cos\alpha} \quad \cdots\cdots (1)$$

where, F_r: Radial load (N), {kgf}
J_r: Radial integral
Z: Number of balls
α: Contact angle (°)

J_r is dependent on the value of ε (Page 111, Table 1), and ε is determined, as explained in Section 5.2, from the radial load and radial clearance.

Fig. 2 shows the relationship between the radial clearance and maximum rolling element load for a 6208 deep groove ball bearing. As can be seen from Fig. 2, the maximum rolling element load increases with increasing radial clearance or reduction in the loaded range. When the radial clearance falls slightly below zero, the loaded range grows widely resulting in minimum in the maximum rolling element load. However, as the compression load on all rolling elements is increased when the clearance is further reduced, the maximum rolling element load begins to increase sharply.

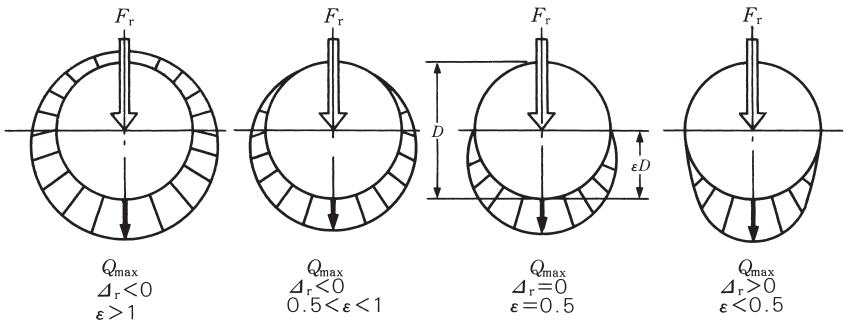

Fig. 1 Radial clearance and load distribution

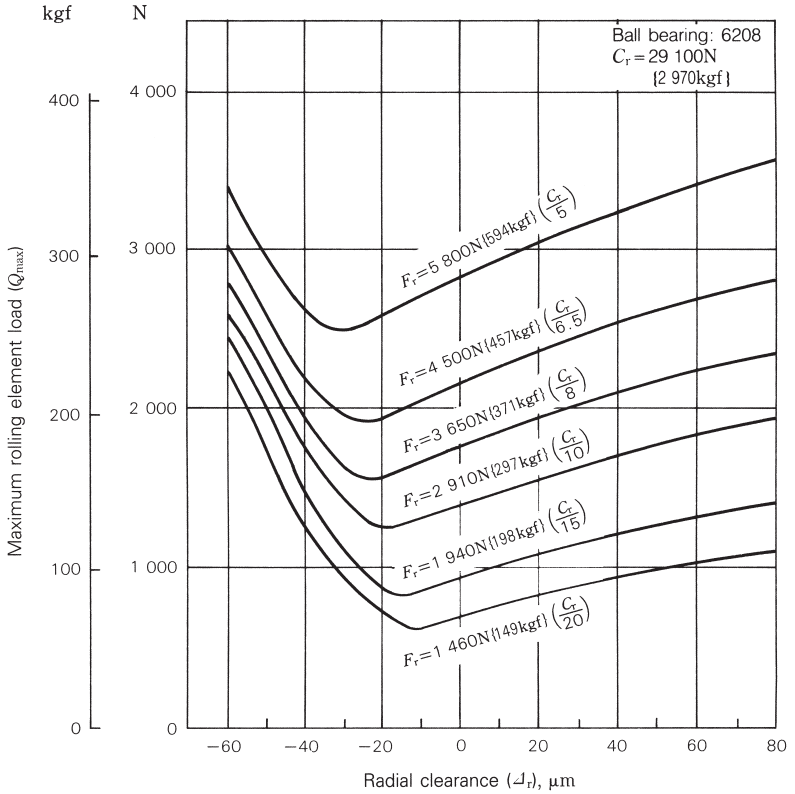

Fig. 2 Radial clearance and maximum rolling element load

5.4 Contact surface pressure and contact ellipse of ball bearings under pure radial loads

Details about the contact between a rolling element and raceway is a classic exercise in the Hertz theory and one where theory and practice have proven to agree well. It also forms the basis for theories on ball bearing life and friction.

Generally, the contact conditions between the inner ring raceway and ball is more severe than those between the outer ring raceway and ball. Moreover, when checking the running trace (rolling contact trace), it is much easier to observe the inner ring raceway than the outer ring raceway. Therefore, we explain the relation of contact ellipse width and load between an inner ring raceway and a ball in a deep groove ball bearing. With no applied load, the ball and inner ring raceway meet at a point. When a load is applied to the bearing, however, elastic deformation is caused and the contact area assumes an elliptical shape as shown in **Fig. 1**.

When a ball bearing is subjected to a load, the resulting maximum contact surface pressure on the elliptical area of contact between a ball and a bearing raceway is P_{max}. The major axis of the ellipse is represented by $2a$ and the minor axis by $2b$. The following relationships were derived from the Hertz equation.

$$P_{max}=\frac{1.5}{\pi}\left\{\frac{3}{E}\left(1-\frac{1}{m^2}\right)\right\}^{-2/3}\frac{1}{\mu\nu}(\Sigma\rho)^{2/3}Q^{1/3}$$

$$=\frac{A_1}{\mu\nu}(\Sigma\rho)^{2/3}Q^{1/3}$$

(MPa), {kgf/mm^2} ..... (1)

where, Constant A_1: 858 for (N-unit), 187 for {kgf-unit}

$$2a=\mu\left\{\frac{24\left(1-\frac{1}{m^2}\right)Q}{E\Sigma\rho}\right\}^{1/3}$$

$$=A_2\mu\left(\frac{Q}{\Sigma\rho}\right)^{1/3}\quad\text{(mm)}\ \cdots\cdots\ (2)$$

where, Constant A_2: 0.0472 for (N-unit), 0.101 for {kgf-unit}

$$2b=\nu\left\{\frac{24\left(1-\frac{1}{m^2}\right)Q}{E\Sigma\rho}\right\}^{1/3}$$

$$=A_2\nu\left(\frac{Q}{\Sigma\rho}\right)^{1/3}\quad\text{(mm)}\ \cdots\cdots\ (3)$$

where, E: Young's modulus (Steel: E=208 000 MPa {21 200 kgf/mm^2})
m: Poisson's number (Steel: 10/3)
Q: Rolling element (ball) load (N), {kgf}
$\Sigma\rho$: Total major curvature

For radial ball bearing,

$$\Sigma\rho=\frac{1}{D_w}\left(4-\frac{1}{f}\pm\frac{2\gamma}{1\mp\gamma}\right)\ \cdots\cdots\ (4)$$

Symbol of ±: The upper is for inner ring.
The lower is for outer ring.

D_w: Ball diameter (mm)
f: Ratio of groove radius to ball diameter
γ: $D_w\cos\alpha/D_{pw}$
D_{pw}: Ball pitch diameter (mm)
α: Contact angle (°)

μ and ν are shown in **Fig. 2** based on $\cos\tau$ in **Equation** (5).

$$\cos\tau=\frac{\frac{1}{f}\pm\frac{2\gamma}{1\mp\gamma}}{4-\frac{1}{f}\pm\frac{2\gamma}{1\mp\gamma}}\ \cdots\cdots\ (5)$$

Symbol of ±: The upper is for the inner ring.
The lower is for the outer ring.

If the maximum rolling element load of the ball bearing under the radial load F_r is Q_{max} and the number of balls is Z, an approximate relation between them is shown in **Equation** (6).

$$Q_{max}=5\frac{F_r}{Z}\ \cdots\cdots\ (6)$$

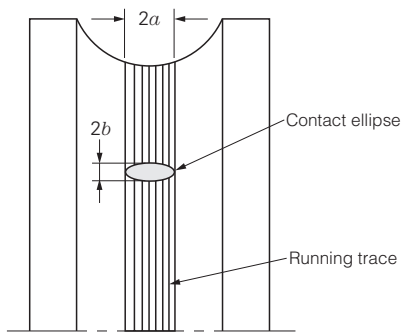

Fig. 1 Inner ring raceway running trace (Rolling contact trace)

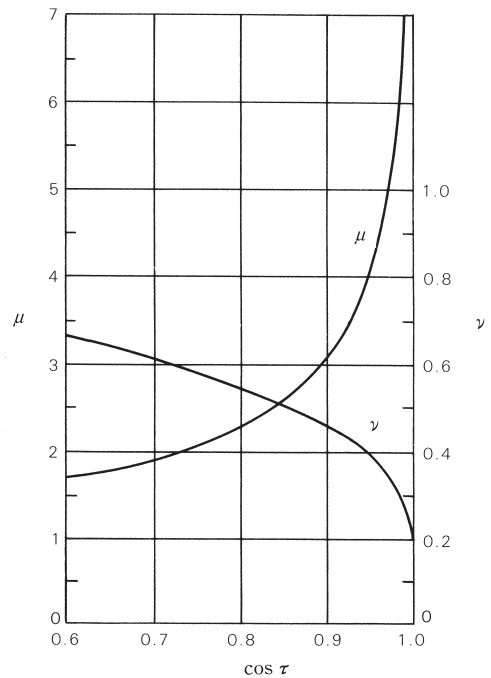

Fig. 2 μ and ν values against $\cos\tau$

Therefore, Equations (1), (2), and (3) can be changed into the following equations by substituting Equations (4) and (6).

$$P_{max} = K_1 \cdot F_r^{1/3} \quad \text{(MPa)} \qquad = 0.218 K_1 \cdot F_r^{1/3} \quad \{\text{kgf/mm}^2\} \quad \cdots\cdots (7)$$

$$2a = K_2 \cdot F_r^{1/3} \quad \text{(N)} \qquad = 2.14 K_2 \cdot F_r^{1/3} \quad \{\text{kgf}\} \quad \text{(mm)} \quad \cdots\cdots (8)$$

$$2b = K_3 \cdot F_r^{1/3} \quad \text{(N)} \qquad = 2.14 K_3 \cdot F_r^{1/3} \quad \{\text{kgf}\} \quad \text{(mm)} \quad \cdots\cdots (9)$$

Table 1 gives values for the constants K_1, K_2, and K_3 for different bearing numbers.

Generally, the ball bearing raceway has a running trace caused by the balls whose width is equivalent to $2a$. We can estimate the applied load by referring to the trace on the raceway. Therefore, we can judge whether or not any abnormal load was sustained by the bearing which was beyond what the bearing was originally designed to carry.

Example

The pure radial load, F_r=3 500 N (10% of basic dynamic load rating), is applied to a deep groove ball bearing, 6210. Calculate the maximum surface pressure, P_{max}, and contact widths of the ball and inner ring raceway, $2a$ and $2b$.

Using the figures of K_1 ~ K_3 in Table 1, the following values can be obtained.

P_{max} = $K_1 \cdot F_r^{1/3}$=143×3 500$^{1/3}$=2 170 (MPa)
$2a$ = $K_2 \cdot F_r^{1/3}$=0.258×3 500$^{1/3}$=3.92 (mm)
$2b$ = $K_3 \cdot F_r^{1/3}$=0.026×3 500$^{1/3}$=0.39 (mm)

Table 1 Values of constants, K_1, K_2, and K_3, for deep groove ball bearings

Bearing bore No.	Bearing series 60			Bearing series 62			Bearing series 63		
	K_1	K_2	K_3	K_1	K_2	K_3	K_1	K_2	K_3
00	324	0.215	0.020	303	0.205	0.019	215	0.404	0.018
01	305	0.205	0.019	226	0.352	0.017	200	0.423	0.019
02	287	0.196	0.019	211	0.336	0.017	184	0.401	0.019
03	274	0.189	0.018	193	0.356	0.017	171	0.415	0.019
04	191	0.332	0.017	172	0.382	0.018	161	0.431	0.020
05	181	0.320	0.016	162	0.367	0.018	142	0.426	0.020
06	160	0.326	0.017	143	0.395	0.019	129	0.450	0.021
07	148	0.342	0.017	128	0.420	0.020	118	0.474	0.021
08	182	0.205	0.021	157	0.262	0.026	112	0.469	0.023
09	166	0.206	0.021	150	0.252	0.025	129	0.308	0.030
10	161	0.201	0.021	143	0.258	0.026	122	0.318	0.031
11	148	0.219	0.023	133	0.269	0.027	116	0.327	0.032
12	144	0.214	0.022	124	0.275	0.028	110	0.336	0.032
13	140	0.209	0.022	120	0.280	0.028	105	0.344	0.033
14	130	0.224	0.023	116	0.284	0.029	100	0.352	0.034
15	127	0.219	0.023	112	0.275	0.028	96.5	0.356	0.035
16	120	0.235	0.024	109	0.293	0.030	92.8	0.364	0.035
17	117	0.229	0.024	104	0.302	0.031	89.4	0.371	0.036
18	111	0.244	0.025	98.7	0.310	0.031	86.3	0.377	0.037
19	108	0.238	0.025	94.3	0.318	0.032	83.4	0.384	0.037
20	108	0.238	0.025	90.3	0.325	0.033	78.6	0.394	0.038
21	102	0.243	0.026	87.2	0.329	0.033	76.7	0.400	0.039
22	98.2	0.268	0.028	83.9	0.336	0.034	72.7	0.412	0.040
24	95.3	0.261	0.027	80.7	0.343	0.035	72.0	0.411	0.040
26	88.1	0.263	0.028	77.8	0.349	0.035	68.5	0.422	0.041
28	85.9	0.257	0.027	77.2	0.348	0.036	65.5	0.431	0.042
30	81.8	0.264	0.028	74.3	0.337	0.035	62.5	0.414	0.041

5.5 Contact surface pressure and contact area under pure radial load (roller bearings)

The following equations, Equations 1 and 2, which were derived from the Hertz equation, give the contact surface pressure P_{max} between two axially-parallel cylinders and the contact area width $2b$ (Fig. 1).

$$P_{max}=\sqrt{\frac{E\cdot\Sigma\rho\cdot Q}{2\pi\left(1-\frac{1}{m^2}\right)L_{we}}}=A_1\sqrt{\frac{\Sigma\rho\cdot Q}{L_w}}$$

(MPa) {kgf/mm^2} ..... (1)

where, constant A_1: 191 ..... (N-unit)
: 60.9 ..... {kgf-unit}

$$2b=\sqrt{\frac{32\left(1-\frac{1}{m^2}\right)Q}{\pi\cdot E\cdot\Sigma\rho\cdot L_w}}=A_2\sqrt{\frac{Q}{\Sigma\rho\cdot L_w}}$$

(mm) ..... (2)

where, constant A_2: 0.00668 ..... (N-unit)
: 0.0209 ..... {kgf-unit}

where, E: Young's modulus (Steel: E=208 000 MPa {21 200 kgf/mm^2})
m: Poisson's number (for steel, m=10/3)
$\Sigma\rho$: Composite curvature for both cylinders
$\Sigma\rho=\rho_{I1}+\rho_{II1}$ (mm^{-1})
ρ_{I1}: Curvature, cylinier I (roller)
$\rho_{I1}=1/D_w/2=2/D_w$ (mm^{-1})
ρ_{II1}: Curvature, cylinier II (raceway)
$\rho_{II1}=1/D_i/2=2/D_i$ (mm^{-1}) for inner ring raceway
$\rho_{II1}=-1/D_e/2=-2/D_e$ (mm^{-1}) for outer ring raceway
Q: Normal load on cylinders (N), {kgf}
L_{we}: Effective contact length of cylinders (mm)

When a radial load F_r is applied on a radial roller bearing, the maximum rolling element load Q_{max} for practical use is given by Equation (3).

$$Q_{max}=\frac{4.6\,F_r}{i\,Z\cos\alpha}\quad \text{(N), \{kgf\}} \quad\cdots\cdots (3)$$

where, i: Number of roller rows
Z: Number of rollers per row
α: Contact angle (°)

The contact surface pressure P_{max} and contact width $2b$ of raceway and roller which sustains the largest load are given by Equations (4) and (5).

$$\left.\begin{aligned}P_{max}&=K_1\sqrt{F_r} &&\text{(MPa)}\\ &=0.319K_1\sqrt{F_r} &&\text{\{kgf/mm}^2\text{\}}\end{aligned}\right\}\quad\cdots\cdots (4)$$

$$\left.\begin{aligned}2b&=K_2\sqrt{F_r} &&\text{(N)}\\ &=3.13K_2\sqrt{F_r} &&\text{\{kgf\}}\end{aligned}\right\}\quad\cdots\cdots (5)$$

The constant K_1 and K_2 of cylindrical roller bearings and tapered roller bearings are listed in Tables 1 to 6 according to the bearing numbers. K_{1i} and K_{2i} are the constants for the contact of roller and inner ring raceway, and K_{1e} and K_{2e} are the constants for the contact of roller and outer ring raceway.

Example

A pure radial load, F_r=4 800 N (10% of basic dynamic load rating), is applied to the cylindrical roller bearing, NU210. Calculate the maximum surface pressure, P_{max}, and contact widths of the roller and raceway, $2b$.

Using the figures of K_{1i}, K_{1e} K_{2i}, and K_{2e} in Table 1, the following values can be obtained.

Contact of roller and inner ring raceway:
$P_{max}=K_{1i}\sqrt{F_r}=17.0\times\sqrt{4\ 800}=1\ 180$ (MPa)
$2b=K_{2i}\sqrt{F_r}=2.55\times10^{-3}\times\sqrt{4\ 800}=0.18$ (mm)

Contact of roller and outer ring raceway:
$P_{max}=K_{1e}\sqrt{F_r}=14.7\times\sqrt{4\ 800}=1\ 020$ (MPa)
$2b=K_{2e}\sqrt{F_r}=2.95\times10^{-3}\times\sqrt{4\ 800}=0.20$ (mm)

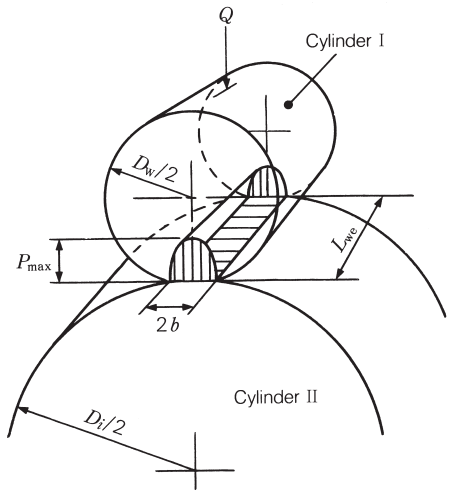

Fig. 1 Contact surface pressure P_{max} and contact width $2b$

Table 1 Constants, K_{1i}, K_{1e}, K_{2i}, and K_{2e}, for cylindrical roller bearings

Bearing No.	Bearing series NU2				Bearing No.	Bearing series NU3			
	K_{1i}	K_{1e}	K_{2i}	K_{2e}		K_{1i}	K_{1e}	K_{2i}	K_{2e}
			$\times 10^{-3}$	$\times 10^{-3}$				$\times 10^{-3}$	$\times 10^{-3}$
NU205W	30.6	25.8	2.90	3.44	NU305W	24.2	19.6	3.03	3.73
NU206W	26.1	22.2	2.87	3.39	NU306W	20.5	16.8	2.89	3.52
NU207W	21.6	18.2	2.83	3.36	NU307W	17.7	14.6	2.76	3.35
NU208W	18.5	15.7	2.70	3.20	NU308W	16.1	13.4	2.76	3.32
NU209W	17.7	15.2	2.63	3.07	NU309W	14.4	11.8	2.85	3.46
NU210W	17.0	14.7	2.55	2.95	NU310W	13.1	10.8	2.79	3.37
NU211W	15.4	13.3	2.54	2.93	NU311W	11.5	9.44	2.76	3.36
NU212W	14.0	12.2	2.53	2.92	NU312W	10.8	8.91	2.76	3.34
NU213W	12.5	10.8	2.44	2.82	NU313W	10.3	8.54	2.79	3.37
NU214W	12.4	10.9	2.45	2.81	NU314W	9.35	7.78	2.68	3.22
NU215W	11.5	10.1	2.44	2.80	NU315W	8.83	7.31	2.77	3.34
NU216W	11.0	9.57	2.49	2.86	NU316W	8.43	7.05	2.68	3.20
NU217W	10.2	8.94	2.48	2.85	NU317W	8.04	6.68	2.76	3.32
NU218W	9.10	7.87	2.45	2.84	NU318W	7.45	6.22	2.68	3.21
NU219W	8.98	7.77	2.56	2.96	NU319W	7.14	5.97	2.68	3.20
NU220W	8.23	7.13	2.47	2.85	NU320W	6.61	5.52	2.66	3.19
NU221W	7.82	6.78	2.47	2.85	NU321W	6.42	5.34	2.76	3.31
NU222W	7.36	6.34	2.53	2.93	NU322W	6.06	5.04	2.78	3.34
NU224W	7.02	6.08	2.53	2.92	NU324W	5.38	4.44	2.75	3.33
NU226W	6.76	5.91	2.46	2.82	NU326W	5.07	4.21	2.75	3.32
NU228W	6.27	5.48	2.47	2.83	NU328W	4.80	3.99	2.75	3.31
NU230W	5.80	5.07	2.47	2.83	NU330W	4.61	3.85	2.79	3.34

Table 2 Constants, K_{1i}, K_{1e}, K_{2i}, and K_{2e}, for cylindrical roller bearings

Bearing No.	Bearing series NU4				Bearing No.	Bearing series NU22			
	K_{1i}	K_{1e}	K_{2i}	K_{2e}		K_{1i}	K_{1e}	K_{2i}	K_{2e}
			$\times 10^{-3}$	$\times 10^{-3}$				$\times 10^{-3}$	$\times 10^{-3}$
NU405W	19.2	15.1	3.08	3.92	NU2205W	25.4	21.4	2.40	2.85
NU406W	16.4	12.9	3.06	3.90	NU2206W	21.1	17.9	2.32	2.73
NU407W	14.6	11.7	2.99	3.74	NU2207W	17.0	14.3	2.22	2.63
NU408W	12.9	10.2	2.96	3.73	NU2208W	15.4	13.0	2.25	2.66
NU409W	12.0	9.65	2.97	3.70	NU2209W	14.7	12.6	2.18	2.55
NU410W	10.9	8.73	2.98	3.73	NU2210W	14.1	12.3	2.12	2.45
NU411W	10.3	8.37	2.87	3.54	NU2211W	13.0	11.3	2.15	2.48
NU412W	9.35	7.56	2.85	3.52	NU2212W	11.3	9.79	2.04	2.35
NU413W	8.90	7.23	2.85	3.51	NU2213W	9.93	8.62	1.94	2.24
NU414W	7.90	6.41	2.86	3.52	NU2214W	9.88	8.64	1.95	2.23
NU415W	7.34	5.92	2.84	3.52	NU2215W	9.54	8.32	2.02	2.32
NU416W	6.84	5.50	2.82	3.51	NU2216W	8.90	7.76	2.02	2.31
NU417M	6.49	5.18	2.83	3.55	NU2217W	8.22	7.17	1.99	2.28
NU418M	6.07	4.87	2.83	3.53	NU2218W	7.46	6.45	2.01	2.33
NU419M	5.76	4.69	2.73	3.36	NU2219W	7.03	6.08	2.00	2.32
NU420M	5.44	4.41	2.72	3.35	NU2220W	6.82	5.90	2.05	2.36
NU421M	5.15	4.17	2.71	3.35	NU2221M	6.44	5.58	2.03	2.34
NU422M	4.87	3.95	2.71	3.34	NU2222W	5.96	5.14	2.05	2.38
NU424M	4.37	3.54	2.72	3.37	NU2224W	5.65	4.89	2.03	2.35
NU426M	3.92	3.16	2.71	3.36	NU2226W	5.28	4.61	1.92	2.20
NU428M	3.80	3.07	2.74	3.38	NU2228W	4.82	4.22	1.90	2.18
NU430M	2.97	2.97	2.65	3.23	NU2230W	4.55	3.98	1.93	2.21

Table 3 Constants, K_{1i}, K_{1e}, K_{2i}, and K_{2e}, for cylindrical roller bearings

Bearing No.	Bearing series NU23				Bearing No.	Bearing series NN30			
	K_{1i}	K_{1e}	K_{2i}	K_{2e}		K_{1i}	K_{1e}	K_{2i}	K_{2e}
			$\times 10^{-3}$	$\times 10^{-3}$				$\times 10^{-3}$	$\times 10^{-3}$
NU2305W	19.0	15.4	2.38	2.93	NN3005	31.3	27.3	2.36	2.72
NU2306W	17.0	14.0	2.41	2.93	NN3006	28.1	24.7	2.36	2.69
NU2307W	15.6	12.9	2.43	2.96	NN3007T	24.3	21.5	2.24	2.53
NU2308W	12.9	10.7	2.22	2.67	NN3008T	23.1	20.4	2.31	2.61
NU2309W	11.9	9.79	2.36	2.86	NN3009T	20.7	18.4	2.25	2.52
NU2310W	10.6	8.76	2.26	2.73	NN3010T	20.1	18.1	2.20	2.45
NU2311W	9.53	7.83	2.29	2.78	NN3011T	17.5	15.6	2.18	2.43
NU2312W	8.85	7.31	2.26	2.74	NN3012T	16.7	15.0	2.09	2.32
NU2313W	8.32	6.90	2.26	2.72	NN3013T	15.9	14.5	2.02	2.22
NU2314W	7.50	6.24	2.15	2.58	NN3014T	14.4	13.0	2.04	2.25
NU2315W	6.98	5.78	2.19	2.64	NN3015T	14.0	12.8	2.01	2.20
NU2316W	6.66	5.58	2.11	2.53	NN3016T	12.6	11.4	1.99	2.19
NU2317W	6.21	5.17	2.14	2.57	NN3017T	12.3	11.2	1.96	2.15
NU2318W	6.11	5.10	2.20	2.63	NN3018T	11.4	10.3	1.98	2.18
NU2319W	5.65	4.73	2.12	2.53	NN3019T	11.1	10.2	1.95	2.14
NU2320W	5.40	4.51	2.18	2.60	NN3020T	10.9	10.0	1.92	2.09
NU2321M	4.80	3.99	2.06	2.48	NN3021T	9.75	8.84	2.00	2.21
NU2322M	4.48	3.73	2.05	2.47	NN3022T	9.04	8.18	2.00	2.20
NU2324M	4.00	3.31	2.05	2.48	NN3024T	8.66	7.90	1.93	2.11
NU2326M	3.62	3.00	1.96	2.37	NN3026T	7.86	7.14	1.99	2.19
NU2328M	3.43	2.86	1.97	2.36	NN3028	7.55	6.90	1.92	2.11
NU2330M	3.24	2.70	1.96	2.34	NN3030	7.08	6.47	1.92	2.10

Table 4 Constants, K_{1i}, K_{1e}, K_{2i}, and K_{2e}, for tapered roller bearings

Bearing No.	Bearing series 302				Bearing No.	Bearing series 303			
	K_{1i}	K_{1e}	K_{2i}	K_{2e}		K_{1i}	K_{1e}	K_{2i}	K_{2e}
			$\times 10^{-3}$	$\times 10^{-3}$				$\times 10^{-3}$	$\times 10^{-3}$
HR30205J	20.6	17.4	1.94	2.29	HR30305J	17.8	14.3	2.34	2.92
HR30206J	17.7	14.9	1.99	2.36	HR30306J	15.7	12.8	2.30	2.83
HR30207J	15.8	13.3	2.07	2.45	HR30307J	13.7	11.1	2.26	2.78
HR30208J	14.5	12.3	2.13	2.52	HR30308J	12.1	10.0	2.09	2.51
HR30209J	13.7	11.7	2.03	2.37	HR30309J	10.9	9.07	2.11	2.54
HR30210J	12.7	11.0	1.96	2.28	HR30310J	10.1	8.37	2.16	2.60
HR30211J	11.4	9.80	2.02	2.36	HR30311J	9.38	7.79	2.19	2.64
HR30212J	11.0	9.41	2.11	2.46	HR30312J	8.66	7.19	2.19	2.64
HR30213J	10.0	8.62	2.05	2.38	HR30313J	8.04	6.68	2.20	2.65
HR30214J	9.62	8.28	2.07	2.40	HR30314J	7.49	6.22	2.20	2.65
HR30215J	9.11	7.89	1.99	2.30	HR30315J	7.09	5.88	2.23	2.68
HR30216J	8.79	7.57	2.12	2.47	HR30316J	6.79	5.64	2.28	2.74
HR30217J	8.04	6.93	2.07	2.40	HR30317J	6.30	5.24	2.22	2.68
HR30218J	7.69	6.63	2.10	2.44	30318	6.42	5.34	2.41	2.89
HR30219J	7.27	6.26	2.11	2.45	30319	6.09	5.06	2.37	2.85
HR30220J	6.74	5.81	2.07	2.40	30320	5.84	4.86	2.43	2.92
HR30221J	6.36	5.48	2.06	2.39	30321	5.62	4.67	2.44	2.94
HR30222J	5.94	5.12	2.03	2.36	HR30322J	4.99	4.15	2.33	2.81
HR30224J	5.74	4.97	2.06	2.38	HR30324J	4.75	3.95	2.39	2.88
30226	5.83	5.07	2.23	2.57	30326	4.69	3.93	2.46	2.94
HR30228J	5.36	4.64	2.24	2.58	30328	4.47	3.75	2.50	2.98
30230	5.10	4.41	2.31	2.67	30330	4.15	3.48	2.50	2.98

Table 5 Constants, K_{1i}, K_{1e}, K_{2i}, and K_{2e}, for tapered roller bearings

Bearing No.	Bearing series 322				Bearing No.	Bearing series 323			
	K_{1i}	K_{1e}	K_{2i}	K_{2e}		K_{1i}	K_{1e}	K_{2i}	K_{2e}
			$\times 10^{-3}$	$\times 10^{-3}$				$\times 10^{-3}$	$\times 10^{-3}$
HR32205	18.5	15.6	1.72	2.04	HR32305J	15.0	12.0	1.93	2.40
HR32206J	15.7	13.2	1.76	2.08	HR32306J	12.9	10.5	1.86	2.28
HR32207J	13.3	11.2	1.73	2.05	HR32307J	11.5	9.38	1.87	2.30
HR32208J	12.8	10.8	1.88	2.22	HR32308J	10.1	8.38	1.71	2.06
HR32209J	12.0	10.3	1.79	2.09	HR32309J	9.22	7.65	1.75	2.11
HR32210J	11.7	10.0	1.80	2.08	HR32310J	8.26	6.86	1.73	2.08
HR32211J	10.4	8.90	1.83	2.14	HR32311J	7.62	6.33	1.74	2.10
HR32212J	9.43	8.08	1.80	2.10	HR32312J	7.13	5.92	1.77	2.13
HR32213J	9.64	7.40	1.82	2.13	HR32313J	6.62	5.50	1.78	2.15
HR32214J	8.58	7.39	1.84	2.14	HR32314J	6.21	5.16	1.79	2.16
HR32215J	8.28	7.18	1.81	2.09	HR32315J	5.80	4.81	1.79	2.15
HR32216J	7.70	6.63	1.86	2.15	HR32316J	5.46	4.54	1.80	2.16
HR32217J	7.38	6.36	1.90	2.21	HR32317J	5.26	4.36	1.83	2.20
HR32218J	6.56	5.65	1.80	2.09	HR32318J	5.00	4.15	1.83	2.20
HR32219J	6.14	5.29	1.78	2.07	32319	4.97	4.13	1.89	2.27
HR32220J	5.77	4.97	1.77	2.06	HR32320J	4.43	3.68	1.84	2.21
HR32221J	5.39	4.64	1.74	2.02	32321	4.36	3.62	1.88	2.27
HR32222J	5.12	4.41	1.75	2.03	HR32322J	4.03	3.35	1.87	2.25
HR32224J	4.82	4.18	1.72	1.98	HR32324J	3.75	3.11	1.87	2.25
32226	4.48	3.90	1.68	1.93	32326	3.59	3.01	1.89	2.26
HR32228J	4.02	3.48	1.67	1.93	32328	3.21	2.71	1.75	2.08
32230	4.06	3.55	1.74	1.99	32330	2.95	2.51	1.65	1.94

Table 6 Constants, K_{1i}, K_{1e}, K_{2i}, and K_{2e}, for tapered roller bearings

Bearing No.	Bearing series 303D				Bearing No.	Bearing series 320			
	K_{1i}	K_{1e}	K_{2i}	K_{2e}		K_{1i}	K_{1e}	K_{2i}	K_{2e}
			$\times 10^{-3}$	$\times 10^{-3}$				$\times 10^{-3}$	$\times 10^{-3}$
30305D	22.0	18.4	2.42	2.91	HR32005XJ	21.1	18.4	1.58	1.82
30306D	19.0	15.8	2.48	2.98	HR32006XJ	18.2	15.9	1.61	1.85
HR30307DJ	14.8	12.4	2.18	2.62	HR32007XJ	16.4	14.4	1.57	1.79
HR30308DJ	13.0	10.8	2.18	2.61	HR32008XJ	14.4	12.7	1.48	1.67
HR30309DJ	11.9	9.94	2.22	2.66	HR32009XJ	13.3	11.8	1.47	1.65
HR30310DJ	10.8	9.02	2.21	2.65	HR32010XJ	13.0	11.6	1.45	1.62
HR30311DJ	10.0	8.37	2.22	2.66	HR32011XJ	11.3	10.0	1.46	1.64
HR30312DJ	9.33	7.79	2.26	2.71	HR32012XJ	10.8	9.69	1.41	1.57
HR30313DJ	8.66	7.23	2.27	2.71	HR32013XJ	10.6	9.57	1.39	1.54
HR30314DJ	8.20	6.85	2.28	2.74	HR32014XJ	9.68	8.70	1.44	1.60
HR30315DJ	7.83	6.54	2.34	2.80	HR32015XJ	9.32	8.43	1.39	1.54
HR30316DJ	7.37	6.15	2.33	2.80	HR32016XJ	8.15	7.35	1.36	1.51
HR30317DJ	6.93	5.79	2.34	2.80	HR32017XJ	8.00	7.25	1.34	1.48
HR30318DJ	6.96	5.81	2.48	2.98	HR32018XJ	7.36	6.64	1.37	1.52
HR30319DJ	6.34	5.30	2.37	2.84	HR32019XJ	7.22	6.54	1.35	1.50
—	—	—	—	—	HR32020XJ	7.10	6.45	1.34	1.47
—	—	—	—	—	HR32021XJ	6.61	5.99	1.36	1.50
—	—	—	—	—	HR32022XJ	6.19	5.59	1.39	1.54
—	—	—	—	—	HR32024XJ	6.10	5.52	1.42	1.56
—	—	—	—	—	HR32026XJ	5.26	4.74	1.41	1.57
—	—	—	—	—	HR32028XJ	5.15	4.67	1.39	1.54
—	—	—	—	—	HR32030XJ	4.77	4.32	1.38	1.53

5.6 Rolling contact trace and load conditions

5.6.1 Ball bearing

When a rolling bearing is rotating while subjected to a load on the raceways of the inner and outer rings and on the surfaces of the rolling elements, heavy stress is generated at the place of contact. For example, when about 10% of the load (normal load) of the C_r, basic dynamic load rating, as radial load, is applied, in the case of deep groove ball bearings, its maximum surface pressure becomes about 2 000 MPa {204 kgf/mm^2} and for a roller bearing, the pressure reaches 1 000 MPa {102 kgf/mm^2}.

As bearings are used under such high contact surface pressure, the contact parts of the rolling elements and raceway may become slightly elastically deformed or wearing may progress depending on lubrication conditions. As a result of this contact trace, light reflected from the raceway surface of a used bearing looks different for the places where a load was not applied.
Parts that were subjected to load reflect light differently and the dull appearance of such parts is called a trace (rolling contact trace). Thus, an examination of the trace can provide insights into the contact and load conditions.

Trace varies depending on the bearing type and conditions. Examination of the trace sometimes allows identification of the cause: radial load only, heavy axial load, moment load, or extreme unevenness of stiffness of housing.

For the case of a deep groove ball bearing used under an inner ring rotation load, only radial load F_r is applied, under the general condition of residual clearance after mounting is Δ_r>0, the load zone ψ becomes narrower than 180° (Fig. 1), traces on inner and outer rings become as shown in Fig. 2.

In addition to a radial load F_r, if an axial load F_a is simultaneously applied, the load zone ψ is widened as shown in Fig. 3. When only an axial load is applied, all rolling elements are uniformly subjected to the load, for both inner and outer rings the load zone becomes ψ=360° and the race is unevenly displaced in the axial direction.

A deviated and inclined trace may be observed on the outer ring as shown in Fig. 4, when an axial load and relative inclination of the inner ring to the outer ring are applied together to a deep groove or angular contact ball bearing used for inner ring rotation load. Or if the deflection is big, a similar trace appears.

As explained above, by comparing the actual trace with the shape of the trace forecasted from the external force considered when the bearing was designed, it is possible to tell if an abnormal axial load was applied to the bearing or if the mounting error was excessive.

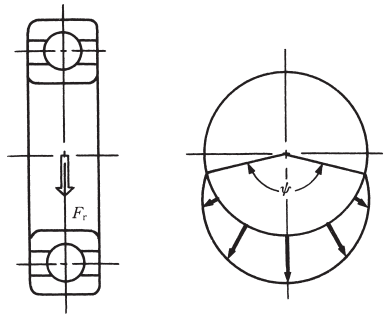

Fig. 1 Load zone under a radial load only

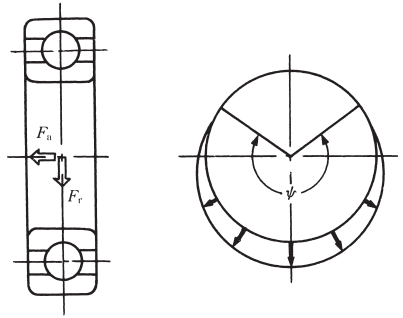

Fig. 3 Load zone for radial load + axial load

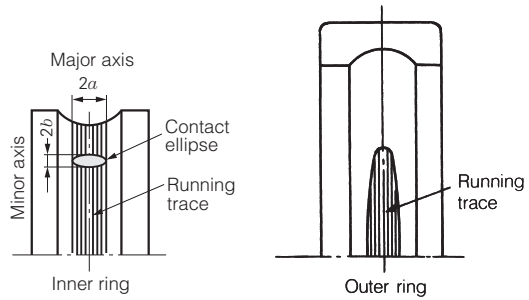

Fig. 2 Trace (rolling contact trace) on raceway surface

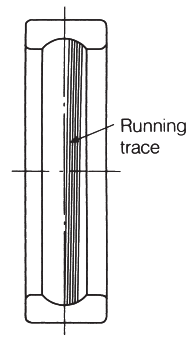

Fig. 4 Deviation and inclination of trace (rolling contact trace) on raceway surface of outer ring

5.6.2 Roller bearing

The relation between load condition and running trace of roller bearings may be described as follows. Usually, when rollers (or raceway) of a roller bearing are not crowned despite there being no relative inclination on inner ring with outer ring, then stress concentration occurs at the end parts where the rollers contact the raceway (Fig. 5 (a)). Noticeable contact appears at both ends of the trace. If the stress on the end parts is excessive, premature flaking occurs. Rollers (or raceway) can be crowned to reduce stress (Fig. 5 (b)). Even if the rollers are crowned, however, if inclination exists between the inner and outer rings, then stress at the contacting part becomes as shown in Fig. 5 (c).

Fig. 6 (a) shows an example of trace on an outer ring raceway for a radial load which is correctly applied to a cylindrical roller bearing and used for inner ring rotation. Compared with this, if there is relative inclination of inner ring to outer ring, as shown in Fig. 6 (b), the trace on raceway has shading in width direction. And the trace looks inclined at the entry and exit of the load zone.

The trace of outer ring becomes as shown in Fig. 7 (a) for double-row tapered roller bearings if only a radial load is applied while inner ring is rotating, or the trace becomes as shown in Fig. 7 (b) if only an axial load is applied.
In addition, traces are produced on both sides of the raceway (displaced by 180°) as shown in Fig. 7 (c) if a radial load is applied under the condition that there is a large relative inclination of the inner ring to the outer ring.

The trace becomes even on the right and left sides of the raceways if a radial load is applied to a spherical roller bearing having the permissible aligning angle of 1 to 2.5°. In the case of an application of an axial load, the trace appears only on one side. A trace is produced that has a difference corresponding to them and is marked on right and left load zones if combined radial and axial loads are applied.

Therefore, the trace becomes even on the left and right sides for a free-end spherical roller bearing that is mainly subjected to radial load. If the length of the trace is greatly different, it indicates that internal axial load caused by thermal expansion of shaft, etc. was not sufficiently absorbed by displacement of the bearing in the axial direction.

Besides the above, the trace on raceway is influenced often by the shaft or housing. By comparison of the bearing outside face contact or pattern of fretting against the degree of trace on raceway, it is possible to tell if there is structural failure or uneven stiffness of shaft or housing.

As explained above, observation of the trace on raceway can help to prevent bearing trouble.

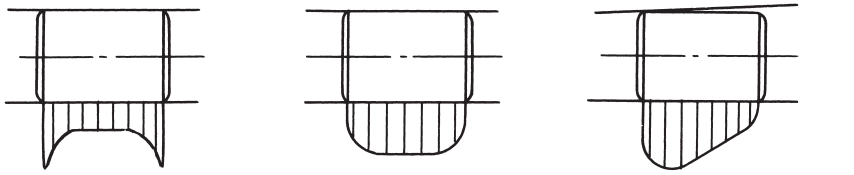

(a) Roller having no crowning (b) Crowned roller (c) Crowned roller and relatively inclined inner ring and outer ring

Fig. 5 Stress distribution of cylindrical roller

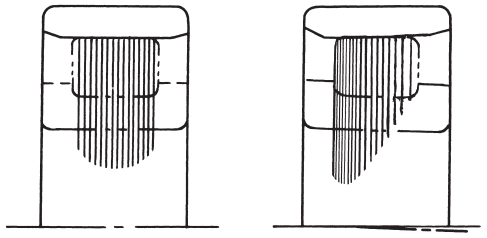

(a) Normal trace (b) When inner ring and outer ring are relatively inclined

Fig. 6 Trace (rolling contact trace) of outer ring of cylindrical roller bearing

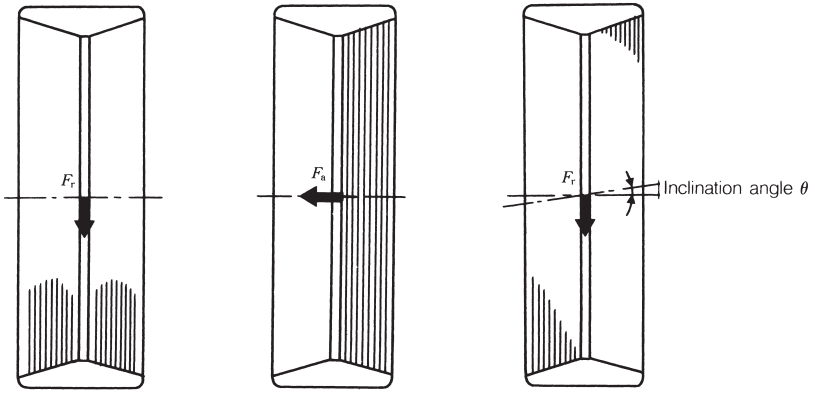

(a) When only a radial load is applied (b) When only an axial load is applied (c) When radial load is applied and inclination is large

Fig. 7 Trace (rolling contact trace) of outer ring of double row tapered roller bearing

5.7 Radial load and displacement of cylindrical roller bearings

One of the most important requirements for bearings to be used in machine-tool applications is that there be as little deflection as possible with applied loading, i.e. that the bearings have high rigidity.

Double-row cylindrical roller bearings are considered to be the most rigid types under radial loads and also best for use at high speeds. NN30K and NNU49K series are the particular radial bearings most often used in machine tool head spindles.

The amount of bearing displacement under a radial load will vary with the amount of internal clearance in the bearings. However, since machine-tool spindle cylindrical roller bearings are adjusted so the internal clearance after mounting is less than several micrometers, we can consider the internal clearance to be zero for most general calculations. The radial elastic displacement δ_r of cylindrical roller bearings can be calculated using Equation (1).

$$\left.\begin{aligned}\delta_r &= 0.000077\frac{Q_{max}^{0.9}}{L_{we}^{0.8}} \quad \text{(N)}\\ &= 0.0006\frac{Q_{max}^{0.9}}{L_{we}^{0.8}} \quad \{\text{kgf}\}\end{aligned}\right\} \text{(mm)} \cdots\cdots\cdots (1)$$

where, Q_{max}: Maximum rolling element load (N), {kgf}

L_{we}: Effective contact length of roller (mm)

If the internal clearance is zero, the relationship between maximum rolling element load Q_{max} and radial load F_r becomes:

$$Q_{max} = \frac{4.08}{iZ} F_r \quad \text{(N), \{kgf\}} \cdots\cdots\cdots\cdots\cdots\cdots\cdots\cdots (2)$$

where, i: Number of rows of rollers in a bearing (double-row bearings: i=2)

Z: Number of rollers per row

F_r: Radial load (N), {kgf}

Combining Equations (1) and (2), it follows that the relation between radial load F_r and radial displacement δ_r becomes.

$$\left.\begin{aligned}\delta_r &= K F_r^{0.9} \quad \text{(N)}\\ &= 7.8K F_r^{0.9} \quad \{\text{kgf}\}\end{aligned}\right\} \text{(mm)} \cdots\cdots\cdots (3)$$

where, $K = \dfrac{0.000146}{Z^{0.9} L_{we}^{0.8}}$

K is a constant determined by the individual double-row cylindrical roller bearing. Table 1 gives values for K for bearing series NN30. Fig. 1 shows the relation between radial load F_r and radial displacement δ_r.

Table 1 Constant K for bearing series NN30

Bearing	K	Bearing	K	Bearing	K
	$\times 10^{-6}$		$\times 10^{-6}$		$\times 10^{-6}$
NN3005	3.31	NN3016T	1.34	NN3032	0.776
NN3006T	3.04	NN3017T	1.30	NN3034	0.721
NN3007T	2.56	NN3018T	1.23	NN3036	0.681
NN3008T	2.52	NN3019T	1.19	NN3038	0.637
NN3009T	2.25	NN3020T	1.15	NN3040	0.642
NN3010T	2.16	NN3021T	1.10	NN3044	0.581
NN3011T	1.91	NN3022T	1.04	NN3048	0.544
NN3012T	1.76	NN3024T	0.966	NN3052	0.526
NN3013T	1.64	NN3026T	0.921	NN3056	0.492
NN3014T	1.53	NN3028	0.861	NN3060	0.474
NN3015T	1.47	NN3030	0.816	NN3064	0.444

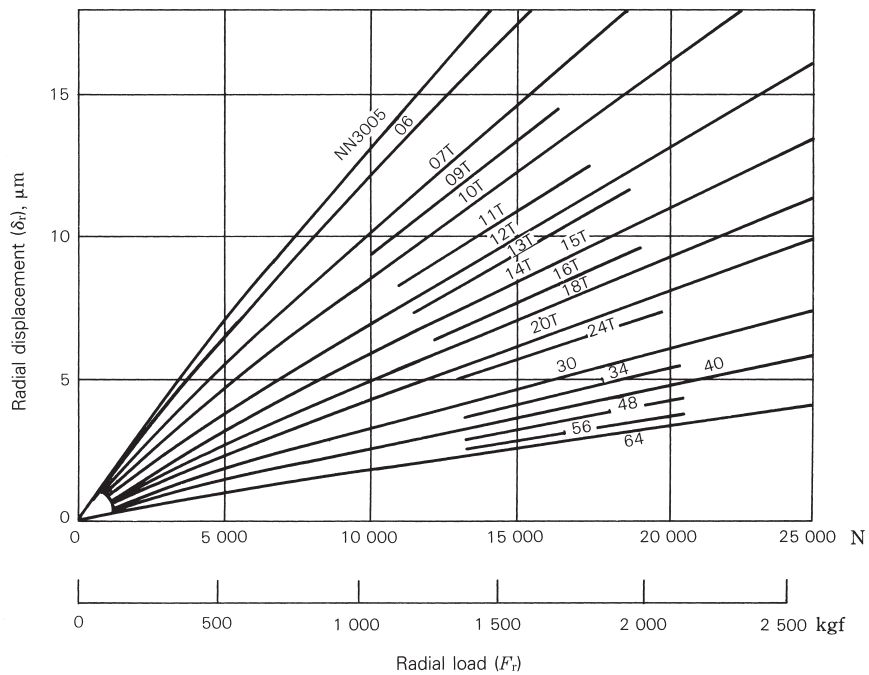

Fig. 1

5.8 Misalignment, maximum rolling-element load and moment for deep groove ball bearings

5.8.1 Misalignment angle of rings and maximum rolling-element load

There are occasions when the inner and outer rings of deep groove bearings are forced to rotate out of parallel, whether from shaft deflection or mounting error. The allowable misalignment can be determined from the relation between the inner or outer ring deflection angle θ and maximum rolling-element load Q_{max}.

For standard groove radii, the relation between θ and Q_{max} (see Fig. 1) is given by Equation (1).

$$Q_{max}=K\,D_w^{\,2}\left\{\sqrt{\left(\frac{R_i}{2m_0}\theta\right)^2+\cos^2\alpha_0}-1\right\}^{3/2}$$

(N), {kgf} ..... (1)

where, K: Constant determined by bearing material and design
Approximately for deep groove ball bearing
K=717 (N-unit)
K=72.7 {kgf-unit}

Q_{max}: Maximum rolling element load (N), {kgf}

D_w: Ball diameter (mm)

R_i: Distance between bearing center and inner ring raceway curvature center (mm)

m_0: $m_0=r_i+r_e-D_w$
r_i and r_e are inner and outer ring groove radii, respectively

θ: Inner and outer ring misalignment angle (rad)

α_0: Initial contact angle (°)

$$\cos\alpha_0=1-\frac{\Delta_r}{2m_0}$$

Δ_r: Radial clearance (mm)

Fig. 2 shows the relationship between θ and Q_{max} for a 6208 ball bearing with various radial clearances Δ_r.

When a radial load F_r equivalent to the basic static load rating C_{0r}=17 800 N {1 820 kgf} or basic dynamic load rating C_r=29 100 N {2 970 kgf} is applied on a bearing, Q_{max} becomes as follows by Equation 8 in Section 5.1.

$F_r=C_{0r}$ Q_{max}=9 915 N {1 011 kgf}
$F_r=C_r$ Q_{max}=16 167 N {1 650 kgf}

Since the allowable misalignment θ during operation will vary depending on the load, it is impossible to make an unqualified statement, but if we reasonably assume Q_{max}=2 000 N {204 kgf}, 20% of Q_{max} when $F_r=C_{0r}$, we can determine from Fig. 2 that θ will be:

Δ_r=0 θ=18′
Δ_r=0.050 mm θ=24.5′

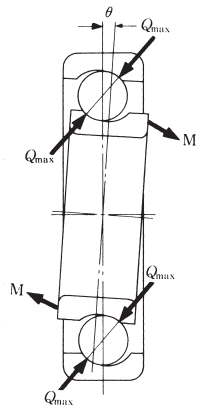

Fig. 1

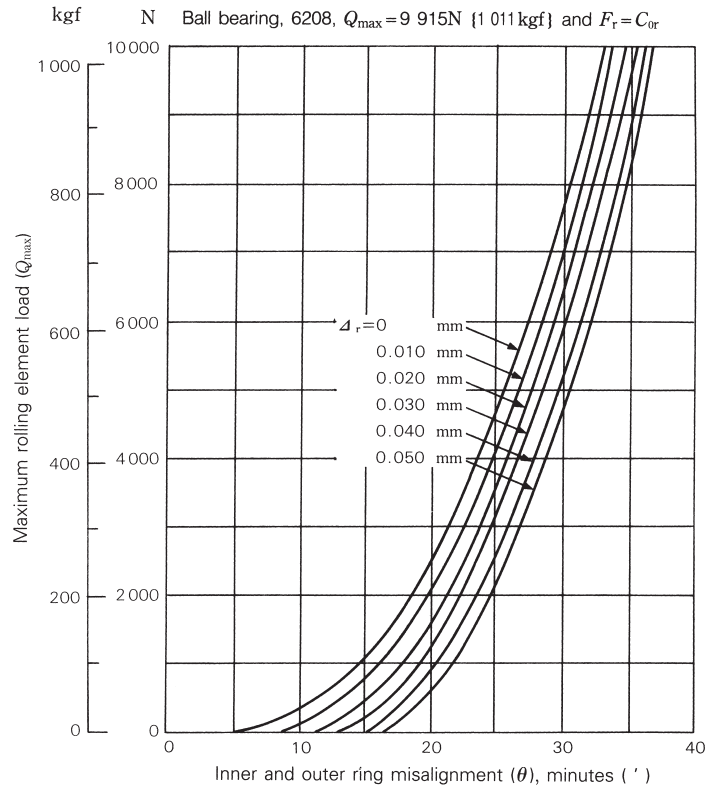

Fig. 2 Inner and outer ring misalignment and maximum rolling element load

5.8.2 Misalignment of inner and outer rings and moment

To determine the angle ψ (Fig. 3) between the positions of the ball and ball under maximum rolling-element load, for standard race way radii, Equation (2) for rolling-element load $Q(\psi)$ can be used like Equation (1) (Page 134).

$$Q(\psi)=K D_w^2 \left\{ \sqrt{\left(\frac{R_i}{m_0}\theta\right)^2 \cos^2\psi+\cos^2\alpha_0}-1 \right\}^{3/2}$$

(N), {kgf} ..... (2)

The moment $M(\psi)$ caused by the relative inner and outer ring misalignment from this $Q(\psi)$ is given by,

$$M(\psi)=\frac{D_{pw}}{2}\cos\psi\, Q(\psi)\sin\alpha(\psi)$$

where, D_{pw}: Ball pitch diameter (mm)
$\alpha(\psi)$, as used here, represents the local rolling element contact angle at the ψ position. It is given by,

$$\sin\alpha(\psi)=\frac{\left(\frac{R_i}{m_0}\theta\right)\cos\psi}{\sqrt{\left(\frac{R_i}{m_0}\theta\right)^2\cos^2\psi+\cos^2\alpha_0}}$$

It is better to consider that the moment M originating from bearing can be replaced with the total moment originating from individual rolling element loads. The relation between the inner and outer ring misalignment angle θ and moment M is as shown by Equation (3):

$$M=\sum_{\psi=0}^{2\pi}\frac{D_{pw}}{2}\cos\psi Q(\psi)\sin\alpha(\psi)$$

$$=\frac{KD_{pw}D_w^2}{2}\Sigma\frac{\left\{\sqrt{\left(\frac{R_i}{m_0}\theta\right)^2\cos^2\psi+\cos^2\alpha_0}-1\right\}^{3/2}\left(\frac{R_i}{m_0}\theta\right)\cos^2\psi}{\sqrt{\left(\frac{R_i}{m_0}\theta\right)^2\cos^2\psi+\cos^2\alpha_0}}$$

(mN·m), {kgf·mm} ..... (3)

where, K: Constant determined by bearing material and design

Figs. 4 shows the calculated results for a 6208 deep groove ball bearing with various internal clearances. The allowable moment for a 6208 bearing with a maximum rolling element load Q_{max} of 2 000 N {204 kgf}, can be estimated using Fig. 2 (Page 135):

Radial clearance Δ_r=0, θ=18′
M=60 N·m {6.2 kgf·mm}

Radial clearance Δ_r=0.050 mm θ=24.5′
M=70 N·m {7.1 kgf·mm}

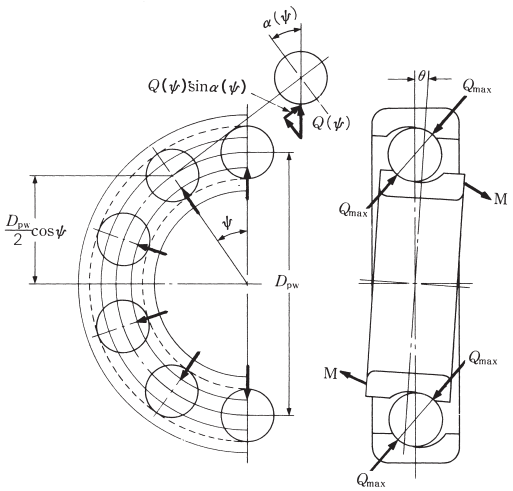

Fig. 3

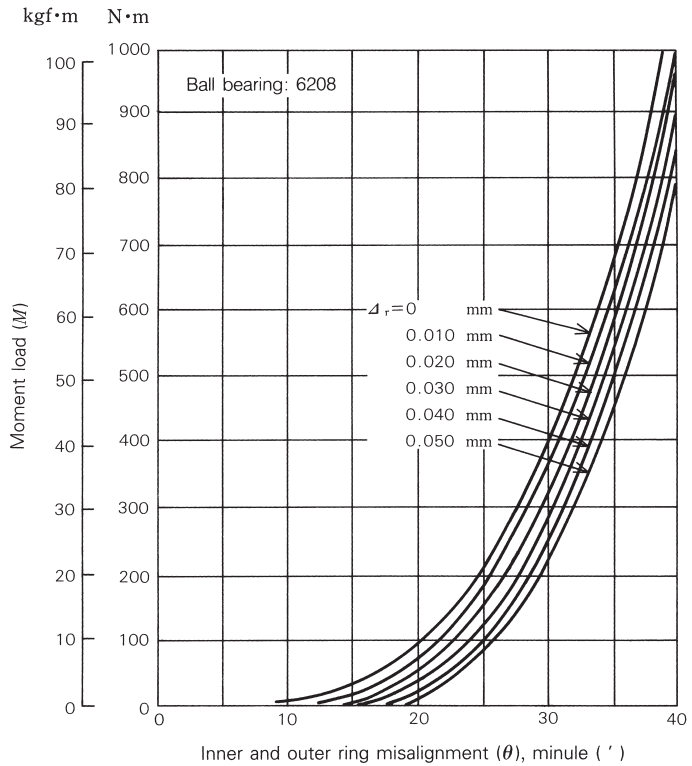

Fig. 4 Inner and outer ring misalignment and moment

5.9 Load distribution of single-direction thrust bearing due to eccentric load

When a pure axial load F_a is applied on a single-direction thrust bearing with a contact angle of α=90°, each rolling element is subjected to a uniform load Q:

$$Q=\frac{F_a}{Z}$$

where, Z: Number of rolling elements

Fig. 1 shows the distribution with any eccentric load F_a applied on a single-direction thrust bearing with a contact angle α=90°.

Based on Fig. 1, the following equations can be derived to determine the total elastic deformation δ_{max} of the rolling element under the maximum load and the elastic deformation of any other rolling element $\delta(\psi)$.

$$\delta_{max}=\delta_T+\frac{\theta D_{pw}}{2} \quad \cdots\cdots (1)$$

$$\delta(\psi)=\delta_T+\frac{\theta D_{pw}}{2}\cos\psi \quad \cdots\cdots (2)$$

From Equation (1) and (2) we obtain,

$$\delta(\psi)=\delta_{max}\left\{1-\frac{1}{2\varepsilon}(1-\cos\psi)\right\} \quad \cdots\cdots (3)$$

where,

$$\varepsilon=\frac{1}{2}\left(1+\frac{2\delta_T}{\theta D_{pw}}\right) \quad \cdots\cdots (4)$$

The load $Q(\psi)$ on any rolling element is proportional to the elastic deformation $\delta(\psi)$ of the contact surface to the t power. Thus when ψ=0, with Q_{max} representing the maximum rolling element load and δ_{max} the elastic deformation, we obtain.

$$\frac{Q(\psi)}{Q_{max}}=\left\{\frac{\delta(\psi)}{\delta_{max}}\right\}^t \quad \cdots\cdots (5)$$

t=1.5 (point contact), t=1.1 (line contact)

From Equations (3) and (5), we obtain,

$$\frac{Q(\psi)}{Q_{max}}=1-\left\{\frac{1}{2\varepsilon}(1-\cos\psi)\right\}^t \quad \cdots\cdots (6)$$

Since the eccentric load F_a acting on a bearing must be the sum of the individual rolling element loads, we obtain (Z is the number of the rolling elements),

$$F_a=\sum_{\psi=0}^{2\pi} Q(\psi)$$

$$=\sum_{\psi=0}^{2\pi} Q_{max}=\left\{1-\frac{1}{2\varepsilon}(1-\cos\psi)\right\}^t$$

$$=Q_{max}\,Z\,J_A \quad \cdots\cdots (7)$$

Based on Fig. 1, the moment M acting on the shaft with ψ=90° as the axis is,

$$M=\sum_{\psi=0}^{2\pi} Q(\psi)\frac{D_{pw}}{2}\cos\psi$$

$$=\sum_{\psi=0}^{2\pi} Q_{max}\frac{D_{pw}}{2}\left\{1-\frac{1}{2\varepsilon}(1-\cos\psi)\right\}^t\cos\psi$$

$$=Q_{max}\,Z\frac{D_{pw}}{2}J_R \quad \cdots\cdots (8)$$

Values for ε and the corresponding J_A and J_R values for point contact and line contact from Equations (7) and (8) are listed in Table 1.

Sample Calculation

Find the maximum rolling element load for a 51130X single-direction thrust ball bearing (ϕ150×ϕ190×31 mm) that sustains an axial load of 10 000 N {1 020 kgf} at a position 80 mm out from the bearing center.

$$e=80,\ D_{pw}\fallingdotseq\frac{1}{2}(150+190)=170$$

$$\frac{2e}{D_{pw}}=\frac{2\times80}{170}=0.941$$

$$Z=32$$

Using Table 1, the value for J_A corresponding to $2e/D_{pw}$=0.941 is 0.157. Substituting these values into Equation (7), we obtain,

$$Q_{max}=\frac{F_a}{Z\,J_A}=\frac{10\ 000}{32\times0.157}=1\ 990\ (N)$$

$$=\frac{1\ 020}{32\times0.157}=203\ \{kgf\}$$

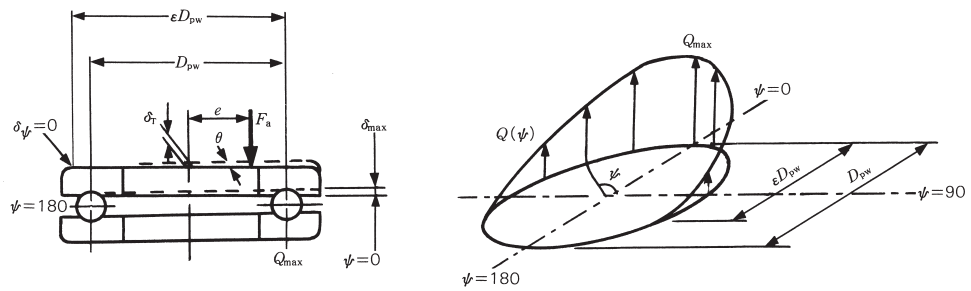

Fig. 1

Table 1 J_R and J_A values for single-direction thrust bearings

ε	Point contact			Line contact		
	$2e/D_{pw}$ $2M/D_{pw}F_a$	J_R	J_A	$2e/D_{pw}$ $2M/D_{pw}F_a$	J_R	J_A
0	1.0000	1/Z	1/Z	1.0000	1/Z	1/Z
0.1	0.9663	0.1156	0.1196	0.9613	0.1268	0.1319
0.2	0.9318	0.1590	0.1707	0.9215	0.1737	0.1885
0.3	0.8964	0.1892	0.2110	0.8805	0.2055	0.2334
0.4	0.8601	0.2117	0.2462	0.8380	0.2286	0.2728
0.5	0.8225	0.2288	0.2782	0.7939	0.2453	0.3090
0.6	0.7835	0.2416	0.3084	0.7480	0.2568	0.3433
0.7	0.7427	0.2505	0.3374	0.6999	0.2636	0.3766
0.8	0.6995	0.2559	0.3658	0.6486	0.2658	0.4098
0.9	0.6529	0.2576	0.3945	0.5920	0.2628	0.4439
1.0	0.6000	0.2546	0.4244	0.5238	0.2523	0.4817
1.25	0.4338	0.2289	0.5044	0.3598	0.2078	0.5775
1.67	0.3088	0.1871	0.6060	0.2340	0.1589	0.6790
2.5	0.1850	0.1339	0.7240	0.1372	0.1075	0.7837
5.0	0.0831	0.0711	0.8558	0.0611	0.0544	0.8909
∞	0	0	1.0000	0	0	1.0000

e: Distance between bearing center and loading point
D_{pw}: Rolling-element pitch diameter

6. Preload and axial displacement

6.1 Position preload and constant-pressure preload

Bearings for machine-tool head spindles, hypoid-gear pinion shafts, and other similar applications are often preloaded to increase bearing rigidity and, thereby, reduce as far as possible undesirable bearing displacement due to applied loads.

Generally, a preload is applied as shown in Fig. 1, using a spacer, shim, etc. to set the displacement dimensionally (position preload), or, as shown in Fig. 2, using a spring (constant pressure preload).

The effect of a position preload on rigidity is apparent in preload graphs such as Fig. 3. This graph is similar to data generally found in bearing makers' catalogs. That is, Fig. 3 shows that the relation between the axial displacement δ_a and external load F_a (axial load) under the preload of F_{a0}. This graph of position preload is derived from the displacement curves for the two side-by-side bearings, A and B.

By substituting a spring displacement curve (a straight line) for the bearing B displacement curve and plotting it together with the displacement curve for bearing A, a graph for a constant-pressure preload is formed.

Fig. 4 is a preload graph for a constant-pressure preload. Because spring rigidity is, as a rule, small compared with bearing rigidity, the displacement curve for the spring is a straight line that is nearly parallel to the horizontal axis of the graph. It also follows that an increase in rigidity under a constant-pressure preload will be nearly the same as an increase in rigidity for a single bearing subjected to an F_{a0} preload.

Fig. 5 compares the rigidity provided by various preload methods on a 7212A angular contact ball bearing.

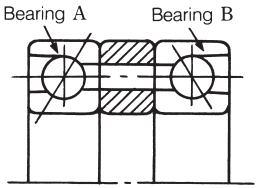

Fig. 1 Position preload

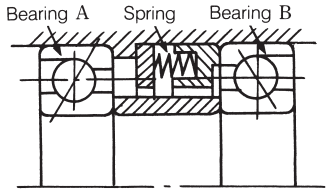

Fig. 2 Constant-pressure preload

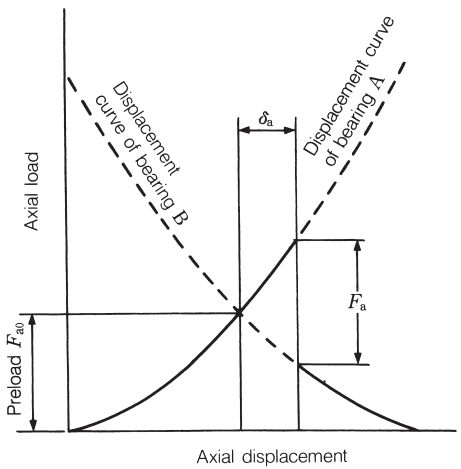

Fig. 3 Preload graph for position preload

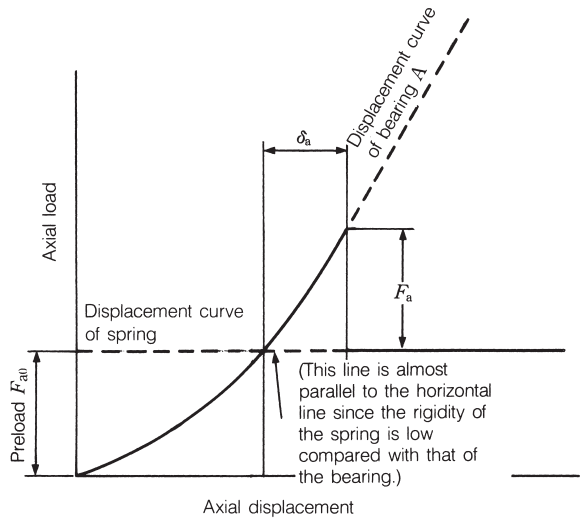

Fig. 4 Preload graph for constant-pressure preload

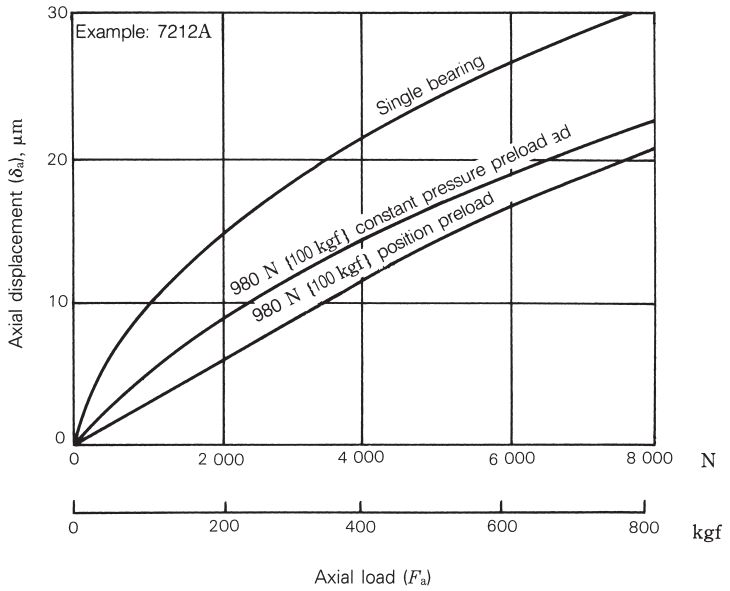

Fig. 5 Comparison of rigidity among different preload methods

6.2 Load and displacement of position-preloaded bearings

Two (or more) ball or tapered roller bearings mounted side by side as a set are termed duplex (or multiple) bearing sets. The bearings most often used in multiple arrangements are single-row angular contact ball bearings for machine tool spindles, since there is a requirement to reduce the bearing displacement under load as much as possible.

There are various ways of assembling sets depending on the effect desired. Duplex angular contact bearings fall into three types of arrangements, Back-to-Back, with lines of force convergent on the bearing back faces, Face-to-Face, with lines of force convergent on the bearing front faces, and Tandem, with lines of force being parallel. The symbols for these are DB, DF, and DT arrangements respectively (Fig. 1).

DB and DF arrangement sets can take axial loads in either direction. Since the distance of the load centers of DB bearing set is longer than that of DF bearing set, they are widely used in applications where there is a moment. DT type sets can only take axial loads in one direction. However, because the two bearings share some load equally between them, a set can be used where the load in one direction is large.

By selecting the DB or DF bearing sets with the proper preloads which have already been adjusted to an appropriate range by the bearing manufacturer, the radial and axial displacements of the bearing inner and outer ring can be reduced as much as allowed by certain limits. However, the DT bearing set cannot be preloaded.

The amount of preload can be adjusted by changing clearance between bearings, δ_{a0}, as shown in Figs. 3 to 5. Preloads are divided into four graduated classification — Extra light (EL), Light (L), Medium (M), and Heavy (H). Therefore, DB and DF bearing sets are often used for applications where shaft misalignments and displacements due to loads must be minimized.

Triplex sets are also available in three types (symbols: DBD, DFD, and DTD) of arrangements as shown in Fig. 2. Sets of four or five bearings can also be used depending on the application requirements.

Duplex bearings are often used with a preload applied. Since the preload affects the rise in bearing temperature during operation, torque, bearing noise, and especially bearing life, it is extremely important to avoid applying an excessive preload.

Generally, the axial displacement δ_a under an axial load F_a for single-row angular contact ball bearings is calculated as follows,

$$\delta_a = c\, F_a^{2/3} \quad \cdots\cdots (1)$$

where, c: Constant depending on the bearing type and dimensions.

Fig. 3 shows the preload curves of duplex DB arrangement, and Figs. 4 and 5 show those for triplex DBD arrangement.

If the inner rings of the duplex bearing set in Fig. 3 are pressed axially, A-side and B-side bearings are deformed δ_{a0A} and δ_{a0B} respectively and the clearance (between the inner rings), δ_{a0}, becomes zero. This condition means that the preload F_{a0} is applied on the bearing set. If an external axial load F_a is applied on the preloaded bearing set from the A-side, then the A-side bearing will be deformed δ_{a1} additionally and the displacement of B-side bearing will be reduced to the same amount as the A-side bearing displacement δ_{a1}. Therefore, the displacements of A- and B-side bearings are $\delta_{aA}=\delta_{a0A}+\delta_{a1}$ and $\delta_{aB}=\delta_{a0B}+\delta_{a1}$ respectively. That is, the load on A-side bearing including the preload is $(F_{a0}+F_a-F_a')$ and the B-side bearing is $(F_{a0}-F_a')$.

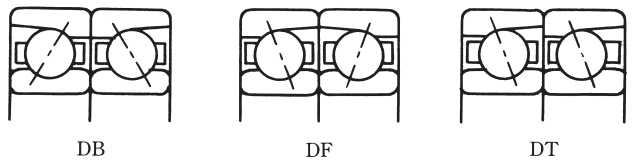

Fig. 1 Duplex bearing arrangements

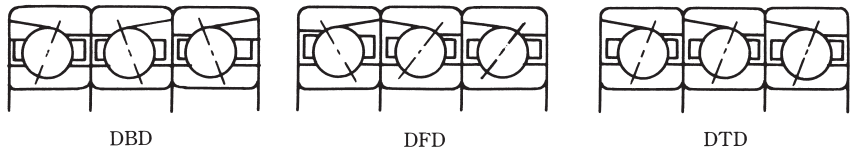

Fig. 2 Triplex bearing arrangements

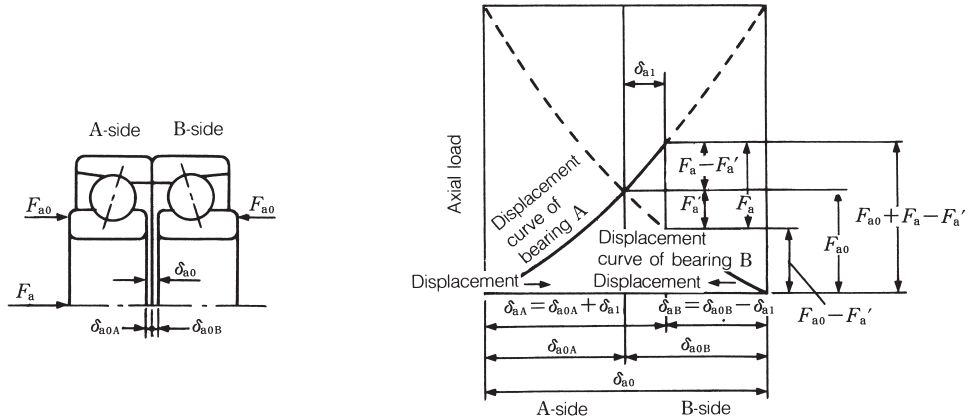

Fig. 3 Preload graph of DB arrangement duplex bearings

If the bearing set has an applied preload, the A-side bearing should have a sufficient life and load capacity for an axial load ($F_{a0}+F_a-F_a'$) under the speed condition. The axial clearance δ_{a0} is shown in **Tables 3** to **7** of Section **6.3** (Pages 151 to 155).

In **Fig. 4**, with an external axial load F_a applied on the AA-side bearings, the axial loads and displacements of AA- and B-side bearings are summarized in **Table 1**.

In **Fig. 5**, with an external axial load F_a applied on the A-side bearing, the axial loads and displacements of A- and BB-side bearings are summarized in **Table 2**.

The examples, **Figs. 6** to **11**, show the relation of the axial loads and axial displacements using duplex DB and triplex DBD arrangements of 7018C and 7018A bearings under several preload ranges.

Table 1

Direction	Displacement	Axial load
AA-side	$\delta_{a0A}+\delta_{a1}$	$F_{a0}+F_a-F_a'$
B-side	$\delta_{a0B}-\delta_{a1}$	$F_{a0}-F_a'$

Table 2

Direction	Displacement	Axial load
A-side	$\delta_{a0A}+\delta_{a1}$	$F_{a0}+F_a-F_a'$
BB-side	$\delta_{a0B}-\delta_{a1}$	$F_{a0}-F_a'$

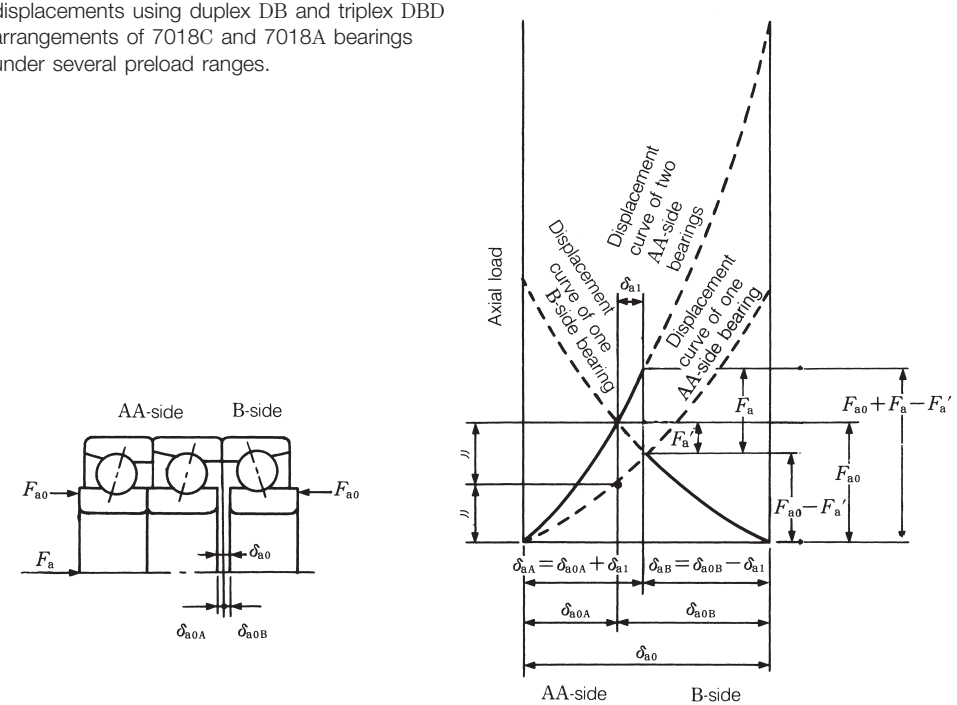

Fig. 4 Preload graph of triplex DBD bearing set
(Axial load is applied from AA-side)

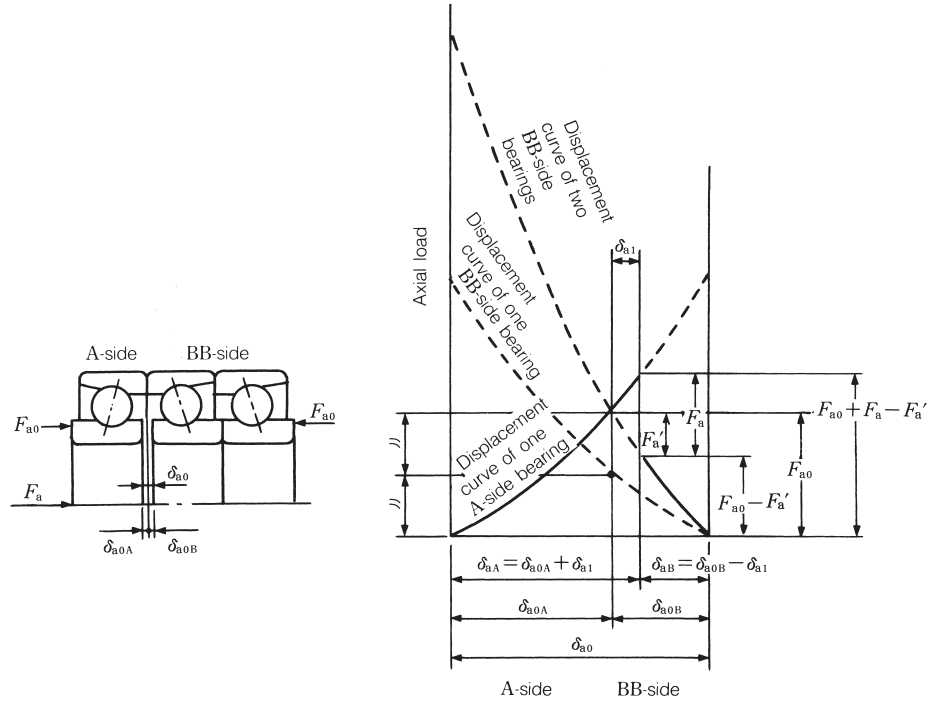

Fig. 5 Preload graph of triplex DBD bearing set
(Axial load is applied from A-side)

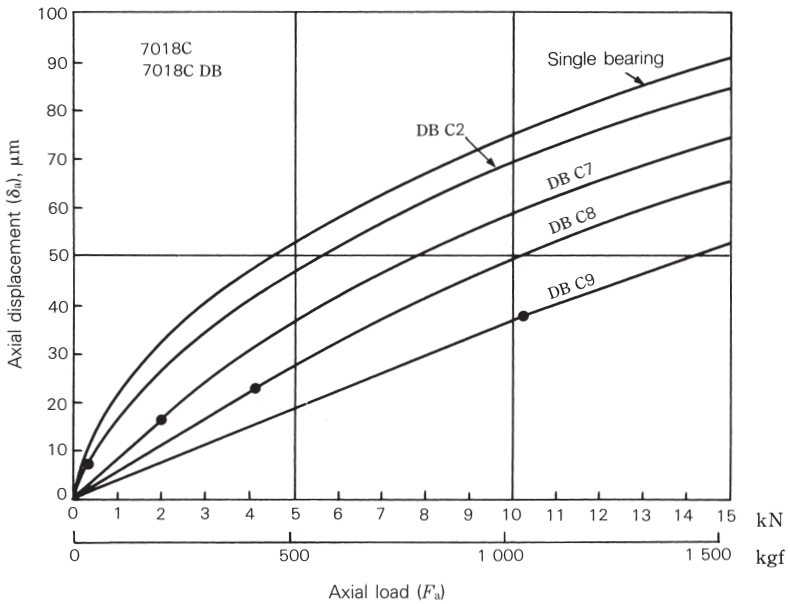

Fig. 6

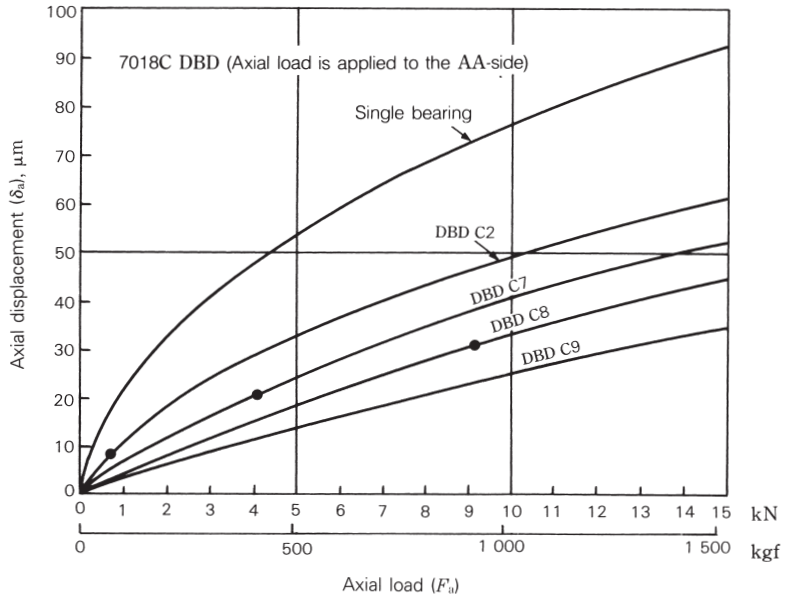

Fig. 7

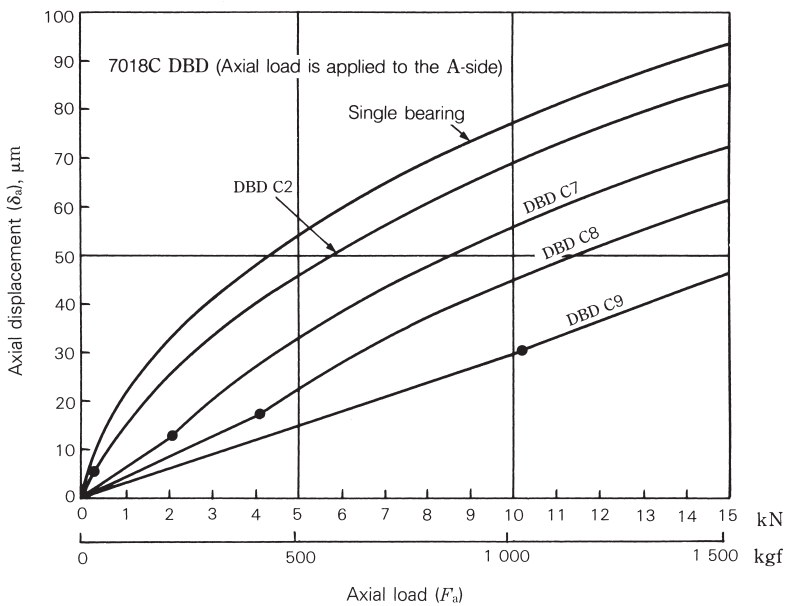

Fig. 8

Remarks A (•) mark on the axial load or displacement curve indicates the point where the preload is zero. Therefore, if the axial load is larger than this, the opposed bearing does not impose a load.

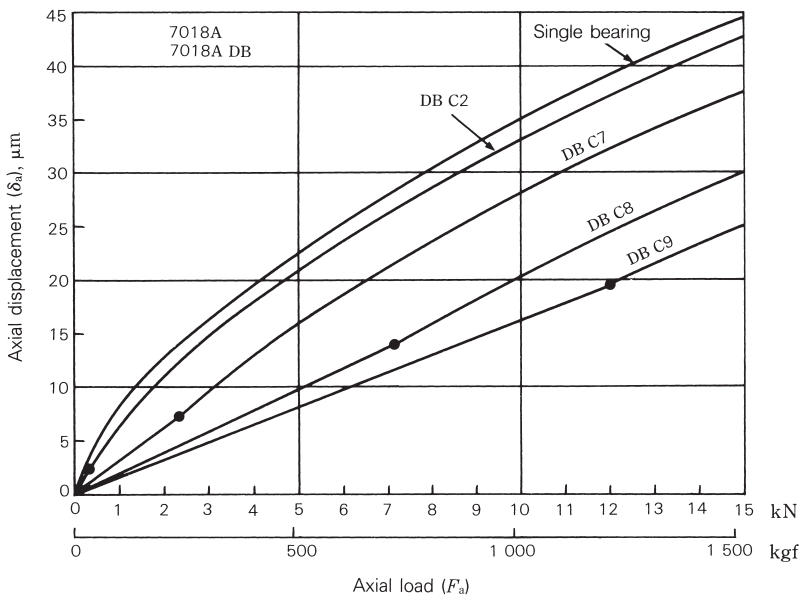

Fig. 9

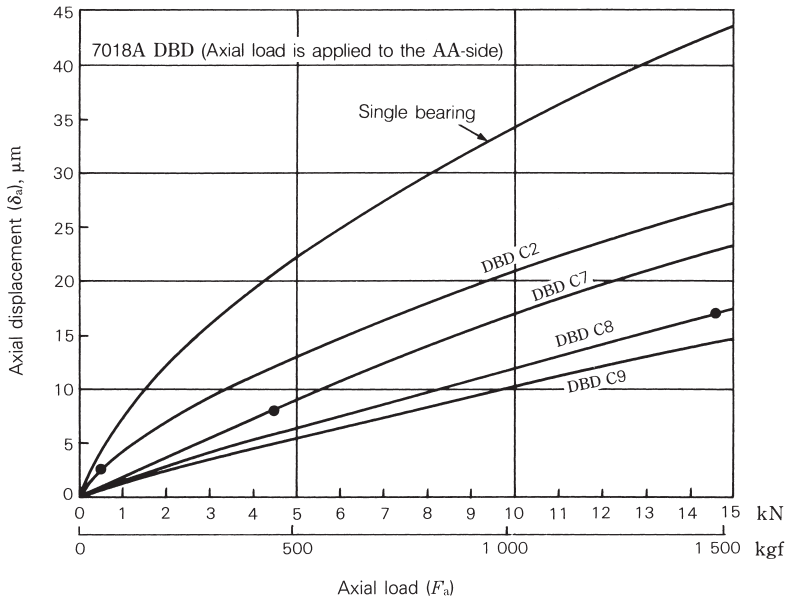

Fig. 10

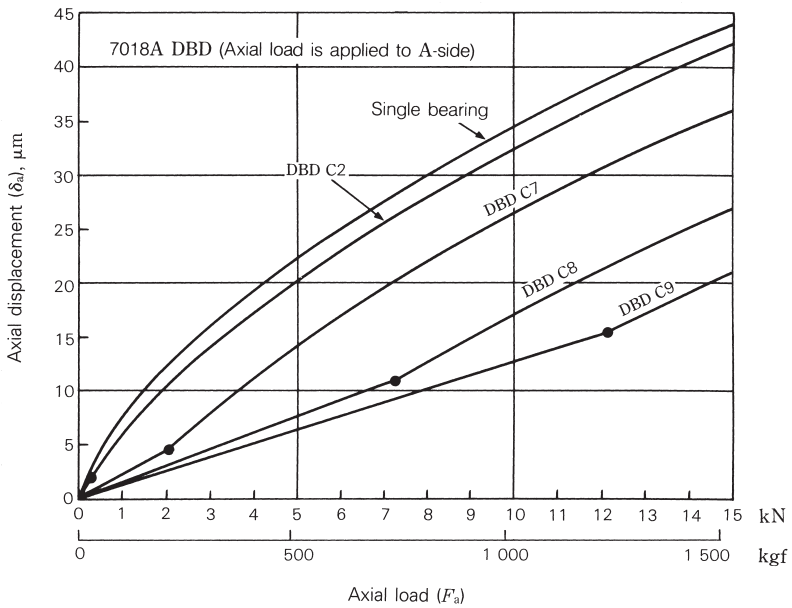

Fig. 11

Remarks A (•) mark on the axial load or displacement curve indicates the point where the preload is zero. Therefore, if the axial load is larger than this, the opposed bearing does not impose a load.

6.3 Average preload for duplex angular contact ball bearings

Angular contact ball bearings are widely used in spindles for grinding, milling, high-speed turning, etc. At NSK, preloads are divided into four graduated classifications — Extra light (EL), Light (L), Medium (M), and Heavy (H) — to allow the customer to freely choose the appropriate preload for the specific application. These four preload classes are expressed in symbols, EL, L, M, and H, respectively, when applied to DB and DF bearing sets.

The average preload and axial clearance (measured) for duplex angular contact ball bearing sets with contact angles 15° and 30° (widely used on machine tool spindles) are given in Tables 3 to 7.

The measuring load when measuring axial clearance is shown in Table 1.

The recommended axial clearance to achieve the proper preload was determined for machine-tool spindles and other applications requiring ISO Class 5 and above high-precision bearing sets. The standard values given in Table 2 are used for the shaft — inner ring and housing — outer ring fits. The housing fits should be selected in the lower part of the standard clearance for bearings in fixed-end applications and the higher part of the standard clearance for bearings in free-end applications.

As general rules when selecting preloads, grinding machine spindles or machining center spindles require extra light to light preloads, whereas lathe spindles, which need rigidity, require medium preloads.

The bearing preloads, if the bearing set is mounted with tight fit, are larger than those shown in Tables 3 to 7. Since excessive preloads cause bearing temperature rise and seizure, etc., it is necessary to pay attention to fitting.

Table 1 Measuring load of axial clearance

Nominal bearing outside diameter D (mm)		Measuring load
over	incl	(N)
10*	50	24.5
50	120	49
120	200	98
200	—	196

*10 mm is included in this range.

Table 2 Target of fitting

Units: μm

Bore or outside diameter d or D (mm)		Shaft and inner ring	Housing and outer ring
over	incl	Target interference	Target clearance
—	18	0 to 2	—
18	30	0 to 2.5	2 to 6
30	50	0 to 2.5	2 to 6
50	80	0 to 3	3 to 8
80	120	0 to 4	3 to 9
120	150	—	4 to 12
150	180	—	4 to 12
180	250	—	5 to 15

Table 3 Average preloads and axial clearance for bearing series 79C

Bearing No.	Extra light EL		Light L		Medium M		Heavy H	
	Preload	Axial clearance	Preload	Axial clearance	Preload	Axial clearance	Preload	Axial clearance
	(N)	(μm)	(N)	(μm)	(N)	(μm)	(N)	(μm)
7900C	7	5	15	2	29	−1	59	−6
7901C	8.6	4	15	2	39	−3	78	−8
7902C	12	3	25	0	49	−4	100	−11
7903C	12	3	25	0	59	−5	120	−12
7904C	19	1	39	−3	78	−8	150	−15
7905C	19	1	39	−2	100	−9	200	−17
7906C	24	0	49	−3	100	−8	200	−16
7907C	34	2	69	−2	150	−9	290	−18
7908C	39	1	78	−3	200	−12	390	−22
7909C	50	0	100	−5	200	−11	390	−21
7910C	50	0	100	−4	250	−13	490	−24
7911C	60	−1	120	−5	290	−15	590	−26
7912C	60	−1	120	−5	290	−15	590	−25
7913C	75	−2	150	−7	340	−16	690	−27
7914C	100	−4	200	−10	490	−22	980	−36
7915C	100	−4	200	−9	490	−21	980	−35
7916C	100	−4	200	−9	490	−21	980	−34
7917C	145	−6	290	−14	640	−25	1 270	−41
7918C	145	−3	290	−9	740	−23	1 470	−39
7919C	145	−3	290	−9	780	−24	1 570	−40
7920C	195	−5	390	−13	880	−28	1 770	−46

Remarks In the axial clearance column, the measured value is given.

Table 4 Average preloads and axial clearance for bearing series 70C

Bearing No.	Extra light EL		Light L		Medium M		Heavy H	
	Preload	Axial clearance	Preload	Axial clearance	Preload	Axial clearance	Preload	Axial clearance
	(N)	(μm)	(N)	(μm)	(N)	(μm)	(N)	(μm)
7000C	12	3	25	0	49	−5	100	−12
7001C	12	3	25	0	59	−6	120	−14
7002C	14	3	29	−1	69	−7	150	−16
7003C	14	2	29	−1	69	−7	150	−16
7004C	24	0	49	−4	120	−12	250	−22
7005C	29	−1	59	−5	150	−14	290	−24
7006C	39	1	78	−3	200	−13	390	−24
7007C	60	−1	120	−7	250	−16	490	−28
7008C	60	−1	120	−6	290	−17	590	−30
7009C	75	−3	150	−8	340	−19	690	−33
7010C	75	−2	150	−8	390	−20	780	−34
7011C	100	−4	200	−11	490	−24	980	−40
7012C	100	−4	200	−10	540	−25	1 080	−42
7013C	125	−6	250	−13	540	−24	1 080	−39
7014C	145	−7	290	−14	740	−30	1 470	−48
7015C	145	−7	290	−14	780	−31	1 570	−49
7016C	195	−6	390	−14	930	−31	1 860	−52
7017C	195	−6	390	−14	980	−32	1 960	−52
7018C	245	−8	490	−18	1 180	−37	2 350	−60
7019C	270	−9	540	−19	1 180	−36	2 350	−58
7020C	270	−9	540	−18	1 270	−37	2 550	−60

Remarks In the axial clearance column, the measured value is given.

Table 5 Average preloads and axial clearance for bearing series 72C

Bearing No.	Extra light EL		Light L		Medium M		Heavy H	
	Preload	Axial clearance	Preload	Axial clearance	Preload	Axial clearance	Preload	Axial clearance
	(N)	(μm)	(N)	(μm)	(N)	(μm)	(N)	(μm)
7200C	14	3	29	−1	69	−8	150	−18
7201C	19	1	39	−3	100	−12	200	−22
7202C	19	1	39	−3	100	−11	200	−21
7203C	24	0	49	−4	150	−16	290	−28
7204C	34	−2	69	−7	200	−20	390	−33
7205C	39	1	78	−4	200	−14	390	−27
7206C	60	−1	120	−7	290	−20	590	−35
7207C	75	−3	150	−10	390	−25	780	−43
7208C	100	−5	200	−13	490	−29	980	−47
7209C	125	−7	250	−16	540	−30	1 080	−49
7210C	125	−7	250	−15	590	−31	1 180	−50
7211C	145	−8	290	−17	780	−38	1 570	−60
7212C	195	−11	390	−22	930	−42	1 860	−67
7213C	220	−12	440	−23	1 080	−44	2 160	−70
7214C	245	−9	490	−20	1 180	−42	2 350	−69
7215C	270	−10	540	−21	1 230	−42	2 450	−68
7216C	295	−12	590	−24	1 370	−47	2 750	−76
7217C	345	−14	690	−27	1 670	−53	3 330	−85
7218C	390	−15	780	−29	1 860	−57	3 730	−90
7219C	440	−18	880	−33	2 060	−63	4 120	−99
7220C	490	−20	980	−36	2 350	−68	4 710	−107

Remarks In the axial clearance column, the measured value is given.

Table 6 Average preloads and axial clearance for bearing series 70A

Bearing No.	Extra light EL		Light L		Medium M		Heavy H	
	Preload	Axial clearance	Preload	Axial clearance	Preload	Axial clearance	Preload	Axial clearance
	(N)	(μm)	(N)	(μm)	(N)	(μm)	(N)	(μm)
7000A	25	0	100	−5	210	−10	330	−15
7001A	25	0	110	−5	220	−10	360	−15
7002A	25	0	110	−5	240	−10	390	−15
7003A	25	0	120	−5	250	−10	420	−15
7004A	25	0	130	−5	280	−10	470	−15
7005A	25	0	140	−5	290	−10	510	−15
7006A	50	0	190	−5	390	−10	640	−15
7007A	50	0	210	−5	420	−10	700	−15
7008A	50	0	220	−5	460	−10	760	−15
7009A	50	0	230	−5	480	−10	1 180	−20
7010A	50	0	250	−5	530	−10	1 270	−20
7011A	50	0	250	−5	880	−15	1 270	−20
7012A	50	0	250	−5	930	−15	1 370	−20
7013A	50	0	270	−5	980	−15	1 470	−20
7014A	50	0	270	−5	1 080	−15	2 060	−25
7015A	50	0	280	−5	1 080	−15	2 160	−25
7016A	100	0	760	−10	1 770	−20	3 040	−30
7017A	100	0	780	−10	1 860	−20	3 240	−30
7018A	100	0	780	−10	2 450	−25	3 920	−35
7019A	100	0	810	−10	2 550	−25	4 120	−35
7020A	100	0	840	−10	2 750	−25	4 310	−35

Remarks In the axial clearance column, the measured value is given.

Table 7 Average preloads and axial clearance for bearing series 72A

Bearing No.	Extra light EL		Light L		Medium M		Heavy H	
	Preload	Axial clearance	Preload	Axial clearance	Preload	Axial clearance	Preload	Axial clearance
	(N)	(μm)	(N)	(μm)	(N)	(μm)	(N)	(μm)
7200A	25	0	100	−5	210	−10	—	—
7201A	25	0	110	−5	220	−10	360	−15
7202A	25	0	110	−5	240	−10	390	−15
7203A	25	0	120	−5	250	−10	410	−15
7204A	25	0	260	−10	440	−15	650	−20
7205A	50	0	350	−10	580	−15	840	−20
7206A	50	0	380	−10	630	−15	910	−20
7207A	50	0	400	−10	660	−15	1 270	−25
7208A	50	0	440	−10	730	−15	1 470	−25
7209A	50	0	450	−10	1 080	−20	1 860	−30
7210A	50	0	480	−10	1 180	−20	2 060	−30
7211A	50	0	490	−10	1 670	−26	2 650	−35
7212A	50	0	510	−10	1 670	−25	2 750	−35
7213A	50	0	550	−10	1 860	−25	3 040	−35
7214A	100	0	1 080	−15	2 650	−30	3 920	−40
7215A	100	0	1 080	−15	2 750	−30	4 220	−40
7216A	100	0	1 080	−15	2 650	−30	4 020	−40
7217A	100	0	1 180	−15	3 430	−35	5 790	−50
7218A	100	0	1 670	−20	4 310	−40	5 980	−50
7219A	360	−5	1 670	−20	4 220	−40	6 670	−55
7220A	370	−5	1 670	−20	5 100	−45	7 650	−60

Remarks In the axial clearance column, the measured value is given.

6.4 Axial displacement of deep groove ball bearings

When an axial load F_a is applied to a radial bearing with a contact angle α_0 and the inner ring is displaced δ_a, the center Oi of the inner ring raceway radius is also moved to Oi' resulting in the contact angle α as shown in Fig. 1. If δ_N represents the elastic deformation of the raceway and ball in the direction of the rolling element load Q, Equation (1) is derived from Fig. 1.

$$(m_0+\delta_N)^2=(m_0\cdot\sin\alpha_0+\delta_a)^2+(m_0\cdot\cos\alpha_0)^2$$

$$\therefore\ \delta_N=m_0\left\{\sqrt{\left(\sin\alpha_0+\frac{\delta_a}{m_0}\right)^2+\cos^2\alpha_0}-1\right\} \quad \cdots\cdots (1)$$

Also there is the following relationship between the rolling element load Q and elastic deformation δ_N.

$$Q=K_N\cdot\delta_N^{3/2} \quad \cdots\cdots (2)$$

where, K_N: Constant depending on bearing material, type, and dimension

$\therefore$ If we introduce the relation of

$$m_0=\left(\frac{r_e}{D_w}+\frac{r_i}{D_w}-1\right)D_w=B\cdot D_w$$

Equations (1) and (2) are,

$$Q=K_N\,(B\cdot D_w)^{3/2}\left\{\sqrt{(\sin\alpha_0+h)^2+\cos^2\alpha_0}-1\right\}^{3/2}$$

where, $h=\dfrac{\delta_a}{m_0}=\dfrac{\delta_a}{B\cdot D_w}$

If we introduce the relation of $K_N=K\cdot\dfrac{\sqrt{D_w}}{B^{3/2}}$

$$Q=K\cdot D_w^2\left\{\sqrt{(\sin\alpha_0+h)^2+\cos^2\alpha_0}-1\right\}^{3/2} \quad \cdots\cdots (3)$$

On the other hand, the relation between the bearing axial load and rolling element load is shown in Equation (4) using Fig. 2:

$$F_a=Z\cdot Q\cdot\sin\alpha \quad \cdots\cdots (4)$$

Based on Fig. 1, we obtain,

$$(m_0+\delta_N)\sin\alpha=m_0\cdot\sin\alpha_0+\delta_a$$

$$\therefore\ \sin\alpha=\frac{m_0\cdot\sin\alpha_0+\delta_a}{m_0+\delta_N}=\frac{\sin\alpha_0+h}{1+\dfrac{\delta_N}{m_0}}$$

If we substitute Equation (1),

$$\sin\alpha=\frac{\sin\alpha_0+h}{\sqrt{(\sin\alpha_0+h)^2+\cos^2\alpha_0}} \quad \cdots\cdots (5)$$

That is, the relation between the bearing axial load F_a and axial displacement δ_a can be obtained by substituting Equations (3) and (5) for Equation (4).

$$F_a=K\cdot Z\cdot D_w^2\cdot\frac{\left\{\sqrt{(\sin\alpha_0+h)^2+\cos^2\alpha_0}-1\right\}^{3/2}\times(\sin\alpha_0+h)}{\sqrt{(\sin\alpha_0+h)^2+\cos^2\alpha_0}} \quad \cdots\cdots (6)$$

where, K: Constant depending on the bearing material and design

D_w: Ball diameter

Z: Number of balls

α_0: Initial contact angle

In case of single-row deep groove ball bearings, the initial contact angle can be obtained using Equation (5) of Section 4.6 (Page 96)

Actual axial deformation varies depending on the bearing mounting conditions, such as the material and thickness of the shaft and housing, and bearing fitting. For details, consult with NSK regarding the axial deformation after mounting.

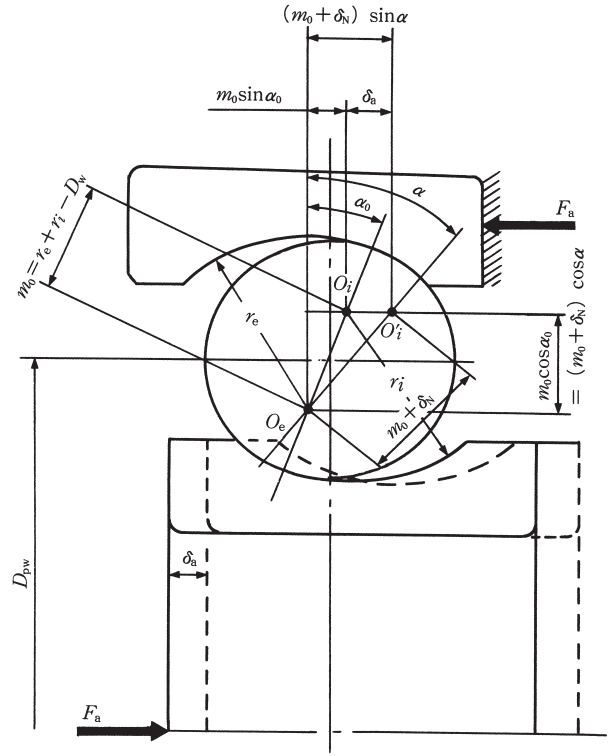

Fig. 1

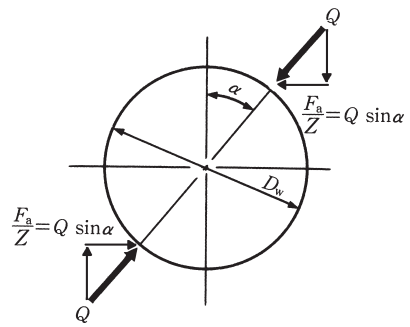

Fig. 2

Fig. 3 gives the relation between axial load and axial displacement for 6210 and 6310 single-row deep groove ball bearings with initial contact angles of α_0=0°, 10°, 15°. The larger the initial contact angle α_0, the more rigid the bearing will be in the axial direction and also the smaller the difference between the axial displacements of 6210 and 6310 under the same axial load. The angle α_0 depends upon the groove radius and the radial clearance.

Fig. 4 gives the relation between axial load and axial displacement for 72 series angular contact ball bearings with initial contact angles of 15° (C), 30° (A), and 40° (B). Because 70 and 73 series bearings with identical contact angles and bore diameters can be considered to have almost the same values as 72 series bearings.

Angular contact ball bearings that sustain loads in the axial direction must maintain their running accuracy and reduce the bearing elastic deformation from applied loads when used as multiple bearing sets with a preload applied.

To determine the preload to keep the elastic deformation caused by applied loads within the required limits, it is important to know the characteristics of load vs. deformation. The relationship between load and displacement can be expressed by **Equation** (6) as $F_a \propto \delta_a^{3/2}$ or $\delta_a \propto F_a^{3/2}$. That is, the axial displacement δ_a is proportional to the axial load F_a to the 2/3 power. When this axial load index is less than one, it indicates the relative axial displacement will be small with only a small increase in the axial load. (**Fig.** 4) The underlying reason for applying a preload is to reduce the amount of displacement.

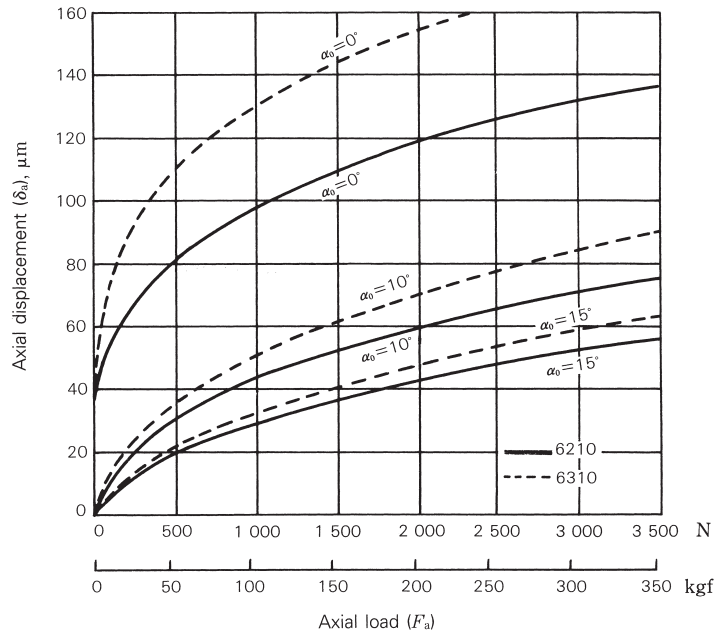

Fig. 3 Axial load and axial displacement of deep groove ball bearings

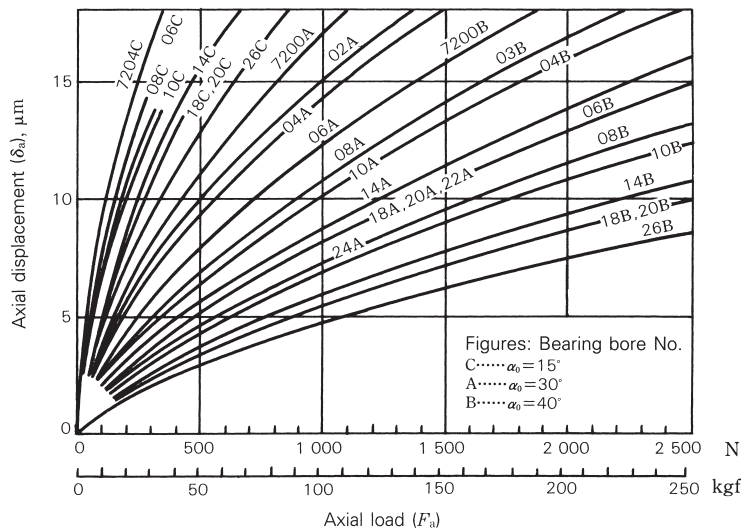

Fig. 4 Axial load and axial displacement of angular contact ball bearings

6.5 Axial displacement of tapered roller bearings

Tapered roller bearings are widely used in pairs like angular contact ball bearings. Care should be taken to select appropriate tapered roller bearings.

For example, the bearings of machine tool head spindles and automobile differential pinions are preloaded to increase shaft rigidity.

When a bearing with an applied preload is to be used in an application, it is essential to have some knowledge of the relationship between axial load and axial displacement. For tapered roller bearings, the axial displacement calculated using Palmgren's method, Equation (1) generally agrees well with actual measured values.

Actual axial deformation varies depending on the bearing mounting conditions, such as the material and thickness of the shaft and housing, and bearing fitting. For details, consult with NSK regarding the axial deformation after mounting.

$$\left.\begin{aligned}\delta_a &= \frac{0.000077}{\sin\alpha}\cdot\frac{Q^{0.9}}{L_{we}^{0.8}} \quad \text{(N)}\\ &= \frac{0.0006}{\sin\alpha}\cdot\frac{Q^{0.9}}{L_{we}^{0.8}} \quad \{\text{kgf}\}\end{aligned}\right\} \quad \cdots\cdots\cdots (1)$$

where, δ_a: Axial displacement of inner, outer ring (mm)

α: Contact angle...1/2 the cup angle (°)

Q: Load on rolling elements (N), {kgf}

$$Q=\frac{F_a}{Z\sin\alpha}$$

L_{we}: Length of effective contact on roller (mm)

F_a: Axial load (N), {kgf}

Z: Number of rollers

Equation (1) can also be expressed as Equation (2).

$$\delta_a = K_a \cdot F_a^{0.9} \quad \cdots\cdots\cdots (2)$$

where,

$$K_a=\frac{0.00007}{(\sin\alpha)^{1.9}\,Z^{0.9}\,L_{we}^{0.8}} \quad \cdots\cdots\cdots \text{(N)}$$

$$=\frac{0.0006}{(\sin\alpha)^{1.9}\,Z^{0.9}\,L_{we}^{0.8}} \quad \cdots\cdots\cdots \{\text{kgf}\}$$

Here, K_a: Coefficient determined by the bearing internal design.

Axial loads and axial displacement for tapered roller bearings are plotted in Fig. 1.

The amount of axial displacement of tapered roller bearings is proportional to the axial load raised to the 0.9 power. The displacement of ball bearings is proportional to the axial load raised to the 0.67 power, thus the preload required to control displacement is much greater for ball bearings than for tapered roller bearings.

Caution should be taken not to make the preload indiscriminately large on tapered roller bearings, since too large of a preload can cause excessive heat, seizure, and reduced bearing life.

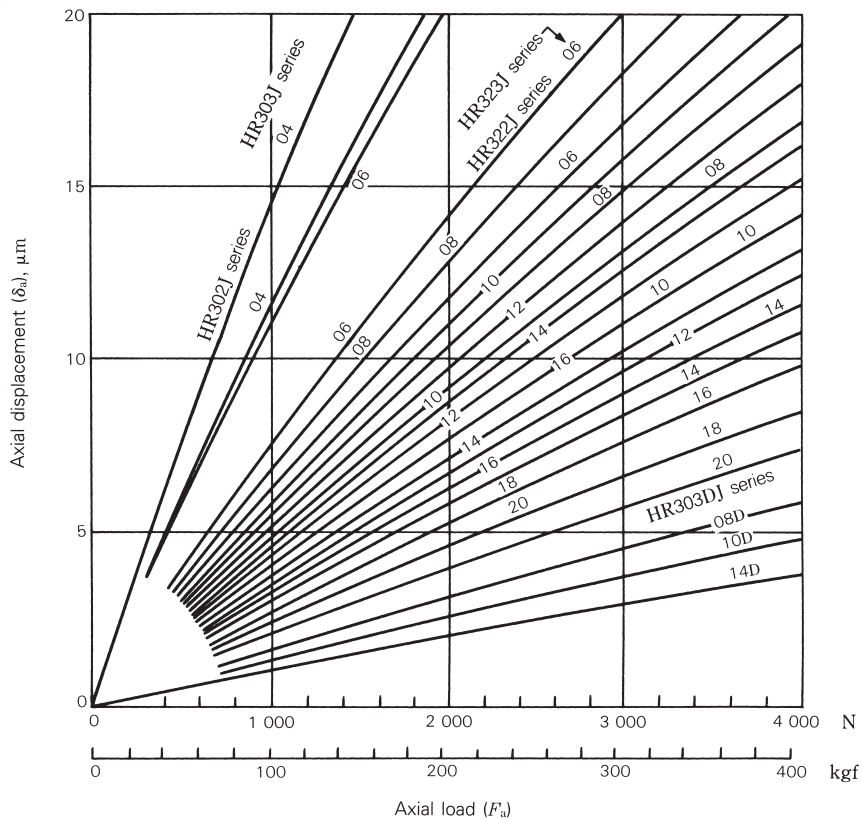

Fig. 1 Axial load and axial displacement for tapered roller bearings

7. Starting and running torques

7.1 Preload and starting torque for angular contact ball bearings

Angular contact ball bearings, like tapered roller bearings, are most often used in pairs rather than alone or in other multiple bearing sets. Back-to-back and face-to-face bearing sets can be preloaded to adjust bearing rigidity. Extra light (EL), Light (L), Medium (M), and Heavy (H) are standard preloads. Friction torque for the bearing will increase in direct proportion to the preload.

The starting torque of angular contact ball bearings is mainly the torque caused by angular slippage between the balls and contact surfaces on the inner and outer rings. Starting torque for the bearing M due to such spin is given by,

$$M=M_s \cdot Z\sin\alpha \ (\mathrm{mN \cdot m}),\ \{\mathrm{kgf \cdot mm}\} \quad \cdots\cdots\cdots\cdots\cdots\cdots (1)$$

where, M_s: Spin friction for contact angle α centered on the shaft,

$$M_s=\frac{3}{8}\mu_s \cdot Q \cdot a\ E\ (k)$$

$(\mathrm{mN \cdot m}),\ \{\mathrm{kgf \cdot mm}\}$

μ_s: Contact-surface slip friction coefficient

Q: Load on rolling elements (N), {kgf}

a: (1/2) of contact-ellipse major axis (mm)

$E\ (k)$: With $k=\sqrt{1-\left(\frac{b}{a}\right)^2}$ as the population parameter, second class complete ellipsoidal integration

b: (1/2) of contact-ellipse minor axis (mm)

Z: Number of balls

α: Contact angle (°)

Actual measurements with 15° angular contact ball bearings correlate well with calculated results using μ_s=0.15 in Equation (1). Fig. 1 shows the calculated friction torque for 70C and 72C series bearings.

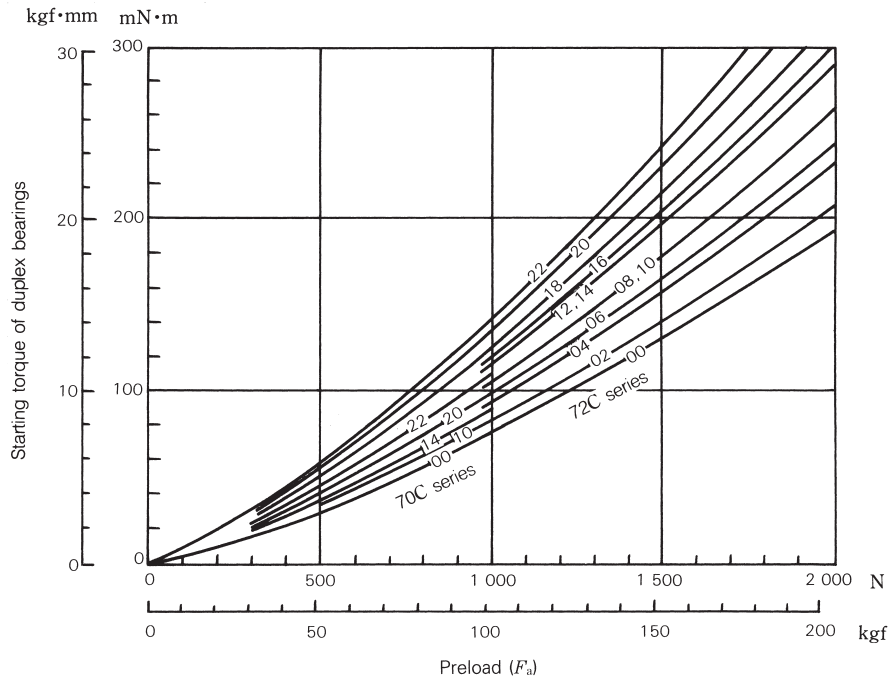

Fig. 1 Preload and starting torque for angular contact ball bearings (α=15°) of DF and DB duplex sets

7.2 Preload and starting torque for tapered roller bearings

The balance of loads on the bearing rollers when a tapered roller bearing is subjected to axial load F_a is expressed by the following three Equations (1), (2), and (3):

$$Q_e=\frac{F_a}{Z\sin\alpha} \quad \cdots\cdots (1)$$

$$Q_i=Q_e\cos 2\beta=\frac{\cos 2\beta}{Z\sin\alpha}F_a \quad \cdots\cdots (2)$$

$$Q_f=Q_e\sin 2\beta=\frac{\sin 2\beta}{Z\sin\alpha}F_a \quad \cdots\cdots (3)$$

where, Q_e: Rolling element load on outer ring (N), {kgf}
Q_i: Rolling element load on inner ring (N), {kgf}
Q_f: Rolling element load on inner-ring large end rib, (N), {kgf} (assume $Q_f \perp Q_i$)
Z: Number of rollers
α: Contact angle...(1/2) of the cup angle (°)
β: (1/2) of tapered roller angle (°)
D_{w1}: Roller large-end diameter (mm) (Fig. 1)
e: Contact point between roller end and rib (Fig. 1)

As represented in Fig. 1, when circumferential load F is applied to the bearing outer ring and the roller turns in the direction of the applied load, the starting torque for contact point C relative to instantaneous center A becomes $e\ \mu_e Q_f$.

Therefore, the balance of frictional torque is,

$$D_{w1}F=e\ \mu_e Q_f \text{ (mN·m), {kgf·mm}} \quad \cdots\cdots (4)$$

where, μ_e: Friction coefficient between inner ring large rib and roller endface

The starting torque M for one bearing is given by,

$$M=F\ Z\ l$$

$$=\frac{e\ \mu_e l\ \sin 2\beta}{D_{w1}\ \sin\alpha}F_a$$

$$\text{(mN·m), {kgf·mm}} \quad \cdots\cdots (5)$$

because, $D_{w1}=2\ \overline{OB}\ \sin\beta$, and $l=\overline{OB}\ \sin\alpha$.
If we substitute these into Equation (5) we obtain,

$$M=e\ \mu_e\ \cos\beta\ F_a \text{ (mN·m), {kgf·mm}} \quad \cdots\cdots (6)$$

The starting torque M is sought considering only the slip friction between the roller end and the inner-ring large-end rib. However, when the load on a tapered roller bearing reaches or exceeds a certain level (around the preload) the slip friction in the space between the roller end and inner-ring large end rib becomes the decisive factor for bearing starting torque. The torque caused by other factors can be ignored. Values for e and β in Equation (5) are determined by the bearing design. Consequently, assuming a value for μ_e, the starting torque can be calculated.

The values for μ_e and for e have to be thought of as a dispersion, thus, even for bearings with the same number, the individual starting torques can be quite diverse. When using a value for e determined by the bearing design, the average value for the bearing starting torque can be estimated using μ_e=0.20 which is the average value determined from various test results.

Fig. 2 shows the results of calculations for various tapered roller bearing series.

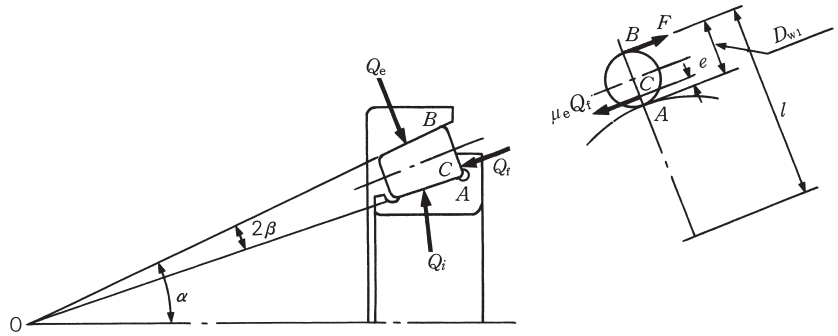

Fig. 1

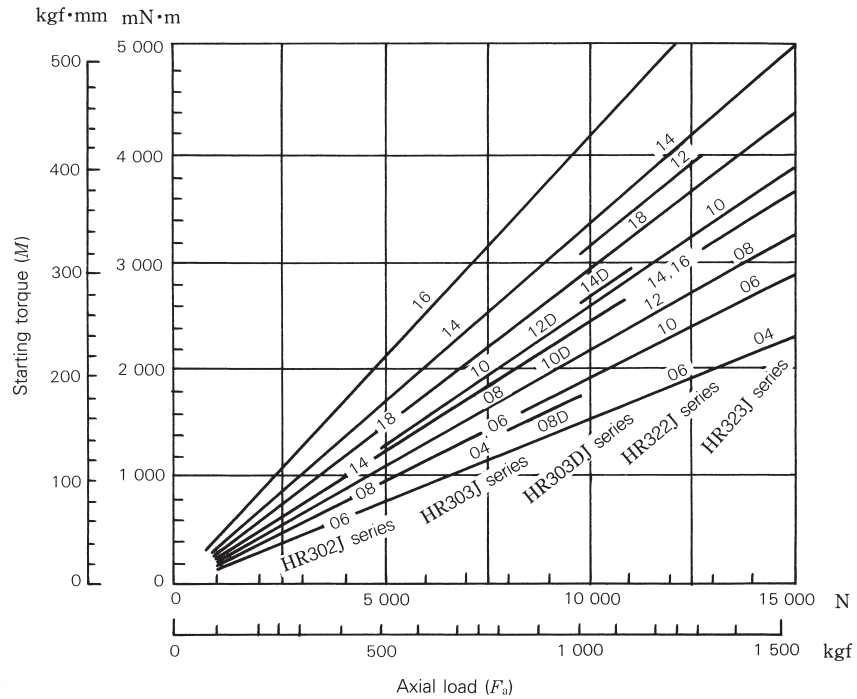

Fig. 2 Axial load and starting torque for tapered roller bearings

7.3 Empirical equation of running torque of high-speed ball bearings

We present here empirical equations for the running torque of high speed ball bearings subject to axial loading and jet lubrication. These equations are based on the results of tests of angular contact ball bearings with bore diameters of 10 to 30 mm, but they can be extrapolated to bigger bearings.

The running torque M can be obtained as the sum of a load term M_l and speed term M_v as follows:

$$M=M_l+M_v \text{ (mN·m), \{kgf·mm\}} \quad \cdots\cdots (1)$$

The load term M_l is the term for friction, which has no relation with speed or fluid friction, and is expressed by **Equation** (2) which is based on experiments.

$$\left.\begin{aligned} M_l&=0.672\times10^{-3}D_{pw}^{0.7}F_a^{1.2} \text{ (mN·m)} \\ &=1.06\times10^{-3}D_{pw}^{0.7}F_a^{1.2} \text{ \{kgf·mm\}} \end{aligned}\right\} \quad \cdots\cdots (2)$$

where, D_{pw}: Pitch diameter of rolling elements (mm)
F_a: Axial load (N), {kgf}

The speed term M_v is that for fluid friction, which depends on angular speed, and is expressed by **Equation** (3).

$$\begin{aligned} M_v&=3.47\times10^{-10}D_{pw}^{3}n_i^{1.4}Z_B^{a}Q^{b} \text{ (mN·m)} \\ &=3.54\times10^{-11}D_{pw}^{3}n_i^{1.4}Z_B^{a}Q^{b} \text{ \{kgf·mm\}} \end{aligned} \quad \cdots\cdots (3)$$

where, n_i: Inner ring speed (min^{-1})
Z_B: Absolute viscosity of oil at outer ring temperature (mPa·s), {cp}
Q: Oil flow rate (kg/min)

The exponents a and b, that affect the oil viscosity and flow rate factors, depend only on the angular speed and are given by **Equations** (4) and (5) as follows:

$$a=24n_i^{-0.37} \quad \cdots\cdots (4)$$
$$b=4\times10^{-9}n_i^{1.6}+0.03 \quad \cdots\cdots (5)$$

An example of the estimation of the running torque of high speed ball bearings is shown in **Fig. 1**. A comparison of values calculated using these equations and actual measurements is shown in **Fig. 2**. When the contact angle exceeds 30°, the influence of spin friction becomes big, so the running torque given by the equations will be low.

Calculation Example

Obtain the running torque of high speed angular contact ball bearing 20BNT02 (ϕ20×ϕ47×14) under the following conditions:

n_i=70 000 min^{-1}
F_a=590 N, {60 kgf}
Lubrication: Jet, oil viscosity: 10 mPa·s {10 cp}
oil flow: 1.5 kg/min

From **Equation** (2),

$$\begin{aligned} M_l&=0.672\times10^{-3}D_{pw}^{0.7}F_a^{1.2} \\ &=0.672\times10^{-3}\times33.5^{0.7}\times590^{1.2} \\ &=16.6\times10^{-3} \text{ (mN·m)} \\ M_l&=1.06\times10^{-3}33.5^{0.7}\times60^{1.2}=1.7 \\ &\text{\{kgf·mm\}} \end{aligned}$$

From **Equations** (4) and (5),

$$\begin{aligned} a&=24n_i^{-0.37} \\ &=24\times70\ 000^{-0.37}=0.39 \\ b&=4\times10^{-9}n_i^{1.6}+0.03 \\ &=4\times10^{-9}\times70\ 000^{1.6}+0.03=0.26 \end{aligned}$$

From **Equation** (3),

$$\begin{aligned} M_v&=3.47\times10^{-10}D_{pw}^{3}n_i^{1.4}Z_B^{a}Q^{b} \\ &=3.47\times10^{-10}\times33.5^{3}\times70\ 000^{1.4}\times10^{0.39}\times1.5^{0.26} \\ &=216 \text{ (mN·m)} \\ M_v&=3.54\times10^{-11}\times33.5^{3}\times70\ 000^{1.4}\times10^{0.39}\times1.5^{0.26} \\ &=22.0 \text{ \{kgf·mm\}} \\ M&=M_l+M_v=16.6+216=232.6 \text{ (mN·m)} \\ M&=M_l+M_v=1.7+22=23.7 \text{ \{kgf·mm\}} \end{aligned}$$

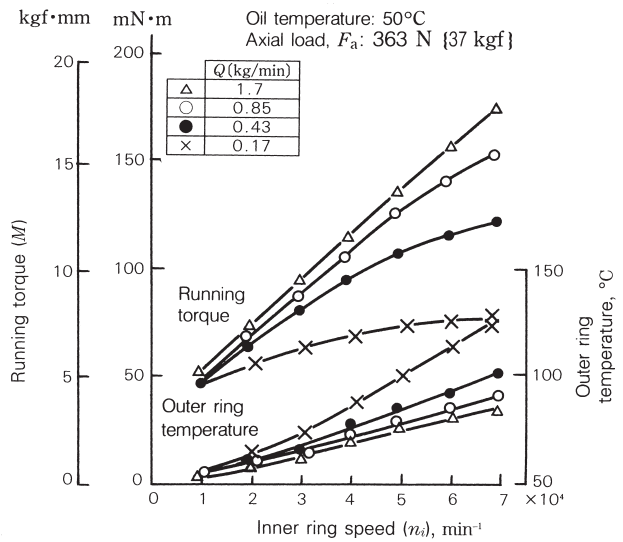

Fig. 1 Typical test example

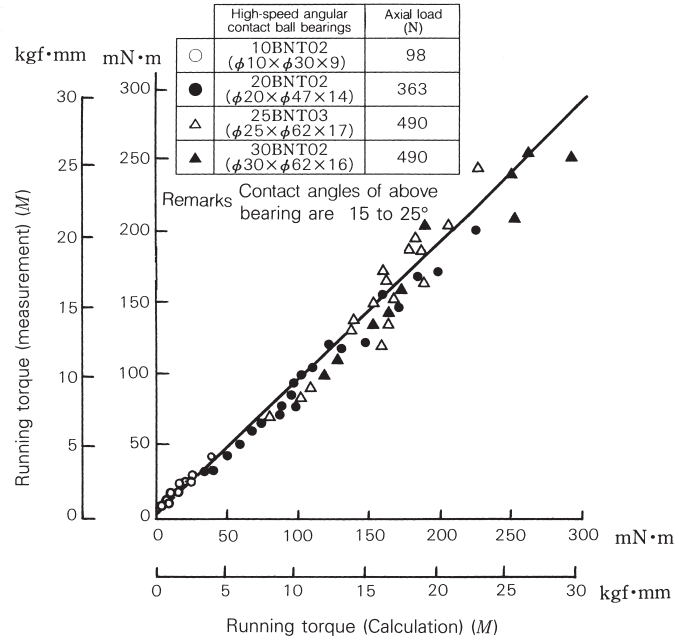

Fig. 2 Comparison of actual measurements and calculated values

7.4 Empirical equations for running torque of tapered roller bearings

When tapered roller bearings operate under axial load, we reanalyzed the torque of tapered roller bearings based on the following two kinds of resistance, which are the major components of friction:

(1) Rolling resistance (friction) of rollers with outer or inner ring raceways — elastic hysteresis and viscous rolling resistance of EHL

(2) Sliding friction between inner ring ribs and roller ends

When an axial load F_a is applied on tapered roller bearings, the loads shown in Fig. 1 are applied on the rollers.

$$Q_e \doteqdot Q_i = \frac{F_a}{Z \sin\alpha} \quad \cdots\cdots (1)$$

$$Q_f = \frac{F_a \sin 2\beta}{Z \sin\alpha} \quad \cdots\cdots (2)$$

where, Q_e: Rolling element load on outer ring
Q_i: Rolling element load on inner ring
Q_f: Rolling element load on inner-ring large end rib
Z: Number of rollers
α: Contact angle…(1/2) of the cup angle
β: (1/2) of tapered roller angle

For simplification, a model using the average diameter D_{we} as shows in Fig. 2 can be used.

Where, M_i, M_e: Rolling resistance (moment)
F_{si}, F_{se}, F_{sf}: Sliding friction
R_i, R_e: Radii at center of inner and outer ring raceways
e: Contact height of roller end face with rib

In Fig. 2, when the balance of sliding friction and moments on the rollers are considered, the following equations are obtained:

$$F_{se} - F_{si} = F_{sf} \quad \cdots\cdots (3)$$

$$M_i + M_e = \frac{D_w}{2} F_{se} + \frac{D_w}{2} F_{si} + \left(\frac{D_w}{2} - e\right) F_{sf} \quad \cdots\cdots (4)$$

When the running torque M applied on the outer (inner) ring is calculated using Equations (3) and (4) and multiplying by Z, which is the number of rollers:

$$M = Z\,(R_e\, F_{se} - M_e)$$

$$= \frac{Z}{D_w}(R_e\, M_i + R_i M_e) + \frac{Z}{D_w} R_e\, e\, F_{sf}$$

$$= M_R + M_S$$

Therefore, the friction on the raceway surface M_R and that on the ribs M_S are separately obtained. Additionally, M_R and M_S are rolling friction and sliding friction respectively.

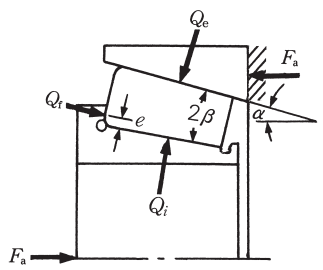

Fig. 1 Loads applied on roller

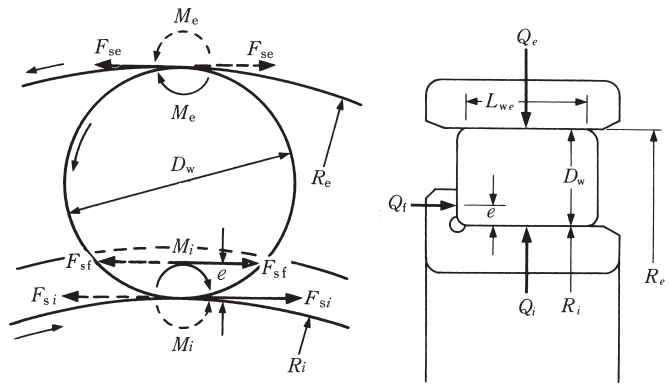

Fig. 2 Model of parts where friction is generated

The running torque M of a tapered roller bearing can be obtained from the rolling friction on the raceway M_R and sliding friction on the ribs M_S.

$$M=M_R+M_S=\frac{Z}{D_w}(R_eM_i+R_iM_e)+\frac{Z}{D_w}R_e\ e\ F_{sf} \quad \cdots\cdots (5)$$

Sliding friction on rib M_S

As a part of M_S, F_{sf} is the tangential load caused by sliding, so we can write $F_{sf} = \mu Q_f$ using the coefficient of dynamic friction μ. Further, by substitution of the axial load F_a, the following equation is obtained:

$$M_S = e\ \mu\ \cos\beta\ F_a \quad \cdots\cdots (6)$$

This is the same as the equation for starting torque, but μ is not constant and it decreases depending on the conditions or running in. For this reason, Equation (6) can be rewritten as follows:

$$M_S=e\ \mu_0\ \cos\beta\ F_a f'\ (\Lambda,\ t,\ \sigma) \quad \cdots\cdots (7)$$

Where μ_0 is approximately 0.2 and $f'\ (\Lambda,\ t,\ \sigma)$ is a function which decreases with running in and oil film formation, but it is set equal to one when starting.

Rolling friction on raceway surface M_R

Most of the rolling friction on the raceway is viscous oil resistance (EHL rolling resistance). M_i and M_e in Equation (5) correspond to it. A theoretical equation exists, but it should be corrected as a result of experiments. We obtained the following equation that includes corrective terms:

$$M_{i,\ e}=\left[f\ (w)\left(\frac{1}{1+0.29L^{0.78}}\right)\frac{4.318}{\alpha_0}(G\cdot U)^{0.658}W^{0.0126}R^2L_{we}\right]_{i,\ e} \quad \cdots\cdots (8)$$

$$f\ (w)=\left(\frac{kF_a}{E'\ D_wL_{we}Z\sin\alpha}\right)^{0.3} \quad \cdots\cdots (9)$$

Therefore, M_R can be obtained using Equations (8) and (9) together with the following equation:

$$M_R=\frac{Z}{D_w}(R_eM_i+R_iM_e)$$

Running torque of bearings M

From these, the running torque of tapered roller bearings M is given by Equation (10)

$$M=\frac{Z}{D_w}(R_eM_i+R_iM_e)+e\ \mu_0\ \cos\beta\ F_af'\ (\Lambda,\ t,\ \sigma) \quad \cdots\cdots (10)$$

As shown in Figs. 3 and 4, the values obtained using Equation (10) correlate rather well with actual measurements. Therefore, estimation of running torque with good accuracy is possible. When needed, please consult NSK.

[Explanation of Symbols]

G, W, U:	EHL dimensionless parameters
L:	Coefficient of thermal load
α_0:	Pressure coefficient of lubricating oil viscosity
R:	Equivalent radius
k:	Constant
E':	Equivalent elastic modulus
α:	Contact angle (Half of cup angle)
R_i, R_e:	Inner and outer ring raceway radii (center)
β:	Half angle of roller
i, e:	Indicate inner ring or outer ring respectively
L_{we}:	Effective roller length

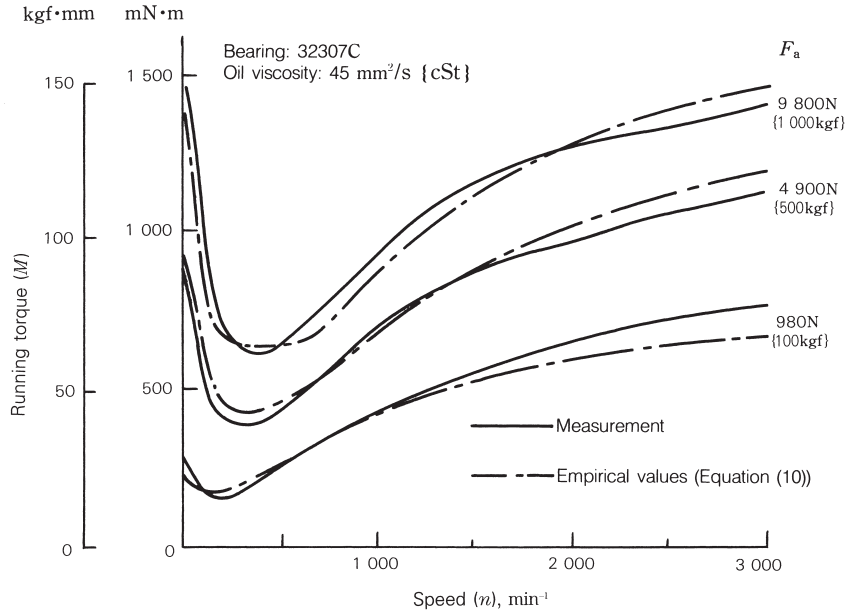

Fig. 3 Comparison of empirical values with actual measurements

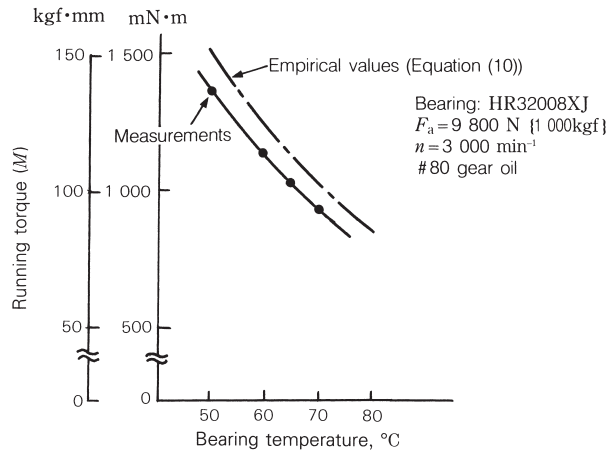

Fig. 4 Viscosity variation and running torque

8. Bearing type and allowable axial load

8.1 Change of contact angle of radial ball bearings and allowable axial load

8.1.1 Change of contact angle due to axial load

When an axial load acts on a radial ball bearing, the rolling element and raceway develop elastic deformation, resulting in an increase in the contact angle and width. When heat generation or seizure has occurred, the bearing should be disassembled and checked for running trace to discover whether there has been a change in the contact angle during operation. In this way, it is possible to see whether an abnormal axial load has been sustained.

The relation shown below can be established among the axial load F_a on a bearing, the load of rolling element Q, and the contact angle α when the load is applied. (See Equations (3), (4), and (5) in Section 6.4)

$$F_a = Z\ Q\ \sin\alpha$$
$$= K\ Z\ D_w^{\ 2}\ \{\sqrt{(\sin\alpha_0+h)^2+\cos^2\alpha_0}-1\}^{3/2}\cdot\sin\alpha \quad \cdots\cdots (1)$$

$$\alpha = \sin^{-1}\frac{\sin\alpha_0+h}{\sqrt{(\sin\alpha_0+h)^2+\cos^2\alpha_0}} \quad \cdots\cdots (2)$$

$$h = \frac{\delta_a}{m_0} = \frac{\delta_a}{r_e+r_i-D_w}$$

Namely, δ_a is the change in Equation (2) to determine α corresponding to the contact angle known from observation of the raceway. Thus, δ_a and α are introduced into Equation (1) to estimate the axial load F_a acting on the bearing. As specifications of a bearing are necessary in this case for calculation, the contact angle α was approximated from the axial load. The basic static load rating C_{0r} is expressed by Equation (3) for the case of a single row radial ball bearing.

$$C_{0r} = f_0\ Z\ D_w^{\ 2}\ \cos\alpha_0 \quad \cdots\cdots (3)$$

where, f_0: Factor determined from the shape of bearing components and applicable stress level

Equation (4) is determined from Equations (1) and (3):

$$\frac{f_0}{C_{0r}}\ F_a = A\ F_a$$
$$= K\ \{\sqrt{(\sin\alpha_0+h)^2+\cos^2\alpha_0}-1\}^{3/2}\cdot\frac{\sin\alpha}{\cos\alpha_0} \quad \cdots\cdots (4)$$

where, K: Constant determined from material and design of bearing

In other words, "h" is assumed and α is determined from Equation (2). Then "h" and α are introduced into Equation (4) to determine $A\ F_a$. This relation is used to show the value A for each bore number of an angular contact ball bearing in Table 1. The relationship between $A\ F_a$ and α is shown in Fig. 1.

Example 1

Change in the contact angle is calculated when the pure axial load F_a = 35.0 kN (50% of basic static load rating) is applied to an angular contact ball bearing 7215C.

A=0.212 is calculated from Table 1 and $A\ F_a$=0.212×35.0=7.42 and α≒26° are obtained from Fig. 1. An initial contact angle of 15° has changed to 26° under the axial load.

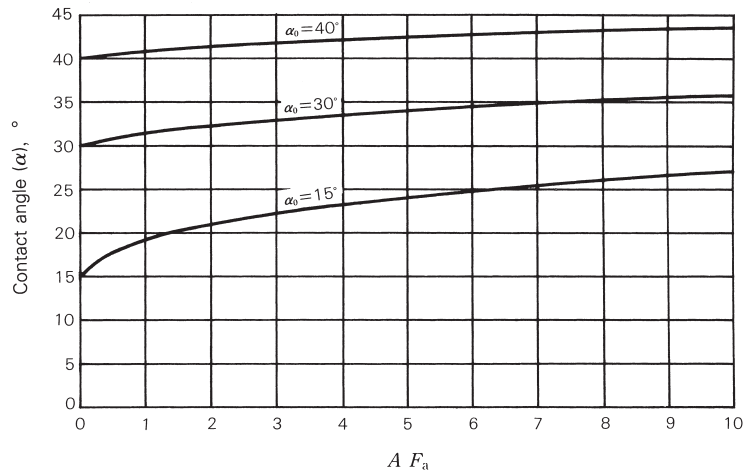

Fig. 1 Change of the contact angle of angular contact ball bearing under axial load

Table 1 Constant A value of angular contact ball bearing

Units: kN^{-1}

Bearing bore No.	Bearing series 70			Bearing series 72			Bearing series 73		
	15°	30°	40°	15°	30°	40°	15°	30°	40°
05	1.97	2.05	2.31	1.26	1.41	1.59	0.838	0.850	0.961
06	1.45	1.51	1.83	0.878	0.979	1.11	0.642	0.651	0.736
07	1.10	1.15	1.38	0.699	0.719	0.813	0.517	0.528	0.597
08	0.966	1.02	1.22	0.562	0.582	0.658	0.414	0.423	0.478
09	0.799	0.842	1.01	0.494	0.511	0.578	0.309	0.316	0.357
10	0.715	0.757	0.901	0.458	0.477	0.540	0.259	0.265	0.300
11	0.540	0.571	0.681	0.362	0.377	0.426	0.221	0.226	0.255
12	0.512	0.542	0.645	0.293	0.305	0.345	0.191	0.195	0.220
13	0.463	0.493	0.584	0.248	0.260	0.294	0.166	0.170	0.192
14	0.365	0.388	0.460	0.226	0.237	0.268	0.146	0.149	0.169
15	0.348	0.370	—	0.212	0.237	0.268	0.129	0.132	0.149
16	0.284	0.302	0.358	0.190	0.199	0.225	0.115	0.118	0.133
17	0.271	0.288	0.341	0.162	0.169	0.192	0.103	0.106	0.120
18	0.228	0.242	0.287	0.140	0.146	0.165	0.0934	0.0955	0.108
19	0.217	0.242	0.273	0.130	0.136	0.153	0.0847	0.0866	0.0979
20	0.207	0.231	0.261	0.115	0.119	0.134	0.0647	0.0722	0.0816

Values for a deep groove ball bearing are similarly shown in Table 2 and Fig. 2.

Example 2

Change in the contact angle is calculated when the pure axial load F_a=24.75 kN (50% of the basic static load rating) is applied to the deep groove ball bearing 6215. Note here that the radial internal clearance is calculated as the median (0.020 mm) of the normal clearance.

The initial contact angle 10° is obtained from Section 4.6 (Fig. 3, Page 99). A=0.303 is determined from Table 2 and $A\ F_a$=0.303×24.75≒7.5 and α≒24° from Fig. 2.

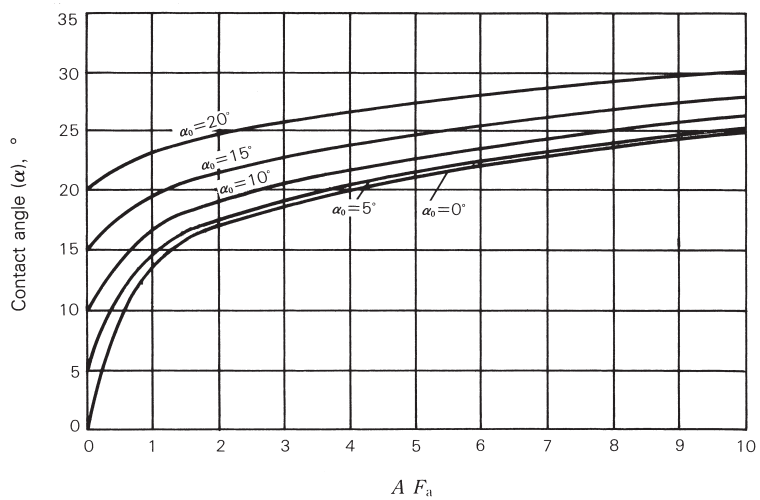

Fig. 2 Change in the contact angle of the deep groove ball bearing under axial load

Table 2 Contact A value of deep groove ball bearing

Units: kN^{-1}

Bearing bore No.	Bearing series 62				
	0°	5°	10°	15°	20°
05	1.76	1.77	1.79	1.83	1.88
06	1.22	1.23	1.24	1.27	1.30
07	0.900	0.903	0.914	0.932	0.958
08	0.784	0.787	0.796	0.811	0.834
09	0.705	0.708	0.716	0.730	0.751
10	0.620	0.622	0.630	0.642	0.660
11	0.490	0.492	0.497	0.507	0.521
12	0.397	0.398	0.403	0.411	0.422
13	0.360	0.361	0.365	0.373	0.383
14	0.328	0.329	0.333	0.340	0.349
15	0.298	0.299	0.303	0.309	0.317
16	0.276	0.277	0.280	0.285	0.293
17	0.235	0.236	0.238	0.243	0.250
18	0.202	0.203	0.206	0.210	0.215
19	0.176	0.177	0.179	0.183	0.188
20	0.155	0.156	0.157	0.160	0.165

8.1.2 Allowable axial load for a deep groove ball bearing

The allowable axial load here means the limit load at which a contact ellipse is generated between the ball and raceway due to a change in the contact angle when a radial bearing, which is under an axial load, rides over the shoulder of the raceway groove. This is different from the limit value of a static equivalent load P_0 which is determined from the basic static load rating C_{0r} using the static axial load factor Y_0. Note also that the contact ellipse may ride over the shoulder even when the axial load on the bearing is below the limit value of P_0.

The allowable axial load $F_{a\ max}$ of a radial ball bearing is determined as follows. The contact angle α for F_a is determined from the right term of Equation (1) and Equation (2) in Section 8.1.1 while Q is calculated as follows:

$$Q=\frac{F_a}{Z\ \sin\alpha}$$

θ of Fig. 1 is also determined from Equation (2) of Section 5.4 as follows:

$$2a=A_2\ \mu\left(\frac{Q}{\Sigma\rho}\right)^{1/3}$$

$$\therefore\ \theta\doteqdot\frac{a}{r}$$

Accordingly, the allowable axial load may be determined as the maximum axial load at which the following relation is established.

$$\gamma\geqq\alpha+\theta$$

As the allowable axial load cannot be determined unless internal specifications of a bearing are known, Fig. 2 shows the result of a calculation to determine the allowable axial load for a deep groove radial ball bearing.

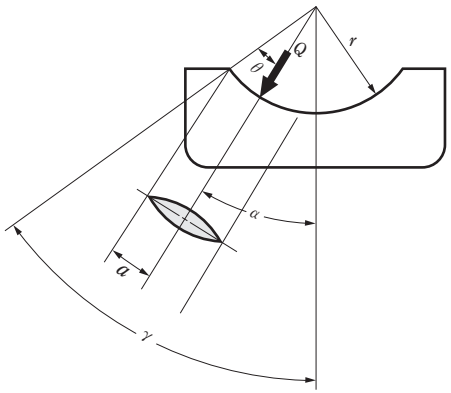

Fig. 1

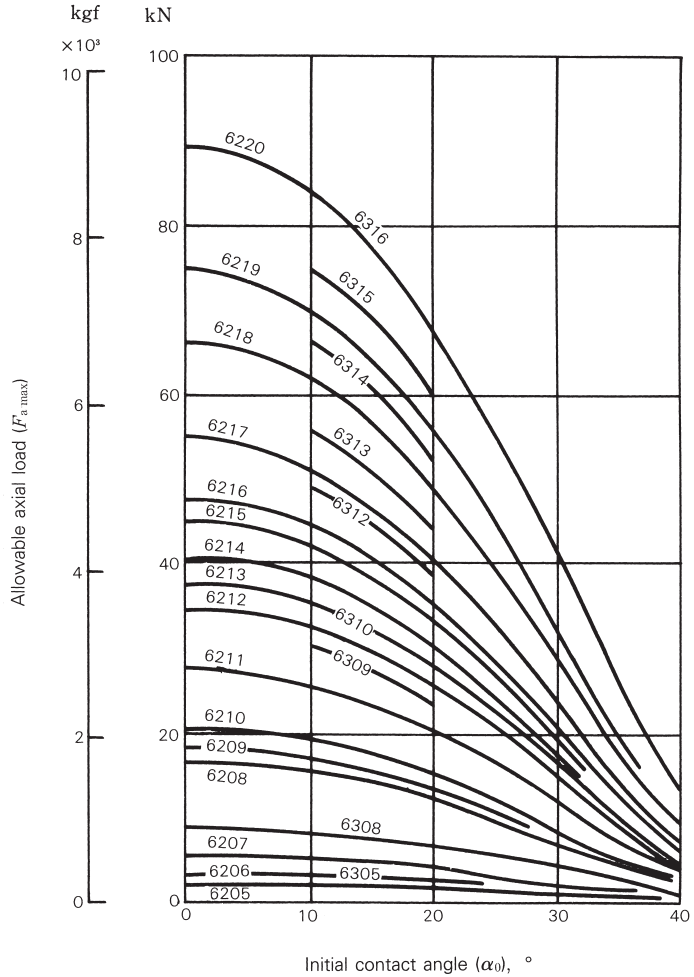

Fig. 2 Allowable axial load for a deep groove ball bearing

8.2 Allowable axial load (break down strength of the ribs) for a cylindrical roller bearings

Both the inner and outer rings may be exposed to an axial load to a certain extent during rotation in a cylindrical roller bearing with ribs. The axial load capacity is limited by heat generation, seizure, etc. at the slip surface between the roller end surface and rib, or the rib strength.

The allowable axial load (the load considered the heat generation between the end face of rollers and the rib face) for the cylindrical roller bearing of the diameter series 3, which is applied continuously under grease or oil lubrication, is shown in Fig. 1.

Grease lubrication (Empirical equation)

$$C_A = 9.8f\left\{\frac{900\ (k\cdot d)^2}{n+1\ 500} - 0.023\times(k\cdot d)^{2.5}\right\}\ \text{(N)}$$

$$= f\left\{\frac{900\ (k\cdot d)^2}{n+1\ 500} - 0.023\times(k\cdot d)^{2.5}\right\}\ \{\text{kgf}\} \quad \cdots\cdots (1)$$

Oil lubrication (Empirical equation)

$$C_A = 9.8f\left\{\frac{490\ (k\cdot d)^2}{n+1\ 000} - 0.000135\times(k\cdot d)^{3.4}\right\}\ \text{(N)}$$

$$= f\left\{\frac{490\ (k\cdot d)^2}{n+1\ 000} - 0.000135\times(k\cdot d)^{3.4}\right\}\ \{\text{kgf}\} \quad \cdots\cdots (2)$$

where, C_A: Allowable axial load (N), {kgf}
d: Bearing bore diameter (mm)
n: Bearing speed (min^{-1})

In the equations (1) and (2), the examination for the rib strength is excluded. Concerning the rib strength, please consult with NSK.

To enable the cylindrical roller bearing to sustain the axial load capacity stably, it is necessary to take into account the following points concerning the bearing and its surroundings.

- ○ Radial load must be applied and the magnitude of radial load should be larger than that of axial load by 2.5 times or more.
- ○ There should be sufficient lubricant between the roller end face and rib.
- ○ Use a lubricant with an additive for extreme pressures.
- ○ Running-in-time should be sufficient.
- ○ Bearing mounting accuracy should be good.
- ○ Don't use a bearing with an unnecessarily large internal clearance.

Moreover, if the bearing speed is very slow or exceeds 50% of the allowable speed in the bearing catalog, or if the bearing bore diameter exceeds 200 mm, it is required for each bearing to be precisely checked for lubrication, cooling method, etc. Please contact NSK in such cases.

f: Load factor

	f value
Continuous loading	1
Intermittent loading	2
Short time loading	3

k: Dimensional factor

	k value
Bearing diameter series 2	0.75
Bearing diameter series 3	1
Bearing diameter series 4	1.2

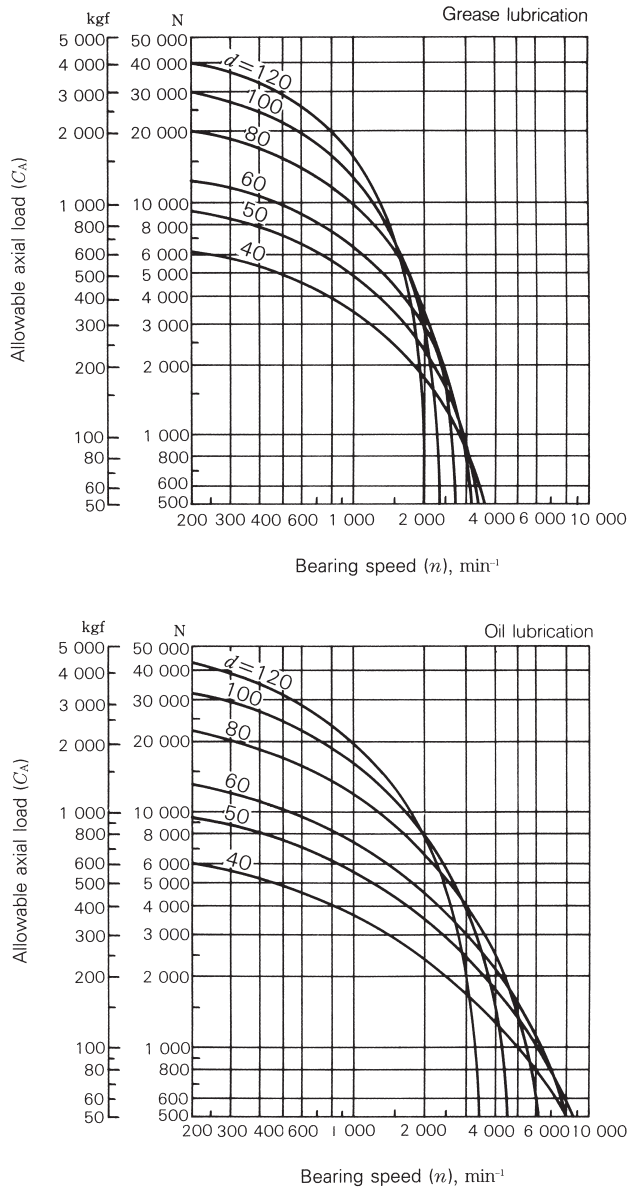

Conditions are continuous loading (f = 1) and bearing diameter series 3 (k = 1.0)

Fig. 1 Allowable axial load for a cylindrical roller bearing

9. Lubrication

9.1 Lubrication amount for the forced lubrication method

When a rolling bearing runs at high speed, the rolling friction of the bearing itself and the churning of lubricant cause heat generation, resulting in substantial temperature rise. Positive removal or dissipation of such generated heat serves greatly to prevent overheating in bearings. The maintenance of a sufficient lubrication oil film ensures stable and continuous operation of bearings at high speed.

Various heat removal or dissipation methods are available. An effective method is to remove the heat directly from bearings by forcing a large quantity of lubricating oil to circulate inside the bearing. This method is called the forced lubrication method. In this case, the amount of oil supplied is mostly determined on the basis of the actual operating conditions. Important factors to be considered include the allowable temperature of the machine or system, radiation effect, and heat generation caused by oil stirring.

Below is an empirical equation which can be used to estimate the amount of forced circulation oil needed for a bearing.

$$\left.\begin{aligned} Q &= \frac{0.19\times10^{-5}}{T_2-T_1}\, d\ \mu\ n\ F\ \text{(N)} \\ &= \frac{1.85\times10^{-5}}{T_2-T_1}\, d\ \mu\ n\ F\ \{\text{kgf}\} \end{aligned}\right\} \quad \cdots\cdots\cdots\cdots\cdots\ (1)$$

where, Q: Oil supply rate (liters/min)
T_1: Oil temperature at the oil inlet (°C)
T_2: Oil temperature at the oil outled (°C)
d: Bearing bore (mm)
μ: Coefficient of dynamic friction (Table 1)
n: Bearing speed (min^{-1})
F: Load on a bearing (N), {kgf}

Systems employing the forced circulation lubrication method include large industrial machinery, such as a paper making machines, presses, steel-making machines, and various speed reducers. Most of these machines incorporate a large bearing. As an example, the calculation of the supply rate for a spherical roller bearing used in a speed reducer is shown below:

Bearing: 22324 CAM E4 C3
d=120 mm
μ=0.0028
Speed: n=1 800 min^{-1}
Bearing load: F=73 500 N, {7 500 kgf}
Temperature difference: Assumed to be T_2-T_1=20°C

$$Q \fallingdotseq \frac{0.19\times10^{-5}}{20}\times120\times0.0028\times1\ 800$$
$$\times73\ 500 \fallingdotseq 4.2$$

The calculated value is about 4 liters/min. This value is only a guideline and may be modified after considering such factors as restrictions on the oil supply and oil outlet bore.

Note that the oil drain pipe and oil drain port must be designed large enough to prevent stagnation of the circulating oil in the housing. For a large bearing with a bore exceeding 200 mm, which is exposed to a heavy load, the oil amount according to Equation (1) is calculated to be slightly larger. However, the user may select a value of about 1/2 to 2/3 of the above calculated value for most practical applications.

Table 1 Coefficients of Dynamic Friction

Bearing Types	Approximate Values of μ
Deep Groove Ball Bearings	0.0013
Angular Contact Ball Bearings	0.0015
Self-Aligning Ball Bearings	0.0010
Thrust Ball Bearings	0.0011
Cylindrical Roller Bearings	0.0010
Tapered Roller Bearings	0.0022
Spherical Roller Bearings	0.0028
Needle Roller Bearings with Cages	0.0015
Full Complement Needle Roller Bearings	0.0025
Spherical Thrust Roller Bearings	0.0028

9.2 Grease filling amount of spindle bearing for machine tools

Recent machine tools, such as machining centers and NC lathes, show a remarkable trend towards increased spindle speeds. The positive results of these higher speeds include enhanced machining efficiency and improved accuracy of the machined surface. But a problem has emerged in line with this trend. Faster spindle speeds cause the spindle temperature to rise which adversely affects the machining accuracy.

In general, grease lubrication is employed with spindle bearings and in particular, for spindle bearings with bores of 150 mm or less. When grease lubrication is employed, filling the bearing with too much grease may cause abnormal heat generation. This is an especially severe problem during the initial operation immediately after filling, and may even result in the deterioration of the grease. It is essential to prevent such a problem by taking sufficient time for a thorough warm-up. In other words, the spindle bearing needs to be accelerated gradually during its initial operation.

Based on its past experience, NSK recommends that spindle bearings for machine tools be filled with the standard amount of grease, which is equivalent to 10% of the cylindrical roller bearing free internal space or 15% of the angular contact ball bearing free internal space, so as to facilitate the initial warm-up wihtout adversely affecting the lubrication performance.

Table 1 shows the standard grease filling amount for bearings used in spindles which is equivalent to 10% of the bearing free space. As an alternative to this table, the simplified equation shown next may be used to estimate the value.

$$V_{10}=f\times10^{-5}\,(D^2-d^2)\,B$$

where, V_{10}: Approximate filling amount (cm^3)
D: Nominal outside diameter (mm)
d: Nominal bore (mm)
B: Nominal bearing width (mm)
f=1.5 for NN30 series and BA10X and BT10X series
f=1.7 for 70 and 72 series
f=1.4 for NN49 series

The grease for high-speed bearings should be a quality grease: use a grease with a synthetic oil as a base if the application involves ball bearings; use a grease with a mineral oil as a base if the application involves roller bearings.

Table 1 Standard grease filling amounts for spindle bearings for machine tools

Units: cm^3

Bearing bore No.	Bearing bore dimension (mm)	Filling amount (per bearing)					
		Cylindrical roller bearing		High-speed angular contact thrust ball bearing BA, BT series	Angular contact ball bearing		High-speed angular contact ball bearing
		NN30 series	N10B series		70 series	72 series	BNC10 series
10	50	1.4	1.1	1.2	1.7	3.1	1.5
11	55	2.0	1.5	2.0	2.3	4.0	2.0
12	60	2.1	1.7	2.0	2.4	4.9	2.0
13	65	2.2	1.8	2.1	2.7	5.7	2.3
14	70	3.2	2.4	3.0	3.6	6.6	3.3
15	75	3.5	2.5	3.2	3.8	7.2	3.6
16	80	4.7	3.3	4.2	5.1	8.8	4.4
17	85	4.9	3.5	4.4	5.3	10.9	4.7
18	90	6.5	4.7	6.0	6.9	13.5	6.2
19	95	6.6	4.8	6.3	7.2	16.3	6.5
20	100	6.8	5.1	6.5	7.4	19.8	6.8
21	105	9.3	6.7	8.4	9.3	23.4	8.1
22	110	11	7.8	10.1	11.9	27.0	10.1
24	120	12.5	8.1	10.8	12.3	32.0	10.8
26	130	18	12.4	16.5	19.5	35.3	16.1
28	140	20	—	17.1	20.7	42.6	17.0
30	150	23	—	21.8	25.8	53.6	21.2
32	160	29	—	26.9	33.8	62.6	25.5
44	170	38	—	32.4	41.6	81.4	33.2

Remarks For the ○○TAC2OD double-direction angular-contact thrust ball bearings, grease should be filled to the same amount as that for the NN30 double-row cylindrical roller bearing.

9.3 Free space and grease filling amount for deep groove ball bearings

Grease lubrication can simplify the bearing's peripheral construction. In place of oil lubrication, grease lubrication is now employed along with enhancement of the grease quality for applications in many fields. It is important to select a grease appropriate to the operating conditions. Due care is also necessary as to the filling amount, since too much or too little grease greatly affects the temperature rise and torque. The amount of grease needed depends on such factors as housing construction, free space, grease brand, and environment. A general guideline is described next.

First, the bearing is filled with an appropriate amount of grease. In this case, it is essential to push grease onto the cage guide surface. Then, the free space, whic excludes the spindle and bearing inside the housing, is filled with an amount of grease as shown next:

1/2 to 2/3 when the bearing speed is 50% or less of the allowable speed specified in the catalog.
1/3 to 1/2 when the bearing speed is 50% or more.

Roughly, low speeds require more grease while high speeds require less grease. Depending on the particular application, the filling amount may have to be reduced further to reduce the torque and to prevent heat generation. When the bearing speed is extremely low, on the other hand, grease may be packed almost full to prevent dust and water entry. Accordingly, it is necessary to know the extent of the housing's free space for the specific bearing to determine the correct filling amount. As a reference, the volume of free space is shown in Table 1 for an open type deep groove ball bearing.

Note that the free space of the open type deep groove ball bearing is the volume obtained by subtracting the volume of the balls and cage from the space formed between inner and outer rings.

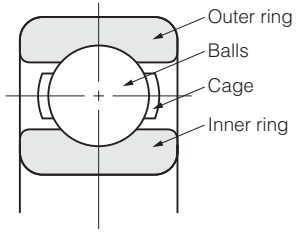

Table 1 Free space of open type deep groove ball bearing

Units: cm^3

Bearing bore No.	Bearing free space			Bearing bore No.	Bearing free space		
	Bearing series				Bearing series		
	60	62	63		60	62	63
00	1.2	1.5	2.9	14	34	61	148
01	1.2	2.1	3.5	15	35	67	180
02	1.6	2.7	4.8	16	47	84	213
03	2.0	3.7	6.4	17	48	104	253
04	4.0	6.0	7.9	18	63	127	297
05	4.6	7.7	12	19	66	155	345
06	6.5	11	19	20	68	184	425
07	9.2	15	25	21	88	216	475
08	11	20	35	22	114	224	555
09	14	23	49	24	122	310	675
10	15	28	64	26	172	355	830
11	22	34	79	28	180	415	1 030
12	23	45	98	30	220	485	1 140
13	24	54	122	32	285	545	1 410

Remarks The table above shows the free space of a bearing using a pressed steel cage. The free space of a bearing using a high-tension brass machined cage is about 50 to 60% of the value in the table.

9.4 Free space of angular contact ball bearings

Angular contact ball bearings are used in various components, such as spindles of machine tools, vertical pump motors, and worm gear reducers.

This kind of bearing is used mostly with grease lubrication. But such grease lubrication may affect the bearing in terms of temperature rise or durability. To allow a bearing to demonstrate its full performance, it is essential to fill the bearing with the proper amount of a suitable grease. A prerequisite for this job is a knowledge of the bearing's free space.

The angular ball bearing is available in various kinds which are independent of the combinations of bearing series, contact angle, and cage type. The free space of the bearing used most frequently is described below. Table 1 shows the free space of a bearing with a pressed cage for general use and Table 2 shows that of a bearing with a high-tension brass machined cage. The contact angle symbols A, B, and C in each table refer to the nominal contact angle of 30°, 40°, and 15° of each bearing.

Table 1 Free space of angular contact ball bearing (1) (with pressed steel cage)

Units: cm^3

Bearing bore No.	Bearing free space			
	Bearing series — Contact angle symbol			
	72-A	72-B	73-A	73-B
00	1.5	1.4	2.9	2.8
01	2.1	2.0	3.7	3.5
02	2.8	2.7	4.8	4.6
03	3.7	3.6	6.2	5.9
04	6.2	5.9	8.4	8.0
05	7.8	7.4	13	12
06	12	11	20	19
07	16	15	26	24
08	20	19	36	34
09	25	24	48	45
10	28	27	63	60

Table 2 Free space of angular contact ball bearing (2) (with high-tension brass machined cage)

Units: cm^3

Bearing bore No.	Bearing free space				
	Bearing series — Contact angle symbol				
	70-C	72-A 72-C	72-B	73-A 73-C	73-B
00	0.9	1.0	1.0	2.2	2.1
01	0.9	1.6	1.6	2.5	2.5
02	1.2	1.9	1.9	3.4	3.3
03	1.6	2.7	2.7	4.6	4.4
04	3.0	4.7	4.2	6.1	5.9
05	3.5	6.0	5.3	9.2	9.0
06	4.3	8.5	8.1	14	13
07	6.5	12	11	18	17
08	8.3	14	14	25	24
09	10	18	17	34	33
10	11	20	20	45	44
11	16	26	25	57	55
12	17	33	31	71	69
13	18	38	37	87	83
14	24	43	42	107	103
15	24	47	45	129	123
16	34	58	57	152	146
17	37	71	70	179	172
18	44	88	85	207	201
19	44	105	105	261	244
20	47	127	127	282	278

9.5 Free space of cylindrical roller bearings

Cylindrical roller bearings employ grease lubrication in many cases because it makes maintenance easier and simplifies the peripheral construction of the housing. It is essential to select a grease brand appropriate for the operating conditions while paying due attention to the filling amount and position of the bearing as well as its housing.

The cylindrical roller bearings can be divided into NU, NJ, N, NF, NH, and NUP types of construction according to the collar, collar ring, and position of the inner or outer ring ribs. Even if bearings belong to the same dimension series, they may have different amounts of free space. The free space also differs depending on whether the cage provided is made from pressed steel or from machined high-tension brass. When determining the grease filling amount, please refer to **Tables 1** and **2** which show the free space of NU type bearings. (By the way, the cylindrical roller bearing type is used most frequently).

For types other than the NU type, the free space can be determined from the free space ratio with the NU type. **Table 3** shows the approximate free space ratio for each type of cylindrical roller bearing. For example, the free space of NJ310 with a pressed steel cage may be calculated approximately at 47 cm^3. This result was calculated by multiplying the free space 52 cm^3 of NU310 in **Table 1** by the space ratio 0.90 for the NJ type (**Table 3**).

Table 1 Free space of cylindrical roller bearing (NU type) (1) (with pressed cage)

Units: cm^3

Bearing bore No.	Bearing free space			
	Bearing series			
	NU2	NU3	NU22	NU23
05	6.6	11	7.8	16
06	9.6	17	12	24
07	14	22	18	35
08	18	31	22	44
09	20	42	23	62
10	23	52	26	80
11	30	68	35	102
12	37	85	45	130
13	44	107	57	156
14	51	124	62	179
15	58	155	70	226
16	71	177	85	260
17	85	210	104	300
18	103	244	134	365
19	132	283	164	415
20	151	335	200	540

Table 2 Free space of cylindrical roller bearing (NU type) (2) (with high-tension brass machined cage)

Units: cm^3

Bearing bore No.	Bearing free space			
	Bearing series			
	NU2	NU3	NU22	NU23
05	5.0	7.6	5.7	10
06	7.4	12	7.9	16
07	9.6	16	12	27
08	12	21	15	32
09	15	29	16	45
10	18	38	17	58
11	22	52	24	77
12	26	62	31	88
13	31	74	43	104
14	37	92	44	129
15	42	102	50	149
16	51	122	60	181
17	64	164	74	200
18	79	193	96	279
19	94	218	116	280
20	115	221	137	355

Table 3 Free space ratio of each type of cylindrical roller bearing

NU Type	NJ Type	N Type	NF Type
1	0.90	1.05	0.95

9.6 Free space of tapered roller bearings

The tapered roller bearing can carry radial load and uni-direction axial loads. It offers high capacity. This type of bearing is used widely in machine systems with relatively severe loading conditions in various combinations by opposing or combining single-row bearings.

With a view towards easier maintenance and inspection, this kind of bearing is lubricated with grease in most cases. It is important to select a grease appropriate to the operating conditions and to use the proper amount of grease for the housing internal space. As a reference, the free space of a tapered roller bearing is shown in Table 1.

The free space of a tapered roller bearing is the space (shadowed portion) of the bearing outer volume less the inner and outer rings and cage, as shown in Fig. 1. The bearing is filled so that grease reaches the inner ring rib surface and pocket surface in sufficient amount. Due attention must also be paid to the grease filling amount and state, especially if grease leakage occurs or maintenance of low running torque is important.

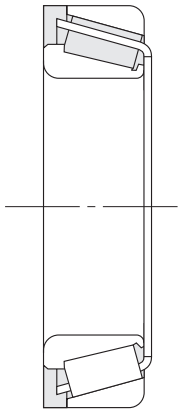

Fig. 1 Free space of tapered roller bearing

Table 1 Free space of tapered roller bearing

Units: cm^3

Bearing bore No.	Bearing free space								
	Bearing series								
	HR329-J	HR320-XJ	HR330-J	HR331-J	HR302-J	HR322-J	HR332-J	HR303-J	HR303-DJ	HR323-J
02	—	—	—	—	—	—	—	4.5	—	—
03	—	—	—	—	3.3	4.3	—	5.7	—	—
04	—	3.5	—	—	5.3	6.6	—	7.2	—	9.2
/22	—	3.6	—	—	—	7.3	—	9.1	—	—
05	—	3.7	4.3	—	6.3	7.4	7.5	11	13	15
/28	—	5.3	—	—	8.8	9.8	10	16	—	—
06	—	6.2	6.7	—	9.2	11	12	18	21	23
/32	—	6.6	—	—	11	13	14	20	—	—
07	4.0	7.5	8.9	—	13	17	18	23	26	35
08	5.8	9.1	11	—	18	23	25	31	35	45
09	—	11	—	18	22	24	26	41	48	58
10	—	12	15	20	23	26	29	55	59	77
11	8.8	19	21	29	30	36	40	72	78	99
12	9.0	20	23	—	39	47	53	88	95	130
13	—	21	25	—	45	62	65	110	120	150
14	17	29	33	—	53	67	69	130	150	190
15	—	30	34	—	58	73	74	160	180	230
16	—	40	—	—	75	91	100	200	200	270
17	—	43	49	76	92	120	130	230	250	320
18	28	58	—	110	110	150	—	260	310	370
19	29	60	—	—	140	170	—	310	350	430
20	37	64	—	150	160	210	240	380	460	580

9.7 Free space of spherical roller bearings

The spherical roller bearing has self-aligning ability and capacity to carry substantially large radial and bi-axial loads. For these reasons, this bearing is used widely in many applications. Application problems include a long span, which causes substantial deflection of the shaft, as well as installation errors and axial misalignment. These bearings may be exposed to a large radial or shock loads. By the way, this bearing is used in plumber blocks.

Grease lubrication is common for spherical roller bearings because it simplifies the seal construction around the housing and makes maintenance and inspection easier. In this case, it is important to select a grease appropriate to the operating conditions and to fill the bearing with the proper amount of grease considering the housing internal space.

As a reference, the bearing free space for conventional types plus four other types (EA, C, CD, and CA) is shown in **Table 1**. Under general operating conditions, it is appropriate to pack a large quantity of grease into the bearing internal space and to pack grease into the housing internal space other than the bearing itself, to the extent of 1/3 to 2/3 that of the free space.

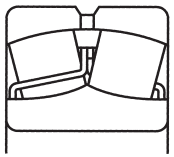

EA type

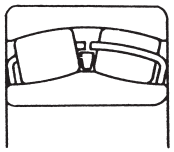

C, CD type

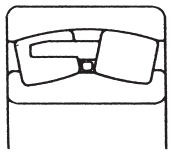

CA type

Table 1 Free space of spherical roller bearing (EA, C, CD, and CA)

Units: cm^3

Bearing bore No.	Bearing free space				
	Bearing series				
	230	231	222	232	223
11	—	—	29	—	78
12	—	—	42	—	96
13	—	—	48	—	113
14	—	—	52	—	139
15	—	—	57	—	170
16	—	—	71	—	206
17	—	—	91	—	234
18	—	—	110	130	283
19	—	—	135	—	327
20	—	—	169	203	410
22	100	150	242	294	560
24	109	228	297	340	700
26	161	240	365	405	955
28	170	292	400	530	1 230
30	209	465	505	680	1 430
32	254	575	680	850	1 710
34	355	610	785	1 090	2 070
36	465	785	810	1 120	2 460
38	565	970	1 160	1 340	2 830
40	715	1 160	1 400	1 640	2 900
44	940	1 500	1 880	2 270	3 750
48	1 030	1 900	2 550	3 550	4 700
52	1 530	2 940	3 300	4 750	5 900
56	1 820	3 150	3 400	4 950	7 250
60	2 200	4 050	4 300	6 200	8 750

Remarks 22211 to 22226, 22311 to 22324 are EA type bearings.
23122 to 23148, 23218 to 23244 are C type bearings.
23022 to 23036, 22228 to 22236 are CD type bearings.
23038 to 23060, 23152 to 23160, 22238 to 22260, 23248 to 23260, and 22326 to 22360 are CA type bearing.

9.8 NSK's dedicated greases

9.8.1 NS7 and NSC greases for induction motor bearings

NS7 and NSC greases have been developed by NSK mainly for lubrication of bearings for induction motors. These greases consist of ingredients such as synthetic oil and lithium soap. Synthetic oil is superior in oxidation, thermal stability, and low-temperature fluidity while lithium soap is superior in water resistance, and shearing stability.

NS7 and NSC greases are applicable over a wide range of temperature from –40°C to +140°C. The viscosity of the base oil is lowest in NS7 and highest in NSC. Namely, NS7 grease is best suited when the low-temperature performance is important and NSC grease for high-temperature performance.

Features
(1) Superior in high-temperature durability, with long grease life
(2) Superior in low-temperature performance, with less abnormal sound and vibration in a bearing at cold start
(3) Superior in high-speed running performance, with little grease leakage
(4) Reduction of the friction torque of a bearing at low and room temperature
(5) Fewer particle inclusions and satisfactory acoustic performance. Moreover, NSC grease can maintain superior acoustic performance over a long period (long acoustic life).
(6) Superior in water resistance
(7) Superior in anti-rusting performance against salt water

Table 1 Characteristics of NS7 and NSC greases

Characteristics	NS7	NSC	Test method
Appearance	Light brown	Light brown	—
Thickener	Li soap	Li soap	—
Base oil	Polyolester diester	Polyolester diphenylether	—
Kinematic viscosity of base oil, mm^2/s 40℃ 100℃	 26.0 5.0	 53.0 8.3	JIS K 2283
Worked penetration, 25℃, 60W	250	235	JIS K 2220: 2003 (Clause 7)
Dropping point, ℃	192	192	JIS K 2220: 2003 (Clause 8)
Corrosiveness, (Copper strip) 100℃, 24 h	Good	Good	JIS K 2220: 2003 (Clause 9)
Evaporation, % 99℃, 22 h	0.30	0.25	JIS K 2220: 2003 (Clause 10)
Oil separation, % 100℃, 24 h	1.2	1.1	JIS K 2220: 2003 (Clause 11)
Oxidative stability, kPa 99℃, 100 h	25	20	JIS K 2220: 2003 (Clause 12)
Worked stability, 25℃, 10^5W	306	332	JIS K 2220: 2003 (Clause 15)
Water wash-out, % 38℃, 1 h	1.4	1.4	JIS K 2220: 2003 (Clause 16)
Low temperature torque, mN·m −30℃ Starting {−40℃} Running	 {115} {25}	 421 84	JIS K 2220: 2003 (Clause 18)
Rust protection test, 0.1%, NaCl 25℃, 48 h, 100% RH	1,1,1	1,1,1	ASTM D 1743

Remarks The value of parentheses is low temperature torque value at −40℃.

Application
* Motor for home electric products (video cassette recorder, air conditioner fan motor, electric oven hood fan motor)
* Motor for office automation equipment (fixed disk drive spindle, floppy disk drive spindle, stepping motor, IC cooling fan motor)
* Industrial motor (blower motor, pump motor, large and medium motor)
* Automotive equipment (starter, distributor, wind shield wiper motor)

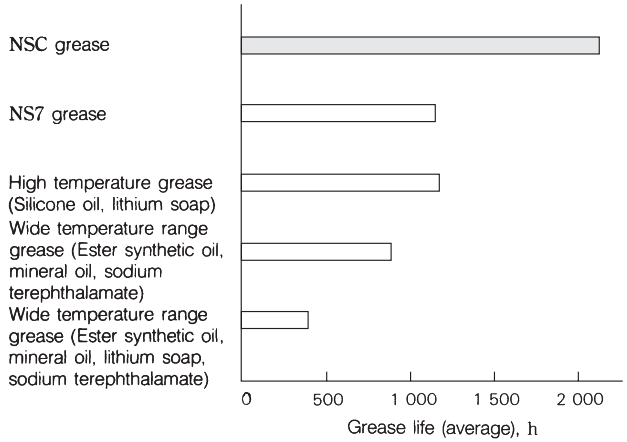

(Test conditions)

Bearing: Non-contact sealed deep groove ball bearing (ϕ25 × ϕ62 × 17 mm)
Bearing outer ring temperature: 140°C
Inner ring speed: 10 000 min^{-1}
Radial load: 98 N {10 kgf}
Axial load: 98 N {10 kgf}
Grease packed volume: 3.4 g

Fig. 1 Grease life

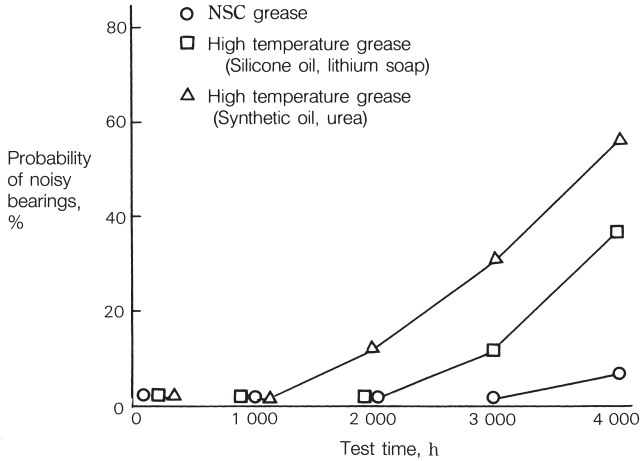

(Test conditions)

Bearing: Non-contact sealed deep groove ball bearing (ϕ8 × ϕ22 × 7 mm)
Ambient temperature: 100°C
Inner ring speed: 5 600 min^{-1}
Axial load: 29.4 N {3 kgf}
Grease packed volume: 0.16 g
Test bearing quantity: 16/test

Fig. 2 Acoustic life

9.8.2 ENS and ENR greases for high-temperature/speed ball bearings

The performances demanded of bearings for electric parts and auxiliary engine equipment installed around the engine are growing more and more severe in order to achieve functional improvement, fuel saving, and life extension of automobiles. These kinds of bearings are mostly operated at high speed and in a high-temperature environment, and they may be subjected to salt or turbid (muddy) water depending on the application and installation position. Certain bearings are also exposed to vibration and high load. ENS and ENR are the greases best suited for bearings used in such stringent conditions.

Features

The ENS and ENR greases use polyester and a urea compound. Polyolester is superior in oxidation and thermal stability and low-temperature fluidity as a base oil while the urea compound is superior in heat and water resistance, shearing stability as a thickener. High-grade additives are also properly combined. Features of this grease are as follows:

(1) Superior in high-temperature durability, with long grease life at a temperature as high as 160°C
(2) Superior shearing stability, with less grease leakage during high-speed rotation and outer ring rotation
(3) Low base oil viscosity and drop point, showing the low torque performance. Less abnormal noise in bearing during a cold start
(4) Superior water resistance of the thickener, which makes softening and outflow difficult even when water may enter the bearing.
(5) Mixing of an adequate rust-preventive agent offers satisfactory rust-prevention performance without any degradation of the grease life. In particular, the ENR grease has powerful rust-preventive capacity, preventing rusting even when water enters a bearing.
(6) However, attention is necessary because it swells the acrylic based materials and deteriorates the fluorine based materials.

Table 1 Characteristics of ENS and ENR grease

Characteristics	ENS	ENR	Test method
Appearance	Milky white	Milky white	—
Thickener	Diurea	Diurea	—
Base oil	Polyolester	Polyolester	—
Kinematic viscosity of base oil, mm^2/s 40℃ 100℃	 30.5 5.4	 30.5 5.4	JIS K 2283
Worked penetration, 25℃, 60W	264	237	JIS K 2220: 2003 (Clause 7)
Dropping point, ℃	≧260	≧260	JIS K 2220: 2003 (Clause 8)
Corrosiveness, (Copper strip) 100℃, 24 h	Good	Good	JIS K 2220: 2003 (Clause 9)
Evaporation, % 99℃, 22 h	0.39	0.48	JIS K 2220: 2003 (Clause 10)
Oil separation, % 100℃, 24 h	1.1	1.4	JIS K 2220: 2003 (Clause 11)
Oxidative stability, kPa 99℃, 100 h	25	30	JIS K 2220: 2003 (Clause 12)
Worked stability, 25℃, 10^5W	310	288	JIS K 2220: 2003 (Clause 15)
Water wash-out, % 79℃, 1 h	2.0	1.0	JIS K 2220: 2003 (Clause 16)
Low temperature torque, −30℃, mN·m Starting Running	 150 60	 230 48	JIS K 2220: 2003 (Clause 18)
Rust protection test, 0.1%, NaCl 25℃, 48 h, 100% RH	1,1,1	1,1,1	ASTM D 1743

Applications

* Electric equipment (electromagnetic clutch, alternator, starter, idler pulley)
* Engine auxiliary equipment (timing belt tensioner, clutch release)
* Office automation equipment (copying machine heat roller)
* Motors (inverter motor, servo motor)

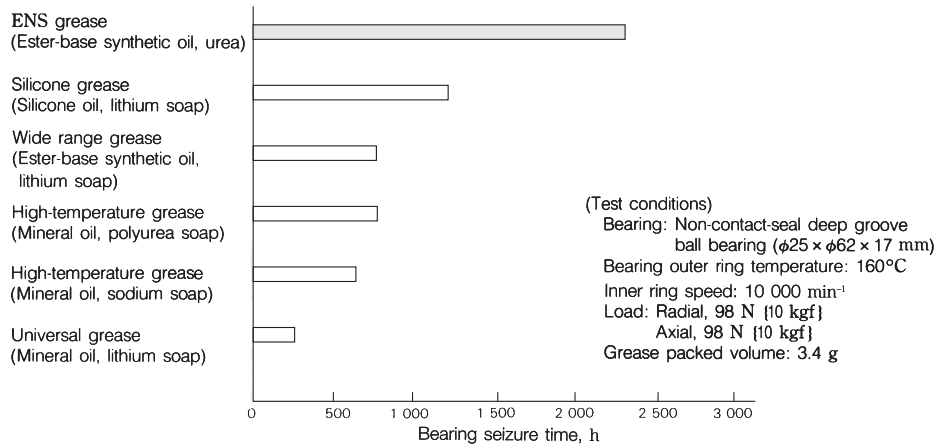

Fig. 1 Grease life

Table 2 Bearing rust-prevention test

Base oil / thickener	ENS Table 1	ENR Table 1	Wide range grease		High-temp grease	
			Ester synthetic oil	Ester synthetic oil and mineral oil	Mineral oil	Mineral oil
Test conditions	Table 1	Table 1	Li soap	Na terephtalamate	Li complex soap	Polyurea
0.1% salt 25℃, 48 h	1,1,1	1,1,1	1,1,1	1,1,1	3,3,3	1,1,1
0.5% salt 52℃, 24 h	2,2,3	1,1,1	1,2,2	1,1,1	—	1,2,2
1.0% salt 52℃, 24 h	—	1,1,1	—	1,2,2	—	—

Test method As per ASTM D 1743
Bearing: Tapered roller bearing 09074R/09194R (φ19.05 × φ49.23 × 23.02 mm)
Relative humidioy: 100 %
Evaluation: 1; No rusting, 2; Minor rusting in three or less points, 3; Worse than Rank 2

9.8.3 EA3 and EA6 greases for commutator motor shafts

An electric fan is used to cool an automotive radiator and air-conditioner compressor. Since an FF model cannot use a cooling fan directly coupled to the engine, an electric fan is used. For this reason, the production of electric fans is growing.

The electric fan is installed near the engine, and the motor bearing temperature reaches around 130 to 160°C and will rise further in the future.

Conventional greases have therefore developed seizure within a shorter period though the speed was lower at 2 000 and 3 000 min^{-1} than that of other electric equipment. One probable reason is entry of carbon brush worn powder into a bearing. Greases best suited for an electric fan motor used in such severe environment and EA3 and EA6.

The cleaner motor tends to have a higher speed to enhance the suction efficiency, and has come to be used at speeds as high as 40 000 to 50 000 min^{-1} these days. Much lower torque, lower noise, and longer life are expected for grease along with speed increase. The grease best suited for such cleaner motor bearing is EA3.

Features and Applications

The EA3 grease uses poly-α-olefine superior in oxidation and thermal stability and low-temperature fluidity as a base oil and urea compound superior in heat and water resistance as a thickener. Moreover, a high-grade additive is added. EA6 is a grease with an EA3 base oil viscosity enhancement to extend the grease life at high temperature.

(1) Superior oxidation stability, wear resistance, and grease sealing performance, preventing entry of carbon brush abrasion powder into a bearing. The grease life in the electric fan motor bearing is long. EA3 is suitable when low-torque performance is important and EA6 is suitable when the bearing temperature exceeds 150°C.

(2) EA3 grease is superior in low-torque and low-noise performances, with superior fluidity, showing superb lubrication performance during rotation as fast as 40 000 to 50 000 min^{-1}. Also, the grease life of a cleaner motor bearing is longer.

(3) Superior rust-preventive performance and less adverse effect on rubber and plastics.

(4) However, attention is necessary because it deteriorates the fluorine based materials.

Table 1 Characteristics of EA3 and EA6 grease

Characteristics	EA3	EA6	Test method
Appearance	Light yellow	Light yellow	—
Thickener	Diurea	Diurea	—
Base oil	Poly-α-olefine oil	Poly-α-olefine oil	—
Kinematic viscosity of base oil, mm^2/s 40℃ 100℃	 47.8 8.0	 112 15	JIS K 2283
Worked penetration, 25℃, 60W	230	220	JIS K 2220: 2003 (Clause 7)
Dropping point, ℃	≧260	≧260	JIS K 2220: 2003 (Clause 8)
Corrosiveness, (Copper strip) 100℃, 24 h	Good	Good	JIS K 2220: 2003 (Clause 9)
Evaporation, % 99℃, 22 h	0.40	0.40	JIS K 2220: 2003 (Clause 10)
Oil separation, % 100℃, 24 h	0.5	0.5	JIS K 2220: 2003 (Clause 11)
Oxidative stability, kPa 99℃, 100 h	25	25	JIS K 2220: 2003 (Clause 12)
Worked stability, 25℃, 10^5W	364	320	JIS K 2220: 2003 (Clause 15)
Water wash-out, % 79℃, 1 h	2.0	1.0	JIS K 2220: 2003 (Clause 16)
Low temperature torque, −30℃, mN·m Starting Running	 150 24	 180 48	JIS K 2220: 2003 (Clause 18)
Rust protection test, 0.1%, NaCl 25℃, 48 h, 100% RH	1,1,1	1,1,1	ASTM D 1743

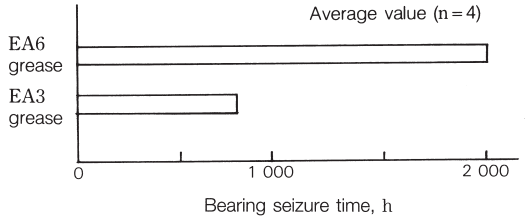

(Test conditions)
Bearing: Non-contact sealed deep groove ball bearing ($\phi8 \times \phi16 \times 4$ mm)
Bearing outer ring temperature: 150 to 160°C
Inner ring speed: 1 700 to 2 000 min^{-1}
Applied voltage: DC 13.5 V
Grease packed volume: 0.06 g

Fig. 1 Durability test with electric fan motors

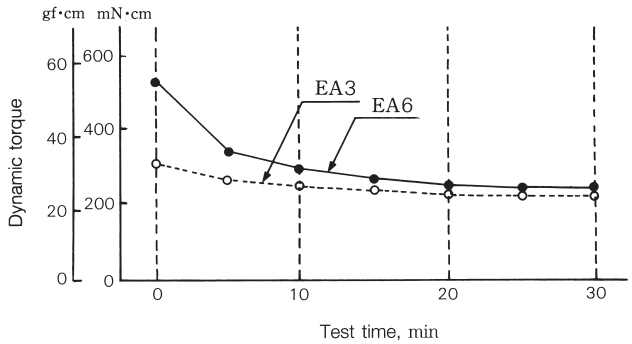

(Test conditions)
Bearing: Non-contact sealed deep groove ball bearing ($\phi8 \times \phi22 \times 7$ mm)
Ambient temperature: 30°C
Inner ring speed: 2 500 min^{-1}
Axial load: 29.4 N {3 kgf}
Grease packed volume: 0.16 g

Fig. 2 Running torque

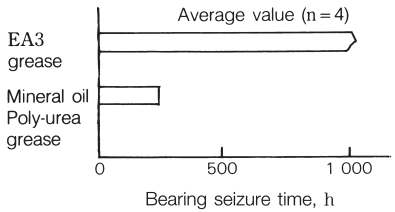

(Test conditions)
Bearing: Non-contact sealed deep groove ball bearing ($\phi8 \times \phi22 \times 7$ mm)
Bearing outer ring temperature: 90°C
Inner ring speed: 50 000 min^{-1}
Axial load: 58.8 N {6 kgf}
Grease packed volume: 0.16 g

Fig. 3 Grease life

9.8.4 WPH grease for water pump bearings

An automotive water pump is a pump to circulate cooling water through the engine. A typical bearing for a water pump is a bearing unit which measures 16 mm in shaft diameter and 30 mm in outer shell diameter and uses either balls with balls or balls with rollers. Though the water pump bearing unit is equipped with a high-performance seal, cooling water may enter the unit. In fact, most water pump bearing failures can be attributed to entry of coolant into the bearing.

Recently, the bearing speed tends to rise in line with performance and efficiency enhancement of engines. Moreover, the bearing temperature rises further along with temperature rise of the cooling water and engine. The bearing load is also growing these days as the number of models employing poly V-belts is growing rapidly.

The grease guaranteeing high reliability and best applicability for water pump bearings and bearing units used in such severe environment is WPH.

Features

The WPH grease uses poly-α-olefine, which is superior in oxidation and thermal stability, as a base oil and a urea compound, which is superior in heat and water resistance, as a thickener. A high-grade additive is also used. Features are as described below:

(1) This grease does not readily soften and outflow even if coolant enters the bearing. Also, this grease can maintain satisfactory lubrication performance over an extended period of time. As a result, this grease can prevent flaking in a bearing.

(2) Superior in high-temperature durability, preventing deterioration and seizure even when the bearing temperature rises.

(3) Superior rust-preventive performance prevents rusting even if water or coolant enters the bearing.

Table 1 Characteristics of WPH grease

Characteristics	WPH	Test method
Appearance	Butter-like milky yellow	—
Thickener	Diurea	—
Base oil	Poly-α-olefine oil	—
Kinematic viscosity of base oil, mm^2/s 40℃ 100℃	 95.8 14.4	JIS K 2283
Worked penetration, 25℃, 60W	240	JIS K 2220: 2003 (Clause 7)
Dropping point,℃	259	JIS K 2220: 2003 (Clause 8)
Corrosiveness, (Copper strip) 100℃, 24 h	Good	JIS K 2220: 2003 (Clause 9)
Evaporation, % 99℃, 22 h	0.20	JIS K 2220: 2003 (Clause 10)
Oil separation, % 100℃, 24 h	0.2	JIS K 2220: 2003 (Clause 11)
Oxidative stability, kPa 99℃, 100 h	20	JIS K 2220: 2003 (Clause 12)
Worked stability, 25℃, 10^5W	306	JIS K 2220: 2003 (Clause 15)
Water wash-out, % 79℃, 1 h	0	JIS K 2220: 2003 (Clause 16)
Low temperature torque, −30℃, mN·m Starting Running	 240 45	JIS K 2220: 2003 (Clause 18)
Rust protection test, 0.1%, NaCl 25℃, 48 h, 100% RH	1,1,1	ASTM D 1743

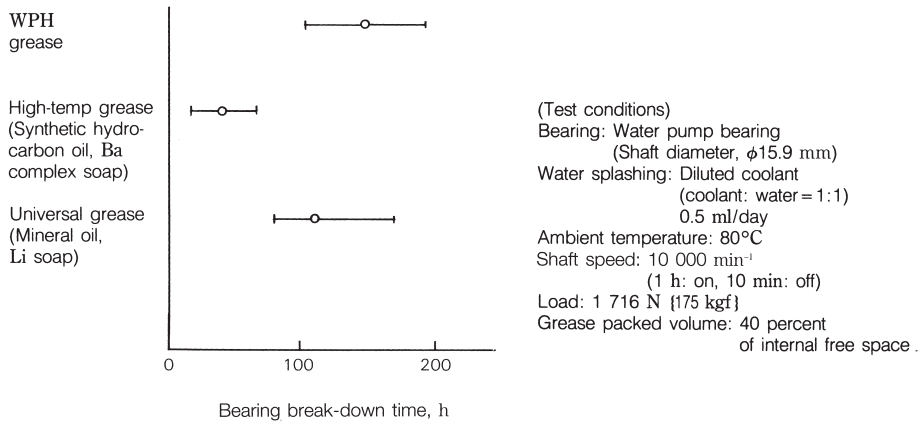

Fig. 1 Water resistant test of grease for water pump bearings

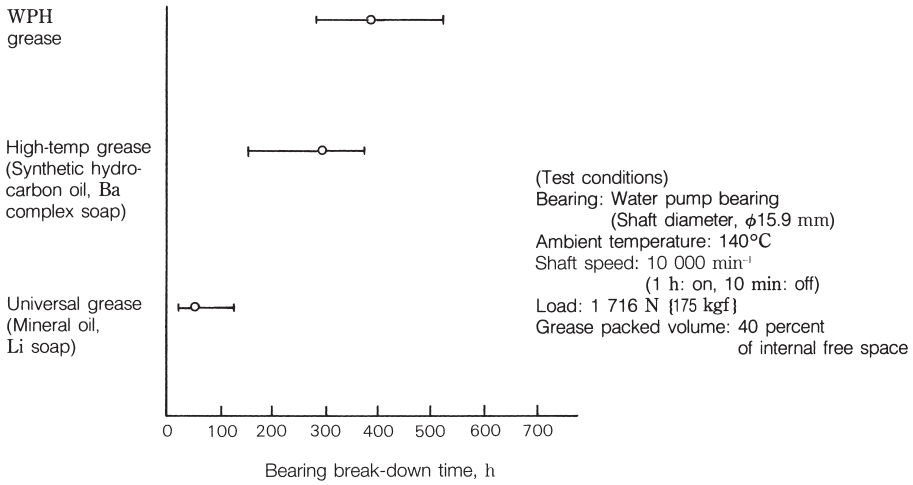

Fig. 2 Life test of water pump bearings

10. Bearing materials

10.1 Comparison of national standards of rolling bearing steel

The dimension series of rolling bearings as mechanical elements have been standardized internationally, and the material to be used for them specified in ISO 683/17 (heat treatment, alloy, and free cutting steels / Part 17 ball and roller bearing steels). However, materials are also standardized according to standards of individual countries and, in some cases, makers are even making their own modifications.

As internationalization of products incorporating bearings and references to the standards of these kinds of steels are increasing nowadays, applicable standards are compared and their features described for some representative bearing steels.

Table 1

Applicable national standards and chemical composition of high-carbon chrome bearing steel

JIS G 4805	ASTM	Other major national standards	Chemical composition (%) C	Si	Mn	Cr	Mo	Others	Application	Remarks
SUJ1	—	—	0.95 to 1.10	0.15 to 0.35	≦0.50	0.90 to 1.20	—	*1	Not used generally	Equivalent to each other though there are slight differences in the ranges.
—	51100	—	0.98 to 1.10	0.15 to 0.35	0.25 to 0.45	0.90 to 1.15	≦0.10	*1		
SUJ2	—	—	0.95 to 1.10	0.15 to 0.35	≦0.50	1.30 to 1.60	—	*1	Typical steel type for small and medium size bearings	Equivalent to each other though there are slight differences in the ranges.
—	A 295-89 52100	—	0.93 to 1.05	0.15 to 0.35	0.25 to 0.45	1.35 to 1.60	≦0.10	P≦0.025 S≦0.015		
—	—	100Cr6 (DIN)	0.90 to 1.05	0.15 to 0.35	0.25 to 0.40	1.40 to 1.65	—	—		
—	—	100C6 (NF)	0.95 to 1.10	0.15 to 0.35	0.20 to 0.40	1.35 to 1.60	≦0.08	P≦0.030 S≦0.025		
—	—	535A99 (BS)	0.95 to 1.10	0.10 to 0.35	0.40 to 0.70	1.20 to 1.60	—	*1		
SUJ3	—	—	0.95 to 1.10	0.40 to 0.70	0.90 to 1.15	0.90 to 1.20	—	*1	For large size bearings	SUJ3 is equivalent to Grade 1. Grade 2 has better quenching capability
—	A 485-03 Grade 1	—	0.90 to 1.05	0.45 to 0.75	0.90 to 1.20	0.90 to 1.20	≦0.10	P≦0.025 S≦0.015		
—	A 485-03 Grade 2	—	0.85 to 1.00	0.50 to 0.80	1.40 to 1.70	1.40 to 1.80	≦0.10	P≦0.025 S≦0.015		
SUJ4	—	—	0.95 to 1.10	0.15 to 0.35	≦0.50	1.30 to 1.60	0.10 to 0.25	*1	Scarcely used	Better quenching capability than SUJ2
SUJ5	—	—	0.95 to 1.10	0.40 to 0.70	0.90 to 1.15	0.90 to 1.20	0.10 to 0.25	*1	For ultralarge size bearings	Though Grade 3 is equivalent to SUJ5, quenching capability of Grade 3 is better than SUJ5.
—	A 485-03 Grade 3	—	0.95 to 1.10	0.15 to 0.35	0.65 to 0.90	1.10 to 1.50	0.20 to 0.30	P≦0.025 S≦0.015		

Notes *1: P≦0.025, S≦0.025
Remarks ASTM: Standard of American Society of Testing Materials, DIN: German Standard, NF: French Standard, BS: British Standard

Table 2 JIS and ASTM standards and chemical composition of carburizing bearing steel

JIS G 4052 G 4053	ASTM A 534-90	C	Chemical composition (%) Si	Mn	Ni	Cr	Mo	Others	Application	Remarks
SCr420H	—	0.17 to 0.23	0.15 to 0.35	0.55 to 0.95	≦0.25	0.85 to 1.25	—	*2	For small bearings	Similar steel type
—	5120H	0.17 to 0.23	0.15 to 0.35	0.60 to 1.00	—	0.60 to 1.00	—	*3		
SCM420H	—	0.17 to 0.23	0.15 to 0.35	0.55 to 0.95	≦0.25	0.85 to 1.25	0.15 to 0.35	*2	For small bearings	Similar steel type, though quenching capability of 4118H is inferior to SCM420H
—	4118H	0.17 to 0.23	0.15 to 0.35	0.60 to 1.00	—	0.30 to 0.70	0.08 to 0.15	*3		
SNCM220H	—	0.17 to 0.23	0.15 to 0.35	0.60 to 0.95	0.35 to 0.75	0.35 to 0.65	0.15 to 0.30	*2	For small bearings	Equivalent, though there are slight differences
—	8620H	0.17 to 0.23	0.15 to 0.35	0.60 to 0.95	0.35 to 0.75	0.35 to 0.65	0.15 to 0.25	*3		
SNCM420H	—	0.17 to 0.23	0.15 to 0.35	0.40 to 0.70	1.55 to 2.00	0.35 to 0.65	0.15 to 0.30	*2	For medium bearings	Equivalent, though there are slight differences
—	4320H	0.17 to 0.23	0.15 to 0.35	0.40 to 0.70	1.55 to 2.00	0.35 to 0.65	0.20 to 0.30	*3		
SNCM815	—	0.12 to 0.18	0.15 to 0.35	0.30 to 0.60	4.00 to 4.50	0.70 to 1.00	0.15 to 0.30	*2	For large bearings	Similar steel type
—	9310H	0.07 to 0.13	0.15 to 0.35	0.40 to 0.70	2.95 to 3.55	1.00 to 1.45	0.08 to 0.15	*3		

Notes *2: P≦0.030, S≦0.030 *3: P≦0.025, S≦0.015

10.2 Long life bearing steel (NSK Z steel)

It is well known that the rolling fatigue life of high-carbon chrome bearing steel (SUJ2, SAE52100) used for rolling bearings is greatly affected by non-metallic inclusions.

Non-metallic inclusions are roughly divided into three-types: sulfide, oxide, and nitride. The life test executed for long periods showed that oxide non-metallic inclusions exert a particularly adverse effect on the rolling fatigue life.

Fig. 1 shows the parameter (oxygen content) indicating the amount of oxide non-metallic inclusions vs. life.

The oxygen amount in steel was minimized as much as possible by reducing impurities (Ti, S) substantially, thereby achieving a decrease in the oxide non-metallic inclusions. The resulting long-life steel is the Z steel.

The Z steel is an achievement of improved steelmaking facility and operating conditions made possible by cooperation with a steel maker on the basis of numerous life test data.

A graph of the oxygen content in steel over the last 25 years is shown in Fig. 2.

The result of the life test with sample material in Fig. 2 is shown in Fig. 3. The life tends to become longer with decreasing oxygen content in steel. The high-quality Z steel has a life span which is about 1.8 times longer than that of conventional degassed steel.

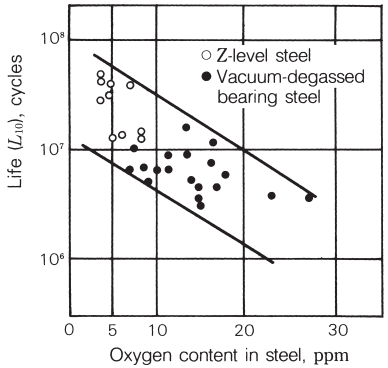

Fig. 1 Oxygen content in steel and life of bearing steel

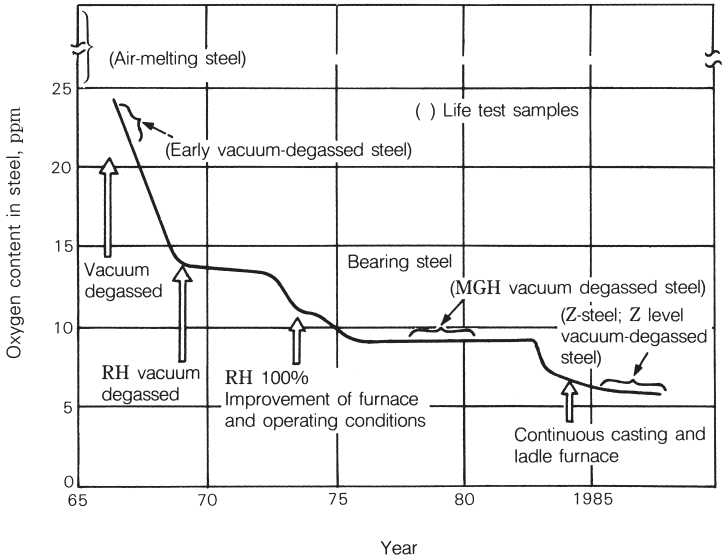

Fig. 2 Transition of oxygen content in NSK bearing steels

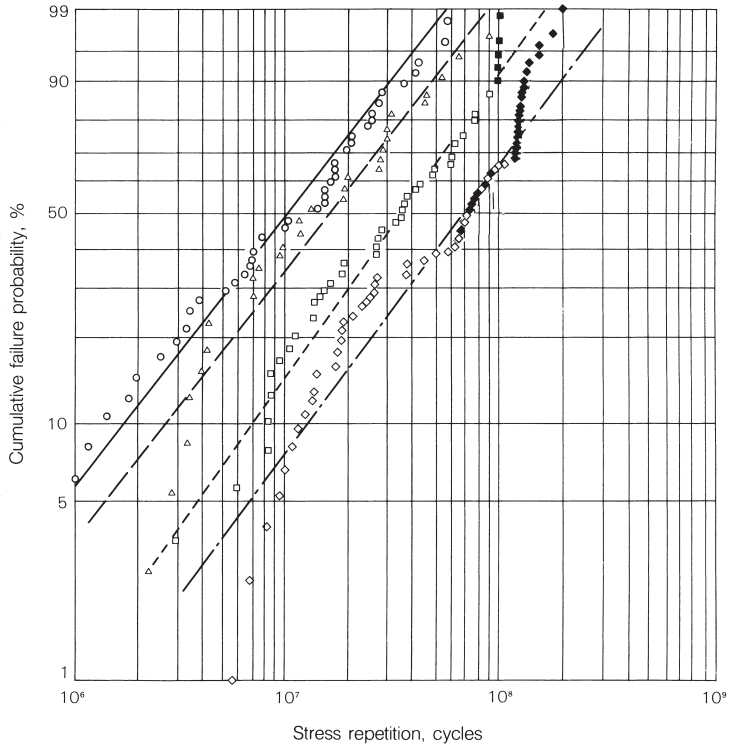

Classification	Test quantity	Failured quantity	Weibull slope	L_{10}	L_{50}
○ Air-melting steel	44	44	1.02	1.67×10^6	1.06×10^7
△ Vacuum degassed steel	30	30	1.10	2.82×10^6	1.55×10^7
□ MGH vacuum degassed steel	46	41	1.16	6.92×10^6	3.47×10^7
◇ Z steel	70	39	1.11	1.26×10^7	6.89×10^7

Remarks Testing of bearings marked dark ■ and ◆ has not been finished testing yet.

Fig. 3 Result of thrust life test of bearing steel

10.3 High temperature bearing materials

Even for rolling bearings with countermeasures against high-temperature, the upper limit of the operating temperature is a maximum of about 400°C because of constraints of lubricant. This kind of bearing may be used in certain cases at around 500 to 600°C if the durable time, running speed, and load are restricted. Materials used for high-temperature bearings should be at a level appropriate to the application purpose in terms of hardness, fatigue strength, structural change, and dimensional stability at the operating temperature. In particular, the hardness is important.

Ferrous materials generally selected for high temperature applications include high-speed steel (SKH4) and AISI M50 of Cr-Mo-V steel. Where heat and corrosion resistances are required, martensitic stainless steel SUS 440C may be used. Chemical components of these materials are shown along with bearings steel SUJ2 in Table 1. Their hardness at high temperature is shown in Fig. 1.

The high-temperature hardness of bearing steel diminishes sharply when the tempering temperature is exceeded. The upper limit of the bearing's operating temperature for a bearing having been subjected to normal tempering (160 to 200°C) is around 120°C. If high-temperature tempering (230 to 280°C) is made, then the bearing may be used up to around 200°C as long as the load is small.

SKH4 has been used with success as a bearing material for X-ray tube and can resist well at 450°C when operated with solid lubricant. M50 is used mostly for high-temperature and high-speed bearings of aircraft, and the upper limit of operating temperature is around 320°C.

Where hardness and corrosion resistance at high temperature are required, SUS 440C, having been subjected to high temperature tempering (470 to 480°C), can have a hardness between SUJ2 and M50. Accordingly, this steel can be used reliably at a maximum temperature of 200°C. In high temperature environments at 600°C or more, even high-speed steel is not sufficient in hardness. Accordingly, hastealloy of Ni alloy or stellite of Co alloy is used.

At a temperature exceeding the above level, fine ceramics may be used such as silicon nitride (Si_3N_4) or silicon carbonate (SiC) which are currently highlighted as high-temperature corrosion resistant materials. Though not yet satisfactory in workability and cost, these materials may eventually be used in increasing quantity.

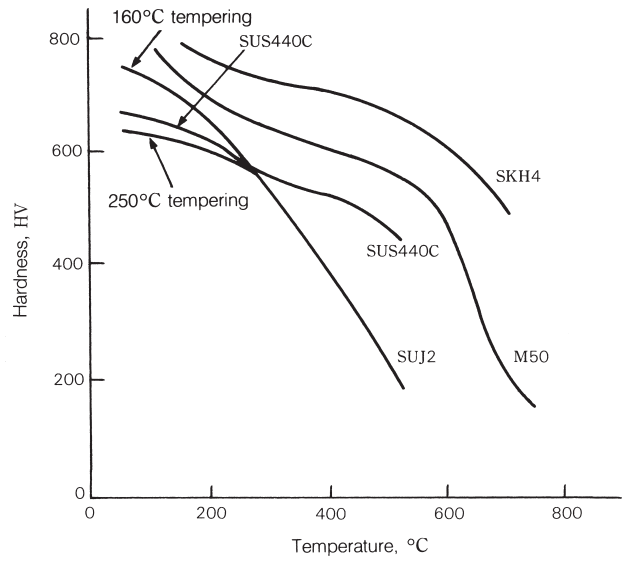

Fig. 1 Hardness of high-temperature materials

Steel type	C	Si
SUJ2	1.02	0.25
SKH4	0.78	≦0.4
M50	0.81	≦0.25
SUS 440C	1.08	≦1.0

Remarks Figures without ≦ mark indicate median of tolerance.

Table 1 High-temperature bearing materials

Chemical composition %							Remarks
Mn	Ni	Cr	Mo	W	V	Co	
≦0.5	—	1.45	—	—	—	—	General use
≦0.4	—	4.15	—	18.0	1.25	10.0	High-temperature use
≦0.35	≦0.10	4.0	4.25	≦0.25	1.0	≦0.25	High-temperature use
≦1.0	≦0.60	17.0	≦0.75	—	—	—	Corrosion resistance/ high temperature

10.4 Dimensional stability of bearing steel

Sectional changes or changes in the dimensions of rolling bearings as time passes during operation is called aging deformation. When the inner ring develops expansion due to such deformation, the result is a decrease in the interference between the shaft and inner ring. This becomes one of the causes of inner ring creep. Creep phenomenon, by which the shaft and inner ring slip mutually, causes the bearing to proceed from heat generation to seizure, resulting in critical damage to the entire machine. Consequently, appropriate measures must be taken against aging deformation of the bearing depending on the application.

Aging deformation of bearings may be attributed to secular thermal decomposition of retained austenite in steel after heat treatment. The bearing develops gradual expansion along with phase transformation.

The dimensional stability of the bearings, therefore, varies in accordance with the relative relationship between the tempering during heat treatment and the bearing's operating temperature. The bearing dimensional stability increases with rising tempering temperature while the retained austenite decomposition gradually expands as the bearing's operating temperature rises.

Fig. 1 shows how temperature influences the bearing's dimensional stability. In the right-hand portion of the figure, the interference between the inner ring and shaft in various shaft tolerance classes is shown as percentages for the shaft diameter. As is evident from Fig. 1, the bearing dimensional stability becomes more unfavorable as the bearing's temperature rises. Under these conditions, the interference between the shaft and inner ring of a general bearing is expected to decrease gradually. In this view, loosening of the fit surface needs to be prevented by using a bearing which has received dimension stabilization treatment.

When the bearing temperature is high, there is a possibility of inner ring creep. Since due attention is necessary for selection of an appropriate bearing, it is essential to consult NSK beforehand.

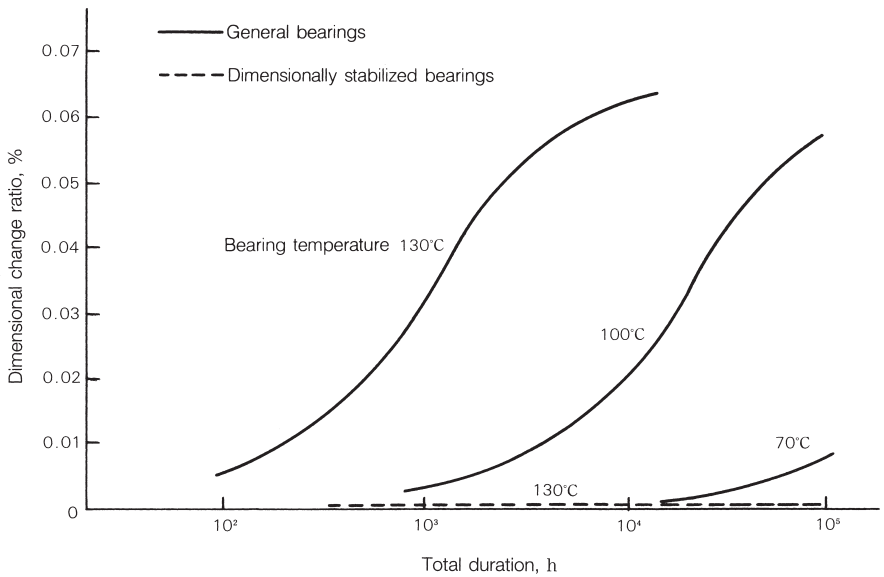

Fig. 1 Bearing temperature and dimensional change ratio

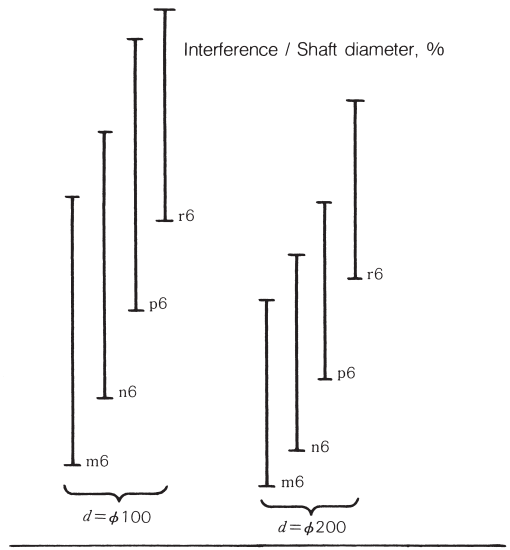

10.5 Characteristics of bearing and shaft/housing materials

Rolling bearings must be able to resist high load, run at high speed, and endure long-time operation. It is also important to know the characteristics of the shaft and housing materials if the bearing performance is to be fully exploited. Physical and mechanical properties or typical materials of a bearing and shaft/housing are shown for reference in Table 1.

	Material	Heat treatment
Bearing	SUJ2	Quenching, tempering
	SUJ2	Spheroidizing annealing
	SCr420	Quenching, low temp tempering
	SAE4320 (SNCM420)	Quenching, low temp tempering
	SNCM815	Quenching, low temp tempering
	SUS440C	Quenching, low temp tempering
	SPCC	Annealing
	S25C	Annealing
	CAC301 (HBsC1)	—
Shaft	S45C	Quenching, 650℃ tempering
	SCr430	Quenching, 520 to 620℃ fast cooling
	SCr440	Quenching, 520 to 620℃ fast cooling
	SCM420	Quenching, 150 to 200℃ air cooling
	SNCM439	Quenching, 650℃ tempering
	SC46	Normalizing
	SUS420J2	1 038℃ oil cooling, 400°C air cooling
Housing	FC200	Casting
	FCD400	Casting
	A1100	Annealing
	AC4C	Casting
	ADC10	Casting
	SUS304	Annealing

Note * JIS standard or reference value.
** Though Rockwell C scale is generally used, Brinel hardness is shown for comparison.
Remarks Proportional limits of SUJ2 and SCr420 are 833 MPa {85 kgf/mm²} and 440 MPa {45 kgf/mm²} respectively as reference.

Table 1 Physical and mechanical properties of bearing and shaft/housing materials

Density g/cm	Specific heat kJ/(kg·K)	Thermal conductivity W/(m·K)	Electric resistance μΩ·cm	Linear expansion coeff. (0 to 100℃) ×10⁻⁶/℃	Young's modulus MPa {kgf/mm²}	Yield point MPa {kgf/mm²}	Tensile strength MPa {kgf/mm²}	Elongation %	Hardness HB	Remarks
7.83	0.47	46	22	12.5	208 000 {21 200}	1 370 {140}	1 570 to 1 960 {160 to 200}	0.5 Max.	650 to 740	High carbon chrome bearing steel No. 2
7.86				11.9		420 {43}	647 {66}	27	180	
7.83		48	21	12.8		882 {90}	1 225 {125}	15	370	Chrome steel
		44	20	11.7		902 {92}	1 009 {103}	16	**293 to 375	Nickel chrome molybdenum steel
7.89		40	35	—		—	*1 080 {110} Min.	*12 Min.	*311 to 375	
7.68	0.46	24	60	10.1	200 000 {20 400}	1 860 {190}	1 960 {200}	—	**580	Martensitic stainless steel
7.86	0.47	59	15	11.6	206 000 {21 000}	—	*275 {28} Min.	*32 Min.	—	Cold rolled steel plate
	0.48	50	17	11.8		323 {33}	431 {44}	33	120	Carbon steel for machine structure
8.5	0.38	123	6.2	19.1	103 000 {10 500}	—	*431 {44} Min.	*20 Min.	—	High-tension brass
7.83	0.48	47	18	12.8	207 000 {21 100}	440 {45}	735 {75}	25	217	Carbon steel for machine structure
			22	12.5	208 000 {21 100}	*637 {65} Min.	*784 {80} Min.	*18 Min.	*229 to 293	Chrome steel
		45	23			*784 {80} Min.	*930 {95} Min.	*13 Min.	*269 to 331	
	0.47	48	21	12.8		—	*930 {95} Min.	*14 Min.	*262 to 352	Chrome molybdenum steel
		38	30	11.3	207 000 {21 100}	920 {94}	1 030 {105}	18	320	Nickel chrome molybdenum steel
—	—	—	—	—	206 000 {21 000}	294 {30}	520 {53}	27	143	Low carbon cast steel
7.75	0.46	22	55	10.4	200 000 {20 400}	1 440 {147}	1 650 {168}	10	400	Martensitic stainless steel
7.3	0.50	43	—		98 000 {10 000}	—	*200 {20} Min.	—	*217 Max.	Gray cast iron
7.0	0.48	20	—	11.7		*250 {26} Min.	*400 {41} Min.	*12 Min.	*201 00Max.	Spheroidal graphite cast iron
2.69	0.90	222	3.0	23.7	70 600 {7 200}	34 {3.5}	78 {8}	35	—	Pure aluminum
2.68	0.88	151	4.2	21.5	72 000 {7 350}	88 {9}	167 {17}	7	—	Aluminum alloy for sand casting
2.74	0.96	96	7.5	22.0	71 000 {7 240}	167 {17}	323 {33}	4	—	Aluminum alloy for die casting
8.03	0.50	15	72	15.7 to 16.8	193 000 {19 700}	245 {25}	588 {60}	60	150	Austenitic stainless steel

10.6 Engineering ceramics as bearing material

Ceramics are superior to metal materials in corrosion, heat, and wear resistance, but limited in application because they are generally fragile. But engineering ceramics that have overcome this problem of fragility are highlighted as materials to replace metals in various fields. Engineering ceramics have already been used widely for cutting tools, valves, nozzles, heat insulation materials, and structural members.

More specifically, ceramic material is highlighted as a bearing material. In practice, the angular contact ball bearing with silicon nitride balls is applied to the head spindle of machine tools. The heat generation characteristics and machine rigidity allow this material to offer functions which have not been available up to now with other materials.

Characteristics of engineering ceramics and bearing steel are shown in **Table 1**. Engineering ceramics have the following advantages as a bearing material over metals:

- ○ Low density for weight reduction and high-speed rotation
- ○ High hardness and small frictional coefficient, and superiority in wear resistance
- ○ Small coefficient of thermal expansion and satisfactory dimensional stability
- ○ Superior heat resistance and less strength degradation at high temperature
- ○ Excellent corrosion resistance
- ○ Superior electric insulation
- ○ Non-magnetic

Development of applications that take advantage of these characteristics are actively underway. For example, bearings for rotary units to handle molten metals, and non-lubricated bearings in clean environments (clean rooms, semiconductor manufacture systems, etc.).

Engineering ceramics include many kinds such as silicon nitride, silicon carbonate, alumina, partially-stabilized zirconia. Each of these materials has its own distinctive properties.

To successfully use ceramics as bearing material, it is essential to know various properties of ceramic materials and to select the material to match the operating conditions. Though suffering from problems of workability and cost, improvement in material design and manufacturing technology will further accelerate application of ceramic bearings in high temperature environments, corrosive environments, and in vacuum environments.

Material	Density g/cm^3	Hardness HV
Silicon nitride (Si_3N_4)	3.1 to 3.3	1 500 to 2 000
Silicon carbonate (SiC)	3.1 to 3.2	1 800 to 2 500
Alumina (Al_2O_3)	3.6 to 3.9	1 900 to 2 700
Partly-stabilized zirconia (ZrO_2)	5.8 to 6.1	1 300 to 1 500
Bearing steel	7.8	700

What is required most of the engineering ceramics as bearing materials is greater reliability in terms of rolling fatigue life. In particular, ceramic bearings are used at high temperatures or high speeds. Thus, any damage will exert an adverse effect on performance of peripheral devices of the machine. Numerous measures have been taken such as processing the raw material powder to sintering and machining in order to enhance the reliability of the rolling life.

Table 1 Properties of engineering ceramics and metal material (bearing steel)

Young's modulus GPa {×10^{4}kgf/mm^2}	Flexural strength MPa {kgf/mm^2}	Fracture toughness MPa·m$^{1/2}$	Linear thermal expansion coeff. ×10^{-6}/℃	Thermal shock resistance ℃	Thermal conductivity W/(m·K) {cal/cm·s℃}	Electric resistance Ω·cm
250 to 330 {2.5 to 3.3}	700 to 1 000 {70 to 100}	5.2 to 7.0	2.5 to 3.3	800 to 1 000	12 to 50 {0.03 to 0.12}	10^{13} to 10^{14}
310 to 450 {3.1 to 4.5}	500 to 900 {50 to 90}	3.0 to 5.0	3.8 to 5.0	400 to 700	46 to 75 {0.11 to 0.18}	100 to 200
300 to 390 {3.0 to 3.9}	300 to 500 {30 to 50}	3.8 to 4.5	6.8 to 8.1	190 to 210	17 to 33 {0.04 to 0.08}	10^{14} to 10^{16}
150 to 210 {1.5 to 2.1}	900 to 1 200 {90 to 120}	8.5 to 10.0	9.2 to 10.5	230 to 350	2 to 3 {0.005 to 0.008}	10^{10} to 10^{12}
208 {2.1}	—	14 to 18	12.5	—	50 {0.12}	10^{-5}

Fig. 1 shows a Weibull plot of the results of a test with radial ball bearings using ceramic balls of silicon nitride of six kinds of HIP (sintered under atmospheric pressure) differing in raw material, structure, and components. The test was conducted, with 3/8" diameter ceramic balls incorporated into inner and outer rings of bearing steel, under conditions of Table 2.

X and Y in Fig. 1 are bearings with NSK-made ceramic balls developed under strict control of the material manufacturing process. A theoretical calculation life (L_{10}) of bearing with steel balls under the same test conditions is 263 hours. It can, therefore, be stated that NSK-made ceramic balls have a life of more than eight times as long as L_{10} of bearings with steel balls. Other ceramic balls develop flaking while suffering wider variance within a shorter period of time.

The flaking pattern shows a unique fatigue appearance (Photo 1), mostly indicating a type of flaking which is generated by foreign metallic material, segregation of the sintering auxiliary agent, or the occurrence of pores.

The commonly highlighted strength characteristics of engineering ceramics are flexural strength, hardness, and K_{IC} (fracture toughness). Apart from these characteristics, the material needs to be free from defects such as pores or segregation of the auxiliary agent. This can be accomplished through cleaning of the material base and optimum sintering.

Accordingly, due and careful consideration of the material maker is necessary during processing stages from raw material powder to sintering in order to transform ceramics into a an extremely reliable engineering bearing material.

Table 2 Test conditions

Test bearing	6206 with 8 ceramic balls and nylon cage
Support bearing	6304
Radial load	3 800 N {390 kgf}
Max. contact surface pressure	2 800 MPa {290 kgf/mm^2}
Speed	3 000 min^{-1}
Lubrication	FBK oil RO-68

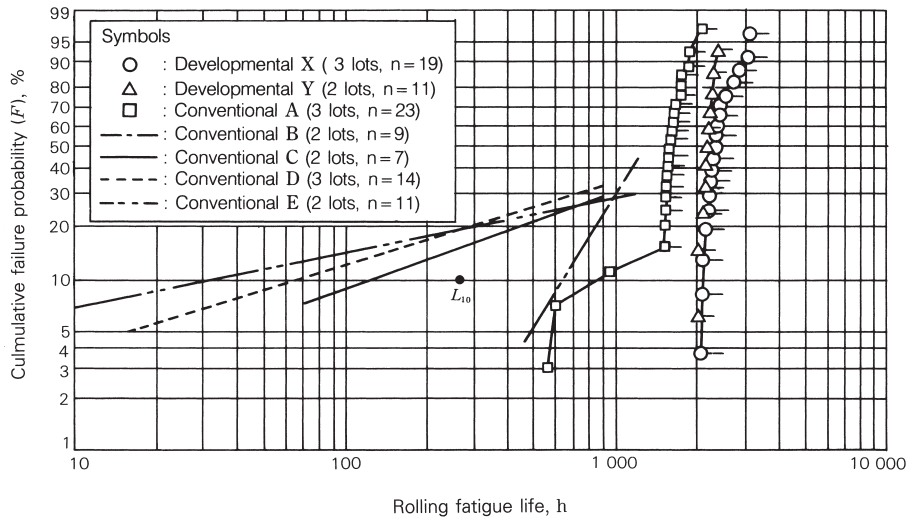

Fig. 1 Weibull plot of life test results

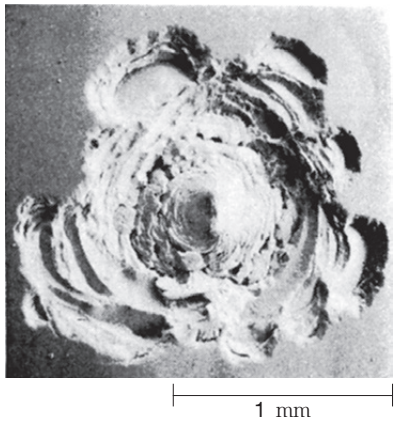

Photo 1 Appearance of flaking

10.7 Physical properties of representative polymers used as bearing material

Because of lightweight, easy formability, and high corrosion resistance, polymer materials are used widely as a material for cages. Polymers may be used independently, but they are usually combined with functional fillers to form a composite material. Composites can be customized to have specific properties. In this way composites can be designed to be bearing materials. For example, fillers can be used to improve such properties as low friction, low wear, non-stick slip characteristic, high limit PV value, non-scrubbing of counterpart material, mechanical properties, and heat resistance, etc.

Table 1 shows characteristics of representative polymer materials used for bearings.

Plastics	Elastic modulus (GPa) (1)
Polyethylene HDPE UHMWPE	 0.11 50.5
Polyamide Nylon 6 Nylon 66	 2.5 3.0
Nylon 11	1.25
Polytetra fluoroethylene PTFE	0.40
Poly buthylene terephthalate PBT	2.7
Polyacetal POM Homo-polymer Co-polymer	 3.2 2.9
Polyether sulfon PES	2.46
Polysulfon PSf	2.5
Polyallylate (Aromatic polyester)	1.3 3.0
Polyphenylene sulfide PPS (GF 40%)	4.2
Polyether ether keton PEEK	1.7
Poly-meta-phenylene isophthalic amide	10 (fiber) 7.7 (mold)
Polypromellitic imide (Aromatic polyimide) PI	3 (film)
	2.5 to 3.2 (mold)
Polyamide imide PAI	4.7
Polyether imide (Aromatic polyimide) PI	3.6
Polyamino bis-maleimide	—

Notes (1) GPa≒10^4 kgf/cm^2=10^2 kgf/mm^2
(2) If there is a slash mark "/" in the thermal deformation temperature column, then the value to the left of the "/" applies to 451 kPa, If there, the value relates to 1.82 MPa.
(3) Reference value

Table 1 Characteristics of representative polymers

Strength GPa (1)	Density g/cm^3	Specific elastic modulus ×10^4mm	Specific strength ×10^4mm	Melting point ℃	Glass transition temp ℃	Thermal deformation temperature ℃ (2)	Continuous operating temperature ℃	Remarks
0.03 0.025	0.96 0.94	12.6 53.2	3.3 2.7	132 136	−20 −20	75/50 75/50	— —	High creep and toughness, softening
0.07 0.08	1.13 1.14	221.2 263.2	6.2 7.0	215 264	50 60	150/57 180/60	80 to 120 80 to 120	High water absorption and toughness
0.04	1.04	120.2	3.8	180	—	150/55	Lower than nylon 6 or 66	Low water absorption
0.028	2.16	18.5	1.3	327	115	120/—	260	High creep, sintering,low friction and adhesion, inert. Stable at 290℃
0.06	1.31	206.1	4.6	225	30	230/215	155	
0.07 0.06	1.42 1.41	225.3 205.7	4.9 4.3	175 165	−13 —	170/120 155/110	— 104	High hardness and toughness, low water absorption
0.086	1.37	179.6	6.3	—	225	210/203	180	Usable up to 200℃ Chemically stable
0.07	1.24	201.6	5.6	—	190	181/175	150	
0.07 0.075	1.35 1.40	96.3 214.3	5.2 5.4	350 350	— —	293 293	300 260 to 300	Inert, high hardness, Used as filler for PTFE Stable up to 320℃
0.14	1.64	256.1	8.5	275	94	>260	220	Hot cured at 360℃
0.093	1.30	130.8	7.2	335	144	152	240	
0.7 0.18	1.38 1.33	724.6 579	50.7 13.5	375 415 (decomposition)	>230 >230	280 280	220 220	Fire retardant, heat resistance fiber
0.17	1.43	203	7.0	Heat de-composition	417 decomposition	360/250	300 (3)	No change in inert gas up to 350℃
0.1	1.43	203	7.0	Heat de-composition	417 decomposition	360/250	260	Usable up to 300℃ for bearing. Sintering, no fusion (molded products)
0.2	1.41	333.3	14.2	—	280	260	210	Usable up to 290℃ as adhesive or enamel Improved polyimide of melting forming
0.107	1.27	240.9	—	—	215	210/200	170	Improved polyimide of melting forming
0.35	1.6	—	21.9	—	—	330 (3)	260	

10.8 Characteristics of nylon material for cages

In various bearings these days, plastic cages have come to replace metal cages increasingly. Advantages of using plastic cages may be summarized as follows:

(1) Lightweight and favorable for use with high-speed rotation
(2) Self-lubricating and low wear. Worn powders are usually not produced when plastic cages are used. As a result, a highly clean internal state is maintained.
(3) Low noise appropriate atm silent environments
(4) Highly corrosion resistant, without rusting
(5) Highly shock resistant, proving durable under high moment loading
(6) Easy molding of complicated shapes, ensures high freedom for selection of cage shape. Thus, better cage performance can be obtained.

As to disadvantages when compared with metal cages, plastic cages have low heat resistance and limited operating temperature range (normally 120°C). Due attention is also necessary for use because plastic cages are sensitive to certain chemicals. Polyamide resin is a representative plastic cage material. Among polyamide resins, nylon 66 is used in large quantity because of its high heat resistance and mechanical properties.

Polyamide resin contains the amide coupling (-NHCO-) with hydrogen bonding capability in the molecular chain and is characterized by its regulation of mechanical properties and water absorption according to the concentration and hydrogen bonding state. High water absorption (Fig. 1) of nylon 66 is generally regarded as a shortcoming because it causes dimensional distortion or deterioration of rigidity. On the other hand, however, water absorption helps enhance flexibility and prevents cage damage during bearing assembly when a cage is required to have a substantial holding interference for the rolling elements. This also causes improvement is toughness which is effective for shock absorption during use. In this way, a so-called shortcoming may be considered as an advantage under certain conditions.

Nylon can be improved substantially in strength and heat resistance by adding a small amount of fiber. Therefore, materials reinforced by glass fiber may be used depending on the cage type and application. In view of maintaining deformation of the cage during assembly of bearings, it is common to use a relatively small amount of glass fiber to reinforce the cage. (Table 1)

Nylon 66 demonstrates vastly superior performance under mild operating conditions and has wide application possibilities as a mainstream plastic cage material. However, it often develops sudden deterioration under severe conditions (in high temperature oil, etc.). Therefore, due attention should be paid to this material during practical operation.

As an example, Table 2 shows the time necessary for the endurance performance of various nylon 66 materials to drop to 50% of the initial value under several different cases.

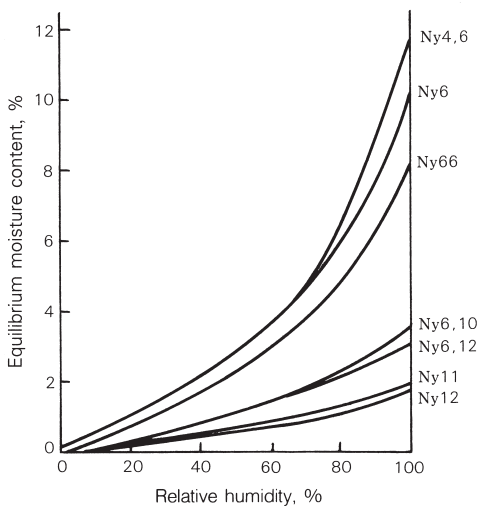

Fig. 1 Equilibrium moisture content and relative humidity of various nylons

Material deterioration in oil varies depending on the kind of oil. Deterioration is excessive if the oil contains an extreme-pressure agent. It is known that sulfurous extreme-pressure agents accelerate deterioration more than phosphorous extreme-pressure agents and such deterioration occurs more rapidly with rising temperatures.

On the other hand, material deteriorates less in grease or air than in oil. Besides, materials reinforced with glass fiber can suppress deterioration of the strength through material deterioration by means of the reinforcement effect of glass fibers, thereby, helping to extend the durability period.

Table 1 Examples of applications with fiber reinforced nylon cages

	Bearing type	Main aplication	Cage material
Ball bearing	Miniature ball bearings	VCR, IC cooling fans	Nylon 66 (Glass fiber content: 0 to 10%)
	Deep groove ball bearings	Alternators, fan motors for air conditioners	
	Angular contact ball bearings	Magnetic clutches, automotive wheels	
Roller bearing	Needle roller bearings	Automotive transmissions	Nylon 66 (Glass fiber content: 10 to 25%)
	Tapered roller bearings	Automotive wheels	
	ET-type cylindrical roller bearings	General	
	H-type spherical roller bearings	General	

Table 2 Environmental resistance of nylon 66 resin

Environment		Temperature, C	Glass content	Hours for the physical property value to drop to 50%, h (500, 1000, 1500, 2000)	Remarks
Oil	Gear oil	120	0 D		Contains an extreme pressure additive
		140	0 A D		
	Synthetic lubricating oil	100	A		Contains an extreme pressure additive
		120	A		
		130	0 A C		
		150	0 B D		
	Hydraulic oil	80	0 D		Contains an extreme pressure additive
		120	0 D		
		150	0 D		
	ATF oil	120	0 D		
		140	0 A D		
	Engine oil	120	0 D		
Grease		80	0 D		
		120	0 D		
		130	A D		
Air		160	0 A C		
		180	0 B		

Class content: A<B<C<D

10.9 Heat-resistant resin materials for cages

Currently, polyamide resin shows superior performance under medium operating environmental conditions. This feature plus its relative inexpensiveness lead to its use in increasing quantities. But, the material suffers from secular material deterioration or aging which creates a practical problem during continuous use at 120°C or more or under constant or intermittent contact with either oils (containing an extreme pressure agent) or acids.

Super-engineering plastics should be used for the cage materials of bearings running in severe environments such as high temperature over 150°C or corrosive chemicals. Though super-engineering plastics have good material properties like heat resistance, chemical resistance, rigidity at high temperature, mechanical strength, they have problems with characteristics required for the cage materials like toughness when molding or bearing assembling, weld strength, fatigue resistance. Also, the material cost is expensive. Table 1 shows the evaluation results of typical super-engineering plastics, which can be injection molded into cage shapes.

Among the materials in Table 1, though the branch type polyphenylene sulfide (PPS) is popularly used, the cage design is restricted since forced-removal from the die is difficult due to poor toughness and brittleness. Moreover, PPS is not always good as a cage material, since the claw, stay, ring, or flange of the cage is easily broken on the bearing assembling line. On the other hand, the heat resistant plastic cage developed by NSK, is made of linear-chain high molecules which have been polymerized from molecular chains. These molecular chains do not contain branch or crosslinking so they have high toughness compared to the former material (branch type PPS). Linear PPS is not only superior in heat resistance, oil resistance, and chemical resistance, but also has good mechanical characteristics such as snap fitting (an important characteristic for cages), and high temperature rigidity.

NSK has reduced the disadvantages associated with linear PPS: difficulty of removing from the die and slow crystallization speed, thereby establishing it as a material suitable for cages. Thus, linear PPS is thought to satisfy the required capabilities for a heat resistant cage material considering the relation between the cost and performance.

Classification	Polyether sulfone (PES)
Resin	Amorphous resin
Continuous temp	180℃
Physical properties	•Poor toughness (Pay attention to cage shape) •Low weld strength •Small fatigue resistance
Environmental properties	•Water absorption (Poor dimensional stability) •Good aging resistance •Poor stress cracking resistance
Material cost (Superiority)	3
Cage application	•Many performance problems •High material price

Table 1 Properties of typical super-engineering plastic materials for cages

Polyether imide (PEI)	Polyamide imide (PAI)	Polyether etherketon (PEEK)	Branch type polyphenylene sulfide (PPS)	Linear type polyphenylene sulfide (L-PPS)
Amorphous resin	Amorphous resin	Crystalline resin	Crystalline resin	Crystalline resin
170℃	210℃	240℃	220℃	220℃
•Poor toughness •Small weld strength •Small fatigue resistance	•Very brittle (No forced-removal molding) •Special heat treatment before use •High rigidity, after heat treatment	•Excellent toughness, wear and fatigue resistance •Small weld strength	•Excellent mechanical properties •Slightly low toughness	•Excellent mechanical properties •Good toughness •Good dimensional stability (No water absorption)
•Good aging resistance •Poor stress cracking resistance	•Good environment resistance	•Good environment resistance	•Good environment resistance	•Good environment resistance (Not affected by most chemicals. Doesn't deteriorate in high temperature oil with extreme pressure additives).
2	5	4	1	1
•Many performance problems •High material cost	•Good performance •High material and molding cost (For special applications)	•Excellent performance •High material cost (For special applications)	•Problems with toughness •Cost is high compared to its performance	•Reasonable cost for its performance (For general applications)

10.10 Features and operating temperature range of ball bearing seal material

The sealed ball bearing is a ball bearing with seals as shown in Figs. 1 and 2. There are two seal types: non-contact seal type and contact seal type. For rubber seal material, nitrile rubber is used for general purpose and poly-acrylic rubber, silicon rubber, and fluoric rubber are used depending on temperature conditions.

These rubbers have their own unique nature and appropriate rubber must be selected by considering the particular application environment and running conditions.

Table 1 shows principal features of each rubber material and the operating temperature range of the bearing seal. The operating temperature range of Table 1 is a guideline for continuous operation. Thermal aging of rubber is related to the temperature and time. Rubber may be used in a much wider range of operating temperatures depending on the operating time and frequency.

In the non-contact seal, heat generation due to friction on the lip can be ignored. And thermal factors, which cause aging of the rubber, are physical changes due to atmospheric and bearing temperatures. Accordingly, increased hardness or loss of elasticity due to thermal aging exerts only a negligible effect on the seal performance. A rubber non-contact seal can thus be used in an expanded range of operating temperatures greater than that for a contact seal.

But there are some disadvantages. The contact seal has a problem with wear occurring at the seal lip due to friction, thermal plastic deformation, and hardening. When friction or plastic deformation occurs, the contact pressure between the lip and slide surface decreases, resulting in a clearance. This clearance is minimum and does not cause excessive degradation of sealing performance (for instance, it does not allow dust entry or grease leakage). In most cases, this minor plastic deformation or slightly increased hardness presents no practical problems.

However, in external environments with dust and water in large quantity, the bearing seal is used as an auxiliary seal and a principal seal should be provided separately. As so far described, the operating temperature range of rubber material is only a guideline for selection. Since heat resistant rubber is expensive, it is important to understand the temperature conditions so that an economical selection can be made. Due attention should also be paid not only to heat resistance, but also to the distinctive features of each rubber.

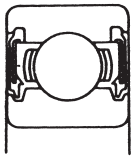

Non-contact rubber seal (VV)

Fig. 1

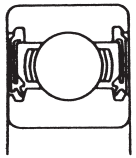

Contact rubber seal (DDU)

Fig. 2

Table 1 Features and operating temperature range of rubber materials

Material		Nitrile rubber	Polyacrylic rubber	Silicon rubber	Fluorine rubber
Key features		○Most popular seal material ○Superior in oil and wear resistances and mechanical properties ○Readily ages under direct sun-rays ○Less expensive than other rubbers	○Superior in heat and oil resistances ○Large compression causes permanent deformation ○Inferior in cold resistance ○One of the less expensive materials among the high temperature materials ○Attention is necessary because it swells the ester oil based grease	○High heat and cold resistances ○Inferior in mechanical properties other than permanent deformation by compression. Pay attention to tear strength ○Pay attention so as to avoid swell caused by low aniline point mineral oil, silicone grease, and silicone oil	○High heat resistance ○Superior in oil and chemical resistances ○Cold resistance similar to nitrile rubber ○Attention is necessary because it deteriorates the urea grease
Operating temperature range (1) (℃)	Non-contact seal	−50 to +130	−30 to +170	−100 to +250	−50 to +220
	Contact seal	−30 to +110	−15 to +150	−70 to +200	−30 to +200

Note (1) This operating temperature is the temperature of seal rubber materials.

11. Load calculation of gears

11.1 Calculation of loads on spur, helical, and double-helical gears

There is an extremely close relationship among the two mechanical elements, gears and rolling bearings. Gear units, which are widely used in machines, are almost always used with bearings. Rating life calculation and selection of bearings to be used in gear units are based on the load at the gear meshing point.

The load at the gear meshing point is calculated as follows:

Spur gear:

$$P_1=P_2=\frac{9\ 550\ 000H}{n_1\left(\frac{d_{p1}}{2}\right)}=\frac{9\ 550\ 000H}{n_2\left(\frac{d_{p2}}{2}\right)} \quad \cdots\cdots \text{(N)}$$

$$=\frac{974\ 000H}{n_1\left(\frac{d_{p1}}{2}\right)}=\frac{974\ 000H}{n_2\left(\frac{d_{p2}}{2}\right)} \quad \cdots\cdots \{\text{kgf}\}$$

$$S_1=S_2=P_1\tan\alpha$$

The magnitudes of the forces P_2 and S_2 applied to the driven gear are the same as P_1 and S_1 respectively, but the direction is opposite.

Helical gear:

$$P_1=P_2=\frac{9\ 550\ 000H}{n_1\left(\frac{d_{p1}}{2}\right)}=\frac{9\ 550\ 000H}{n_2\left(\frac{d_{p2}}{2}\right)} \quad \cdots\cdots \text{(N)}$$

$$=\frac{974\ 000H}{n_1\left(\frac{d_{p1}}{2}\right)}=\frac{974\ 000H}{n_2\left(\frac{d_{p2}}{2}\right)} \quad \cdots\cdots \{\text{kgf}\}$$

$$S_1=S_2=\frac{P_1\tan\alpha_n}{\cos\beta}$$

$$T_1=T_2=P_1\tan\beta$$

The magnitudes of the forces P_2, S_2, and T_2 applied to the driven gear are the same as P_1, S_1, and T_1 respectively, but the direction is opposite.

Double-helical gear:

$$P_1=P_2=\frac{9\ 550\ 000H}{n_1\left(\frac{d_{p1}}{2}\right)}=\frac{9\ 550\ 000H}{n_2\left(\frac{d_{p2}}{2}\right)} \quad \cdots\cdots \text{(N)}$$

$$=\frac{974\ 000H}{n_1\left(\frac{d_{p1}}{2}\right)}=\frac{974\ 000H}{n_2\left(\frac{d_{p2}}{2}\right)} \quad \cdots\cdots \{\text{kgf}\}$$

$$S_1=S_2=\frac{P_1\tan\alpha_n}{\cos\beta}$$

where, P: Tangential force (N), {kgf}
S: Separating force (N), {kgf}
T: Thrust (N), {kgf}
H: Transmitted power (kW)
n: Speed (min^{-1})
d_p: Pitch diameter (mm)
α: Gear pressure angle
α_n: Gear normal pressure angle
β: Twist angle
Subscript 1: Driving gear
Subscript 2: Driving gear

In the case of double-helical gears, thrust of the helical gears offsets each other and thus only tangential and separating forces act. For the directions of tangential, separating, and thrust forces, please refer to Figs. 1 and 2.

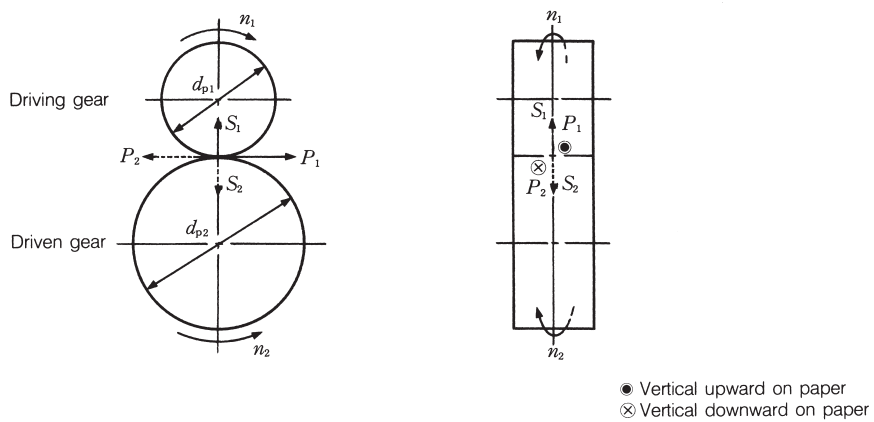

Fig. 1 Spur gear

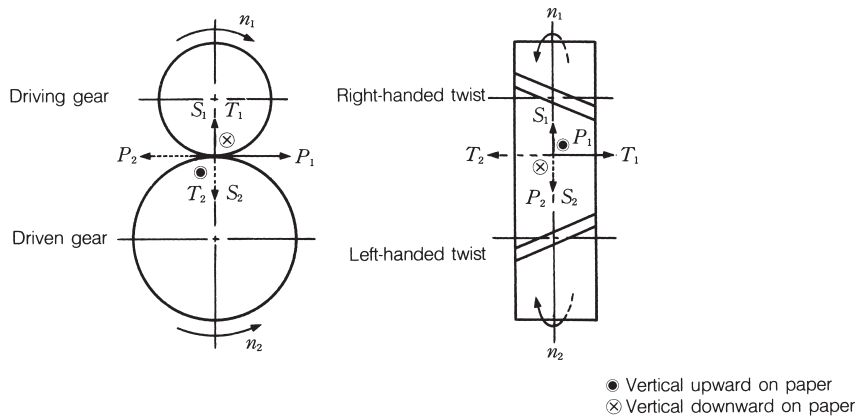

Fig. 2 Helical gear

The thrust direction of the helical gear varies depending on the gear running direction, gear twist direction, and whether the gear is driving or driven.
The directions are as follows:

The force on the bearing is determined as follows:

Tangential force:

$$P_1=P_2=\frac{9\ 550\ 000H}{n_1\left(\frac{d_{p1}}{2}\right)}=\frac{9\ 550\ 000H}{n_2\left(\frac{d_{p2}}{2}\right)} \quad \cdots\cdots \text{(N)}$$

$$=\frac{974\ 000H}{n_1\left(\frac{d_{p1}}{2}\right)}=\frac{974\ 000H}{n_2\left(\frac{d_{p2}}{2}\right)} \quad \cdots\cdots \{\text{kgf}\}$$

Separating force: $S_1=S_2=P_1\frac{\tan\alpha_n}{\cos\beta}$

Thrust: $T_1=T_2=P_1\cdot\tan\beta$

The same method can be applied to bearings C and D.

Table 1

Load classification		Bearing A	Bearing B
Radial load	From P_1	$P_A=\frac{b}{a+b}P_1$ ⊗	$P_B=\frac{a}{a+b}P_1$ ⊗
	From S_1	$S_A=\frac{b}{a+b}S_1$ ↑	$S_B=\frac{a}{a+b}S_1$ ↑
	From T_1	$U_A=\frac{d_{p1}/2}{a+b}T_1$ ↑	$U_B=\frac{d_{p1}/2}{a+b}T_1$ ↓
Combined radial load		$F_{rA}=\sqrt{P_A^2+(S_A+U_A)^2}$	$F_{rB}=\sqrt{P_B^2+(S_B-U_B)^2}$
Axial load		$F_a=T_1$ ←	

Load direction is shown referring to left side of Fig. 3.

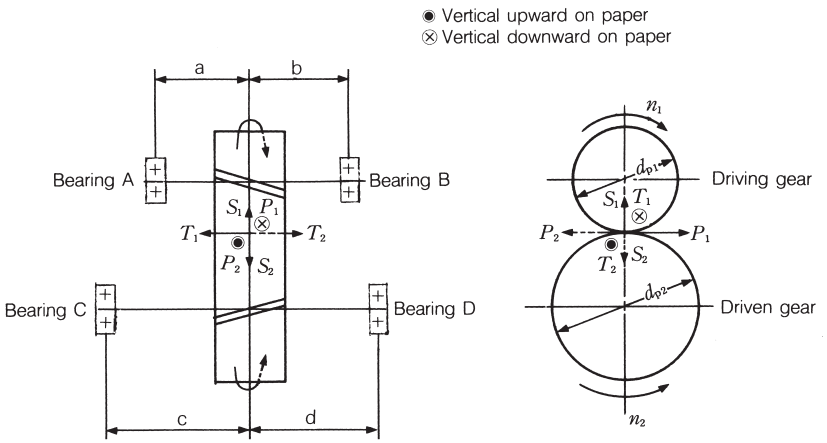

Fig. 3

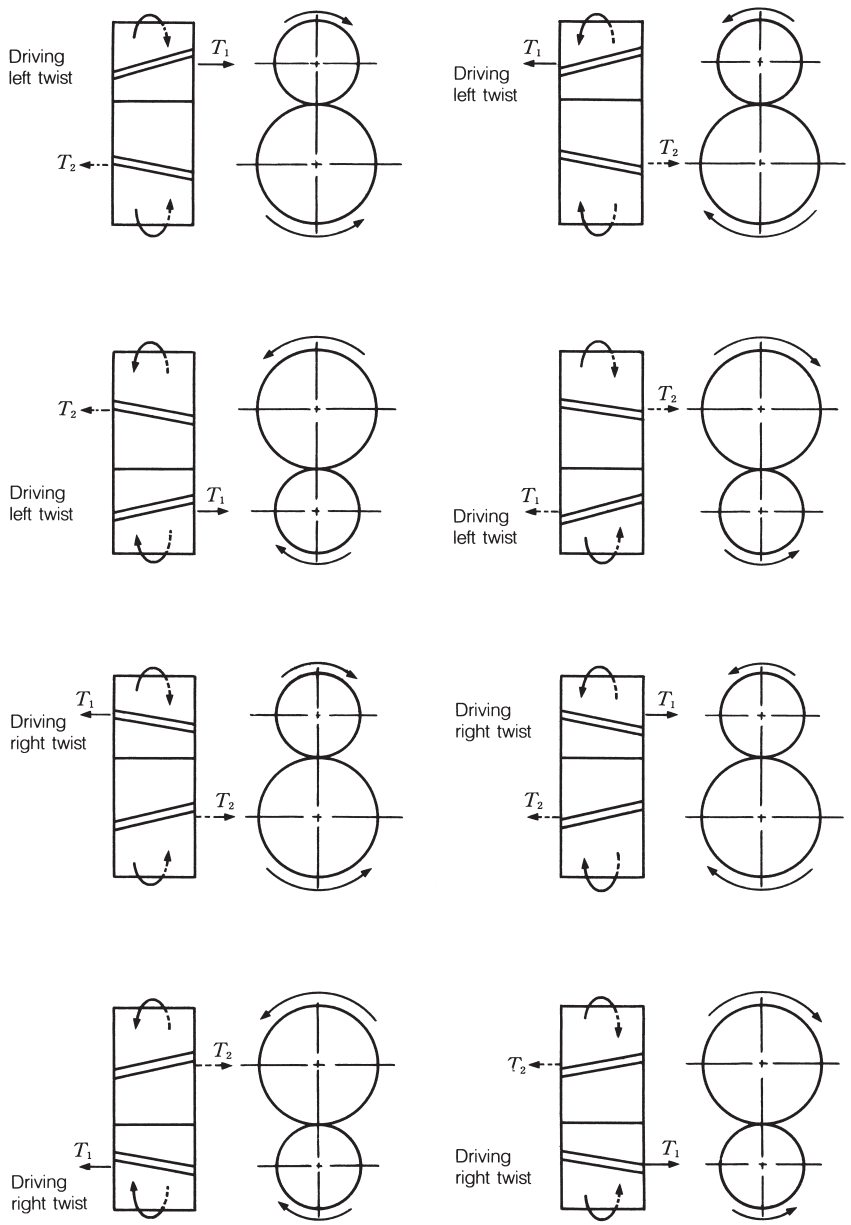

Fig. 4 Thrust direction

11.2 Calculation of load acting on straight bevel gears

The load at the meshing point of straight bevel gears is calculated as follows:

$$P_1=P_2=\frac{9\ 550\ 000H}{n_1\left(\frac{D_{m1}}{2}\right)}=\frac{9\ 550\ 000H}{n_2\left(\frac{D_{m2}}{2}\right)} \quad \cdots\cdots \text{(N)}$$

$$=\frac{974\ 000H}{n_1\left(\frac{D_{m1}}{2}\right)}=\frac{974\ 000H}{n_2\left(\frac{D_{m2}}{2}\right)} \quad \cdots\cdots \{\text{kgf}\}$$

$D_{m1}=d_{p1}-w\ \sin\delta_1$
$D_{m2}=d_{p2}-w\ \sin\delta_2$

$S_1=P_1\tan\alpha_n\ \cos\delta_1$
$S_2=P_2\tan\alpha_n\ \cos\delta_2$

$T_1=P_1\tan\alpha_n\ \cos\delta_1$
$T_2=P_2\tan\alpha_n\ \cos\delta_2$

where, D_m: Average pitch diameter (mm)
d_p: Pitch diameter (mm)
w: Gear width (pitch line length) (mm)
α_n: Gear normal pressure angle
δ: Pitch cone angle

Generally, $\delta_1+\delta_2=90°$. In this case, S_1 and T_2 (or S_2 and T_1) are the same in magnitude but opposite in direction. S/P and T/P for δ are shown in Fig. 3. The load on the bearing can be calculated as shown below.

Table 1

◉ Vertical upward on paper
⊗ Vertical downward on paper

Load classification		Bearing A	Bearing B	Bearing C	Bearing D
Radial load	From P	$P_A=\frac{b}{a}P_1$ ◉	$P_B=\frac{a+b}{a}P_1$ ⊗	$P_C=\frac{d}{c+d}P_2$ ◉	$P_D=\frac{c}{c+d}P_2$ ◉
	From S	$S_A=\frac{b}{a}S_1$ ↓	$S_B=\frac{a+b}{a}S_1$ ↑	$S_C=\frac{d}{c+d}S_2$ →	$S_D=\frac{c}{c+d}S_2$ →
	From T	$U_A=\frac{D_{m1}}{2\cdot a}T_1$ ↑	$U_B=\frac{D_{m1}}{2\cdot a}T_1$ ↓	$U_C=\frac{D_{m2}}{2(c+d)}T_2$ ←	$U_D=\frac{D_{m2}}{2(c+d)}T_2$ →
Combined radial load		$F_{rA}=\sqrt{P_A^2+(S_A-U_A)^2}$	$F_{rB}=\sqrt{P_B^2+(S_B-U_B)^2}$	$F_{rC}=\sqrt{P_C^2+(S_C-U_C)^2}$	$F_{rD}=\sqrt{P_D^2+(S_D+U_D)^2}$
Axial load		$F_a=T_1$ ←		$F_a=T_2$ ↓	

Load direction is shown referring to Fig. 2.

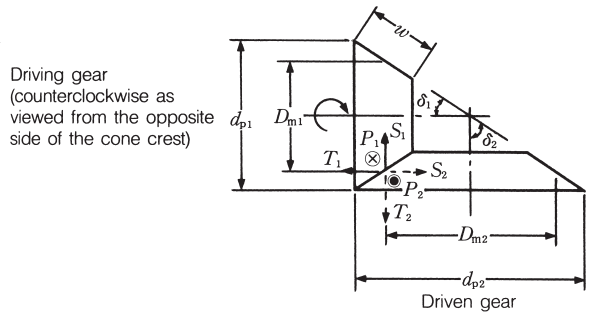

Fig. 1

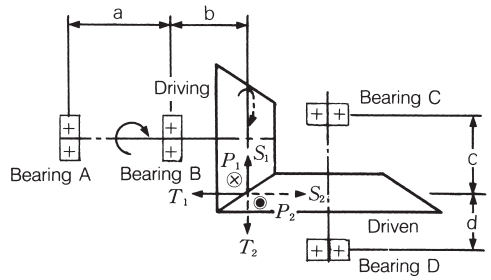

Fig. 2

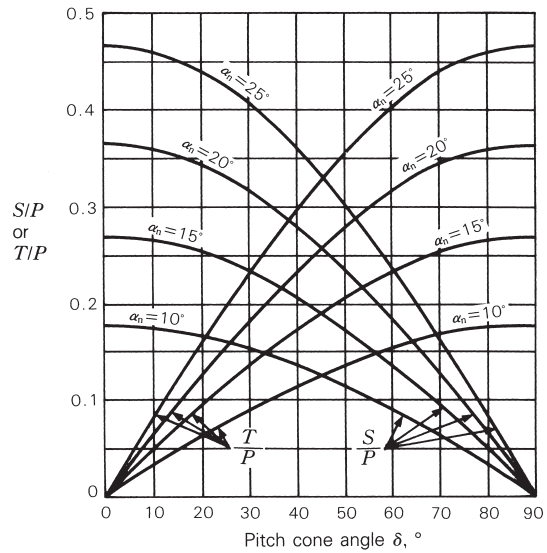

Fig. 3

11.3 Calculation of load on spiral bevel gears

In the case of spiral bevel gears, the magnitude and direction of loads at the meshing point vary depending on the running direction and gear twist direction. The running is either clockwise or counterclockwise as viewed from the side opposite of the gears (Fig. 1). The gear twist direction is classified as shown in Fig. 2. The force at the meshing point is calculated as follows:

$$P_1=P_2=\frac{9\ 550\ 000H}{n_1\left(\frac{D_{m1}}{2}\right)}=\frac{9\ 550\ 000H}{n_2\left(\frac{D_{m2}}{2}\right)} \quad \cdots\cdots \text{(N)}$$

$$=\frac{974\ 000H}{n_1\left(\frac{D_{m1}}{2}\right)}=\frac{974\ 000H}{n_2\left(\frac{D_{m2}}{2}\right)} \quad \cdots\cdots \{\text{kgf}\}$$

where, α_n: Gear normal pressure angle
β: Twisting angle
δ: Pitch cone angle
w: Gear width (mm)
D_m: Average pitch diameter (mm)
d_p: Pitch diameter (mm)

Note that the following applies:
$D_{m1}=d_{p1}-w\sin\delta_1$
$D_{m2}=d_{p2}-w\sin\delta_2$

The separating force S and T are as follows depending on the running direction and gear twist direction:

(1) Clockwise with right twisting or counterclockwise with left twisting

Driving gear
Separating force

$$S_1=\frac{P}{\cos\beta}(\tan\alpha_n\cos\delta_1+\sin\beta\sin\delta_1)$$

Thrust

$$T_1=\frac{P}{\cos\beta}(\tan\alpha_n\sin\delta_1-\sin\beta\cos\delta_1)$$

Driven gear
Separating force

$$S_2=\frac{P}{\cos\beta}(\tan\alpha_n\cos\delta_2-\sin\beta\sin\delta_2)$$

Thrust

$$T_2=\frac{P}{\cos\beta}(\tan\alpha_n\sin\delta_2+\sin\beta\cos\delta_2)$$

(2) Counterclockwise with right twist or clockwise with left twist

Driving gear
Separating force

$$S_1=\frac{P}{\cos\beta}(\tan\alpha_n\cos\delta_1-\sin\beta\sin\delta_1)$$

Thrust

$$T_1=\frac{P}{\cos\beta}(\tan\alpha_n\sin\delta_1+\sin\beta\cos\delta_1)$$

Driven gear
Separating force

$$S_2=\frac{P}{\cos\beta}(\tan\alpha_n\cos\delta_2+\sin\beta\sin\delta_2)$$

Thrust

$$T_2=\frac{P}{\cos\beta}(\tan\alpha_n\sin\delta_2-\sin\beta\cos\delta_2)$$

The positive (plus) calculation result means that the load is acting in a direction to separate the gears while a negative (minus) one means that the load is acting in a direction to bring the gears nearer.

Generally, $\delta_1+\delta_2=90°$. In this case, T_1 and S_2 (S_1 and T_2) are the same in magnitude but opposite in direction. The load on the bearing can be calculated by the same method as described in Section 11.2, "Calculation of load acting on straight bevel gears."

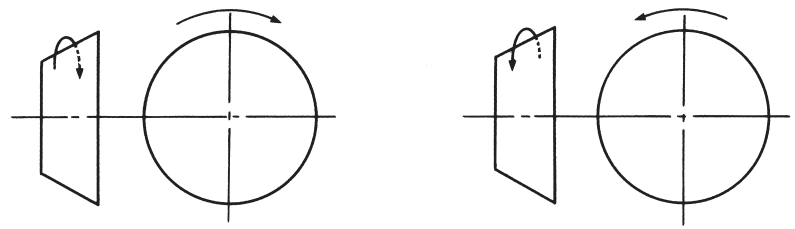

Fig. 1

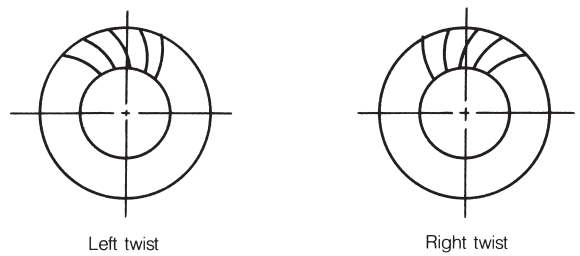

Fig. 2

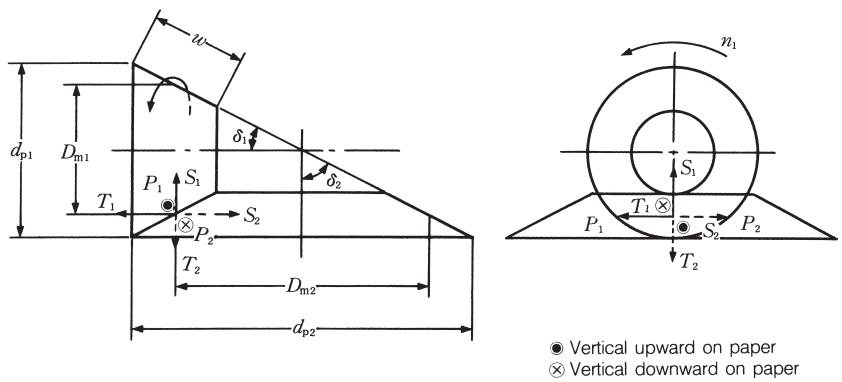

Fig. 3

11.4 Calculation of load acting on hypoid gears

The force acting at the meshing point of hypoid gears is calculated as follows:

$$P_1=\frac{9\ 550\ 000H}{n_1\left(\frac{D_{m1}}{2}\right)}=\frac{\cos\beta_1}{\cos\beta_2}P_2 \quad \cdots\cdots \text{(N)}$$

$$=\frac{974\ 000H}{n_1\left(\frac{D_{m1}}{2}\right)}=\frac{\cos\beta_1}{\cos\beta_2}P_2 \quad \cdots\cdots \text{\{kgf\}}$$

$$P_2=\frac{9\ 550\ 000H}{n_2\left(\frac{D_{m2}}{2}\right)} \quad \cdots\cdots \text{(N)}$$

$$=\frac{974\ 000H}{n_2\left(\frac{D_{m2}}{2}\right)} \quad \cdots\cdots \text{\{kgf\}}$$

$$D_{m1}=D_{m2}\frac{z_1}{z_2}\cdot\frac{\cos\beta_1}{\cos\beta_2}$$

$$D_{m2}=d_{p2}-w_2\sin\delta_2$$

where, α_n: Gear normal pressure angle
β: Twisting angle
δ: Pitch cone angle
w: Gear width (mm)
D_m: Average pitch diameter (mm)
d_p: Pitch diameter (mm)
z: Number of teeth

The separating force S and T are as follows depending on the running direction and gear twist direction:

(1) Clockwise with right twisting or counterclockwise with left twisting

Driving gear
Separating force

$$S_1=\frac{P_1}{\cos\beta_1}(\tan\alpha_n\cos\delta_1+\sin\beta_1\sin\delta_1)$$

Thrust

$$T_1=\frac{P_1}{\cos\beta_1}(\tan\alpha_n\sin\delta_1-\sin\beta_1\cos\delta_1)$$

Driven gear
Separating force

$$S_2=\frac{P_2}{\cos\beta_2}(\tan\alpha_n\cos\delta_2-\sin\beta_2\sin\delta_2)$$

Thrust

$$T_2=\frac{P_2}{\cos\beta_2}(\tan\alpha_n\sin\delta_2+\sin\beta_2\cos\delta_2)$$

(2) Counterclockwise with right twist or clockwise with left twist

Driving gear
Separating force

$$S_1=\frac{P_1}{\cos\beta_1}(\tan\alpha_n\cos\delta_1-\sin\beta_1\sin\delta_1)$$

Thrust

$$T_1=\frac{P_1}{\cos\beta_1}(\tan\alpha_n\sin\delta_1+\sin\beta_1\cos\delta_1)$$

Driven gear
Separating force

$$S_2=\frac{P_2}{\cos\beta_2}(\tan\alpha_n\cos\delta_2+\sin\beta_2\sin\delta_2)$$

Thrust

$$T_2=\frac{P_2}{\cos\beta_2}(\tan\alpha_n\sin\delta_2-\sin\beta_2\cos\delta_2)$$

The positive (plus) calculation result means that the load is acting in a direction to separate the gears while a negative (minus) one means that the load is acting in a direction to bring the gears nearer.

For the running direction and gear twist direction, refer to Section 11.3, “Calculation of load on spiral bevel gears.” The load on the bearing can be calculated by the same method as described in Section 11.2, “Calculation of load acting on straight bevel gears.”

The next calculation diagram is used to determine the approximate value and direction of separating force S and thrust T.

[How To Use]
The method of determining the separating force S is shown. The thrust T can also be determined in a similar manner.

1. Take the gear normal pressure angle α_n from the vertical scale on the left side of the diagram.
2. Determine the intersection between the pitch cone angle δ and the twist angle β. Determine one point which is either above or below the β=0 line according to the rotating direction and gear twist direction.
3. Draw a line connecting the two points and read the point at which the line cuts through the right vertical scale. This reading gives the ratio (S/P, %) of the separating force S to the tangential force P in percentage.

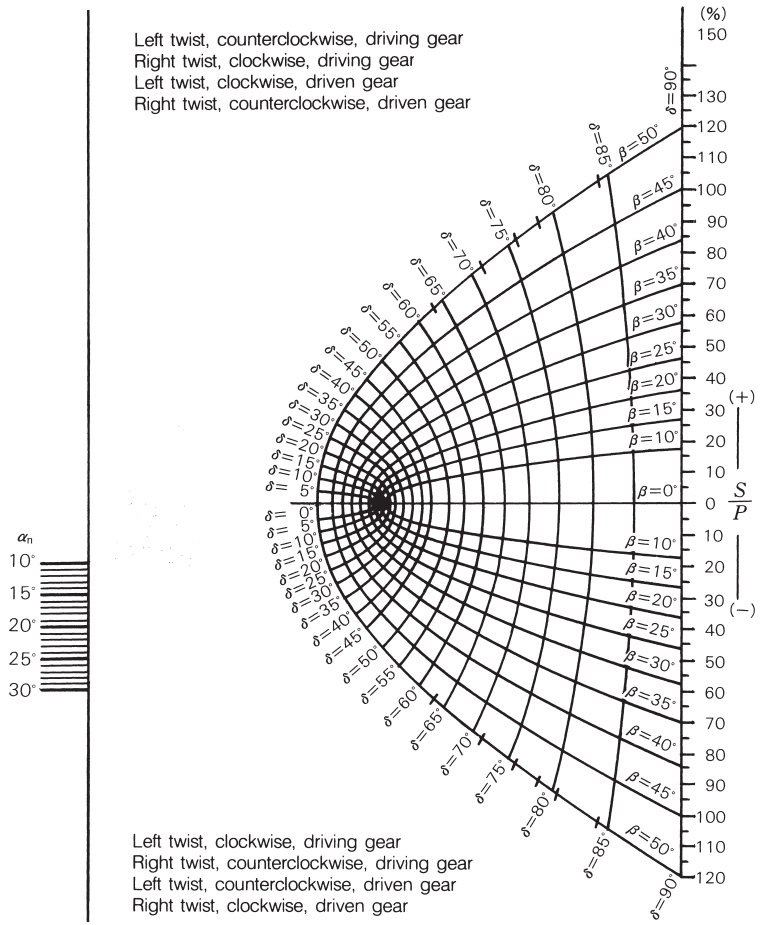

Calculation diagram of separating force S

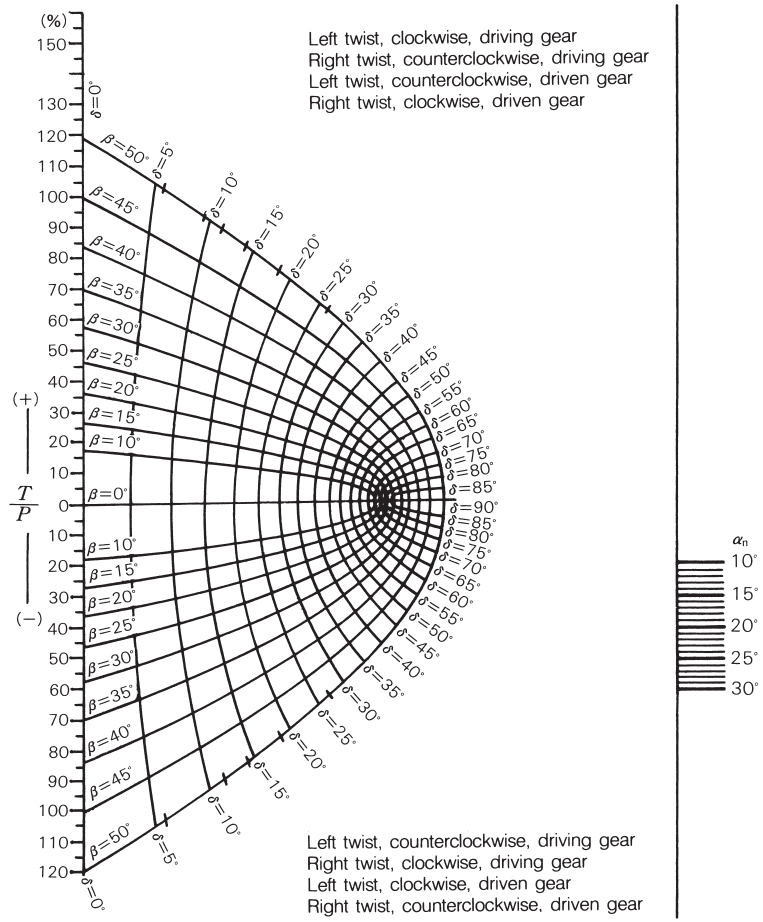

Calculation diagram of thrust T

11.5 Calculation of load on worm gear

A worm gear is a kind of spigot gear, which can produce a high reduction ratio with small volume. The load at a meshing point of worm gears is calculated as shown in **Table 1**. Symbols of **Table 1** are as follows:

i: Gear ratio $\left(i=\dfrac{Z_2}{Z_w}\right)$

η: Worm gear efficiency $\left[\eta=\dfrac{\tan\gamma}{\tan(\gamma+\psi)}\right]$

γ: Advance angle $\left(\gamma=\tan^{1}\dfrac{d_{p2}}{id_{p1}}\right)$

ψ: For the frictional angle, the value obtained from $V_R=\dfrac{\pi d_{p1}n_1}{\cos\gamma}\times\dfrac{10^{-3}}{60}$ as shown in **Fig. 1** is used.

When V_R is 0.2 m/s or less, then use ψ=8°.
When V_R exceeds 6 m/s, use ψ=1°4′.

α_n: Gear normal pressure angle
α_a: Shaft plane pressure angle
Z_w: No. of threads (No. of teeth of worm gear)
Z_2: No. of teeth of worm wheel
Subscript 1: For driving worm gear
Subscript 2: For driving worm gear

In a worm gear, there are four combinations of interaction at the meshing point as shown below depending on the twist directions and rotating directions of the worm gear.

The load on the bearing is obtained from the magnitude and direction of each component at the meshing point of the worm gears according to the method shown in **Table 1** of Section **11.1**, Calculation of loads on spur, helical, and double-helical gears.

Table 1

Force	Worm	Worm wheel
Tangential P	$\dfrac{9\,550\,000H}{n_1\left(\dfrac{d_{p1}}{2}\right)}$ ……(N) $\dfrac{974\,000H}{n_1\left(\dfrac{d_{p1}}{2}\right)}$ ……{kgf}	$\dfrac{9\,550\,000Hi\eta}{n_1\left(\dfrac{d_{p2}}{2}\right)}=\dfrac{P_1\,\eta}{\tan\gamma}=\dfrac{P_1}{\tan(\gamma+\psi)}$ ……(N) $\dfrac{974\,000Hi\eta}{n_1\left(\dfrac{d_{p2}}{2}\right)}=\dfrac{P_1\,\eta}{\tan\gamma}=\dfrac{P_1}{\tan(\gamma+\psi)}$ ……{kgf}
Thrust T	$\dfrac{9\,550\,000H\eta}{n_1\left(\dfrac{d_{p2}}{2}\right)}=\dfrac{P_1\,\eta}{\tan\gamma}=\dfrac{P_1}{\tan(\gamma+\psi)}$ ……(N) $\dfrac{974\,000H\eta}{n_1\left(\dfrac{d_{p2}}{2}\right)}=\dfrac{P_1\,\eta}{\tan\gamma}=\dfrac{P_1}{\tan(\gamma+\psi)}$ ……{kgf}	$\dfrac{9\,550\,000H}{n_1\left(\dfrac{d_{p1}}{2}\right)}$ ……(N) $\dfrac{974\,000H}{n_1\left(\dfrac{d_{p1}}{2}\right)}$ ……{kgf}
Separating S	$\dfrac{P_1\tan\alpha_n}{\sin(\gamma+\psi)}=\dfrac{P_1\tan\alpha_a}{\tan(\gamma+\psi)}$ ……(N), {kgf}	$\dfrac{P_1\tan\alpha_n}{\sin(\gamma+\psi)}=\dfrac{P_1\tan\alpha_a}{\tan(\gamma+\psi)}$ ……(N), {kgf}

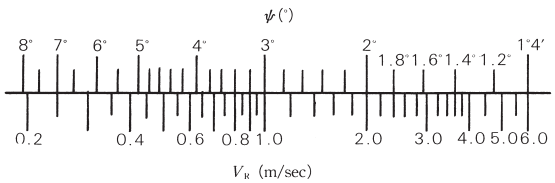

Fig. 1

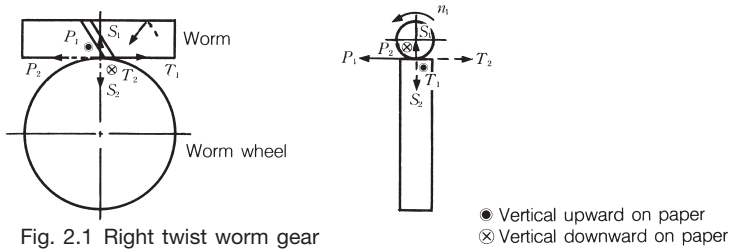

Fig. 2.1 Right twist worm gear

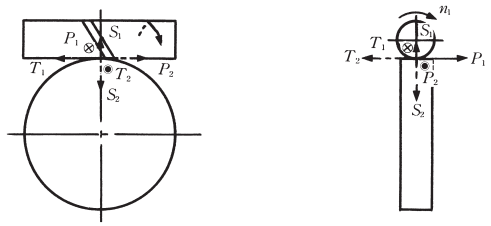

Fig. 2.2 Right twist worm gear (Worm rotation is opposite that of Fig. 2.1)

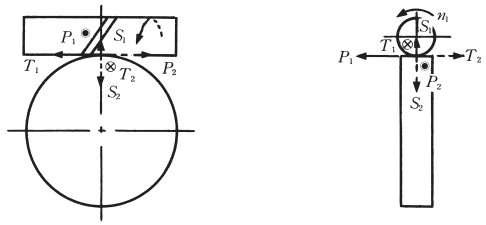

Fig. 2.3 Left twist worm gear

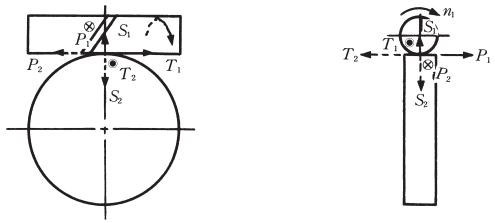

Fig. 2.4 Left twist worm gear (Worm rotation is opposite that of Fig. 2.3)

12. General miscellaneous information

12.1 JIS concerning rolling bearings

Rolling bearings are critical mechanical elements which are used in a wide variety of machines. They are standardized internationally by ISO (International Organization for Standardization). Standards concerning rolling bearings can also be found in DIN (Germany), ANSI (USA), and BS (England). In Japan, the conventional JIS standards related to rolling bearings are arranged systematically and revised in accordance to the JIS standards enacted in 1965. Since then, these have been individually revised in reference to the ISO standards or compliance with the actual state of production and sales.

Most of the standard bearings manufactured in Japan are based on the JIS standards. BAS (Japan Bearing Association Standards), on the other hand, acts as a supplement to JIS. Table 1 lists JIS standards related to bearings.

Table 1 JIS related to rolling bearing

No.	Standard classification	Standard No.	Title of Standard
1	General code	B 1511	Rolling bearings — General code
2	Common standards of bearings	B 0005	Technical drawings — Rolling bearings — Part 1: General simplified representation — Part 2: Detailed simplified representation
3		B 0104	Rolling bearings — Vocabulary
4		B 0124	Rolling bearings — Symbols for quantities
5		B 1512	Rolling bearings — Boundary dimensions
6		B 1513	Rolling bearings — Designation
7		B 1514	Rolling bearings — Tolerances of bearings — Part 1: Radial bearings — Part 2: Thrust bearings — Part 3: Chamfer dimensions-Maximum values
8		B 1515	Rolling bearings — Tolerances — Part 1: Terms and definitions — Part 2: Measuring and gauging principles and methods
9		B 1516	Making on rolling bearings and packagings
10		B 1517	Packaging of rolling bearings
11		B 1518	Dynamic load ratings and rating life for rolling bearings
12		B 1519	Static load ratings for rolling bearings
13		B 1520	Rolling bearings — Radial internal clearance
14		B 1548	Rolling bearings — Measuring methods of A-weighted sound pressure levels
15		B 1566	Mounting dimensions and fits for rolling bearings
16		G 4805	High carbon chromium bearing steels
17	Individual standards of bearings	B 1521	Rolling bearings — Deep groove ball bearings
18		B 1522	Rolling bearings — Angular contact ball bearings
19		B 1523	Rolling bearings — Self-aligning ball bearings
20		B 1532	Rolling bearings — Thrust ball bearings with flat back faces
21		B 1533	Rolling bearings — Cylindrical roller bearings
22		B 1534	Rolling bearings — Tapered roller bearings
23		B 1535	Rolling bearings — Self-aligning roller bearings
24		B 1536	Rolling bearings-Boundary dimensions and tolerances of needle roller bearings — Part 1: Dimension series 48, 49 and 69 — Part 2: Drawn cup without inner ring — Part 3: Radial needle roller and cage assemblies — Part 4: Thrust needle roller and cage assemblies, thrust washers — Part 5: Track rollers
25		B 1539	Rolling bearings — Self-aligning thrust roller bearings
26		B 1557	Rolling bearings — Insert bearing units
27		B 1558	Rolling bearings — Insert bearings
28	Standards of bearing parts	B 1501	Steel balls for ball bearings
29		B 1506	Rolling bearings — Rollers
30		B 1509	Rolling bearings — Radial bearings with locating snap ring — Dimensions and tolerances
31	Standards of bearing accessorie	B 1551	Rolling bearing accessories — Plummer block housings
32		B 1552	Rolling bearings — Adapter assemblies, Adapter sleeves and Withdrawal sleeves
33		B 1554	Rolling bearings — Locknuts and locking devices
34		B 1559	Rolling bearings — Cast and pressed housings for insert bearings
35	Reference standard	K 2220	Lubricating grease

12.2 Amount of permanent deformation at point where inner and outer rings contact rolling element

When two materials are in contact, a point within the contact zone develops local permanent deformation if it is exposed to a load exceeding the elastic limit of the material. The rolling and raceway surfaces of a bearing, which appear to be perfect to a human eye, are found to be imperfect when observed by microscope even though the surfaces are extremely hard and finished to an extreme accuracy. Therefore, the true contact area is surprisingly small when compared with the apparent contact area, because the surface is actually jagged and rough with asperities or sharp points. These local points develop permanent deformation when exposed to a relatively small load. Such microscopic permanent deformations seldom affect the function of the bearing. Usually, the only major change is that light is reflected differently from the raceway surface (running marks, etc.).

As the load grows further, the amount of permanent deformation increases corresponding to the degree identifiable on the macroscopic scale in the final stage. Fig. 1 shows the manner of this change. While the load is small, the elastic displacement during point contact in a ball bearing is proportional to the p-th power of the load Q (p=2/3 for ball bearings and p=0.9 for roller bearings) in compliance with the Hertz theory. The amount of permanent deformation grows as the load increases, resulting in substantial deviation of the elastic displacement from the theoretical value.

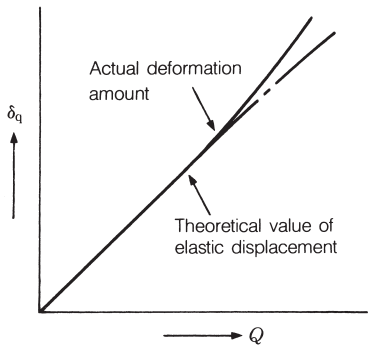

Fig. 1

For normal bearings, about 1/3 of the gross amount of permanent deformation δ_q occurs in rolling element and about 2/3 in the bearing ring.

12.2.1 Ball bearings

The amount of permanent deformation δ_q can also be expressed in relation to the load Q. Equation (1) shows the relationship between δ_q and Q for ball bearings:

$$\delta_q = 1.30\times10^{-7}\frac{Q^2}{D_w}(\rho_{I1}+\rho_{II1})\ (\rho_{I2}+\rho_{II2}) \quad \cdots\cdots (N)$$

$$= 1.25\times10^{-5}\frac{Q^2}{D_w}(\rho_{I1}+\rho_{II1})\ (\rho_{I2}+\rho_{II2}) \quad \cdots\cdots \{kgf\}$$

$$(mm) \quad \cdots\cdots (1)$$

where, δ_q: Gross amount of permanent deformation between the rolling element and bearing ring (mm)
Q: Load of rolling element (N), {kgf}
D_w: Diameter of rolling element (mm)
ρ_{I1}, ρ_{I2} and ρ_{II1}, ρ_{II2}: Take the reciprocal of the main radius of curvature of the area where materials I and II make contact (Units: 1/mm).

When the equation is rewritten using the relation between δ_q and Q, Equation (2) is obtained:

$$\left.\begin{aligned}\delta_q &= K\cdot Q^2 \quad (N)\\ &= 96.2K\cdot Q^2 \quad \{kgf\}\end{aligned}\right\}\ (mm) \quad \cdots\cdots (2)$$

The value of the constant K is as shown for the bearing series and bore number in Table 1. K_i applies to the contact between the inner ring and rolling element while K_e to that between the outer ring and rolling element.

Table 1 Value of the constant K for deep groove ball bearings

Bearing bore No.	Bearing series 60		Bearing series 62		Bearing series 63	
	K_i	K_e	K_i	K_e	K_i	K_e
	$\times10^{-10}$	$\times10^{-10}$	$\times10^{-10}$	$\times10^{-10}$	$\times10^{-10}$	$\times10^{-10}$
00	2.10	4.12	2.01	2.16	0.220	0.808
01	2.03	1.25	0.376	1.13	0.157	0.449
02	1.94	2.21	0.358	1.16	0.145	0.469
03	1.89	2.24	0.236	0.792	0.107	0.353
04	0.279	0.975	0.139	0.481	0.0808	0.226
05	0.270	0.997	0.133	0.494	0.0597	0.218
06	0.180	0.703	0.0747	0.237	0.0379	0.119
07	0.127	0.511	0.0460	0.178	0.0255	0.0968
08	0.417	0.311	0.129	0.0864	0.0206	0.0692
09	0.312	0.234	0.127	0.0875	0.0436	0.0270
10	0.308	0.236	0.104	0.0720	0.0333	0.0207
11	0.187	0.140	0.0728	0.0501	0.0262	0.0162
12	0.185	0.141	0.0547	0.0377	0.0208	0.0218
13	0.183	0.142	0.0469	0.0326	0.0169	0.0105
14	0.119	0.0914	0.0407	0.0283	0.0138	0.00863
15	0.118	0.0920	0.0402	0.0286	0.0117	0.00733
16	0.0814	0.0624	0.0309	0.0218	0.00982	0.00616
17	0.0808	0.0628	0.0243	0.0170	0.00832	0.00523
18	0.0581	0.0446	0.0194	0.0136	0.00710	0.00447
19	0.0576	0.0449	0.0158	0.0110	0.00611	0.00386
20	0.0574	0.0450	0.0130	0.00900	0.00465	0.00292
22	0.0296	0.0225	0.00928	0.00639	0.00326	0.00203
24	0.0293	0.0227	0.00783	0.00544	0.00320	0.00205
26	0.0229	0.0178	0.00666	0.00467	0.00255	0.00164
28	0.0227	0.0179	0.00656	0.00472	0.00209	0.00134
30	0.0181	0.0143	0.00647	0.00477	0.00205	0.00136

As an example, the δ_q and Q relation may be illustrated as shown in **Fig. 2** for the 62 series of deep groove ball bearings.

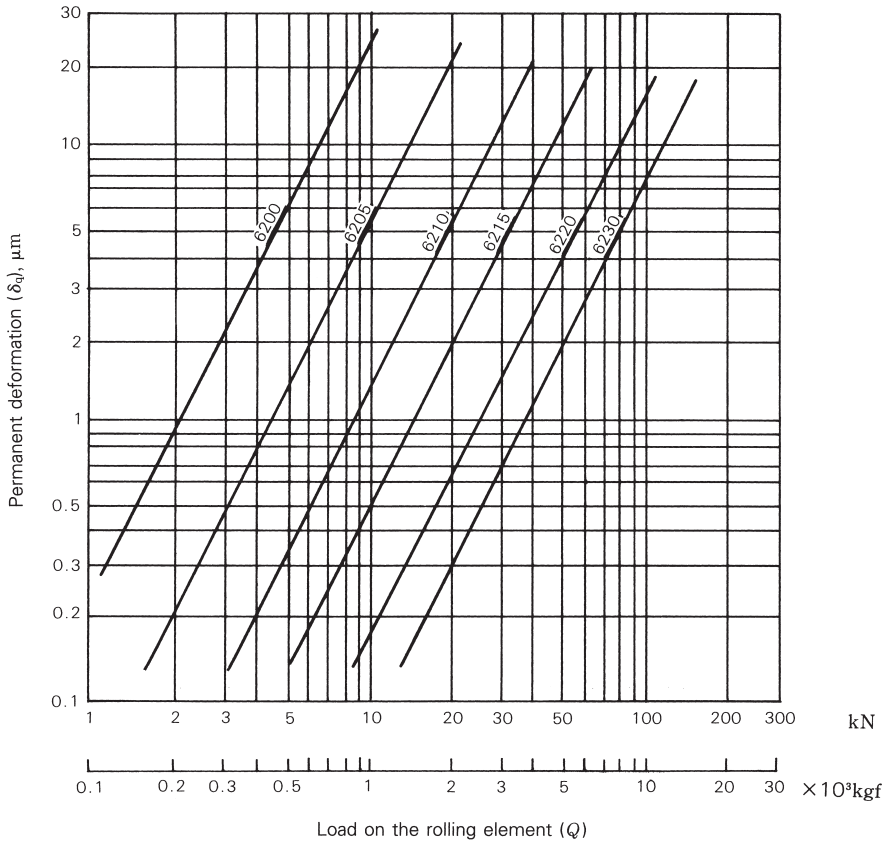

Fig. 2 Load and permanent deformation of rolling element

12.2.2 Roller bearings

In the case of roller bearings, the permanent deformation δ_q and load Q between the rolling element and bearing ring may be related as shown in **Equation (3)**.

$$\left.\begin{aligned}\delta_q &= 2.12\times10^{-11}\cdot\frac{1}{\sqrt{D_w}}\cdot\left(\frac{Q}{L_{we}}\right)^3\cdot(\rho_I+\rho_{II})^{3/2} \quad \cdots\cdots\cdots\cdots (\mathrm{N})\\ &= 2.00\times10^{-8}\cdot\frac{1}{\sqrt{D_w}}\cdot\left(\frac{Q}{L_{we}}\right)^3\cdot(\rho_I+\rho_{II})^{3/2} \quad \cdots\cdots\cdots\cdots \{\mathrm{kgf}\}\end{aligned}\right\}$$

$$(\mathrm{mm}) \quad \cdots\cdots\cdots\cdots (3)$$

where, L_{we}: Effective length of roller (mm)

ρ_I, ρ_{II}: Reciprocal of the main radius of curvature at the point where materials I and II contact (1/mm)

Other symbols for quantities are the same as in **Equation (1)** of **12.2.1**. When the equation is rewritten using the relation between δ_q and Q, then the next **Equation (4)** is obtained:

$$\left.\begin{aligned}\delta_q &= K\cdot Q^3 \quad (\mathrm{N})\\ &= 943K\cdot Q^2 \quad \{\mathrm{kgf}\}\end{aligned}\right\} (\mathrm{mm}) \quad \cdots\cdots\cdots\cdots (4)$$

The value of the constant K is as shown for the bearing number in **Table 2**. K_i applies to the contact between the inner ring and rolling element while K_e to that between the outer ring and rolling element.

As an example, the δ_q and Q relation may be illustrated as shown in **Fig. 3** for the NU2 series of cylindrical roller bearings.

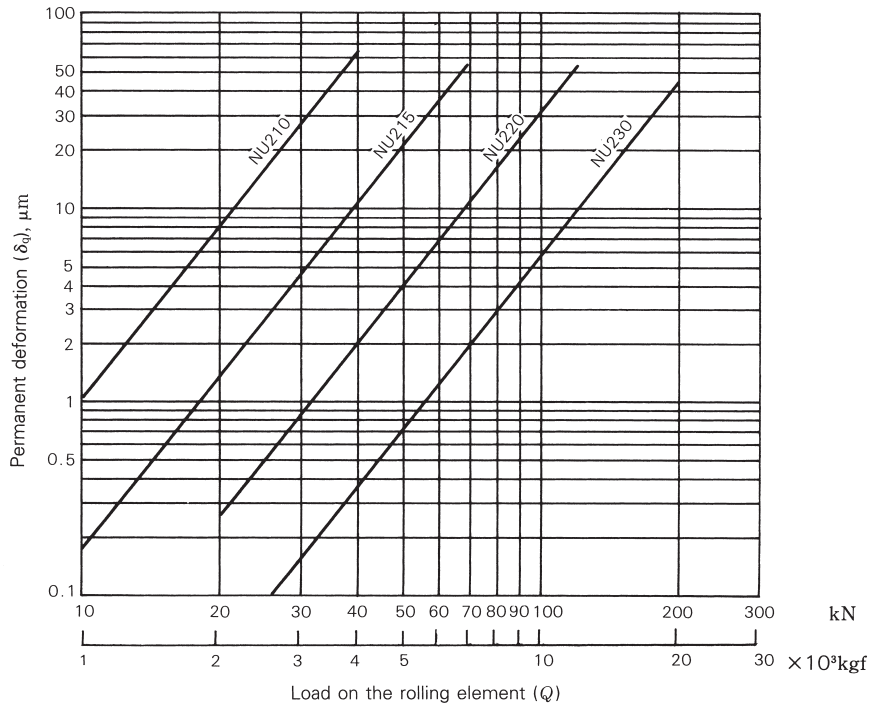

Fig. 3 Load and permanent deformation of rolling element

Table 2 Value of the constant K for cylindrical roller bearings

Bearing series NU2			Bearing series NU3		
Brg No.	K_i	K_e	Brg No.	K_i	K_e
	$\times 10^{-16}$	$\times 10^{-16}$		$\times 10^{-16}$	$\times 10^{-16}$
NU205W	113	67.5	NU305W	20.4	10.9
NU206W	50.7	30.9	NU306W	11.3	6.32
NU207W	19.1	11.4	NU307W	6.83	3.81
NU208W	10.8	6.53	NU308W	4.24	2.43
NU209W	10.6	6.64	NU309W	1.92	1.07
NU210W	10.4	6.74	NU310W	1.51	0.856
NU211W	6.23	4.06	NU311W	0.786	0.435
NU212W	3.93	2.57	NU312W	0.575	0.323
NU213W	2.58	1.69	NU313W	0.460	0.262
NU214W	2.54	1.70	NU314W	0.347	0.200
NU215W	1.74	1.15	NU315W	0.211	0.120
NU216W	1.38	0.915	NU316W	0.207	0.121
NU217W	0.976	0.648	NU317W	0.132	0.0761
NU218W	0.530	0.343	NU318W	0.112	0.0650
NU219W	0.426	0.277	NU319W	0.0903	0.0529
NU220W	0.324	0.210	NU320W	0.0611	0.0357
NU221W	0.249	0.162	NU321W	0.0428	0.0247
NU222W	0.156	0.0995	NU322W	0.0325	0.0187
NU224W	0.123	0.0800	NU324W	0.0176	0.00992
NU226W	0.121	0.0810	NU326W	0.0132	0.00750
NU228W	0.0836	0.0559	NU328W	0.0100	0.00576
NU230W	0.0565	0.0378	NU330W	0.00832	0.00484

Bearing series NU4		
Brg No.	K_i	K_e
	$\times 10^{-16}$	$\times 10^{-16}$
NU405W	4.69	2.28
NU406W	2.09	1.01
NU407W	1.61	0.821
NU408W	0.835	0.418
NU409W	0.607	0.312
NU410W	0.373	0.191
NU411W	0.363	0.194
NU412W	0.220	0.116
NU413W	0.173	0.0926
NU414W	0.0954	0.0509
NU415W	0.0651	0.0342
NU416W	0.0455	0.0237
NU417M	0.0349	0.0178
NU418M	0.0251	0.0130
NU419M	0.0245	0.0132
NU420M	0.0182	0.00972
NU421M	0.0137	0.00729
NU422M	0.0104	0.00559
NU424M	0.00611	0.00323
NU426M	0.00353	0.00185
NU428M	0.00303	0.00161
NU430M	0.00296	0.00163

12.3 Rotation and revolution speed of rolling element

When the rolling element rotates without slip between bearing rings, the distance which the rolling element rolls on the inner ring raceway is equal to that on the outer ring raceway. This fact allows establishment of a relationship among rolling speed n_i and n_e of the inner and outer rings and the number of rotation n_a of rolling elements.

The revolution speed of the rolling element can be determined as the arithmetic mean of the circumferential speed on the inner ring raceway and that on the outer ring raceway (generally with either the inner or outer ring being stationary). The rotation and revolution of the rolling element can be related as expressed by Equations (1) through (4).

No. of rotation

$$n_a=\left(\frac{D_{pw}}{D_w}-\frac{D_w\cos^2\alpha}{D_{pw}}\right)\frac{n_e-n_i}{2}$$

(min^{-1}) ..... (1)

Rotational circumferential speed

$$v_a=\frac{\pi D_w}{60\times10^3}\left(\frac{D_{pw}}{D_w}-\frac{D_w\cos^2\alpha}{D_{pw}}\right)\frac{n_e-n_i}{2}$$

(m/s) ..... (2)

No. of revolutions (No. of cage rotation)

$$n_c=\left(1-\frac{D_w\cos\alpha}{D_{pw}}\right)\frac{n_i}{2}+\left(1+\frac{D_w\cos\alpha}{D_{pw}}\right)\frac{n_e}{2}$$

(min^{-1}) ..... (3)

Revolutional circumferential speed
(cage speed at rolling element pitch diameter)

$$v_c=\frac{\pi D_{pw}}{60\times10^3}\left[\left(1-\frac{D_w\cos\alpha}{D_{pw}}\right)\frac{n_i}{2}+\left(1+\frac{D_w\cos\alpha}{D_{pw}}\right)\frac{n_e}{2}\right]$$

(m/s) ..... (4)

where, D_{pw}: Pitch diameter of rolling elements (mm)
D_w: Diameter of rolling element (mm)
α: Contact angle (°)
n_e: Outer ring speed (min^{-1})
n_i: Inner ring speed (min^{-1})

The rotation and revolution of the rolling element is shown in Table 1 for inner ring rotating (n_e=0) and outer ring rotating (n_i=0) respectively at $0°\leqq\alpha<90°$ and at α=90°.

As an example, Table 2 shows the rotation speed n_a and revolution speed n_c of the rolling element during rotating of the inner ring of ball bearings 6210 and 6310.

Contact angle	Rotation/revolution speed
$0°\leqq\alpha<90°$	n_a (min^{-1})
	v_a (m/s)
	n_c (min^{-1})
	v_c (m/s)
$\alpha=90°$	n_a (min^{-1})
	v_a (m/s)
	n_c (min^{-1})
	v_c (m/s)

Table 2 n_a and n_c for ball bearings 6210 and 6310

Ball bearing	γ	n_a	n_c
6210	0.181	$-2.67n_i$	$0.41n_i$
6310	0.232	$-2.04n_i$	$0.38n_i$

Remarks $\gamma=\frac{D_w\cos\alpha}{D_{pw}}$

Table 1 Rolling element's rotation speed n_a, rotational circumferential speed v_a, revolution speed n_c, and revolutional circumferential speed v_c

	Inner ring rolling (n_e=0)	Outer ring rolling (n_i=0)
	$-\left(\frac{1}{\gamma}-\gamma\right)\frac{n_i}{2}\cdot\cos\alpha$	$\left(\frac{1}{\gamma}-\gamma\right)\frac{n_e}{2}\cdot\cos\alpha$
	$\frac{\pi D_w}{60\times10^3}n_a$	
	$(1-\gamma)\frac{n_i}{2}$	$(1+\gamma)\frac{n_e}{2}$
	$\frac{\pi D_{pw}}{60\times10^3}n_c$	
	$-\frac{1}{\gamma}\cdot\frac{n_i}{2}$	$\frac{1}{\gamma}\cdot\frac{n_e}{2}$
	$\frac{\pi D_w}{60\times10^3}n_a$	
	$\frac{n_i}{2}$	$\frac{n_e}{2}$
	$\frac{\pi D_{pw}}{60\times10^3}n_C$	

Reference 1. ±: The "+" symbol indicates clockwise rotation while the "−" symbol indicates counterclockwise rotation.
2. $\gamma=\frac{D_w\cos\alpha}{D_{pw}}$ $(0°\leqq\alpha<90°)$, $\gamma=\frac{D_w}{D_{pw}}(\alpha=90°)$

12.4 Bearing speed and cage slip speed

One of the features of a rolling bearing is that its friction is smaller than that of a slide bearing. This may be attributed to the fact that rolling friction is smaller than slip friction. However, even a rolling bearing inevitably develops some slip friction.

Slip friction occurs mainly between the cage and rolling element, on the guide surface of the cage, between the rolling element and raceway surface (slip caused by the elastic displacement), and between the collar and roller end surface in the roller bearing.

The most critical factor for a high speed bearing is the slip friction between the cage and rolling element and that on the guide surface of the cage. The allowable speed of a bearing may finally be governed by this slip friction. The PV value may be used as a parameter to indicate the speed limit in the slide bearing and can also be applied to the slip portion of the rolling bearing. "P" is the contact pressure between the rolling element and cage or that between the guide surface of the cage. "P" is not much affected by the load on the bearing in the normal operation state. "V" is a slip speed.

Accordingly, the speed limit of a rolling bearing can be expressed nearly completely by the slip speed, that is, the bearing size and speed.

Conventionally, the $D_{pw}\times n$ value ($d_m n$ value) has often been used as a guideline to indicate the allowable speed of a bearing. But this is nothing but the slip speed inside the bearing. With the outer ring stationary and the inner ring rotating, the relative slip speed V_e on the guide surface of the outer ring guiding cage is expressed by Equation (1):

$$V_e=\frac{\pi}{120\times10^3}(1-\gamma)\,d_{e1}n_i$$

$$=K_e n_i \text{ (m/s)} \quad \cdots\cdots (1)$$

where, d_{e1}: Diameter of the guide surface (mm)

γ: Parameter to indicate the inside design of the bearing

$$\gamma=\frac{D_w\cos\alpha}{D_{pw}}$$

D_w: Diameter of rolling element (mm)
α: Bearing contact angle (°)
D_{pw} (or d_m): Pitch diameter of rolling elements (mm)
n_i: Inner ring rotating speed (min^{-1})

$$K_e=\frac{\pi\, d_{e1}}{120\times10^3}(1-\gamma)$$

Table 2 shows the value of the constant K_e for deep groove ball bearings, 62 and 63 series, and cylindrical roller bearings, NU2 and NU3 series. Assuming V_i for the slip speed of the inner ring guiding cage and V_a for the maximum slip speed of the rolling element for the cage, the relation may be approximated as follows:

$V_i \fallingdotseq$(1.15 to 1.18) V_e (diameter series 2)
$\fallingdotseq$(1.20 to 1.22) V_e (diameter series 3)
$V_a \fallingdotseq$(1.05 to 1.07) V_e (diameter series 2)
$\fallingdotseq$(1.07 to 1.09) V_e (diameter series 3)

Example of calculation with deep groove ball bearing

Table 1 shows $D_{pw}\times n$ ($d_m n$) and the slip speed for 6210 and 6310 when n_i=4 500 min^{-1}.

Table 1

Ball bearing	$D_{pw}\times n$ ($\times10^4$)	V_e(m/s) outer ring guide	V_a(m/s)	V_i(m/s) inner ring guide
6210	31.5	7.5	8.0	8.7
6310	36.9	8.5	9.1	10.3

Remarks

Assuming h_e for the groove depth in Equation (1);

$$d_{e1}=D_{pw}+D_w-2h_e=D_{pw}\left(1+\frac{D_w-2h_e}{D_{pw}}\right)$$

$$V_e=\frac{\pi}{120\times10^3}(1-\gamma)\left(1+\frac{D_w-2h_e}{D_{pw}}\right)D_{pw}\cdot n$$

$$=K_e'\cdot D_{pw}\cdot n$$

The constant K_e' is determined for each bearing and is approximately within the range shown below:

K_e'=(0.23 ~ 0.245)$\times10^{-4}$

Table 2 Constant K_e for 62 and 63 series ball bearings and NU2 and NU3 series roller bearings

Bearing bore No.	Bearing series 62	63	NU2	NU3
	$\times10^{-5}$	$\times10^{-5}$	$\times10^{-5}$	$\times10^{-5}$
00	48	49	—	—
01	50	52	—	—
02	59	66	—	—
03	67	74	—	—
04	77	81	79	84
05	92	103	92	102
06	110	121	110	123
07	125	133	126	136
08	142	149	144	155
09	155	171	157	171
10	168	189	172	189
11	184	201	189	206
12	206	218	208	224
13	221	235	226	259
14	233	252	239	261
15	249	270	251	278
16	264	287	270	298
17	281	305	288	314
18	298	323	304	333
19	316	340	323	352
20	334	366	341	376
21	350	379	361	392
22	368	406	378	416
24	400	441	408	449
26	430	475	441	486
28	470	511	478	523
30	510	551	515	559
32	550	585	551	599
34	585	615	588	635
36	607	655	615	670
38	642	695	651	707
40	682	725	689	747

12.5 Centrifugal force of rolling elements

Under normal operating conditions, the centrifugal force on a rolling element is negligible when compared with the load on the bearing and thus not taken into account during calculation of the effective life of the bearing. However, if the bearing is running at high speed, then even if the load is small, the effect of the centrifugal force on the rolling element cannot be ignored. The deep groove ball bearing and cylindrical roller bearing suffer a decrease in the effective life because of the centrifugal force on the rolling element. In the case of an angular contact ball bearing, the contact angle of the inner ring increases and that of the outer ring decreases from the initial value, resulting in relative variation in the fatigue probability.

Apart from details of the effect on the life, the centrifugal force F_c of the rolling element during rotating of the inner ring is expressed by Equations (1) and (2) respectively for a ball bearing and roller bearing.

Ball bearing

$$F_c = K_B n_i^2 \quad \cdots\cdots (1)$$

$$K_B = 5.580\times10^{-12} D_w^3 D_{pw} (1-\gamma)^2 \quad \cdots\cdots (N)$$
$$= 0.569\times10^{-12} D_w^3 D_{pw} (1-\gamma)^2 \quad \cdots\cdots \{kgf\}$$

Roller bearing

$$F_c = K_R n_i^2 \quad \cdots\cdots (2)$$

$$K_R = 8.385\times10^{-12} D_w^2 L_w D_{pw} (1-\gamma)^2 \quad \cdots\cdots (N)$$
$$= 0.855\times10^{-12} D_w^2 L_w D_{pw} (1-\gamma)^2 \quad \cdots\cdots \{kgf\}$$

where, D_w: Diameter of roller element (mm)
D_{pw}: Pitch diameter of rolling elements (mm)
γ: Parameter to indicate the internal design of the bearing

$$\gamma = \frac{D_w \cos\alpha}{D_{pw}}$$

α: Contact angle of bearing (°)
L_w: Length of roller (mm)
n_i: Inner ring rotating speed (min^{-1})

Table 1 shows the K values (K_B and K_R) for both series of NU2 & NU3 roller bearings and the 62 & 63 ball bearings.

Table 1 Constant K for 62 and 63 series ball bearings and for NU2 and NU3 series roller bearings

Bearing bore No.	Bearing series 62		Bearing series 63		Bearing series NU2		Bearing series NU3	
	K		K		K		K	
	$\times10^{-8}$	$\times10^{-8}$	$\times10^{-8}$	$\times10^{-8}$	$\times10^{-8}$	$\times10^{-8}$	$\times10^{-8}$	$\times10^{-8}$
00	0.78	{ 0.08}	2.16	{ 0.22}	—		—	
01	1.37	{ 0.14}	3.14	{ 0.32}	—		—	
02	1.77	{ 0.18}	4.41	{ 0.45}	—		—	
03	2.94	{ 0.30}	6.67	{ 0.68}	—		—	
04	5.49	{ 0.56}	9.41	{ 0.96}	5.00	{ 0.51}	9.51	{ 0.97}
05	6.86	{ 0.70}	15.7	{ 1.6 }	6.08	{ 0.62}	16.7	{ 1.7 }
06	13.7	{ 1.4 }	29.4	{ 3.0 }	11.8	{ 1.2 }	28.4	{ 2.9 }
07	25.5	{ 2.6 }	47.1	{ 4.8 }	22.6	{ 2.3 }	41.2	{ 4.2 }
08	36.3	{ 3.7 }	73.5	{ 7.5 }	35.3	{ 3.6 }	63.7	{ 6.5 }
09	41.2	{ 4.2 }	129	{ 13.2 }	39.2	{ 4.0 }	109	{ 11.1 }
10	53.9	{ 5.5 }	186	{ 19.0 }	43.1	{ 4.4 }	149	{ 15.2 }
11	84.3	{ 8.6 }	251	{ 25.6 }	63.7	{ 6.5 }	234	{ 23.9 }
12	128	{ 13.1 }	341	{ 34.8 }	91.2	{ 9.3 }	305	{ 31.1 }
13	161	{ 16.4 }	455	{ 46.4 }	127	{ 12.9 }	391	{ 39.9 }
14	195	{ 19.9 }	595	{ 60.7 }	135	{ 13.8 }	494	{ 50.4 }
15	213	{ 21.7 }	765	{ 78.0 }	176	{ 17.9 }	693	{ 70.7 }
16	290	{ 29.6 }	969	{ 98.8 }	233	{ 23.8 }	758	{ 77.3 }
17	391	{ 39.9 }	1 216	{ 124 }	302	{ 30.8 }	1 020	{ 104 }
18	518	{ 52.8 }	1 491	{ 152 }	448	{ 45.7 }	1 236	{ 126 }
19	672	{ 68.5 }	1 824	{ 186 }	559	{ 57.0 }	1 471	{ 150 }
20	862	{ 87.9 }	2 560	{ 261 }	689	{ 70.3 }	1 961	{ 200 }
21	1 079	{110 }	3 011	{ 307 }	844	{ 86.1 }	2 501	{ 255 }
22	1 344	{137 }	4 080	{ 416 }	1 167	{119 }	3 207	{ 327 }
24	1 736	{177 }	4 570	{ 466 }	1 422	{145 }	4 884	{ 498 }
26	2 177	{222 }	6 160	{ 628 }	1 569	{160 }	6 257	{ 638 }
28	2 442	{249 }	8 140	{ 830 }	2 157	{220 }	7 904	{ 806 }
30	2 707	{276 }	9 003	{ 918 }	2 903	{296 }	9 807	{1 000 }
32	2 962	{302 }	11 572	{1 180 }	3 825	{390 }	10 787	{1 100 }
34	4 168	{425 }	16 966	{1 730 }	4 952	{505 }	13 925	{1 420 }

Remarks The value given in braces { } is the calculated result for constant K in units of kgf.

12.6 Temperature rise and dimensional change

Rolling bearings are extremely precise mechanical elements. Any change in dimensional accuracy due to temperature cannot be ignored. Accordingly, it is specified as a rule that measurement of a bearing must be made at 20°C and that the dimensions to be set forth in the standards must be expressed by values at 20°C.

Dimensional change due to temperature change not only affects the dimensional accuracy, but also causes change in the internal clearance of a bearing during operation. Dimensional change may cause interference between the inner ring and shaft or between the outer ring and housing bore. It is also possible to achieve shrink fitting with large interference by utilizing dimensional change induced by temperature difference. The dimensional change Δl due to temperature rise can be expressed as in Equation (1) below:

$$\Delta l = \Delta T \, \alpha \, l \quad (\mathrm{mm}) \quad \cdots\cdots (1)$$

where, Δl: Dimentional change (mm)
ΔT: temperature rise (°C)
α: Coefficient of linear expansion for bearing steel
$\alpha = 12.5 \times 10^{-6}$ (1/°C)
l: Original dimension (mm)

Equation (1) may be illustrated as shown in Fig. 1. In the following cases, Fig. 1 can be utilized to easily obtain an approximate numerical values for dimensional change:

(1) To correct dimensional measurements according to the ambient air temperature
(2) To find the change in bearing internal clearance due to temperature difference between inner and outer rings during operation
(3) To find the relationship between the interference and heating temperature during shrink fitting
(4) To find the change in the interference when a temperature difference exists on the fit surface

Example
To what temperature should the inner ring be heated if an inner ring of 110 mm in bore is to be shrink fitted to a shaft belonging to the n6 tolerance range class?

The maximum interference between the n6 shaft of 110 in diameter and the inner ring is 0.065. To enable insertion of the inner ring with ease on the shaft, there must be a clearance of 0.03 to 0.04. Accordingly, the amount to expand the inner ring must be 0.095 to 0.105. Intersection of a vertical axis Δl=0.105 and a horizontal axis l=110 is determined on a diagram. ΔT is located in the temperature range between 70°C and 80°C ($\Delta T \fallingdotseq 77$°C). Therefore, it is enough to set the inner ring heating temperature to the room temperature +80°C.

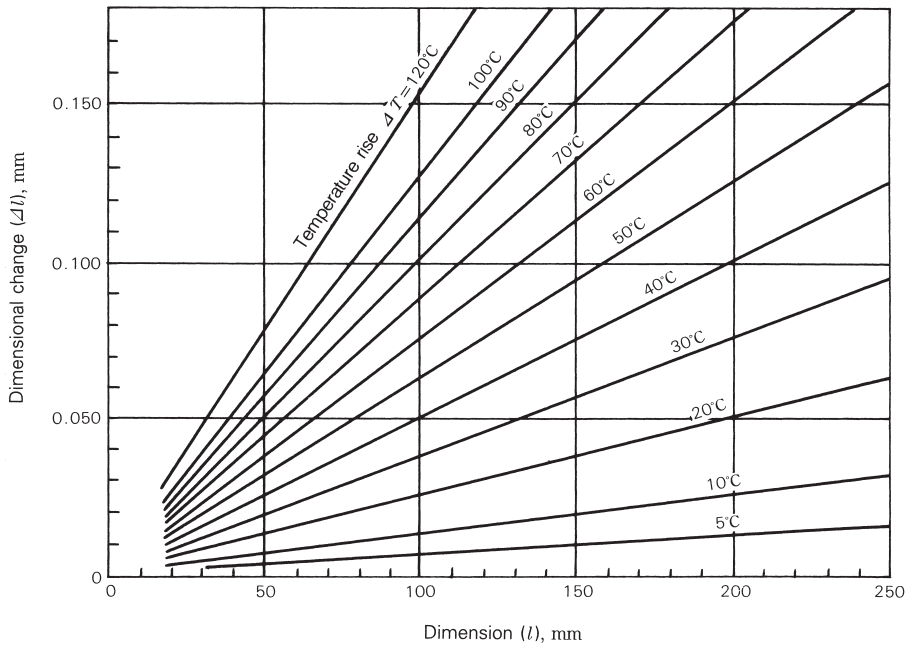

Fig. 1 Temperature rise and dimensional change of bearing steel

12.7 Bearing volume and apparent specific gravity

The bearing bore is expressed by "d" (mm), the bearing outside diameter by "D" (mm), and the width by "B" (mm). The volume "V" of a bearing is expressed as follows:

$$V=\frac{\pi}{4}(D^2-d^2)\,B\times10^{-3}\ (\mathrm{cm}^3) \quad \cdots\cdots (1)$$

Table 1 shows the bearing volume for the principal dimension series of radial bearings. In the case of a tapered roller bearing, the volume is a calculated value assuming the assembly width as "B". When the bearing mass is expressed by "W" (kg), $W/V=k$ may be considered as an apparent specific gravity and the value of "k" is nearly constant according to the type of bearings.

Table 2 shows the values of "k" for radial bearings of each dimension series. When the mass of a bearing not included in the standard dimension series is to be determined, the approximate mass value may be known by using the apparent specific gravity "k" if the bearing volume "V" has been determined.

Table 1 Volume of radial bearing

Units: cm^3

Bearing bore No.	Radial bearing (excluding tapered roller bearing)					Tapered roller bearing		
	Dimension series					Dimension series		
	10	30	02	22	03	23	20	02	03
00	3.6	5.4	5.6	8.8	9.7	15.0	—	—	—
01	4.0	6.0	6.9	9.7	11.5	16.3	—	—	—
02	5.4	7.9	8.4	11.0	15.7	20.5	—	—	17.2
03	7.4	10.3	12.3	16.5	21.1	28.6	—	13.6	23.0
04	12.9	17.1	19.9	25.6	27.1	38.0	—	21.7	29.4
05	14.9	20.0	24.5	29.4	43.0	60.6	—	26.5	46.1
06	21.7	31.7	36.9	46.2	63.9	90.8	28.4	39.3	69.8
07	28.8	41.1	52.9	71.5	85.3	126	37.0	56.8	92.4
08	35.6	50.0	67.9	86.7	117	168	45.2	74.5	129
09	45.2	65.0	77.6	93.9	157	225	56.5	84.9	170
10	49.0	70.5	88.0	101	203	301	61.3	95.6	220
11	71.7	104	115	137	259	384	92	125	281
12	76.7	111	147	187	324	480	98	159	350
13	81.6	118	184	249	398	580	104	198	434
14	113	170	202	261	484	705	142	221	525
15	119	179	221	275	580	860	150	241	627
16	159	239	269	342	689	1 020	204	293	750
17	175	270	336	432	810	1 190	230	366	880
18	217	334	412	550	945	1 410	289	446	1 020
19	226	348	500	671	1 095	1 630	301	538	1 200
20	236	362	598	809	1 340	2 080	313	650	1 460
21	298	469	709	985	1 530	2 390	400	767	1 660
22	369	594	833	1 160	1 790	2 860	502	898	1 950
24	396	649	1 000	1 450	2 300	3 590	536	1 090	2 480
26	598	945	1 130	1 810	2 800	4 490	818	1 240	3 080
28	632	1 020	1 415	2 290	3 430	5 640	866	1 540	3 740
30	773	1 240	1 780	2 890	4 080	6 770	1 060	1 940	4 520

Table 2 Bearing type and apparent specific gravity (k)

Bearing type	Principal bearing series	Apparent specific gravity, k
Single row deep groove ball bearing (with pressed cage)	60, 62, 63	5.3
NU type cylindrical roller bearing	NU10, NU2, NU3	6.8
N type cylindrical roller bearing	N10, N2, N3	6.5
Tapered roller bearing	320, 302, 303	5.5
Spherical roller bearing	230, 222, 223	6.4

12.8 Projection amount of cage in tapered roller bearing

The cage of a tapered roller bearing is made of a steel plate press construction and projects perpendicularly from the side of the outer ring as shown in Fig. 1. It is essential to design the bearing mounting to prevent the cage from contacting such parts as the housing and spacer. It is also recommended to employ the dimension larger than specified in JIS B 1566 "Mounting Dimensions and Fit for Rolling Bearing" and S_a and S_b of the bearing catalog in view of securing the grease retaining space in the case of grease lubrication and in view of improving the oil flow in the case of oil lubrication.

However, if the dimension cannot be designed smaller due to a dimensional restriction in the axial direction, then mounting dimensions S_a and S_b should be selected by adding as large as possible space to the maximum projection values δ_1 and δ_2 (Table 1) to the cage from the outer ring side.

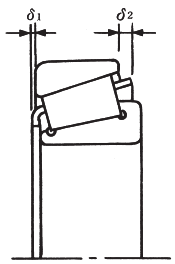

Fig. 1 Projection of a cage

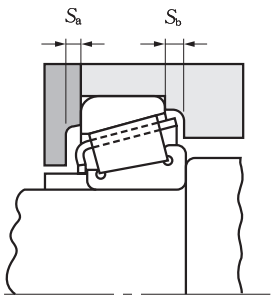

Fig. 2 Dimensions related to bearing mounting

Bearing bore No.	HR329J		HR320XJ	
	δ_1	δ_2	δ_1	δ_2
02	—	—	—	—
03	—	—	—	—
04	—	—	1.5	2.9
/22	—	—	1.6	3.1
05	—	—	1.9	3.5
/28	—	—	1.9	3.5
06	—	—	2.0	3.1
/32	—	—	2.0	3.9
07	1.3	2.7	2.5	3.7
08	1.9	2.9	2.3	4.2
09	—	—	2.9	4.7
10	—	—	3.0	4.6
11	1.9	3.3	3.1	5.1
12	2.3	3.5	3.1	5.0
13	—	—	2.5	5.9
14	2.5	4.1	2.9	5.6
15	—	—	3.5	5.5
16	—	—	4.5	7.2
17	—	—	4.2	6.5
18	3.4	5.5	4.4	7.2
19	3.3	5.2	4.5	7.1
20	3.4	5.1	4.5	7.1

Table 1 Projection of a cage of tapered roller bearing

Units: mm

Bearing series															
HR330J		HR331J		HR302J		HR322J		HR332J		HR303J		HR303DJ		HR323J	
δ_1	δ_2	δ_1	δ_2	δ_1	δ_2	δ_1	δ_2	δ_1	δ_2	δ_1	δ_2	δ_1	δ_2	δ_1	δ_2
—	—	—	—	—	—	—	—	—	—	1.2	3.3	—	—	—	—
—	—	—	—	0.7	2.0	0.3	3.0	—	—	1.4	3.7	—	—	—	—
—	—	—	—	1.0	2.9	0.6	3.5	—	—	0.9	3.7	—	—	1.3	3.2
—	—	—	—	—	—	0.9	3.8	—	—	1.1	2.9	—	—	—	—
2.0	3.1	—	—	0.8	2.9	0.9	3.8	2.0	3.3	1.6	3.4	—	—	1.5	4.5
—	—	—	—	1.4	3.4	1.5	3.4	1.8	3.8	1.5	4.8	—	—	—	—
2.0	4.0	—	—	1.4	3.4	1.5	3.3	2.1	4.6	2.1	3.9	—	—	1.6	4.0
—	—	—	—	0.7	3.3	1.6	2.8	2.2	4.4	—	—	—	—	—	—
2.2	3.4	—	—	2.0	3.1	1.7	4.3	2.6	4.7	2.9	4.8	2.1	4.8	1.1	4.1
2.2	3.2	—	—	1.1	4.7	1.4	5.1	3.1	5.5	1.8	4.9	2.0	5.0	0.5	4.5
—	—	3.3	4.7	1.8	3.9	1.9	5.1	3.7	6.0	2.5	5.1	2.3	5.5	2.0	5.2
2.4	4.4	3.3	5.1	1.8	5.5	1.7	6.2	3.3	5.8	2.2	5.9	3.7	6.8	1.5	5.7
2.9	4.8	3.3	6.3	2.7	4.8	2.1	4.5	3.5	6.6	2.6	5.7	3.3	6.0	1.8	6.4
2.9	5.1	—	—	1.2	5.9	3.4	4.2	3.9	7.0	3.1	6.5	3.2	8.0	2.7	6.5
3.0	5.1	—	—	3.9	4.8	2.8	4.0	4.9	7.4	3.1	6.2	3.9	10.0	2.3	7.4
3.5	5.5	—	—	3.3	5.3	2.7	5.0	5.5	7.0	3.2	6.5	3.8	8.2	2.1	7.2
3.5	5.4	—	—	3.9	5.3	2.8	4.7	5.0	7.9	3.0	7.6	3.7	8.6	1.8	7.7
—	—	—	—	3.1	5.5	3.1	4.6	4.7	7.6	2.2	7.8	3.4	9.2	2.2	7.9
3.7	6.0	4.8	7.6	3.1	6.3	2.1	5.8	4.6	8.7	3.4	8.5	4.0	10.3	2.8	9.8
—	—	4.8	7.5	3.6	5.1	2.6	5.1	—	—	—	—	3.2	9.6	2.1	8.9
—	—	—	—	3.5	5.9	1.9	5.4	—	—	—	—	3.0	10.3	—	—
—	—	3.8	8.8	3.2	6.9	2.0	5.6	3.8	9.4	—	—	—	—	2.1	10.3

12.9 Natural frequency of individual bearing rings

The natural frequencies of individual bearing rings of a rolling bearing are mainly composed of radial vibration and axial vibration. The natural frequency in the radial direction is a vibration mode as shown in Fig. 1. These illustrated modes are in the radial direction and include modes of various dimensions according to the circumferential shape, such as a primary (elliptical), secondary (triangular), tertiary (square), and other modes.

As shown in Fig. 1, the number of nodes in the primary mode is four, with the number of waves due to deformation being two. The number of waves is three and four respectively in the secondary and tertiary modes. In regards to the radial natural frequency of individual bearing rings, Equation (1) is based on the theory of thin circular arc rod and agrees well with measured values:

$$f_{RiN}=\frac{1}{2\pi}\sqrt{\frac{Eg}{\gamma}\frac{I_x}{AR^4}}\frac{n\,(n^2-1)}{\sqrt{n^2-1}}\quad\text{(Hz)}\ \cdots\cdots\cdots\ (1)$$

where, f_{RiN}: i-th natural frequency of individual bearing rings in the radial directios (Hz)
E: Young's modulus (MPa) {kgf/mm^2}
γ: Specific weight (N/mm^3) {kgf/mm^3}
g: Gravity acceleration (mm/s^2)
n: Number of deformation waves in each mode (i+1)
I_x: Sectional secondary moment at neutral axis of the bearing ring (mm^4)
A: Sectional area of bearing ring (mm^2)
R: Radius of neutral axis of bearing ring (mm)

The value of the sectional secondary moment is needed before using Equation (1). But it is troublesome to determine this value exactly for a bearing ring with a complicated cross-sectional shape. Equation (2) is best used when the radial natural frequency is known approximately for the outer ring of a radial ball bearing. Then, the natural frequency can easily be determined by using the constant determined from the bore, outside diameter, and cross-sectional shape of the bearing.

$$f_{RiN}=9.41\times10^5\frac{K\,(D-d)}{\{D-K\,(D-d)\}^2}\times\frac{n\,(n^2-1)}{\sqrt{n^2-1}}\quad\text{(Hz)}\ \cdots\cdots\cdots\ (2)$$

where, d: Bearing bore (mm)
D: Bearing outside diameter (mm)
K: Constant determined from the cross-sectional shape
K=0.125 (outer ring with seal grooves)
K=0.150 (outer ring of an open type)

Another principal mode is the one in the axial direction. The vibration direction of this mode is in the axial direction and the modes range from the primary to tertiary as shown in Fig. 2. The figure shows the case as viewed from the side. As in the case of the radial vibration modes, the number of waves of deformation in primary, secondary, and tertiary is two, three, and four respectively. As for the natural frequency of individual bearing rings in the axial direction, there is an approximation Equation (3), which is obtained by synthesizing an equation based upon the theory of circular arc rods and another based on the non-extension theory of cylindrical shells:

$$f_{AiN}=\frac{\frac{\sqrt{3}}{6\pi}n\,(n^2-1)\,\rho}{(1-\nu^2)\left(\frac{\rho}{\kappa}\right)^2\frac{n^2\,(n^2+1)\,\rho^2+3}{n^2\rho^2+6\,(1-\nu)}+n^2+\lambda}\times\frac{1}{R}\sqrt{\frac{Eg}{\gamma}}\quad\text{(Hz)}\ \cdots\cdots\cdots\ (3)$$

where, $\kappa=H/2R$
$\rho=B/2R$

$$\lambda=\frac{1+\nu}{2-1.26\sigma\,(1-\sigma^4/12)}$$

$$\sigma=\min\left(\frac{\kappa}{\rho},\frac{\rho}{\kappa}\right)$$

where, f_{AiN}: i-th natural frequency of individual bearing rings is the axial direction (Hz)
E: Young's modulus (MPa) {kgf/mm^2}
γ: Specific weight (N/mm^3) {kgf/mm^3}
g: Gravity acceleration (mm/s^2)
n: Number of deformation waves in each mode (i+1)
R: Radius of neutral axis of bearing ring (mm)
H: Thickness of bearing ring (mm)
B: Width of bearing ring (mm)
ν: Poisson's ratio

This equation applies to a rectangular sectional shape and agrees well with actual measurements in the low-dimension mode even in the case of a bearing ring. But this calculation is difficult. Therefore, Equation (4) is best used when the natural frequency in the axial direction is known approximately for the outer ring of the ball bearing. Calculation can then be made using the numerical values obtained from the bearing's bore, outside diameter, width, and outer ring sectional shape.

$$f_{AiN}=\frac{9.41\times10^5 n\,(n^2-1)\,R_0^2}{B\sqrt{\frac{0.91}{H_0^2}\cdot\frac{n^2\,(n^2+1)\,R_0^2+3}{n^2R_0^2+4.2}+n^2+\frac{1.3}{2-1.26H_0+0.105H_0^5}}}\quad\text{(Hz)}\ \cdots\cdots\cdots\ (4)$$

where, $R_0=B/\{D-K\,(D-d)\}$
$H_0=K\,(D-d)/B$

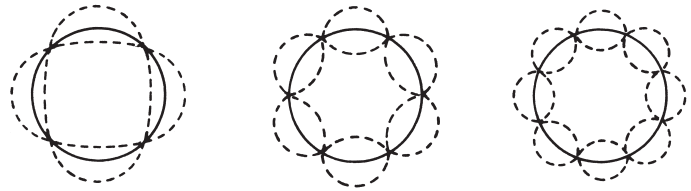

Primary mode (n=2) Secondary mode (n=3) Tertiary mode (n=4)

Fig. 1 Primary to tertiary vibration modes in the radial direction

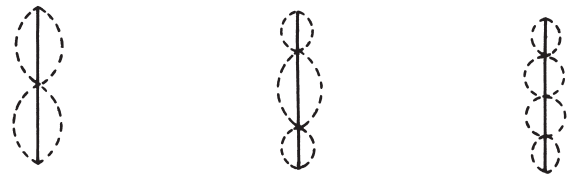

Primary mode (n=2) Secondary mode (n=3) Tertiary mode (n=4)

Fig. 2 Primary to tertiary vibration modes in the axial direction

12.10 Vibration and noise of bearings

The vibration and noise occurring in a rolling bearing are very diverse. Some examples are shown in Table 1. This table shows the vibration and noise of bearings while classifying them roughly into those inherent in the bearing design which occur regardless of the present superb technology and those caused by other reasons, both are further subdivided into several groups. The boundaries among these groups, however, are not absolute. Although vibration and noise due to the bearing structure may be related to the magnitude of the bearing accuracy, nevertheless, vibration attributed to accuracy may not be eliminated completely by improving the accuracy, because there exists certain effects generated by the parts surrounding the bearing.

Arrows in the table show the relationship between the vibration and noise.

Generally, vibration and noise are in a causal sequence but they may be confused. Under normal bearing running conditions, however, around 1 kHz may be used as a boundary line to separate vibration from noise. Namely, by convention, the frequency range of about 1 kHz or less will be treated as vibration while that above this range will be treated as noise.

Typical vibration and noise, as shown in Table 1, have already been clarified as to their causes and present less practical problems. But the environmental changes as encountered these days during operation of a bearing have come to generate new kinds of vibration and noise. In particular, there are cases of abnormal noise in the low temperature environment, which can often be attributed to friction inside of a bearing. If the vibration and noise (including new kinds of abnormal noise) of a bearing are to be prevented or reduced, it is essential to define and understand the phenomenon by focusing on vibration and noise beforehand. As portable tape recorders with satisfactory performance are commonly available these days, it is recommended to use a tape recorder to record the actual sound of the vibration or noise.

Table 1 Vibration and noise of rolling bearing

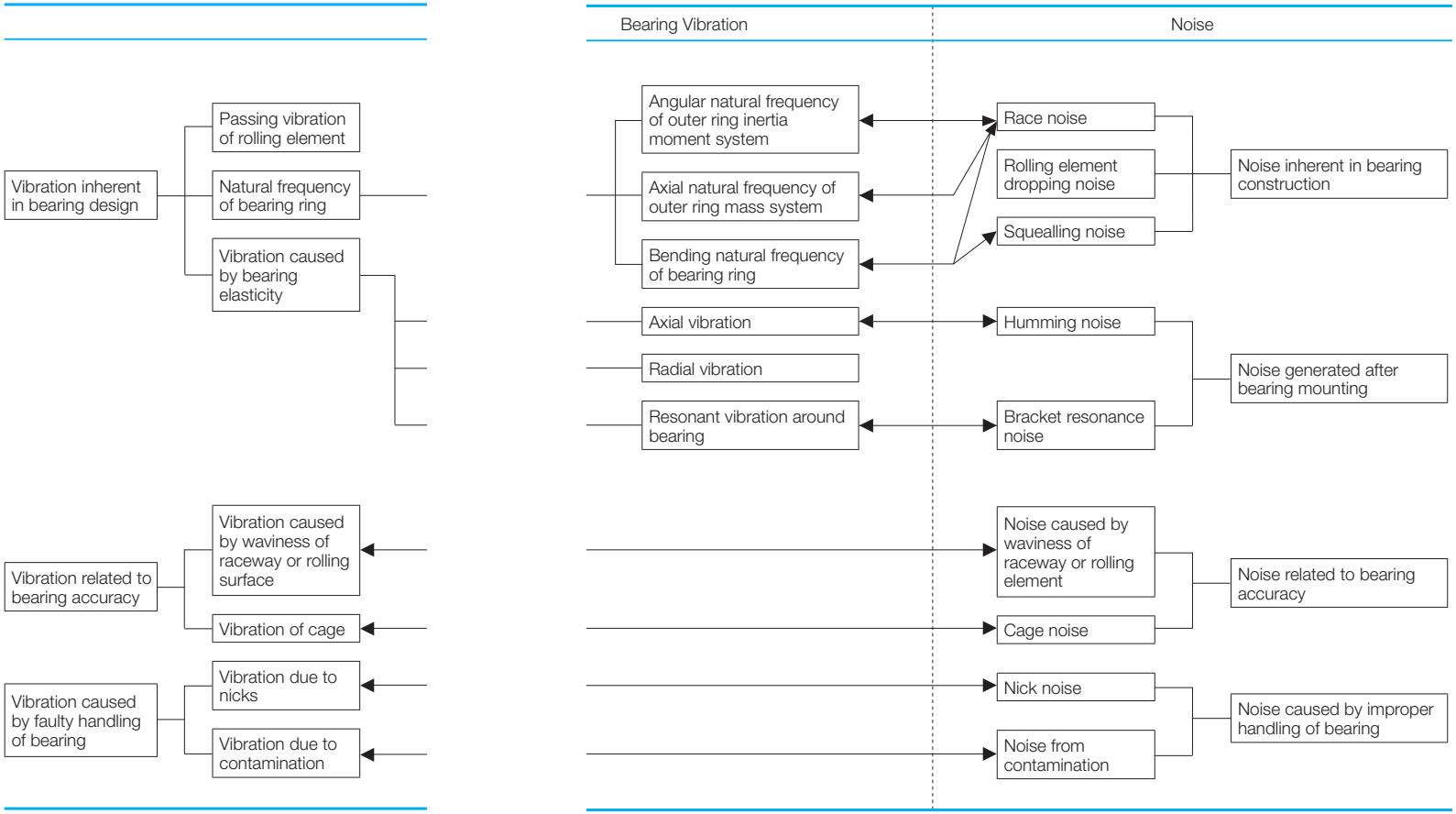

12.11 Application of FEM to design of bearing system

Before a rolling bearing is selected in the design stage of a machine, it is often necessary to undertake a study of dynamic and thermal problems (mechanical structure and neighboring bearing parts) in addition to the dimensions, accuracy, and material of the shaft and housing. For example, in the prediction of the actual load distribution and life of a bearing installed in a machine, there are problems with overload or creep caused by differences in thermal deformation due to a combination of factors such as dissimilar materials, or estimation of temperature rise or temperature distribution.

NSK designs optimum bearings by using Finite Element Methods (FEM) to analyze the shaft and bearing system. Let's consider an example where FEM is used to solve a problem related to heat conduction.

Fig. 1 shows an example of calculating the temperature distribution in the steady state of a rolling mill bearing while considering the bearing heat resistance or heat resistance in the fit section when the outside surface of a shaft and housing is cooled with water. In this analysis, the amount of decrease in the internal clearance of a bearing due to temperature rise or the amount of increase needed for fitting between the shaft and inner ring can be found.

Fig. 2 shows a calculation for the change in the temperature distribution as a function of time after the start of operation for the headstock of a lathe. Fig. 3 shows a calculation example for the temperature change in the principal bearing components. In this example, it is predicted that the bearing preload increases immediately after rotation starts and reaches the maximum value in about 10 minutes.

When performing heat analysis of a bearing system by FEM, it is difficult to calculate the heat generation or to set the boundary conditions to the ambient environment. NSK is proceeding to accumulate an FEM analytical database and to improve its analysis technology in order to effectively harness the tremendous power of FEM.

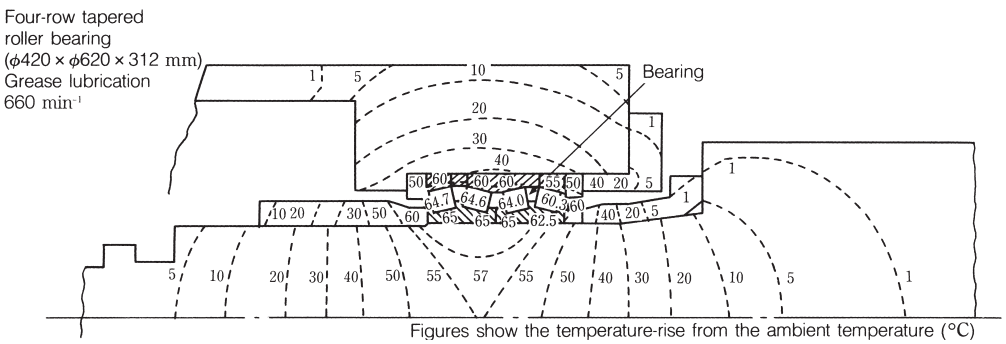

Fig. 1 Calculation example of temperature distribution for the intermediate roll of a rolling mill

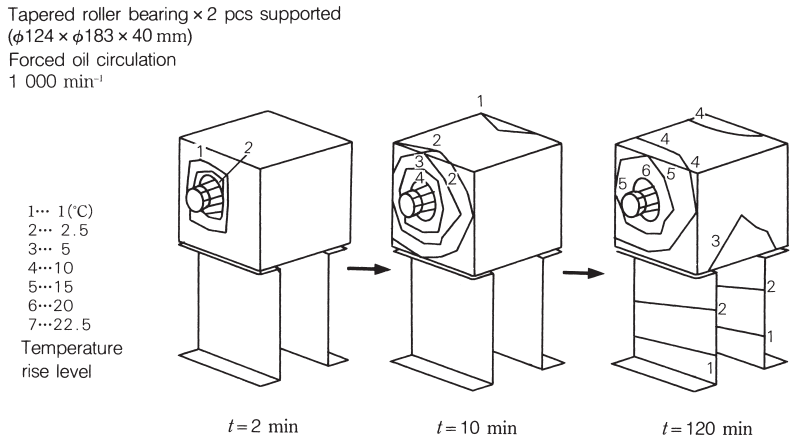

Fig. 2 Calculation example of temperature rise in headstock of lathe

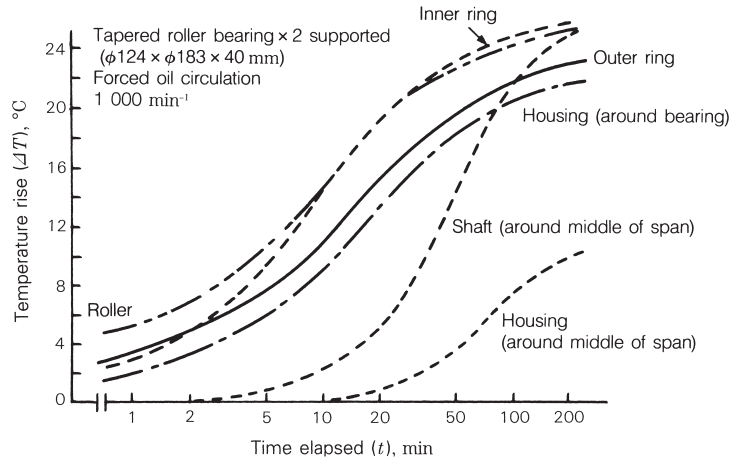

Fig. 3 Calculation example of temperature rise in bearing system

As an example of applying the FEM-based analysis, we introduce here the result of a study on the effect of the shape of a rocker plate supporting the housing of a plate rolling mill both on the life of a tapered roller bearing (ϕ489×ϕ635 in dia. ×321) and on the housing stress. Fig. 4 shows an approximated view of the housing and rocker plate under analysis. The following points are the rerults of analysis made while changing the relief amount l at the top surface of the rocker plate:

(1) The maximum value σ_{max} of the stress (maximum main stress) on a housing occurs at the bottom of the housing.

(2) σ_{max} increases with increase in l. But it is small relative to the fatigue limit of the material.

(3) The load distribution in the rolling element of the bearing varies greatly depending on l. The bearing life reaches a maximum at around l/L=0.7.

(4) In this example, l/L=0.5 to 0.7 is considered to be the most appropriate in view of the stress in the housing and the bearing life. Fig. 5 shows the result of calculation on the housing stress distribution and shape as well as the rolling element load distribution when l/L≒0.55.

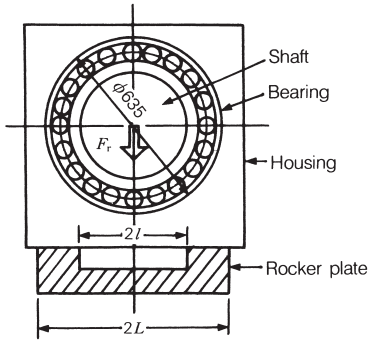

Fig. 4 Rolling mill housing and rocker plate

Fig. 6 shows the result of a calculation on the housing stress and bearing life as a function of change in l.

FEM-based analysis plays a crucial role in the design of bearing systems. Finite Element Methods are applicable in widely-varying fields as shown in Table 1. Apart from these, FEM is used to analyze individual bearing components and contribute to NSK's high-level bearing design capabilities and achievements. Two examples are the analysis of the strength of a rib of a roller bearing and the analysis of the natural mode of a cage.

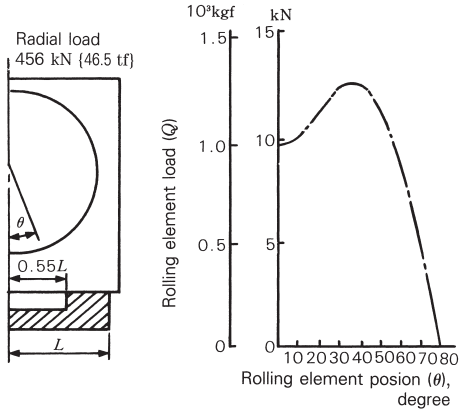

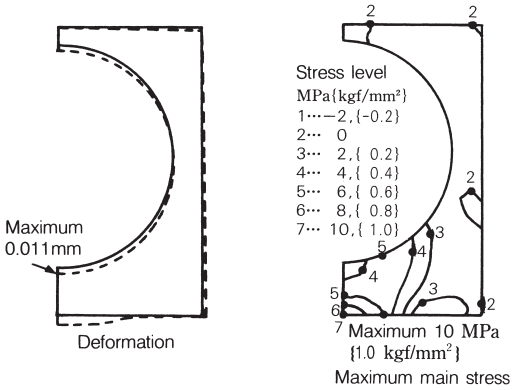

Fig. 5 Calculation example of housing stress and rolling element load distribution of bearing

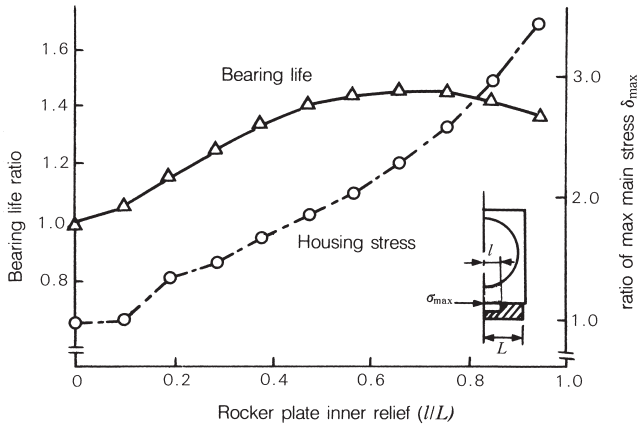

Fig. 6 Calculation of housing stress and bearing life

Table 1 Examples of FEM analysis of bearing systems

Bearing application	Examples	Purpose of analysis
Automobile	•Hub unit •Tension pulley •Differential gear and surrounding •Steering joint	Strength, rigidity, creep, deformation, bearing life
Electric equipment	•Motor bracket •Alternator •Suction Motor Bearing for Cleaner •Pivot Ball Bearing Unit for HDDs	Vibration, rigidity, deformation, bearing life
Steel machinery	•Roll neck bearing peripheral structure (cold rolling, hot rolling, temper mill) •Adjusting screw thrust block •CC roll housing	Strength, rigidity, deformation, temperature distribution, bearing life
Machine tool	•Machining center spindle •Grinding spindle •Lathe spindle •Table drive system peripheral structure	Vibration, rigidity, temperature distribution, bearing life
Others	•Jet engine spindle •Railway rolling stock •Semiconductor-related equipment •Engine block •Slewing bearing's peripheral	Strength, rigidity, thermal deformation, vibration, deformation, bearing life

13. NSK special bearings

13.1 Ultra-precision ball bearings for gyroscopes

(1) Gyroscope bearings

Gyroscopes are used to detect and determine traveling position and angular velocity in airplanes and ships. Gyros are structurally divided into two groups depending on the number of directions and speeds of movement to be detected: those with one degree of freedom and those with two degrees of freedom. (See Fig. 1)
The performance of a gyro depends on the characteristics of the bearing. Thus, a gyro bearing is required to demonstrate top grade performance among the ultra-precision miniature bearings. Gyros have two sets of bearings. One set supports the rotor shaft running at high speed and the other set supports the frame (gimbal). Both must have stable, low frictional torque. Principal types and application environments of rolling bearings for gyros are shown in Table 1.

The inch series of ultra-precision bearings are almost exclusively used for rotors and gimbals. Boundary dimensions and typical NSK bearing numbers are shown in Table 2.

Special-shaped bearings dedicated to gyro applications are also used in large quantity.

Table 1 Type and running conditions of gyro bearings

Application	Principal bearing type	Typical running conditions
Rotor	Angular contact ball bearing End-cap ball bearing	12 000, 24 000 min^{-1} or 36 000 min^{-1}, 60 to 80℃ helium gas
Gimbal	Deep groove ball bearing Other special-shaped bearings	Oscillation within ±2° Normal temperatures to 80℃, Silicon oil or air

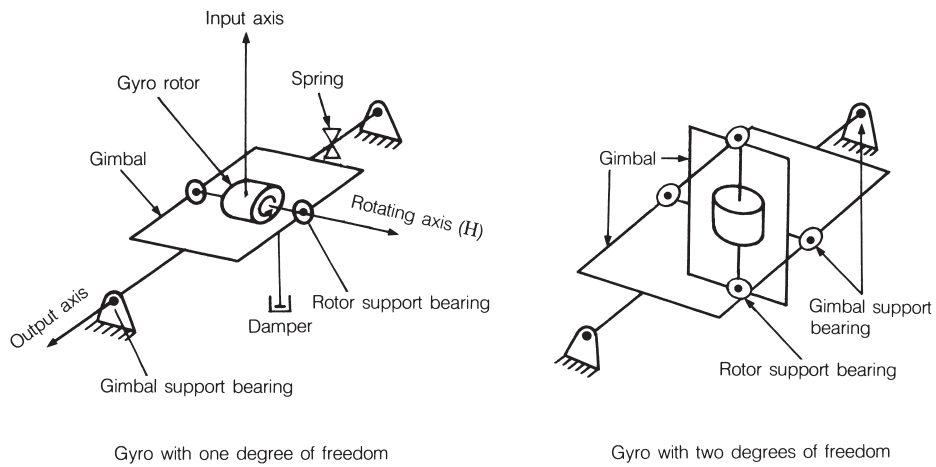

Fig. 1 Gyro type

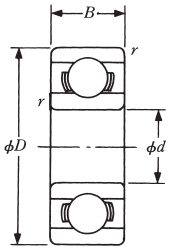

Open type

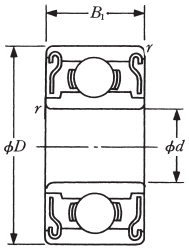

Shielded on both sides type

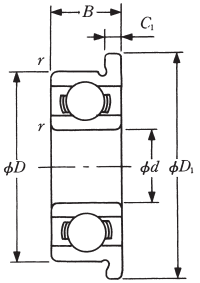

Open type with flange

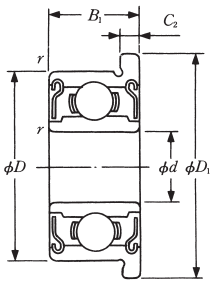

Shielded on both sides type with flange

Table 2 Boundary dimensions and bearing number of gyroscope bearings

Boundary dimensions (mm)					Bearing numbers		Boundary dimensions (mm)			Bearing numbers	
d	D	B	B_1	r (min.)	Open	Both-side shielded	D_1	C_1	C_2	Open, with flange	Both-side shielded, with flange
1.016	3.175	1.191	—	0.1	R 09	—	—	—	—	—	—
1.191	3.967	1.588	2.380	0.1	R 0	R 0 ZZ	5.156	0.330	0.790	FR 0	FR 0 ZZ
1.397	4.762	1.984	2.779	0.1	*R 1	R 1 ZZ	5.944	0.580	0.790	FR 1	FR 1 ZZ
1.984	6.350	2.380	3.571	0.1	*R 1-4	R 1-4 ZZ	7.518	0.580	0.790	FR 1-4	FR 1-4 ZZ
2.380	4.762	1.588	—	0.1	*R 133	—	5.944	0.460	—	FR 133	—
	4.762	—	2.380	0.1	—	R 133 ZZS	5.944	—	0.790	—	FR 133 ZZS
	7.938	2.779	3.571	0.15	*R 1-5	R 1-5 ZZ	9.119	0.580	0.790	FR 1-5	FR 1-5 ZZ
3.175	6.350	2.380	2.779	0.1	*R 144	R 144 ZZ	7.518	0.580	0.790	FR 144	FR 144 ZZ
	7.938	2.779	3.571	0.1	R 2-5	R 2-5 ZZ	9.119	0.580	0.790	FR 2-5	FR 2-5 ZZ
	9.525	2.779	3.571	0.15	*R 2-6	R 2-6 ZZS	10.719	0.580	0.790	FR 2-6	FR 2-6 ZZS
	9.525	3.967	3.967	0.3	*R 2	R 2 ZZ	11.176	0.760	0.760	FR 2	FR 2 ZZ
	12.700	4.366	4.366	0.3	R 2 A	R 2 AZZ	—	—	—	—	—
3.967	7.938	2.779	3.175	0.1	R 155	R 155 ZZS	9.119	0.580	0.910	FR 155	FR 155 ZZS
4.762	7.938	2.779	3.175	0.1	R 156	R 156 ZZS	9.119	0.580	0.910	FR 156	FR 156 ZZS
	9.525	3.175	3.175	0.1	R 166	R 166 ZZ	10.719	0.580	0.790	FR 166	FR 166 ZZ
	12.700	3.967	4.978	0.3	*R 3	R 3 ZZ	14.351	1.070	1.070	FR 3	FR 3 ZZ
6.350	9.525	3.175	3.175	0.1	R 168 B	R 168 BZZ	10.719	0.580	0.910	FR 168 B	FR 168 BZZ
	12.700	3.175	4.762	0.15	R 188	R 188 ZZ	13.894	0.580	1.140	FR 188	FR 188 ZZ
	15.875	4.978	4.978	0.3	*R 4 B	R 4 BZZ	17.526	1.070	1.070	FR 4 B	FR 4 BZZ
	19.050	5.558	7.142	0.4	*R 4 AA	R 4 AAZZ	—	—	—	—	—
7.938	12.700	3.967	3.967	0.15	R 1810	R 1810 ZZ	13.894	0.790	0.790	FR 1810	FR 1810 ZZ
9.525	22.225	5.558	7.142	0.4	R 6	R 6 ZZ	24.613	1.570	1.570	FR 6	FR 6 ZZ

* Angular contact type bearing is also available for rotor.

(2) Characteristics of gyroscope bearings

(2.1) Rotor bearing

The rotor bearing is required to offer extremely-low, torque at high speed, and free from variation and long term stability. To meet these demands, the bearing uses an oil-immersed cage in most cases. A lubrication method of injecting the lubricating oil dissolved with solvent into a bearing is also available, but this method requires adequate concentration adjustment because the frictional torque is affected by the oil amount (Fig. 2). In such an event, the oil amount is adjusted through centrifugal separation to obtain variation-free running torque. A special bearing type, in which an end cap is integrated with the outer ring, may also be used (Fig. 3).

(2.2) Gimbal bearing

Requirements on the gimbal bearing as a gyro output axis include low frictional torque and vibration resistance. Table 3 shows the maximum starting frictional torque for typical bearings. Much smaller starting torque can be obtained through precision machining of the raceway groove and special design of the cage.

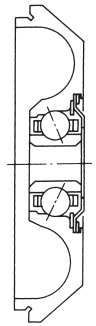

Fig. 3 Typical end-cap ball bearing

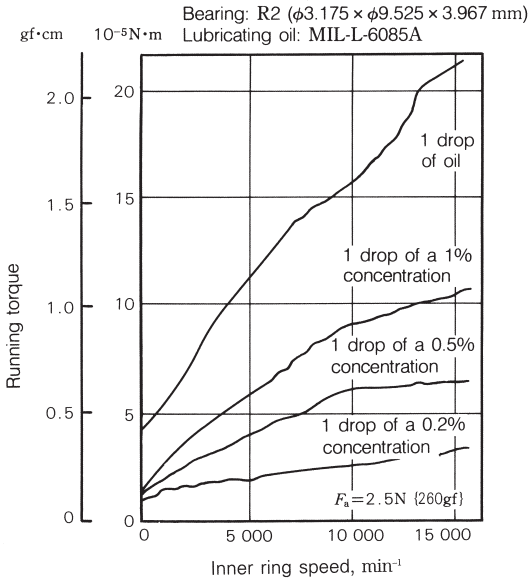

Fig. 2 Oil amount and running torque

Table 3 Maximum starting torque

Bearing No.	Measuring load mN {gf}	Radial internal clearance (μm)				
		MC2 3 to 8	MC3 5 to 10	MC4 8 to 13	MC5 13 to 20	MC6 20 to 28
		Maximum starting torque (μN·m) {mgf·mm}				
R1	735 {75}	7.95 {810}	7.35 {750}	6.75 {690}	6.10 {620}	5.20 {530}
R1-5	735 {75}	13.2 {1 350}	12.3 {1 250}	11.8 {1 200}	10.7 {1 090}	9.70 {990}
R144	735 {75}	8.92 {910}	8.35 {840}	7.65 {780}	6.85 {700}	6.08 {620}
R2	735 {75}	14.7 {1 500}	13.7 {1 400}	12.7 {1 300}	11.8 {1 200}	11.4 {1 160}
R3	3 900 {400}	63.5 {6 500}	54.0 {5 500}	54.0 {5 500}	49.0 {5 000}	44.0 {4 500}
R4B	3 900 {400}	68.5 {7 000}	59.0 {6 000}	59.0 {6 000}	54.0 {5 500}	49.0 {5 000}

Table 4 Specifications of bearings for rotors and gimbals

Item	Rotor bearing	Gimbal bearing
Bearing type	Angular contact ball	Deep groove ball or angular contact ball
Bearing accuracy	CLASS 7P or above	CLASS 5P or CLASS 7P
Lubrication method	Oil-immersed cage and self-lubrication (dual use grease available)	Oil lubrication, filled with an adequate quantity
Cage	Laminated phenol	Steel sheet (low torque design)
Ball accuracy	Around Grade 3	Around Grade 5 or above
Bearing contact angle (°)	20 to 28	—

13.2 Bearings for vacuum use —ball bearings for X-ray tube—

A ball bearing for a rotary anode of an X-ray tube is used under severe conditions such as high vacuum, high temperature, and high speed. An X-ray tube is constructed as shown in Fig. 1, with the internal pressure set below 0.13 mPa (10^{-6} Torr). Thermoelectrons flow from a cathode (filament) toward an anode (target) to generate X-rays at the anode.

A rotor is a part of a motor and driven electromagnetically from the outside. Common speeds range from 3 000 to 10 000 min^{-1}. The anode rotation involves inner ring or outer ring rotation (Fig. 2). Generally, inner ring rotation enables high rigidity and low bearing temperature, but the construction becomes complicated.

Because of heat generation of the anode, the bearing reaches the maximum temperature of 400 to 500°C on the anode side and the bearing on the opposite side reaches a temperature of 200 to 300°C. The bearing is therefore made from high-speed tool steel which is superior in heat resistance.

Most X-ray tubes are used for medical purposes and thus silent rotation is essential. However, difficulty of enhancing the rigidity because of its construction and change in the bearing internal clearance under heavy temperature fluctuation are hindrances to vibration proof.

In this respect, minute care must be taken during the design of a bearing and its neighboring parts. The common range of bearing bores is 6 to 10 mm. Fig. 3 shows examples of typical constructions.

(a) is a type with pressed cage.
(b) has the entire outer ring raceway shaped as a cylindrical surface.
(c) has one side of the outer ring raceway shaped as a cylindrical surface to relieve deviation of inner and outer rings (such as caused by thermal expansion) in the axial direction.

Note that (b) and (c) normally apply to full complement type ball bearings.

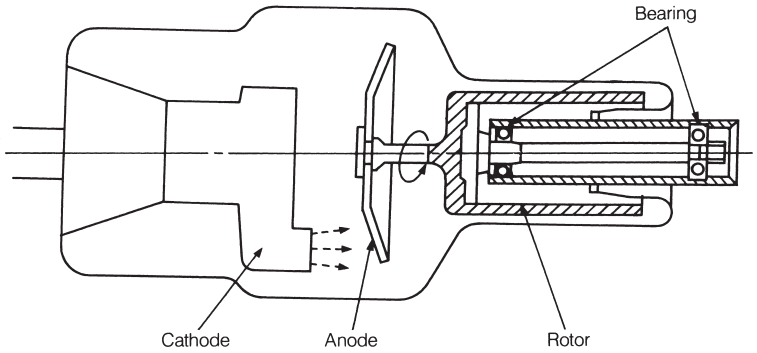

Fig. 1 Typical construction of X-ray tube

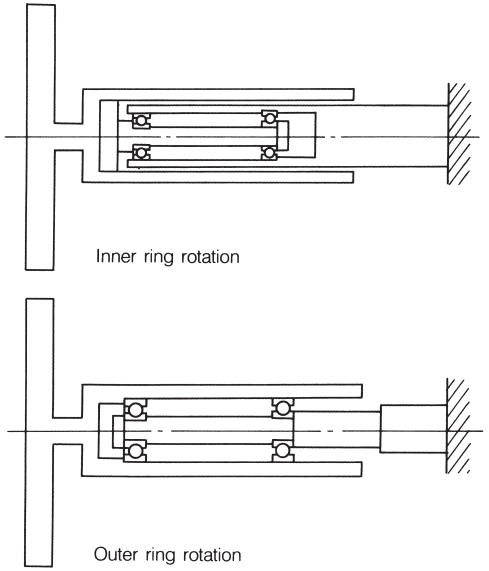

Fig. 2 Anode bearing and rotating ring

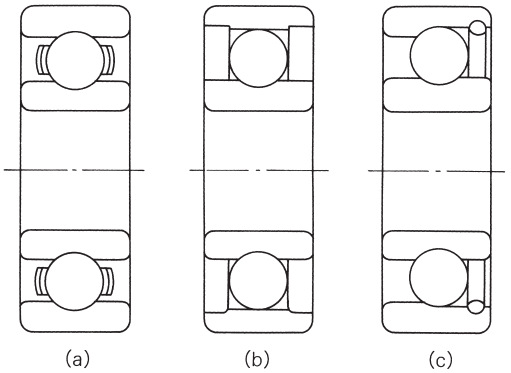

Fig. 3 Typical construction of X-ray tube bearings

One of the greatest challenges facing X-ray tube ball bearings is the lubrication method. Because of the vacuum and high temperature environment, a solid lubricant is used with one of the methods described below:
(1) Provision of laminated solid lubrication (molybdenum disulfide) to the pocket surface of a cage
(2) Provision of thin film of mild metal (silver or lead) over the surface of balls, inner ring/outer ring raceway

The method (2) above applies mostly to full-complement type ball bearings and the thin film is provided by plating, ion plating, etc. The results of a durability test performed on a ball bearing with a soft metal coating in a vacuum are shown in **Fig. 4**. By the way, **Fig. 4** shows a comparison of the endurance time for different conditions of ball bearings (8 mm in bore and 22 mm in outside diameter) that are rotated at 9 000 min^{-1} under an axial load of 20 N {2 kgf} at 0.13 mPa {10^{-6} Torr} while at room temperature. **Fig. 5** shows a graph of the change in running torque as a function of time.

The raceway wear becomes substantial only when the balls are made of ceramics and there is no lubrication. However, if a lubrication film is provided for the raceway, then the torque variation becomes small and stable. **Fig. 6** shows an example of a test with the housing temperature set at 300°C for a ball bearing of 9.5 mm in bore and 22 mm in outside diameter which rotates at 9 000 min^{-1} under an axial load of 5 N {0.5 kgf} or 20 N {2 kgf}.

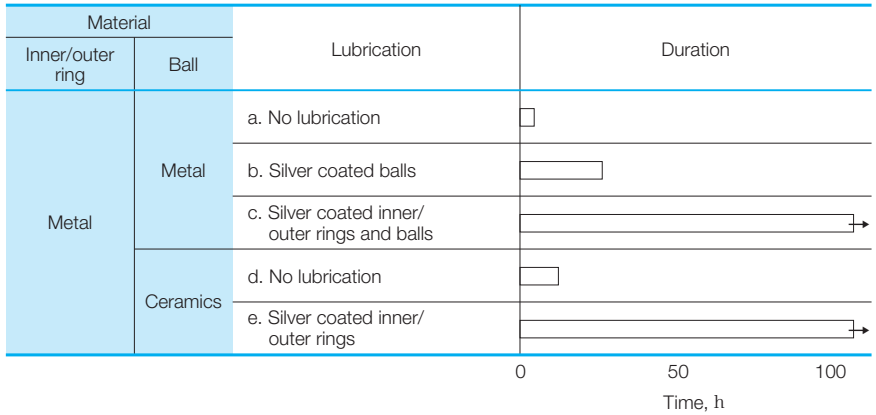

Fig. 4 Lubricating conditions and durable time (room temperature)

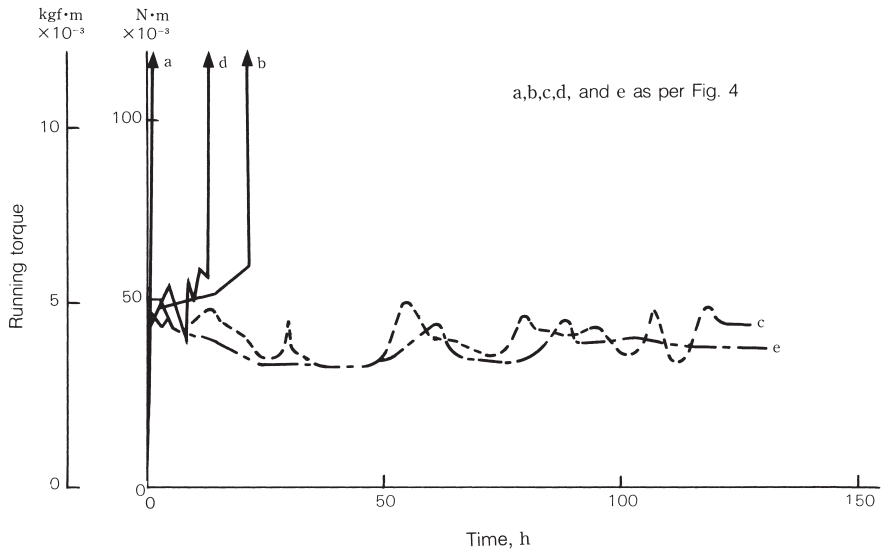

Fig. 5 Torque and duration

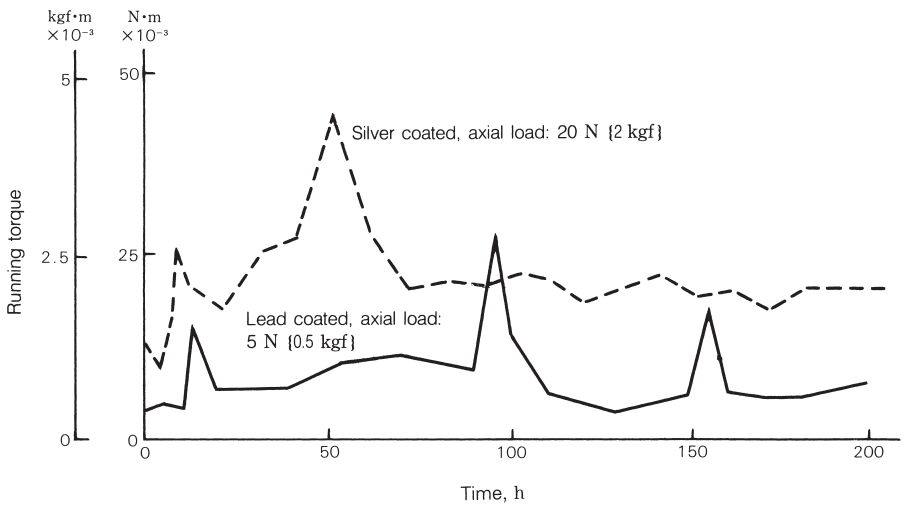

Fig. 6 Lubricating conditions and duration at high temperature

13.3 Ball bearing for high vacuum

A ball bearing coated with a solid lubricant is available for high-vacuum use where normal lubricants or grease cannot be used. **Table 1** shows the bearing number and boundary dimensions of these bearings. They can be classified into a type with a cage or a type without cage (full complement type) which is available with a flange or a shield to suit the specific application.

A bearing with a cage can be made to achieve low-torque stable rotation at low speeds by selecting a cage material and shape suited to the application. At high speeds, however, slip friction grows between the cage and ball.

Table 1 Boundary dimensions of a high-vacuum ball bearings

Bearing No.	Boundary dimensions (mm)		
	d	D	B
U-694hS	4	11	4
U-625hS	5	16	5
U-626hS	6	19	6
U-627hS	7	22	7
U-608hS	8	22	7
U-629hS	9	26	8
U-6000hS	10	26	8
U-6200hS	10	30	9
U-6001hS	12	28	8
U-6201hS	12	32	10
U-6002hS	15	32	9
U-6202hS	15	35	11
U-6003hS	17	35	10
U-6203hS	17	40	12
U-6004hS	20	42	12
U-6204hS	20	47	14
U-6005hS	25	47	12
U-6205hS	25	52	15
U-6006hS	30	55	13
U-6206hS	30	62	16
U-6007hS	35	62	14
U-6207hS	35	72	17
U-6008hS	40	68	15
U-6208hS	40	80	18

Remarks This bearing type is available in open, shielded, and full-complement types. The material used is SAE 51440C.

Accordingly, a full-complement type ball bearing is better suited for high speeds. When compared to a bearing with a cage, the full-complement type ball bearing develops slightly larger running torque due to slide contact between balls, but develops less wear and less torque fluctuation. As a result, a full-complement type ball bearing is used for a wide range of speeds from low to high.

Solid lubricants used include laminated structures of soft metals such as Ag (silver) and Pb (lead) and molybdenum disulfide (MoS_2). **Table 2** and **Figs. 1** through **3** show typical friction and wear characteristics of bearings lubricated via a thin film of solid lubricants at 100 to 9 000 min^{-1}. As is known from **Table 2**, Ag is used when low wear is demanded while Pb and MoS_2 are used when low torque is demanded.

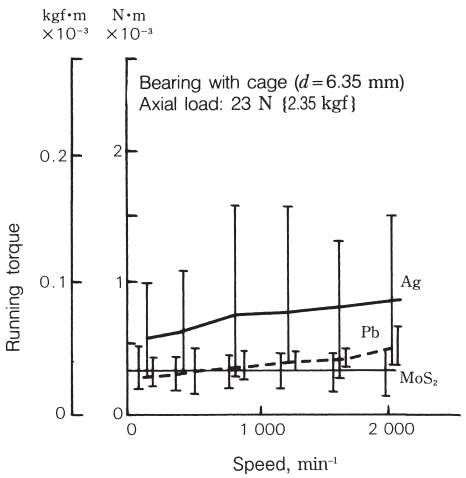

Fig. 1 Speed and running torque

Table 2 Characteristics of high-vacuum ball bearing

Kind of coating	Friction characteristics				Wear amount
	Torque	Relationship with rotating speed		Relationship with axial load with Fig. 3	
		Relatively low speed Fig. 1	Relatively high speed Fig. 2		
Ag	Large △	Almost no change ○	Increase along with rotating speed △	Rapid increase along with load △	Less ○
Pb	Normal ○	Almost no change ○	Increase along with rotating speed △	Increase slightly along with load △	More than Ag △
MoS_2	Small ○	Almost no change ○	Almost no change ○	Increase slightly along with load ○	More than Ag △

Remarks ○: Superior △: Relatively inferior

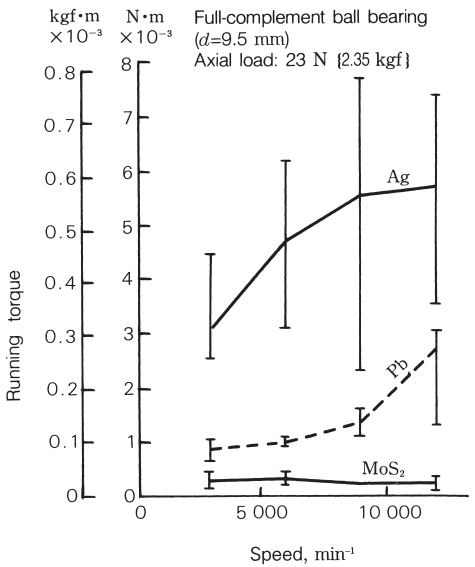

Fig. 2 Speed and running torque

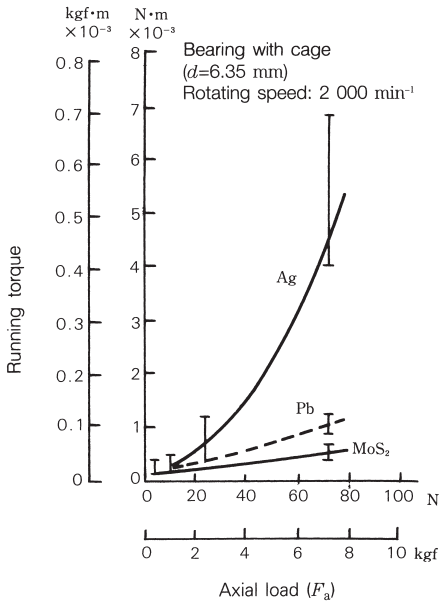

Fig. 3 Axial load and running torque

13.4 Light-contact-sealed ball bearings

Bearings are required to have low torque combined with high sealing effectiveness in order to meet the machine requirements of small-size, light-weight, and low-energy-comsumption.

NSK has developed DDW seals to meet these requirements. They have the following advantages compared with DDU seals, which are NSK's standard contact seals.

(1) There is light contact between the main seal lip and inner ring because the support for the main lip is long and thin resulting in low torque.
(2) The main lip contacts the bevelled portion of the inner ring seal groove where, if there is centrifugal force, the dust moves outward, so the dust resistance is excellent.
(3) The main lip has outward contact with the inner ring seal groove, so internal pressure does not open the seal and allow grease leakage.

The available bearing bore diameters are 10 to 50 mm now. Please consult NSK about other sizes.

In the case of nitrile rubber, the color code is as follows:

DDW (light-contact seal): Green
DDU (standard contact seal): Brown
VV (non-contact seal): Black

Fig. 1 shows the design of DDW sealed bearings and Fig. 2 shows the results of evaluation tests.

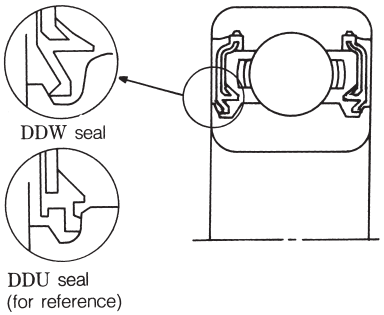

Fig. 1 DDW sealed bearing

1. Starting torque

Temperature: Ambient temperature

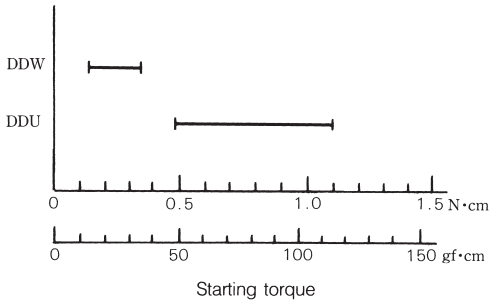

2. Dust resistance

Speed: 6 700 min⁻¹
Radial load: 147 N {15 kgf}
Temperature: 100°C
Dust amount: 200 g/test machine

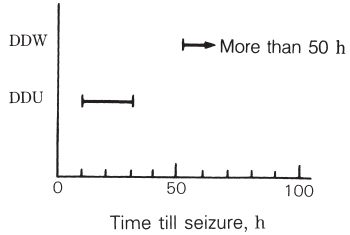

3. Grease leakage (high speed)

Speed: 20 000 min⁻¹
Radial load: 147 N {15 kgf}
Temperature: 100°C
Test time: 24 h

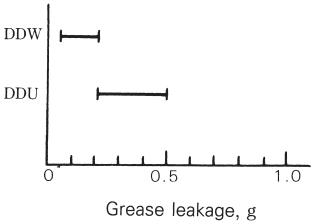

Test bearings: 6203 4 bearings/test
Grease: Ester-base lithium grease, 45% of free space

Fig. 2 Evaluation test results of DDW sealed bearings

13.5 Bearing with integral shaft

In consideration of the need for improved Audio-Visual (AV) and Office Automation (OA) equipment, bearings used in rotary mechanisms of small precision motors and so forth are increasingly demanded to demonstrate much higher performance. Enhanced quality of Video Cassette Recorders (VCR) and Digital Audio Terminals (DAT), increased density of Hard Disk Drives (HDD), and improved printing quality of Laser Beam Printers (LBP) have imposed severe requirements on equipment. These severe design requirements cover improvement of the runout accuracy (rotational repetitive runout, non-repetitive runout), low-noise, and reduction of power consumption as well as being easy-to-assemble. An NSK bearing with integral shaft is available and meets these exacting demands.

The bearing with integral shaft is a unit, which has no inner ring while having the raceway groove directly on the shaft to incorporate a preload spring between both outer rings (Fig. 1). This type of bearing has the following advantages over normal bearings:

(1) Improved recording/reproduction accuracy
- ○Integration of the shaft and inner ring, thereby eliminating movement of the shaft caused by fitting between the shaft and inner ring
- ○Thick-wall design of the outer ring as required, thereby reducing deformation of the outer ring due to interference

(2) Reduced power consumption of motor
- ○Integration of the shaft and inner ring, thereby reducing the ball pitch diameter for the same shaft diameter and resulting in a decrease of torque

(3) High shaft rigidity and compactness
- ○Integration of the shaft and inner ring, thereby reducing the bearing's outside diameter for a given size shaft diameter.

(Example) 684ZZ: Shaft diameter 4 mm, outside diameter 9 mm (without shaft)
4BVD: Shaft diameter 4 mm, outside diameter 8 mm (with integral shaft)

(4) Aiming at "easy-to-assemble" designs
- ○No parts are required for preload adjustment and preloading
- ○No need for selective fitting and adhesion securing of the shaft and inner ring

Specifications on the NSK bearing with integral shaft are shown in Table 1.

Table 1 Specifications on bearing with integral shaft

	Boundary dimensions (mm)			Basic load Ratings (N)		{kgf}	
d	D_1	D_2	W	C_r	C_{or}	C_r	C_{or}
3	6.45	7.05	3.5	435	124	45	13
4	8	10	4	550	173	56	18
5	9	10	4	640	223	65	23
6	10	12	4	710	271	73	28
7	13	15	5	980	365	100	37
8	15	17	6	1 330	505	135	52

Remarks Consult NSK for the shaft length.

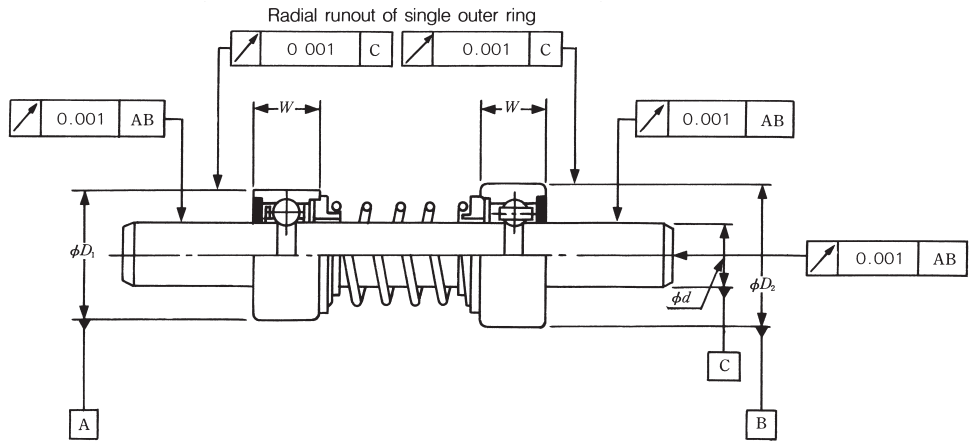

Fig. 1 Composition and runout accuracy of bearing with integral shaft

13.6 Bearings for electromagnetic clutches in car air-conditioners

The electromagnetic clutch is an important part and is necessary to activate the compressor of a car air-conditioner. The performance required of an electromagnetic clutch bearing differs depending on the type of compressor.

Table 1 shows the relationship between the compressor type and the application conditions for electromagnetic clutch bearings.

Values shown in Table 1 are the maximum during practical operation. A bench test is made under more severe conditions to confirm the durability of the bearing.

The electromagnetic clutch bearing must prove durable under these conditions. Principal performances required of the bearing are listed below:

○ Durability at high speed
○ Durability at high temperature
○ Bearing angular clearance should be kept small to assure maintenance of a proper clearance between disk and armature

When deciding the bearing specifications, the appropriateness of the following points should be considered:

○ Bearing internal design for high speed and longer life
○ Long-life grease for high temperatures and high speeds
○ Proper radial clearance
○ Effective sealing system with low grease leakage and superior in terms of dust proof and water proof

Most of the bearings for electromagnetic clutches have a bore in the range of 30 to 45 mm. One common arrangement is to use a pair of single-row deep groove ball bearings, and another is to use a double-row angular contact ball bearing.

A bearing for an electromagnetic clutch is required to have high speed, long grease life, proper internal clearance, and superior seal effectiveness. NSK bearings for electromagnetic clutches have the dimensions and features described below to meet the above performance requirements:

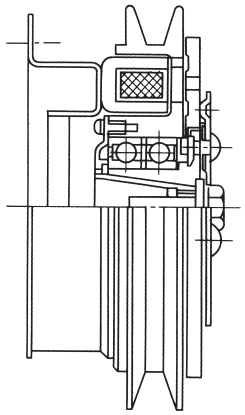

Fig. 1 Electromagnetic clutch for a reciprocating type compressor

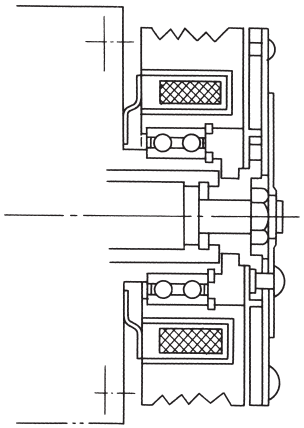

Fig. 2 Electromagnetic clutch for axial type and rotary type compressors

(1) Bearing type and dimensions

An electromagnetic clutch bearing is described below, and its representative bearing numbers and boundary dimensions are shown in Table 2.

Table 1 Compressor type and bearing running conditions

Running conditions of clutch bearing		Compressor type			
		Reciprocating	Vane	Scroll	Swash Plate
Rotating ring	Clutch ON	Inner and outer rings	Outer ring	Outer ring	Outer ring
	Clutch OFF	Outer ring	Outer ring	Outer ring	Outer ring
Maximum speed (min^{-1})		5 500	7 000	12 000	9 000
Maximum bearing temperature (℃) Inner ring		120	120	120	160

Table 2 Boundary dimensions of electromagnetic clutch bearings

Bearing type	Bearing No.	Boundary dimensions (mm)			
		d	D	B	r (min.)
Single-row deep groove ball bearing (2 bearings)	6006	30	55	13×2	1
	6008	40	68	15×2	1
Double-row angular contact ball bearing	30BD40	30	55	23	1
	35BD219	35	55	20	0.6
	40BD219	40	62	24	0.6
	30BD4718	30	47	18	0.5
	35BD5020	35	50	20	0.3
	35BD5220	35	52	20	0.5

(1.1) Double-row angular contact ball bearings
This type of bearing is used in the greatest quantity as an electromagnetic clutch bearing and common features include those listed below:
- ○Easier to handle and superior in economy to a combination of single-row deep groove ball bearings
- ○Use of plastic cage (long life)
- ○Securing of a contact angle (generally 25°) favorable for pulley overhang

(1.2) Combination of single-row deep groove ball bearings
In most cases, this type is replaced by double-row angular contact ball bearings. At present, they are still used in relatively large vehicles and general industrial machinery.

(2) Dedicated grease
NSK has developed dedicated greases MA6, MA8 and HA2 that ensure long life under high-temperature and high-speed conditions. These greases are already in practical use. The main features of MA6, MA8 and HA2 greases can be described as follows:
- ○Superior in resistance at high temperature. Long grease life is ensured even at the high temperature of 160°C.
- ○Less grease leakage due to superior shearing stability
- ○Ensures longer grease life and high anti-rusting performance by the addition of a suitable anti-rusting agent.

(3) Bearing seal
The following performances are required of a bearing seal for an electromagnetic clutch:

- ○Less grease leakage
- ○Superior dust and water resistance
- ○Small torque

NSK seals have a good balance of the above performances (Table 3). NSK offers the types of seals shown on the next page.

Table 3 Type and performance of NSK bearing seals

Seal performance	Seal type		
	DU	DUK	DUM
Grease leakage	Fair	Good	Superior
Seal effectiveness (dust and water resistance)	Fair	Good	Superior
Torque	Good	Good	Good
Seal groove-seal lip contact condition	Contact (with air hole)	Contact (without air hole)	Contact (without air hole)

13.7 Sealed clean bearings for transmissions

A sealed clean bearing for a transmission is a bearing with a special seal that can prevent entry of foreign matters into a gear box and thereby extend the fatigue life of a bearing substantially.

This type of bearing has proven in actual transmission endurance tests to have a durability life which is 6 to 10 times longer than that of standard ball bearings.

The special seal prevents harmful, extremely-small foreign matters suspended in the gear oil from entering the gear box. Thereby minimizing the number of dents and foreign matter that become embedded in the raceway. The bearing fatigue pattern is thus changed from a surface fatigue pattern to an internal fatigue pattern (a reference to be used in judgment of the bearing fatigue), which contributes to extension of the bearing life. This is not much affected by the recent trend to use low viscosity gear oil, either. In these respects, this kind of bearing is better than open type bearings.

Sealed clean bearings as described above are generally called transmission (TM) ball bearings. They are dedicated bearings for use in transmission applications and have the following major features:

1. Satisfactory design and specifications for a transmission bearing
2. Grease with an affinity for gear oil is filled to assist initial lubrication
3. The seal lip construction allows inflow of lubricating oil while preventing entry of foreign matters. (Fig. 1)
4. Lower torque when compared with normal contact seal bearings

These TM ball bearings are produced as series products as shown in Table 1. TM ball bearings have the same nominal dimensions as the open type bearing series 62 and 63 currently in use. Thus, they can readily be substitued.

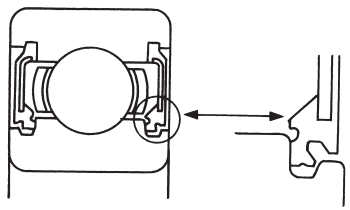

Fig. 1 Sectional and expanded views

Table 1 Specifications of TM ball bearings

Bearing No.	Boundary dimensions (mm)			Basic load ratings (N)		{kgf}	
	d	D	B	C_r	C_{0r}	C_r	C_{0r}
TM203	17	40	12	9 550	4 800	975	490
TM303	17	47	14	13 600	6 650	1 390	675
TM204	20	47	14	12 800	6 600	1 300	670
TM304	20	52	15	15 900	7 900	1 620	805
TM2/22	22	50	14	12 900	6 800	1 320	695
TM3/22	22	56	16	18 400	9 250	1 870	940
TM205	25	52	15	14 000	7 850	1 430	800
TM305	25	62	17	20 600	11 200	2 100	1 150
TM2/28	28	58	16	16 600	9 500	1 700	970
TM3/28	28	68	18	26 700	14 000	2 730	1 430
TM206	30	62	16	19 500	11 300	1 980	1 150
TM306	30	72	19	26 700	15 000	2 720	1 530
TM2/32	32	65	17	20 700	11 600	2 120	1 190
TM3/32	32	75	20	29 400	17 000	3 000	1 730
TM207	35	72	17	25 700	15 300	2 620	1 560
TM307	35	80	21	33 500	19 200	3 400	1 960
TM208	40	80	18	29 100	17 800	2 970	1 820
TM308	40	90	23	40 500	24 000	4 150	2 450
TM209	45	85	19	31 500	20 400	3 200	2 080
TM309	45	100	25	53 000	32 000	5 400	3 250
TM210	50	90	20	35 000	23 200	3 600	2 370
TM310	50	110	27	62 000	38 500	6 300	3 900
TM211	55	100	21	43 500	29 300	4 450	2 980
TM311	55	120	29	71 500	44 500	7 300	4 550
TM212	60	110	22	52 500	36 000	5 350	3 700
TM312	60	130	31	82 000	52 000	8 350	5 300
TM213	65	120	23	57 500	40 000	5 850	4 100
TM313	65	140	33	92 500	60 000	9 450	6 100
TM214	70	125	24	62 000	44 000	6 350	4 500
TM314	70	150	35	104 000	68 000	10 600	6 950

13.8 Double-row cylindrical roller bearings, NN30 T series (with polyamide resin cage)

For machine tool spindle systems which require particularly high rigidity, double-row cylindrical roller bearings (NN30 series) are used in increasing quantities. New machine tools are required to have the following improvements: reduction of the machining time, enhancement of the surface finishing accuracy through reduction of cutting resistance, extension of the tool life, and performance of light, high-speed cutting of materials such as aluminum, graphite, and copper.

NSK has developed double-row cylindrical roller bearings to meet these requirements. These bearings have polyamide cages which are far superior in high speed, low friction, and low noise over conventional types. Key features are listed below:

(1) Superiority in high speed

The polyamide cage is extremely light (about 1/6 that of copper alloy) and satisfactory in self-lubrication, with a lower coefficient of friction. As a result, heat generation is small and superior high speed characteristics are obtainable during high-speed rotation.

(2) Low noise

Low coefficient of friction, superior vibration absorption, and dampening contribute to reduction of the cage-induced noise to a level lower than that of conventional types.

(3) Extension of grease life

The polyamide cage avoids metallic contact with rollers while offering superior wear resistance. Accordingly, grease discoloration and deterioration due to wear of the cage is minimized, helping to further extend the grease life.

Polyamide cage are also used in single-row cylindrical roller bearings (N10 series). They are used mainly as bearings for the rear side of the spindle and are now marketed as the N10B T series.

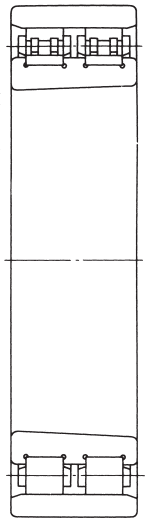

Fig. 1

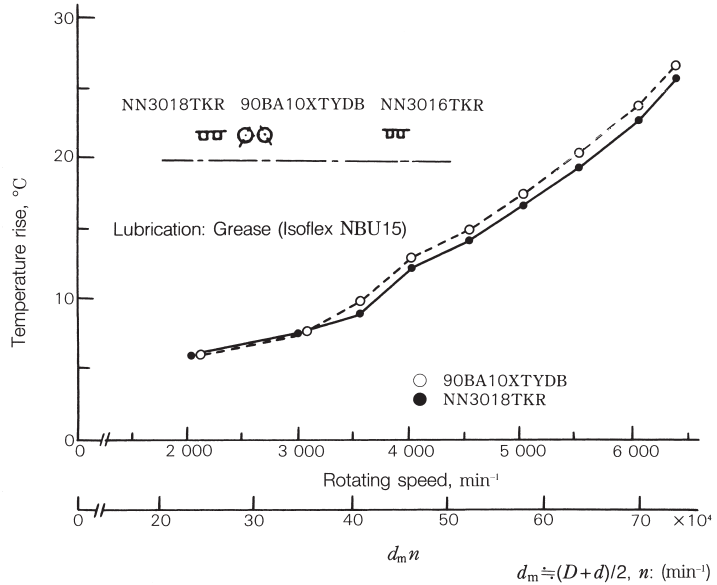

Fig. 2 Rotating speed and temperature rise

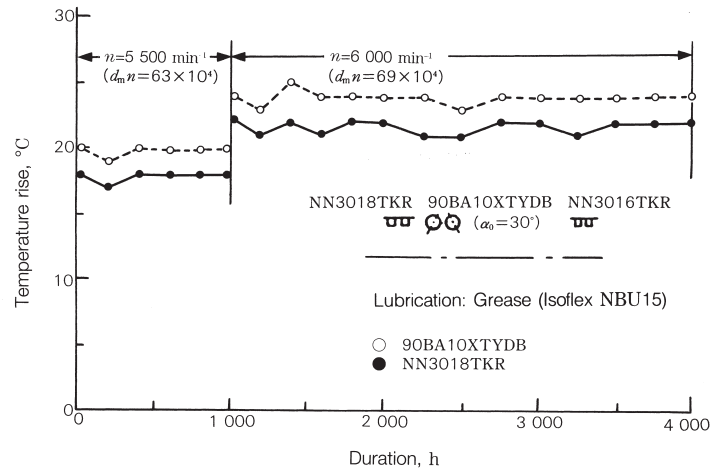

Fig. 3 Temperature change during endurance test

13.9 Single-row cylindrical roller bearings, N10B T series (cage made of polyamide resin)

Bearings to support the rear portion of the head spindle in machining centers and NC lathes are exposed to the belt tension and transmission gear reaction. Accordingly, double-row cylindrical roller bearings with large load capacity are used.

The number of applications are increasing for a drive system with a motor directly coupled or a motor built-in system with a motor arranged directly inside the spindle to meet the demand for faster spindle speeds. In this case, the single-row cylindrical roller bearing has come to be increasingly used because it can reduce the load acting on the rear support bearing and minimize heat generation in the bearing.

NSK has developed the N10B T series of bearings with polyamide cages for single-row cylindrical roller bearings (N10 series).

Key features of these bearings are listed below:

(1) The tapered bore bearing has been included, in addition to the cylindrical bore bearing, into series products. The tapered bore bearing allows easy setting of a proper radial internal clearance through adjustment of the axial push-in amount of the inner ring.
(2) The use of a developed polyamide cage proves favorable for use with grease and oil-air lubrication.

The developed polyamide cage is the same as the one used in the NN30B T series. Polyamide cages extend the grease life beyond that obtained with conventional copper alloy machined cages. Moreover, change of the cage guide method from the inner ring guide to the roller guide makes it easier to supply lubricating oil to the target zone between the cage bore surface and inner ring outside surface by an oil-air lubrication.

Accordingly, the design specifications are different from those of the conventional N10 series (as described in the bearing general catalog and the precision rolling bearing catalog for machining tools).

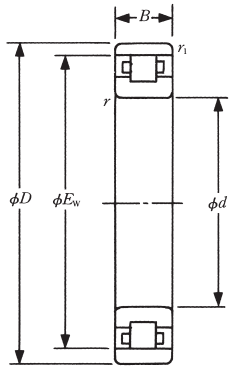

Cylindrical bore

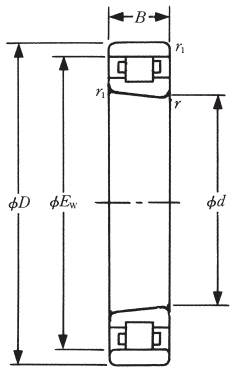

Tapered bore

Bearing No.		Boundary dimensions (mm)						Basic load ratings (N)		{kgf}	
Cylindrical bore	Tapered bore	d	D	B	r (min.)	r_1 (min.)	E_w	C_r	C_{0r}	C_r	C_{0r}
N1007B T	N1007B TKR	35	62	14	1	0.6	55	22 900	25 000	2 340	2 550
N1008B T	N1008B TKR	40	68	15	1	0.6	61	25 200	27 700	2 570	2 830
N1009B T	N1009B TKR	45	75	16	1	0.6	67.5	30 000	34 500	3 100	3 500
N1010B T	N1010B TKR	50	80	16	1	0.6	72.5	31 000	36 500	3 150	3 700
N1011B T	N1011B TKR	55	90	18	1.1	1	81	40 500	48 500	4 100	4 900
N1012B T	N1012B TKR	60	95	18	1.1	1	86.1	42 500	53 000	4 350	5 400
N1013B T	N1013B TKR	65	100	18	1.1	1	91	45 000	58 000	4 600	5 900
N1014B T	N1014B TKR	70	110	20	1.1	1	100	55 000	71 500	5 650	7 300
N1015B T	N1015B TKR	75	115	20	1.1	1	105	56 500	74 500	5 750	7 600
N1016B T	N1016B TKR	80	125	22	1.1	1	113	69 500	93 000	7 100	9 500
N1017B T	N1017B TKR	85	130	22	1.1	1	118	71 000	97 000	7 250	9 900
N1018B T	N1018B TKR	90	140	24	1.5	1.1	127	83 500	114 000	8 500	11 600
N1019B T	N1019B TKR	95	145	24	1.5	1.1	132	85 000	119 000	8 700	12 100
N1020B T	N1020B TKR	100	150	24	1.5	1.1	137	87 000	124 000	8 850	12 600
N1021B T	N1021B TKR	105	160	26	2	1.1	146	112 000	155 000	11 400	15 800
N1022B T	N1022B TKR	110	170	28	2	1.1	155	130 000	180 000	13 200	18 400
N1024B T	N1024B TKR	120	180	28	2	1.1	165	136 000	196 000	13 800	20 000
N1026B T	N1026B TKR	130	200	33	2	1.1	182	166 000	238 000	16 900	24 300

13.10 Sealed clean bearings for rolling mill roll neck

A large quantity of roll cooling water (or rolling oil) or scales is splasthed around the roll neck bearing of the rolling mill. Moreover, the roll and chock must be removed and installed quickly. In this environment, the oil seal provided on the chock may be readily damaged and the roll neck bearing may be exposed to entry of cooling water or scale.

Upon investigation, used grease from the bearing was found to be high in water content. Also, the bearing raceway often shows numerous dents due to inclusion of foreign matter, indicating progress of fatigue on the raceway surface.

The roll neck sealed clean bearing, which NSK has developed on the basis of the above investigation and analytical results, is already employed in large quantity inside and outside of Japan.

Features of the roll neck sealed clean bearing are listed below:

(1) Reduce the frequency of grease replenishment. The conventional man-hour needed for grease supply each day per bearing becomes totally unnecessary. In this way, maintenance costs can be reduced substantially.
(2) Seals are incorporated on both ends of the bearing, thus eliminating the possibility of damaging a seal during handling and effectively preventing entry of water and scale into the bearing. As a result, the rolling fatigue life can be improved substantially and there are fewer accidental seizures.
(3) The grease consumption can be reduced. For example, when assuming a case of three turns of chock for the cold rolling mill work rolls of five stands, the total number of bearings becomes 60 (4 × 5 stands × 3 turns) and, in this case, 10 to 15 tons of grease can be saved annually.
(4) The cleaning interval of a bearing can be extended. Conventional interval of partial cleaning every three months or so can be extended to every six months or more, thereby reducing the amount of maintenance work. However, the optimum interval needs to be determined after considering and experimenting with the particular conditions of the specific rolling mill.
(5) Reduction of the grease supply man-hour and of the grease consumption can decrease the contamination around a roll mill and roll shop and thus improves the cleanliness of the work environment.

Fig. 1 shows a typical assembly of a sealed clean bearing for the roll neck. Table 1 shows typical dimensions of a representative sealed clean bearing. For details, refer to the NSK catalog “Large-Size Rolling Bearings”, CAT. No. E125.

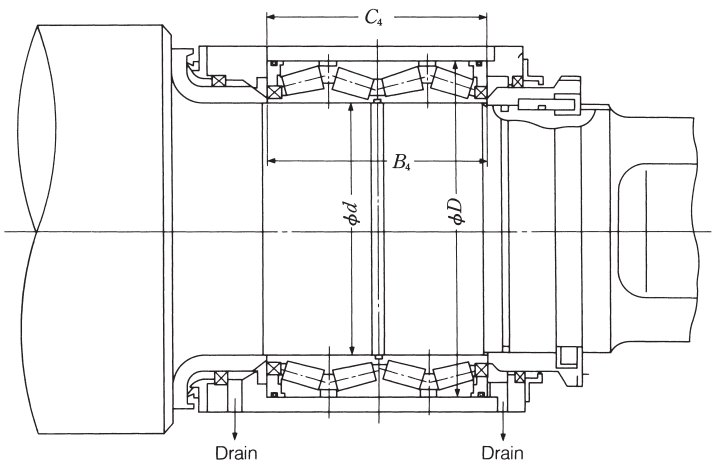

Fig. 1 Typical assembly of sealed clean bearing for roll neck

Table 1 Boundary dimensions of a sealed clean bearing for a roll neck

Bearing No.	Boundary dimensions (mm)			
	d	D	B_4	C_4
STF 343 KVS 4551 Eg	343.052	457.098	254.000	254.000
STF 457 KVS 5951 Eg	457.200	596.900	276.225	279.400
STF 482 KVS 6151 Eg	482.600	615.950	330.200	330.200

13.11 Bearings for chain conveyors

Many chain conveyors are used to transport semi-finished products and finished products (coil, etc.) between processes in a steelmaking plant. Bearings dedicated to these chain conveyors are used. The inner ring is fixed to the pin connecting the link plates while the outer ring functions as a wheel to carry the load on the rail by rolling.

Though varying in design depending on the purpose, typical conveyors used in steelmaking plant are shown in Figs. 1 and 2.

The bearing for chain conveyors rotates with outer rings at extremely low speed while being exposed to relatively heavy load and shock load. They are also used in poor environments with lots of water and scale at high temperature. In view of enhancing the breakdown strength by providing the roller (outer ring) with high wear resistance, a thick-wall design is employed and carburization or special heat treatment is made to increase the shock resistance. A full-complement type cylindrical roller bearing is designed to sustain these heavy loads. A double-row cylindrical roller bearing is not needed usually.

Either the S type (side seal type, Fig. 3) or labyrinth type (Figs. 4 and 5) is available. Thus, dust-proof and water-resistance as well as grease sealing are ensured. In particular, the S type has achieved further improvements in seal effectiveness through the use of a contact seal.

Normally, the outer ring outside has a cylindrical surface. There are various types: some with the outer ring width longer than the inner ring width (Figs. 3 and 4) and some with the outer ring and inner ring widths nearly equal (Fig. 5). Features of the chain conveyor bearing may be summarized as follows:

(1) The rollers (outer rings) are thick and made resistant to shock load and wear through carburization or special heat treatment.
(2) Special tempering allows use at high temperature.
(3) Optimum grease is filled for maintenance free operation, ensuring superior durability and economic feasibility.
(4) The seal construction is superior in grease sealing and dust- and water-proof, with a measure incorporated to prevent dislodgement of the seal by shock. In particular, the S type, which uses a contact seal, can realize improved sealing. The benefits of improved sealing include extension of the bearing life, substantial reduction of both supply grease and supply man-hours, and even cleaner surroundings.

Typical specifications on this bearing are shown in Table 1. Please contact NSK for information on bearings not shown in Table 1.

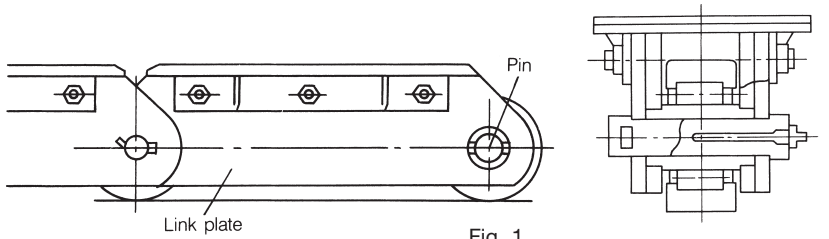

Fig. 1

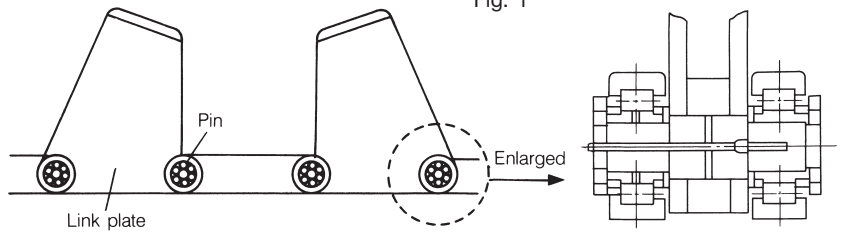

Fig. 2

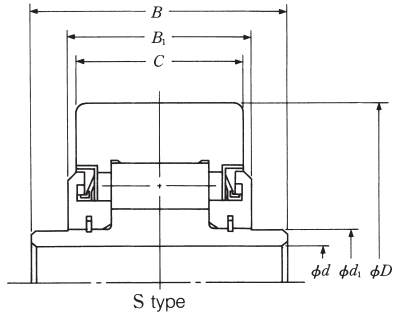

Fig. 3

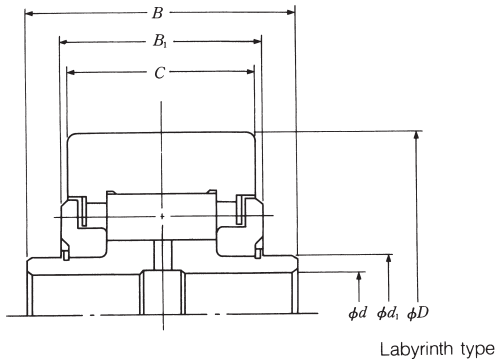

Fig. 4

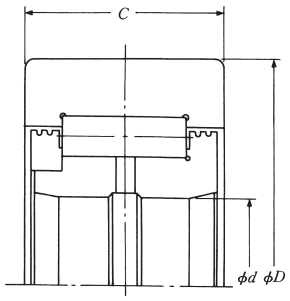

Fig. 5

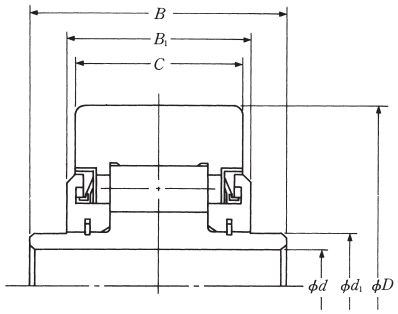

Fig. 3

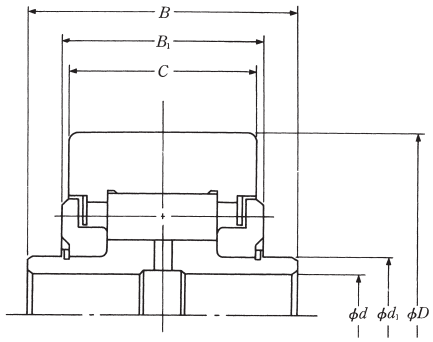

Fig. 4

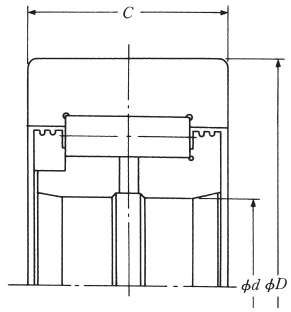

Fig. 5

Table 1 Representative chain conveyor bearings

Bearing No.		Example figure	Dimensions (mm)						Basic load ratings							
									S-type				Labyrinth type			
									(N)		{kgf}		(N)		{kgf}	
S-type	Labyrinth type		d	d_1	D	C	B	B_1	C_r	C_{0r}	C_r	C_{0r}	C_r	C_{0r}	C_r	C_{0r}
—	28RCV05	4	28.2	44.03	125	50	91.4	65	—	—	—	—	198 000	233 000	20 200	23 800
28RCV13	28RCV06	3,4	28.2	39.95	125	55	85.4	60	160 000	177 000	16 400	18 100	175 000	198 000	17 800	20 200
30RCV16	30RCV07	3,4	30.2	45	135	71	110	78	275 000	330 000	28 000	34 000	285 000	350 000	29 100	35 500
30RCV17	30RCV09	3,4	30.3	50.03	135	65	103	78	253 000	298 000	25 800	30 500	253 000	298 000	25 800	30 500
30RCV21	30RCV05	3,4	30.2	45	135	55	94	62	196 000	215 000	20 000	22 000	196 000	215 000	20 000	22 000
30RCV23	—	3	30.3	50.03	135	65	111	78	253 000	298 000	25 800	30 500	—	—	—	—
30RCV25	—	3	30.3	50.03	135	65	105	70	242 000	282 000	24 700	28 700	—	—	—	—
38RCV07	—	3	38.25	55.75	150	70	114.2	83.2	294 000	350 000	30 000	35 500	—	—	—	—
38RCV13	38RCV05	3,4	38.7	56	150	70	114.2	76	294 000	350 000	30 000	35 500	305 000	365 000	31 000	37 500
38RCV19	—	3	38.7	56	150	70	116	78	294 000	350 000	30 000	35 500	—	—	—	—
—	38RCV06	4	38.25	55.75	150	70	114.2	75	—	—	—	—	305 000	365 000	31 000	37 500
41RCV07	41RCV05	3,4	41.75	64.16	175	80	125	85	380 000	485 000	39 000	49 500	380 000	485 000	39 000	49 500
—	41RCV06	4	41.75	64.16	175	85	134.8	90.5	—	—	—	—	415 000	540 000	42 000	55 000
45RCV09	45RCV06	3,4	45.3	70.03	180	90	140.6	95	435 000	590 000	44 500	60 000	485 000	690 000	49 500	70 500
—	48RCV02	5	48.2	—	140	50	—	—	—	—	—	—	229 000	278 000	23 400	28 400
—	70RCV02	5	70	—	180	80	—	—	—	—	—	—	380 000	675 000	39 000	69 000

13.12 RCC bearings for railway rolling stock

Recent trains as well as the rolling stock are required to be high speeds and maintenance-free to satisfy the technical trends and environments.

Among the railway rolling stock, the axlebox bearings which run under the severe conditions such as large vibration and strong shocks when passing the rail joints or points, harsh environments with dust, rain and snow, are required to be high reliability for a long time.

NSK developed RCC bearings (Sealed cylindrical roller bearings for railway axle) to meet the above requirements. The RCC (Rotating end Cap type Cylindrical roller bearing) is a sealed bearing unit in which specially designed oil seals are attached directly to both ends of a double-row cylindrical roller bearing with double collars and filled with a dedicated long-life grease. (Fig. 1) The exclusive greases are the greases which are popularly used at AAR (Association of American Railroads) or long-life grease for axlebox developed by NSK.

The RCC bearings have the following features.

1. Unit construction, enabling easy handling.
2. The axle end can be exposed simply by removing an end cap, facilitating flaw detection of the axles or grinding of axles.
3. The roller and cage sub-unit can be removed from inner and outer rings during disassembly, making cleaning and inspection easier.
4. This unit bearing has an anti-rusting coating applied over the outer ring outside. An adaptor to be set on the outer ring is enough for a bearing box, thereby making the construction around the bearing simpler and reducing the weight.

Now, due to the good results, RCC bearings are widely used in new electric and passenger cars of both private and semi-national (JR) railways in Japan. Specifications of principal NSK RCC bearing units are shown in Table 1.

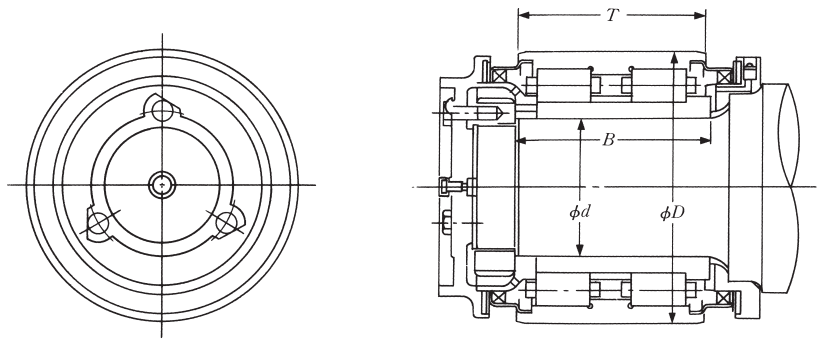

Fig. 1 Construction of RCC bearing

Table 1 Specifications on RCC bearing units

Unit No.	Boundary dimensions (mm)			Basic dynamic load rating	Bearing No. (reference)
	d	D	B	T	C_r (N)	
J-801	130	240	160	160	825 000	130JRF03A
J-803	120	220	188	175	850 000	120JRF04A
J-805	120	220	157	155	765 000	120JRF06
J-806	120	220	172	160	765 000	120JRF07
J-807	130	240	160	160	825 000	130JRF03
J-810A	120	220	185.5	160	765 000	120JRF09
J-811	120	220	204	160	815 000	120JRT07
J-814	130	230	185.5	160	800 000	130JRF05
J-816	130	240	160	160	825 000	130JRF03A
J-817	120	220	175	175	850 000	120JRF04J
J-818	90	154	107	115	315 000	90JRF01
J-819	120	230	185.5	170	945 000	120JRF10
J-820	85	154	135	105	365 000	85JRF01

Worldwide Sales Offices

P: Phone F: Fax ☆: Head Office

NSK LTD.-HEADQUARTERS, TOKYO, JAPAN

Nissei Bldg., 1-6-3 Ohsaki, Shinagawa-ku, Tokyo 141-8560, Japan
P: +81-3-3779-7111 F: +81-3-3779-7431

●Africa

South Africa:

NSK SOUTH AFRICA (PTY) LTD.

SANDTON 25 Galaxy Avenue, Linbro Business Park, Sandton 2146, South Africa
P: +27-011-458-3600 F: +27-011-458-3608

●Asia and Oceania

Australia:

NSK AUSTRALIA PTY. LTD.

MELBOURNE ☆ 100 Logis Boulevard, Dandenong South, Victoria, 3175, Australia
P: +61-3-9765-4400 F: +61-3-9765-4466

SYDNEY Suite A315, 20 Lexington Drive, Bella Vista, New South Wales, 2153, Australia
P: +61-2-9839-2300 F: +61-2-8824-5794

BRISBANE 1/69 Selhurst Street, Coopers Plains, Queensland 4108, Australia
P: +61-7-3347-2600 F: +61-7-3345-5376

PERTH Unit 1, 71 Tacoma Circuit, Canning Vale, Western Australia 6155, Australia
P: +61-8-9256-5000 F: +61-8-9256-1044

New Zealand:

NSK NEW ZEALAND LTD.

AUCKLAND Unit F, 70 Business Parade South, Highbrook, Business Park Auckland 2013, New Zealand
P: +64-9-276-4992 F: +64-9-276-4082

China:

NSK (SHANGHAI) TRADING CO., LTD.

JIANGSU No.8 NSK Rd., Huaqiao Economic Development Zone, Kunshan, Jiangsu, China (215332)
P: +86-512-5796-3000 F: +86-512-5796-3300

NSK (CHINA) INVESTMENT CO., LTD.

JIANGSU ☆ No.8 NSK Rd., Huaqiao Economic Development Zone, Kunshan, Jiangsu, China (215332)
P: +86-512-5796-3000 F: +86-512-5796-3300

BEIJING Room 1906, Beijing Fortune Bldg., No.5 Dong San Huan Bei Lu, Chao Yang District, Beijing, China (100004)
P: +86-10-6590-8161 F: +86-10-6590-8166

TIAN JIN Unit 4604, 46/F., Metropolitan Tower, 183 Nanjing Road, Heping District, Tianjin, China (300051)
P: +86-22-8319-5030 F: +86-22-8319-5033

CHANGCHUN Room 902-03, Changchun Hongwell International Plaza, No.3299 Renmin Street, Changchun, Jilin, China (130061)
P: +86-431-8898-8682 F: +86-431-8898-8670

SHENYANG No.7, 15 Street, Shenyang Economic & Technological Development Area, Shenyang, Liaoning, China (110141)
P: +86-24-2550-5017 F: +86-24-2334-2058

DALIAN Room 1805 Xiwang Tower, No.136 Zhongshan Road, Zhongshan District, Dalian, Liaoning, China (116001)
P: +86-411-8800-8168 F: +86-411-8800-8160

NANJING Room A1 22F, Golden Eagle International Plaza, No.89 Hanzhong Road, Nanjing, Jiangsu, China (210029)
P: +86-25-8472-6671 F: +86-25-8472-6687

FUZHOU Room 1801-1811, B1#1A Class Office Building, Wanda Plaza, No.8 Aojiang Road, Fuzhou, China (350009)
P: +86-591-8380-1030 F: +86-591-8380-1225

WUHAN Room 1512, No.198Yuncai Road, Office Building, Oceanwide City Square, JiangHan, District, WuHan, China (400039)
P: +86-27-8556-9630 F: +86-27-8556-9615

QINGDAO Room 802, Farglory International Plaza, No.26 Xianggang Zhong Road, Shinan District, Qingdao, Shandong, China (266071)
P: +86-532-5568-3877 F: +86-532-5568-3876

GUANGZHOU Room 1011-16, Yuexiu Financial Tower, No.28 Zhujiang Road East, Zhujiang New Town, Guangzhou, Guangdong, China (510627)
P: +86-20-3817-7800 F: +86-20-3786-4501

CHANGSHA Room 3209, Huayuan International Center, No.36, Section 2, Xiangjiang Middle Road, Tianxin District, Changsha, Hunan, China (410002)
P: +86-731-8571-3100 F: +86-731-8571-3255

LUOYANG Room 408, Building A, Zhong hong Excellence Center, No.1 Wu huan Street, Luo long District, Luoyang, Henan, China (471000)
P: +86-379-6069-6188 F: +86-379-6069-6180

XI'AN Room 1007, B Changan Metropolls Center, No.88 Nanguanzheng Steet, Xi'an, Shanxi, China (710068)
P: +86-29-8765-1896 F: +86-29-8765-1895

CHONGQING Room 612, Commercial Apartment, Athestel Hotel, No.288, Keyuan Rd.4, Jiulongpo District, Chongqing, China (400039)
P: +86-23-6806-5310 F: +86-23-6806-5292

CHENGDU Room1117, Lippo Tower, No.62 North Kehua Road, Chengdu, Sichuan, China (610041)
P: +86-28-8528-3680 F: +86-28-8528-3690

NSK CHINA SALES CO., LTD.

JIANGSU No.8 NSK Rd., Huaqiao Economic Development Zone, Kunshan, Jiangsu, China (215332)
P: +86-512-5796-3000 F: +86-512-5796-3300

NSK HONG KONG LTD.

HONG KONG ☆ Suite 705, 7th Floor, South Tower, World Finance Centre, Harbour City, T.S.T, Kowloon, Hong Kong, China
P: +852-2739-9933 F: +852-2739-9323

SHENZHEN Room 624-626, 6/F, Kerry Center, Renminnan Road, Shenzhen, Guangdong, China
P: +86-755-25904886 F: +86-755-25904883

Taiwan:

TAIWAN NSK PRECISION CO., LTD.

TAIPEI ☆ 10F-A6, No.168, Sec.3, Nanjing East Rd., Zhongshan Dist., Taipei City 104, Taiwan
P: +886-2-2772-3355 F: +886-2-2772-3300

TAICHUNG 3F. -2, No. 540, Sec. 3, Taiwan Blvd., Xitun Dist., Taichung City 407, Taiwan
P: +886-4-2708-3393 F: +886-4-2708-3395

TAINAN Rm. A1, 9F., No.189, Sec. 1, Yongfu Rd., West Central Dist., Tainan City 700, Taiwan
P: +886-6-215-6058 F: +886-6-215-5518

India:

NSK BEARINGS INDIA PRIVATE LTD.

CHENNAI ☆ TVH Beliciaa Towers, 2nd Floor, Block I, No.71/1, MRC Nagar Main Road, MRC Nagar, Chennai, Tamil Nadu, India - 600028
P: +91-44-28479600

GURGAON Unit No. 202, 2nd Floor, 'A' Block, Iris Tech Park, Sector-48, Sohna Road, Gurgaon, Haryana, India-122018
P: +91-124-4838000

MUMBAI 91 Spring Board Business Hub Private Limited, Godrej & Boyce, Gate No 2, Plant No 6, LBS Marg, Opposite Vikhroli Bus Depot, Vikhroli West, Mumbai, Maharashtra 400079, India
P: +91-9987617968

JAMSHEDPUR 36, Maharani Mansion Ground Floor, Circuit House Area P.O.- Bistupur, East Singhbhum, Jamshedpur, Jharkhand, India-831011
P: +91-657–2421144

Indonesia:

PT. NSK INDONESIA

JAKARTA Summitmas II, 6th Floor, Jl. Jend Sudirman Kav. 61-62, Jakarta 12190, Indonesia
P: +62-21-252-3458 F: +62-21-252-3223

Korea:

NSK KOREA CO., LTD.

SEOUL Posco Center (West Wing) 9F, 440, Teheran-ro, Gangnam-gu, Seoul, 06194, Korea
P: +82-2-3287-0300 F: +82-2-3287-0345

Malaysia:

NSK BEARINGS (MALAYSIA) SDN. BHD.

SHAH ALAM ☆ No. 2, Jalan Pemaju, U1/15, Seksyen U1, Hicom Glenmarie Industrial Park, 40150 Shah Alam, Selangor, Malaysia
P: +60-3-7803-8859 F: +60-3-7806-5982

PRAI No.24, Jalan kikik, Taman Inderawasih, 13600 Prai, Penang, Malaysia
P: +60-4-3902275 F: +60-4-3991830

JOHOR BAHRU 88 Jalan Ros Merah 2/17, Taman Johor Jaya, 81100 Johor Bahru, Johor, Malaysia
P: +60-7-3546290 F: +60-7-3546291

IPOH No.10&10A, Jalan Industri Paloh, Kawasan Perindustrian Ringan Paloh, 30200 Ipoh, Perak,Malaysia
P: +60-5-2555000 F: +60-5-2553373

Philippines:

NSK REPRESENTATIVE OFFICE

MANILA 8th Floor The Salcedo Towers 169 H.V. Dela Costa St.,Salcedo Villege Makati City, Philippines 1227
P: +63-2-893-9543 F: +63-2-893-9173

Singapore:

NSK INTERNATIONAL (SINGAPORE) PTE LTD.

SINGAPORE 238A, Thomson Road, #24-01/05, Novena Square Tower A, Singapore 307684
P: +65-6496-8000 F: +65-6250-0247

Thailand:

NSK BEARINGS (THAILAND) CO.,LTD.

BANGKOK 26 Soi Onnuch 55/1 Pravet Subdistrict, Pravet District, Bangkok 10250, Thailand
P: +66-2320-2555 F: +66-2320-2826

Vietnam:

NSK VIETNAM CO., LTD.

HANOI ☆ Techno Center, Room 204-205, Thang Long Industrial Park, Dong Anh District, Hanoi, Vietnam
P: +84-24-3955-0159 F: +84-24-3955-0158

HO CHI MINH CITY REPRESENTATIVE OFFICE Unit 609, The Landmark Building, 5B Ton Duc Thang Street,District 1, Ho Chi Minh City, Vietnam
P: +84-28-3822-7907 F: +84-28-3822-7910

Worldwide Sales Offices

P: Phone F: Fax ☆: Head Office

●Europe

United Kingdom:

NSK EUROPE LTD. (EUROPEAN HEADQUARTERS)

MAIDENHEAD Belmont Place, Belmont Road, Maidenhead, Berkshire SL6 6TB, U.K.
P: +44-1628-509-800 F: +44-1628-509-808

NSK UK LTD.

NEWARK Northern Road, Newark, Nottinghamshire NG24 2JF, U.K.
P: +44-1636-605-123 F: +44-1636-605-000

France:

NSK FRANCE S.A.S.

PARIS Quartier de l'Europe, 2 Rue Georges Guynemer, 78283 Guyancourt, France
P: +33-1-30-57-39-39 F: +33-1-30-57-00-01

Germany:

NSK DEUTSCHLAND GMBH

DUSSELDORF ☆ Harkortstrasse 15, D-40880 Ratingen, Germany
P: +49-2102-4810 F: +49-2102-4812-290

STUTTGART Liebknechtstrasse 33, D-70565 Stuttgart-Vaihingen, Germany
P: +49-711-79082-0 F: +49-711-79082-289

WOLFSBURG Tischlerstrasse 3, D-38440 Wolfsburg, Germany
P: +49-5361-27647-10 F: +49-5361-27647-70

Italy:

NSK ITALIA S.P.A.

MILANO Via Garibaldi 215, Garbagnate Milanese (Milano) 20024, Italy
P: +39-299-5191 F: +39-299-025778

Netherlands:

NSK EUROPEAN DISTRIBUTION CENTRE B.V.

TILBURG Brakman 54, 5047 SW Tilburg, Netherlands
P: +31-13-4647647 F: +31-13-4641082

Poland:

NSK POLSKA SP.Z O.O.

WARSAW Ul. Migdalowa 4/73, 02-796, Warsaw, Poland
P: +48-22-645-1525 F: +48-22-645-1529

Spain:

NSK SPAIN S.A.

BARCELONA C/Tarragona, 161 Cuerpo Bajo, 2a Planta, 08014, Barcelona, Spain
P: +34-93-289-2763 F: +34-93-433-5776

Turkey:

NSK RULMANLARI ORTA DOGU TIC. LTD. STI.

ISTANBUL Cevizli Mahallesi. D-100 Güney Yanyolu, Kuriş Kule İş Merkezi No:2 Kat:4, P.K.: 34846, Cevizli-Kartal-Istanbul, Turkey
P: +90-216-5000-675 F: +90-216-5000-676

United Arab Emirates:

NSK BEARINGS GULF TRADING CO.

DUBAI JAFZA View 19, Floor 24 Office LB192402/3, PO Box 262163, Downtown Jebel Ali, Dubai, U.A.E
P: +971-(0)4-804-8200 F: +971-(0)4-884-7227

●North and South America

United States of America:

NSK AMERICAS, INC. (AMERICAN HEADQUARTERS)

ANN ARBOR 4200 Goss Road, Ann Arbor, Michigan 48105, U.S.A.
P: +1-734-913-7500 F: +1-734-913-7511

NSK CORPORATION

ANN ARBOR 4200 Goss Road, Ann Arbor, Michigan 48105, U.S.A.
P: +1-734-913-7500 F: +1-734-913-7511

NSK PRECISION AMERICA, INC.

FRANKLIN ☆ 3450 Bearing Drive, Franklin, Indiana 46131, U.S.A.
P: +1-317-738-5000 F: +1-317-738-5050

SAN JOSE 780 Montague Expressway, Suite 505, San Jose, California, 95131, U.S.A.
P: +1-408-944-9400 F: +1-408-944-9405

NSK LATIN AMERICA, INC.

MIAMI 11601 NW 107 Street, Suite 200, Miami Florida, 33178, U.S.A.
P: +1-305-477-0605 F: +1-305-477-0377

Canada:

NSK CANADA INC.

TORONTO ☆ 317 Rutherford Road South, Brampton, Ontario, L6W 3R5, Canada
P: +1-888-603-7667 F: +1-905-890-1938

MONTREAL 2150-32E Avenue Lachine, Quebec, Canada H8T 3H7
P: +1-514-633-1220 F: +1-800-800-2788

Argentina:

NSK ARGENTINA SRL

BUENOS AIRES Garcia del Rio 2477 Piso 7 Oficina "A" (1429) Buenos Aires-Argentina
P: +54-11-4704-5100 F: +54-11-4704-0033

Brazil:

NSK BRASIL LTDA.

SUZANO ☆ Av. Vereador João Batista Fitipaldi, 66, Vila Maluf, Suzano-SP-Brazil-CEP 08685-000
P: +55-11-4744-2500

JOINVILLE Rua Blumenau, 178, sala 910, Centro, Joinville-SC-Brazil-CEP 89204-250
P: +55-47-3422-2239

Peru:

NSK PERU S.A.C.

LIMA Calle Teniente Enrique Palacios 360 Oficina 311 Miraflores, Lima, Peru
P: +51-493-4385

Mexico:

NSK RODAMIENTOS MEXICANA, S.A. DE C.V.

SILAO, GUANAJUATO Circuito Mexiamora Oriente No. 331, Parque Industrial Santa Fe I, Puerto Interior. Silao, Guanajuato, Mexico. C.P. 36275
P: +52-472-500-9500 F: +52-472-103-9403

<As of October 2024>

For the latest information, please refer to the NSK website.

www.nsk.com

Every care has been taken to ensure the accuracy of data in this publication, but NSK Ltd. accepts no liability for any loss or damage incurred from errors or omissions. As we pursue continuous improvement, all content (text, images, product appearances, specifications, etc.) contained in this publication is subject to change without notice. Unauthorized copying and/or use of the contents of this publication is strictly prohibited. Please investigate and follow the latest product export laws, regulations, and permit procedures when exporting to other countries.

MEMO

MOTION & CONTROL™

NSK

Eco-awareness and reliability in motion

NSK used environmentally friendly paper and printing methods for this publication.

CAT. No. E728h 2024 Z-11 Printed in Japan ©NSK Ltd. First edition published in SEP. 1991